

**Dissertation zur Erlangung des Doktorgrades
der Fakultät für Chemie und Pharmazie
der Ludwig-Maximilians-Universität München**

**Analysis and suppression of mutant presenilin *sel-12*
in *Caenorhabditis elegans***

von

Stefan Eimer

aus

Kronach

2003

Erklärung

Diese Dissertation wurde im Sinne von § 13 Abs. 3 bzw. 4 der Promotionsordnung vom 29. Januar 1998 von Herrn Prof. Dr. Ralf Baumeister betreut.

Ehrenwörtliche Versicherung

Diese Dissertation wurde selbständig, ohne unerlaubte Hilfe angefertigt.

München, am 15.01.2003

Stefan Eimer

Dissertation eingereicht am 16. Januar 2003

1. Gutachter: Prof. Dr. Ralf Baumeister
2. Gutachter: Prof. Dr. Michael Meisterernst

Mündliche Prüfung am 02. Juni 2003

FÜR MEINE ELTERN

Danksagungen

Herrn Prof. Dr. Ralf Baumeister danke ich für die Vergabe des Themas und die hervorragenden Rahmenbedingungen in seinem Labor. Ferner weiß ich es zu schätzen, daß er mir die Freiheit gegeben hat, meine eigenen Ideen zu entwickeln und zu testen.

Mein besonderer Dank gilt auch Prof. Dr. Michael Meisterernst für seine vielseitige Hilfe und Unterstützung, für anregende Diskussionen, die Zeit an gemeinsamen Projekten sowie für die Erstellung des Zweitgutachtens.

Bei allen gegenwärtigen und ehemaligen Mitarbeitern der Arbeitsgruppe Baumeister bedanke ich mich für die Zusammenarbeit und Diskussionen. Ein spezieller Dank gilt dem Team der ersten Stunde Inge, Sascha, Nicole und Roland für ihren Teamgeist und ihre Hilfsbereitschaft. Mein ganz besonderer Dank gilt Roland Donhauser für seine erstklassige technische Unterstützung und vielseitige Hilfe, die einen entscheidenden Beitrag zu dieser Arbeit geleistet haben.

Ferner möchte ich Dr. Inge Röckelein, die hinter meinem Rücken so manche farbenfrohe Wunder vollbrachte, für ihre Kameradschaft und für die gemeinsame Zeit an Hefe-Projekten danken.

Dr. Sascha Röhrig gilt mein Dank für stimulierende Diskussionen, seine versierte Hilfe in allen Computerfragen und die vielen Tore beim "work out". Roland und Sascha sei darüber hinaus hier noch einmal für ihre ruhige und besonnene Art gedankt, die die allgemeine Stimmung ungemein positiv und ausgleichend beeinflusste.

Dr. Nicole Wittenburg möchte ich für die Einweisung in die unbekanntes Welten der Verhaltensforschung in *C. elegans* und für ihre stete Hilfe während und nach der Doktorarbeit danken.

Melissa Grimm gilt mein Dank für eine gute Zusammenarbeit und für den laborbegleitenden Englischunterricht.

Dr. Bernard Lakowski möchte ich für die langen und vielseitigen Diskussionen sowie für die äußerst fruchtbare Zusammenarbeit danken. Ferner danke ich ihm, daß er mir mit seinem fundierten Rat immer zur Seite stand.

Christine Goebel gilt mein Dank für ihre unkonventionelle Hilfe auf dem Projekt und, gemeinsam mit Bianca Sperl, für die ordnende Hand, ohne die das Labor so manche Wunder erlebt hätte. Ihrer beider Einsatz für die "allgemeinen Dinge" gilt meine Hochachtung.

Meinen beiden Diplomanden Andreas Böttcher und Ingo Hüser möchte ich für ihre Geduld und Begeisterungsfähigkeit danken. Es war für mich eine große Ehre einen Teil ihrer Ausbildung begleitet und mitgestaltet zu haben.

Prof. Dr. Christian Haass und Dr. Harald Steiner danke ich für ihre motivierende Zusammenarbeit und Diskussionen. Prof. Dr. Christian Haass möchte ich insbesondere dafür danken, daß er mein Interesse an Presenilinen weckte.

Prof. Dr. Ronald Plasterk und Dr. Henri GAM van Luenen gilt mein Dank für ihre freundliche Aufnahme in ihrer Arbeitsgruppe und Hilfe während dieser Zeit.

Dr. Bettina Meier danke ich, die Begeisterung an der Forschung mit mir geteilt zu haben sowie für ihre seelische Unterstützung. Zudem danke ich ihr dafür, mich immer wieder auf den Boden der Tatsachen zurückgeholt zu haben.

Bei meinen Eltern möchte ich mich für ihr Vertrauen und ihre rückhaltlose Unterstützung während meiner gesamten Ausbildung bedanken.

Die vorliegende Arbeit wurde in der Zeit vom Januar 1998 bis Juli 2002 im Labor von Prof. Dr. Ralf Baumeister am Genzentrum und am Adolf-Butenandt-Institut der Ludwig-Maximilian-Universität in München angefertigt.

Im Verlauf dieser Arbeit wurden folgende Veröffentlichungen angefertigt:

Baumeister R and **Eimer S** (1998)
Amyloid Aggregates, Presenilins, and Alzheimer's Disease
Angew. Chem. Int. Ed. **37** (21): 2978-2982.

Rockelein I, Rohrig S, Donhauser R, **Eimer S**, Baumeister R. (2000)
Identification of amino acid residues in the *Caenorhabditis elegans* POU protein UNC-86 that mediate UNC-86-MEC-3-DNA ternary complex formation.
Mol Cell Biol **20**: 4806-4813.

Okochi M, **Eimer S**, Bottcher A, Baumeister R, Romig H, Walter J, Capell A, Steiner H, Haass C. (2000) A loss of function mutant of the presenilin homologue *sel-12* undergoes aberrant endoproteolysis in *Caenorhabditis elegans* and increased A β 42 generation in human cells. J Biol Chem **275**: 40925-40932.

Wittenburg N, **Eimer S**, Lakowski B, Rohrig S, Rudolph C, Baumeister R. (2000)
Presenilin is required for proper morphology and function of neurons in *C.elegans*.
Nature **406**: 306-309.

Eimer S., Donhauser R. and Baumeister R. (2002)
The *C. elegans* presenilin *sel-12* is required for mesodermal patterning and muscle function.
Dev Biol, **251**: 178-192.

Eimer S., Lakowski B, Donhauser R. and Baumeister R. (2002)
Loss of *spr-5* bypasses the requirement for the presenilin *sel-12* by stage-specific derepression of *hop-1*.
EMBO Journal **21**: 5787-5796.

Lakowski B., **Eimer S.**, Göbel C., Böttcher A., Wagler B. and Baumeister R. (2003)
Two suppressors of *sel-12* encode C2H2 zinc finger proteins that regulate presenilin transcription in *C. elegans*.
Development **130**: 2117-2128.

Yamasaki A., **Eimer S.**, Baumeister R., Haass C. and Steiner H. (2003)
Expression of the *C. elegans* presenilin *spe-4* in human cells: functional implications for γ -secretase assembly and activity.
in preparation.

Summary:		II
Chapter I:	Introduction	1
Chapter II:	Amyloid Aggregates, Presenilins, and Alzheimer's Disease	49
Chapter III:	A loss of function mutant of the presenilin homologue SEL-12 undergoes aberrant endoproteolysis in <i>Caenorhabditis elegans</i> and increased A β 42 generation in human cells	55
Chapter IV	Presenilin is required for proper morphology and function of neurons in <i>C. elegans</i>	64
Chapter V	The <i>C. elegans</i> presenilin <i>sel-12</i> is required for mesodermal patterning and muscle function	69
Chapter VI	Loss of <i>spr-5</i> bypasses the requirement for the presenilin <i>sel-12</i> by stage-specific de-repression of <i>hop-1</i>	85
Chapter VII	Two suppressors of <i>sel-12</i> encode C2H2 zinc finger proteins that regulate presenilin transcription in <i>C. elegans</i>	96
Chapter VIII	SPE-4, the third presenilin ortholog in <i>C. elegans</i> , is a non functional presenilin	130
Curriculum vitae		148
Abbreviations		149

Summary

sel-12 and *hop-1* are two *C. elegans* genes which are structurally and functionally homologous to the human presenilins, PS1 and PS2. Mutations in the human presenilins contribute to the majority of familial Alzheimer's disease cases. Work in *C. elegans* also revealed that presenilins are involved in Notch signaling as a reduction of *sel-12* presenilin activity is able to suppress the phenotypes associated with *lin-12*/Notch gain-of-function mutations. Several lines of evidence suggest that presenilins are an active protease that mediate the transmembrane cleavage event that releases the LIN-12/Notch intracellular domain from the membrane. This step is crucial for nuclear Notch signaling. As a consequence, loss of all presenilin activity, in a *sel-12*; *hop-1* double mutant, causes phenotypes associated with the complete absence of all Notch signaling in *C. elegans*.

Loss of *sel-12* function in *C. elegans* leads to a highly penetrant egg-laying defect (Egl) which resembles the Egl defect present in *lin-12* hypomorphic alleles. The inability of *sel-12* mutant animals to lay eggs is shown here to be caused by two defects: (i) a π cell specification defect which results in a blockage of the vulva-uterine connection and (ii) a sex-muscle patterning defect leading to morphologically abnormal and misattached vulva-muscles.

In order to find new molecules that are able to influence presenilin mediated signaling we screened for extragenic suppressors of the *sel-12* Egl defect. In several screens four *spr* genes (suppressor of presenilin) were identified, which are able to suppress both *sel-12* defects in the egg-laying system. The *spr* genes are not able to influence LIN-12/Notch signaling directly but require the activity of the second *C. elegans* presenilin *hop-1* for *sel-12* suppression. Molecular analysis of SPR-5 revealed that it belongs to a conserved family of FAD containing polyamine-oxidase like proteins. The human homologue is found to be an integral component of the CoREST transcriptional co-repressor complex. Further analysis of the other *spr* genes revealed that SPR-1 is the *C. elegans* homolog of the human CoREST protein, which is also a component of the CoREST complex. Based on the physical interaction of SPR-5 and SPR-1 presented here, it is likely that a CoREST like complex also exists in *C. elegans*. Mutations in this complex lead to a stage specific de-repression of *hop-1* expression which is then able to substitute for *sel-12* presenilin activity during development of the egg-laying system.

Summary

The two remaining suppressors, *spr-3* and *spr-4*, encode nuclear C2H2 zinc finger proteins that have been shown to up-regulate *hop-1* transcription in a similar way and thus may be involved in nuclear targeting of the *C. elegans* CoREST complex.

Additionally, *sel-12* is highly expressed in neurons, which suggests that it may also be required for neuronal function. Experiments presented here show that *sel-12* is also involved in the function and morphology of the AIY interneurons, which control the thermotaxis behaviour in *C. elegans*.

CHAPTER I

Introduction

Alzheimer's disease

Alzheimer's disease (AD) is a progressive, degenerative neurological disorder that results in dementia, with impaired memory, thinking and reasoning. It is one of the major causes of death in the developed countries. The primary risk factor for Alzheimer's disease is old age. Therefore the number of people affected by Alzheimer's disease increases markedly with advancing age. Only 5-10% of the population that are over 65 years old develop Alzheimer's symptoms, while the probability increases to 30-50% for those that are over 85 years old. Thus the risk of Alzheimer's disease doubles every five years after the age of 65 (Evans et al., 1989; Kawas et al., 2000). There is no obvious bias between sexes, since men and women are almost equally affected.

The major behavioural hallmarks of Alzheimer's disease are progressive loss of memory and language. As a consequence of the impairment of judgement and planning, Alzheimer's disease is often accompanied by personality changes resulting in depression, uneasiness, paranoia, delusion, or aggression. An unambiguous diagnosis is often difficult due to the behavioural alterations which overlap with other age related dementia. Most of the Alzheimer's cases can only be confirmed with the identification of specific brain abnormalities after death.

One of the hallmarks of Alzheimer's disease is the presence of characteristic extracellular amyloid plaques in the brains of patients and in most cases neurofibrillary tangles which appear as intraneuronal lesions (Figure 1). Additional pathogenic alteration found in the brains of AD patients are microgliosis, astrocytosis, selective neuronal degeneration and neuronal loss and multiple neurotransmitter deficits.

Analysis of the amyloid plaques found in the brains of AD patients revealed that they are mainly composed of a short peptide of 40-42 amino acids, termed amyloid beta ($A\beta$) peptide. This $A\beta$ peptide is cleaved from a larger membrane protein, the amyloid precursor protein (APP), through two subsequent proteolytic events (Figure 2). The $A\beta$ protein is secreted by all cells throughout the body, but is produced in particularly large amounts in the brain and in the vascular system. The amyloid plaques are seeded outside the cells and develop in the space between the neurons. The amyloid plaques form early in the disease process, before any surrounding neuronal damage is evident. Plaque formation precedes the appearance of AD symptoms by up to 10-20 years. As the plaques grow in size they destroy the surrounding neurons and possess the space formerly occupied by the neurons (Figure 1). In the process of aggregation other cellular proteins are also deposited in the amyloid plaques.

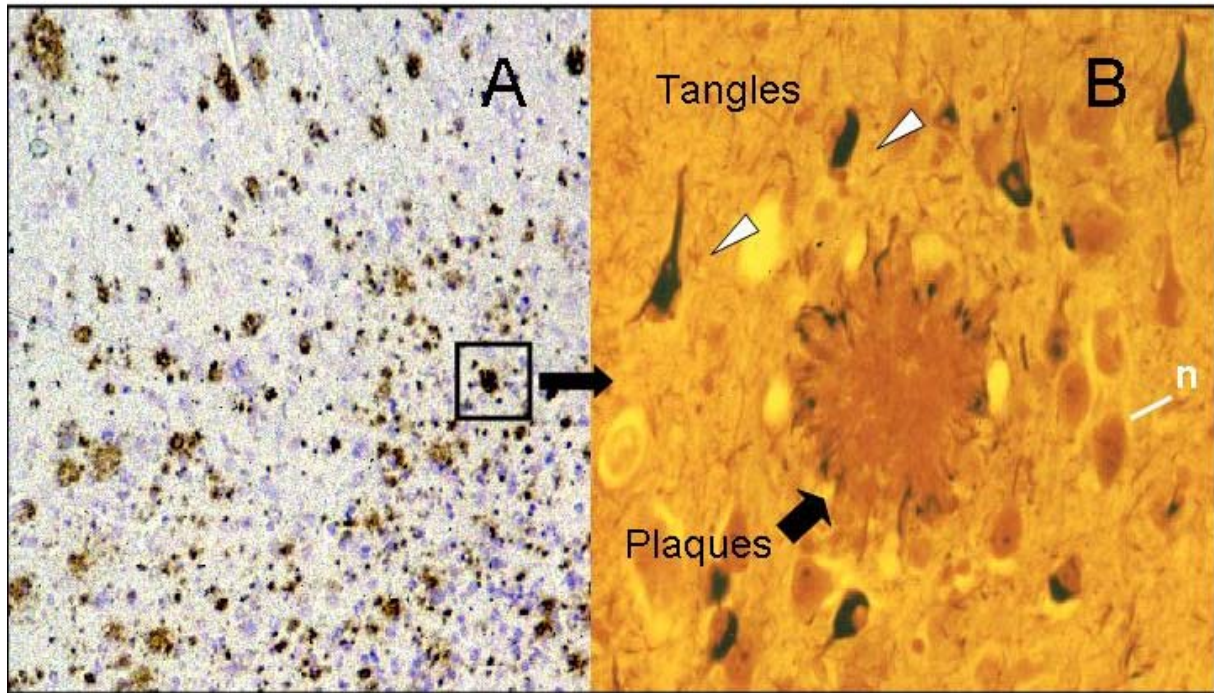


Figure 1: (A) Alzheimer's disease brain showing the typical amyloid plaques. (B) Magnification of the boxed area. Extracellular amyloid plaques (arrow) and intraneuronal tangles (arrowheads) are marked as well as the cell body of a neuron (n) (picture taken from Selkoe, 1999).

A second hallmark of AD brains is often the presence of intraneuronal lesions called tangles (Figure 1). Tangles are filamentous inclusions composed of hyperphosphorylated forms of the microtubule associated protein Tau. Alterations of the cellular Tau protein can lead to the formation of paired helical filaments (PHF) appearing as intraneuronal tangles at autopsy (Johnson and Hartigan, 1999). The Tau protein normally is involved in the stabilisation of microtubules (Xie et al., 1998). Tangles of Tau protein are a defining characteristic of a large number of neurodegenerative diseases and are therefore thought to be a secondary consequence of a primary neuronal injury and thus, an indication of disease progression (David et al., 2002).

Genes involved in Alzheimer's disease

Most of the AD cases occur sporadically and with a late onset after the age of 85. However, 5-10 % of the AD cases are characterised by an early onset (average onset between the age of 30 and 55 years) and by a rapid disease progression. Most of these AD cases exhibit an autosomal dominant transmission within the families (St George-Hyslop, 1998). This stable inheritance made it possible to map and identify the genes, which, when mutated, lead to familial AD (FAD). A summary of the verified genes causing FAD is shown in Table 1.

Table 1: Confirmed genetic loci contributing to the incidence of Alzheimer's disease and their effect on A β production

Chromosome	Genes affected	consequence
21	amyloid precursor protein (APP)	increase in A β production
19	ApoE4 polymorphism	density of A β plaques and vascular deposits
14	Presenilin 1 (PS1)	ratio of A β ₄₂ / A β ₄₀ increases
1	Presenilin 2 (PS2)	ratio of A β ₄₂ / A β ₄₀ increases

A β , amyloid β -protein; Table modified from (Selkoe, 2001).

Additionally, it was also obvious that genetic risk factors exist that contribute to late onset AD. The first susceptibility gene identified for the common form of late onset AD was the apolipoprotein E (ApoE) (Strittmatter et al., 1993).

ApoE

ApoE is a major serum lipoprotein that is involved in metabolism, transport and storage of cholesterol (Weisgraber et al., 1994). Three common isoforms of ApoE e2, e3, and e4, exist as a result of amino acid substitutions at codons 112 and 158. Lipoproteins containing ApoE e4 are cleared more efficiently from blood than those containing ApoE e2 and ApoE e3. ApoE does not cross the blood-brain barrier but is synthesized by astrocytes in the brain. There, it is thought to be involved in the mobilization and redistribution of cholesterol and phospholipids during membrane remodeling associated with plasticity and synaptogenesis. Individuals carrying one or two copies of the ApoE e4 allele have a significantly increased risk of developing AD as compared to individuals carrying no ApoE e4 allele (Dal Forno et

al., 2002). However, the ApoE genotype does not strongly affect the severity of the disease or its progression, nor does it strongly affect the age of onset of the disease. In contrast to ApoE e4, the e2 allele may confer a slightly protective effect (Talbot et al., 1994). Apolipoprotein E is found in amyloid plaques and neurofibrillary tangles. It binds to β -amyloid peptide in cerebrospinal fluid. *In vitro* studies have indicated that ApoE isoforms may differentially affect β -amyloid deposition and β -amyloid fibril formation (Wisniewski et al., 1994). Furthermore, a deletion of the ApoE gene in APP overexpressing mice completely abolishes amyloid plaque formation, without affecting the A β steady state levels. In contrast, transgenic mice that overexpress a mutated version of human APP and either the human ApoE e4 or e3 allele show a drastically reduced clearance of A β deposition in the brain (Brendza et al., 2002; Holtzman et al., 2000; Poirier, 2000). These experiments suggest that an interaction between ApoE and β -amyloid peptide is somehow linked to β -amyloid deposition and amyloid plaque formation. However, the role of ApoE may be indirect. ApoE is involved in cholesterol metabolism and transport and might therefore influence β -amyloid aggregation. It has been demonstrated that lowering the cholesterol content in neurons by extracting cholesterol out of membranes reduces β -amyloid production and thus reduces aggregation (Fassbender et al., 2001; Simons et al., 1998). Blocking cholesterol synthesis in neurons by blocking the hydroxymethylglutaryl-CoA (HMG-CoA) reductase through the drugs of the statins family also inhibits β -secretase cleavage of APP (Frears et al., 1999). This is further supported by the recent finding that *Drosophila* mutations that lower the concentration of cholesterol ester lead to neurodegeneration and an aberrant processing of the *Drosophila* APP like protein (APPL) (Tschape et al., 2002). As the generation of the β -amyloid protein seems to be highly sensitive to cholesterol levels it might be possible that a slight alteration of the cholesterol metabolism induced by different ApoE alleles may have an impact on the development of AD.

APP

Since the β -amyloid peptide, which is processed from the amyloid precursor protein (APP), is the main constituent of the amyloid plaques found in AD brains, it was very suggestive to find linkage of FAD to the APP region on chromosome 21 (Table 1). Furthermore, chromosome 21 is present in three copies in Down syndrome patients, which develop symptoms of AD in their 30s. The APP gene encodes a type I transmembrane domain protein which is transported to the cell surface. Three main isoforms exist, which are derived from a single

gene by alternative splicing (Selkoe, 2001). The most common form of APP in neurons is a 695 amino acid long version (Figure 2)(Sisodia et al., 1993). Although the physiological function of APP is still unclear, it is localized to synapses and thought to be involved in the process of synaptic transmission (Sisodia et al., 1993). However, mice carrying a deletion of the APP gene appear phenotypically normal (Zheng et al., 1996). However, these mice do show an increased sensitivity to kainic acid induced seizures with an increased rates of cell death (Steinbach et al., 1998). In addition, it has been shown that the secreted form of APP has neuroprotective properties *in vitro* (Mattson et al., 1993; Smith-Swintosky et al., 1994) and *in vivo* (Perez et al., 1997). Therefore, APP might play an excitoprotective role, rising the threshold levels for neurotoxicity. In contrast to the knock out mice, overexpression of APP in transgenic mice leads to a variable phenotype which depend on the APP construct used and on the genetic background (Andra et al., 1996; Carlson et al., 1997; Steinbach et al., 1998). For example, overexpression of APP in the brain leads to learning and memory deficits and to the formation of amyloid like deposits in the brain and vasculature of transgenic mice (Calhoun et al., 1999; Czech et al., 1994; Dewachter et al., 2001; Hsia et al., 1999; Koistinaho et al., 2001; Sturchler-Pierrat et al., 1997). Overexpression of the *Drosophila melanogaster* APP homolog, APPL, in flies results in a disruption of axonal transport (Torroja et al., 1999). In spite of the different phenotypes found in the various animal models, a conclusive model of APP function has not been worked out yet.

However, the biochemical consequences of the FAD mutations on APP processing are well established (Figure 2). All FAD mutations lead to an increased production of the 42 amino acid long variant of the amyloid β peptide, increasing the $A\beta_{42}/A\beta_{40}$ ratio (Table 1). Since $A\beta_{42}$ exhibits a much higher tendency to aggregate than $A\beta_{40}$, this is thought to increase the probability of plaque formation and therefore AD (Jarrett et al., 1993a; Jarrett et al., 1993b). APP is proteolytically processed by three different proteases called α -, β - and γ -secretase (Figure 2)(Selkoe, 2001). The β -amyloid peptide is released by the sequential action of the β - and γ -secretases, whereas the cleavage of APP by the α -secretase occurs within the β -amyloid domain and thus prevents the generation of $A\beta$ (Figure2) (Price et al., 1998; Selkoe, 2001). The mutations in APP associated with the autosomal dominant form of FAD cluster around the α -, β - and γ -secretase cleavage sites (Figure 2). $A\beta$ is always present in the brain even in healthy individuals due to constitutive processing of APP by the β - and γ -secretases. However, the majority of $A\beta$ generated is $A\beta_{40}$ with only a few percent being $A\beta_{42}$. In FAD patients the $A\beta_{42}/A\beta_{40}$ ratio is shifted towards the amyloidogenic $A\beta_{42}$. Consequently, the FAD mutations in APP act either by shifting the β - and γ -secretase

cleavage events towards the generation of A β ₄₂ or by reducing the α -secretase cleavage, which also results in more A β due to increased β - and γ -secretase cleavage. Since in FAD patients more of the highly amyloidogenic A β ₄₂ is produced, it is much more likely that an amyloid plaque is seeded over time, leading to an earlier onset of AD in those patients.

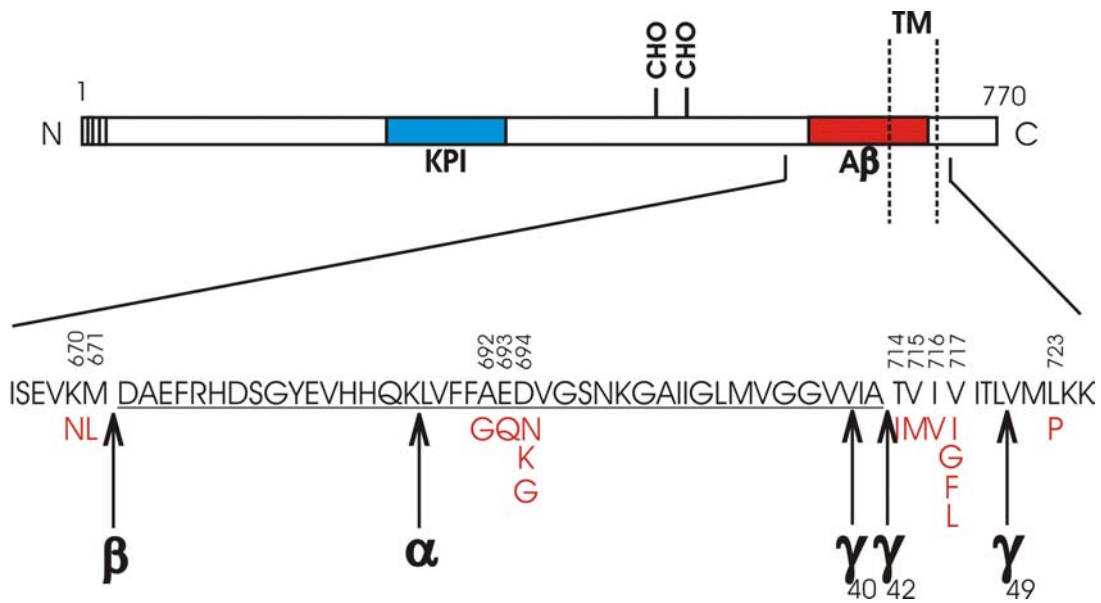


Figure 2: Schematic representation of the most abundant form of the amyloid precursor protein (APP) containing the secretion signal sequence at the amino terminus and a kunitz type inhibitory (KPI) domain. The position of the amyloid peptide sequence (A β) relative to the transmembrane domain (TM) is shown. The positions of the α -, β - γ -secretase cleavage sites are marked along with familial Alzheimer's disease (FAD) linked mutations found in APP, which cluster around the sites of cleavage.

Recently, a more carboxyterminal γ -secretase cleavage product was reported, which end at position 49, called A β ₄₉ (Figure 2). The site of cleavage within APP corresponds to the site 3 cleavage of the Notch receptor. This cleavage has also been shown to be dependent on presenilin activity (Okochi et al., 2002; Sastre et al., 2001).

Presenilins

Shortly after the first FAD mutations in APP were identified, a second FAD locus on human chromosome 14 was discovered. The gene identified to cause early onset AD when mutated was later called presenilin 1 (PS1) (Table 1)(Hardy, 1997; Price et al., 1998; Tanzi, 1999). Most of the PS1 mutations linked to FAD cases are characteristic to cause a very early disease onset (as early as 25) (Campion et al., 1995; Wisniewski et al., 1998) and rapid disease progression. In addition, mapping of the FAD locus on chromosome 1 revealed that a

hPS1	1	MTELPAPLSYFQNAQMS	EDNHL	SNTVRSQNDNRERQEHNDRRS-LGH
Dr PS	1	MADLVQNAANNV	LNDGMDT	SRHTSSSTAAP-----PSR
Xl PS α	1			MNDTSER-----RS-NEN
hPS2	1	MLTFMADSEEEVCDERTS	LMSAESPTPRS	SCQEGRQGFEDGENTA-QWR
Xl PS β	1	MIKLSDESEDECNERTS	LITSESPPLPSYQDGVQAS	EGLETSY-HRE
Dm PS	1	MAAVNLQASCSSGLASEDDANVGS	QIGAAERLERPPRRRQQQRN	
SEL-12	1			MPSTRRQQEG-----GGADAE

hPS1	47	PEPLSN	GRPQGN	S-----RQVVEQ-----DEEED
Dr PS	33	NEVELNGQ	PPTAPP	S-----PQVVTDS-----EEDED
Xl PS α	13	SESQSN	QTQSSS	S-----QQVLEQ-----DEEED
hPS2	49	SQENEEDG	EEDPDRYVCSGVPGR	S-----PPGLE
Xl PS β	47	RQPDSTQ	NNEDVPNGRTSGADAYNSETT	S-----VENE
Dm PS	44	NYGSSNQ	DQPDAAI	LAVPNVVMREPCGSRPSRLTGGRSGSGGPPTNEME
SEL-12	17	THTVYGTN	LITNRNSQE	S-----DENVV
HOP-1	1			M

hPS1	71	EELTLKYGAKHVIMLFV	PVTL	CMVVVVATIKSVSFYTRKDG-QLIYTPF	
Dr PS	59	EELTLKYGAKHVIMLF	PVTL	CMVVVVATIKSVSFYTRKDGQQLIYTPF	
Xl PS α	37	EELTLKYGAKHVIMLFV	PVTL	CMVVVVATIKSVSFYTRFDG-QLIYTPF	
hPS2	77	EELTLKYGAKHVIMLFV	PVTL	CMVVVVATIKSVRFYTKNG-QLIYTTF	
Xl PS β	80	EELTLKYGARHVIMLFV	PVTL	CMVVVVATIKSVSFYTKDG-QLIYTPF	
Dm PS	93	EEQGLKYGAQHVIKL	FVPVSL	CMVVVATINSISFYNSTDV-YLLYTPF	
SEL-12	39	EEAELKYGASHVH	LFPVSL	CMALVVFMTNTITFYSONN	GRHLLYTPF
HOP-1	2	PRTKRVS	SKTITG	VLYPVAICMLFVAINV	KLSQPEQQEQS-KVVYGLF

TM1

hPS1	119	TEDTETVGQRALHS	SILNAA	IMISVIVVMTILLVVLKYRCYKVIHAWLI
Dr PS	108	REDTETVGQRALH	SMLNAI	IMISVIVVMTLLVVLKYRCYKVIQAWLF
Xl PS α	85	TEDTESVGQRAL	NSILNAT	IMISVIVVMTILLVVLKYRCYKVIHGWLI
hPS2	125	TEDTPSVGQRL	NSVNL	TLIMISVIVVMTIFLVVLKYRCYKFIHGWLI
Xl PS β	128	SEDTTSGERL	NSVNL	TLIMISVIVVMTIFLVVLKYRCYKFIHGWLI
Dm PS	141	HEQSPEPSVK	FWSALAN	SLILMSVVVMTFLLIVLKYRCYRIHGWLI
SEL-12	88	VRETDSIVE	KGLMSL	GNALVMLCVVLMVLLIVFYKYKFIHGWLI
HOP-1	50	HS-----YDTAD	SGTITL	YLGFLIITSLGVFCYQMKFYKAIKVYVL

TM2

hPS1	168	ISSLLLLLFFS	FIYLGEV	FKTYNVAVDYITVALLIWNFGVVMGMSIHWK	
Dr PS	157	FSNLLLLLFFS	IYLGEV	FKTYNVAMDYFTLALLIWNFGVVMGICIHWK	
Xl PS α	134	ISSLLLLLFFS	YIYLGEV	FKTYNVAVDYITLALLIWNFGVVMGICIHWK	
hPS2	174	MSSLMLLF	FTYIYLGEV	LKTYNVAMDYPTLLITVWNFGAVGMVCIHWK	
Xl PS β	177	LSSLMLLF	FTYIYLSEV	FKTYNTAMDYPTLFMVIWNFGAVGMICIHWK	
Dm PS	190	LSSFMLLF	FTYIYLE	ELLRAYNTAMDYPTALLIMWNFGVVMGMSIHWQ	
SEL-12	137	VSSFLLLF	FTTYVQ	EVLKSEFVSPSALLVLFGLGNVGVLMGMCIHWK	
HOP-1	93	ANSIGITL	VYSVFHF	FORIAEAQSI	PVSVPTFFFLIQFGGLGITCLHWK

TM3

TM4

hPS1	217	GPLRLQQAYL	LIMISAL	MALVFIKYLPEWTAWLILAVISVYDLVAVLCPK	
Dr PS	206	GPLRLQQAYL	LIMISAL	MALVFIKYLPEWTAWLILAAISVYDLLAVLCPK	
Xl PS α	183	GPLLQQAYL	LIMISAL	MALVFIKYLPEWTTWLILAVISVYDLVAVLSPK	
hPS2	223	GPLVLQQAYL	LIMISAL	MALVFIKYLPEWSAWVILGAVISVYDLVAVLCPK	
Xl PS β	226	GPLQLQQAYL	LIMISAL	MALVFIKYLPEWSAWVILGAVISVYDLLAVLCPK	
Dm PS	239	GPLRLQQGYL	I	FVAALMALVFIKYLPEWTAWAVLAAISTWDLIAVLSPR	
SEL-12	186	GPLRLQQGYL	I	TMSALMALVFIKYLPEWTVWFVLFVISWDLVAVLTPK	
HOP-1	142	SHRRLH	QFYLI	MLAGLTAIFILNILE	DWTVWMALTAISEWDIVAVLTPC

TM5

TM6

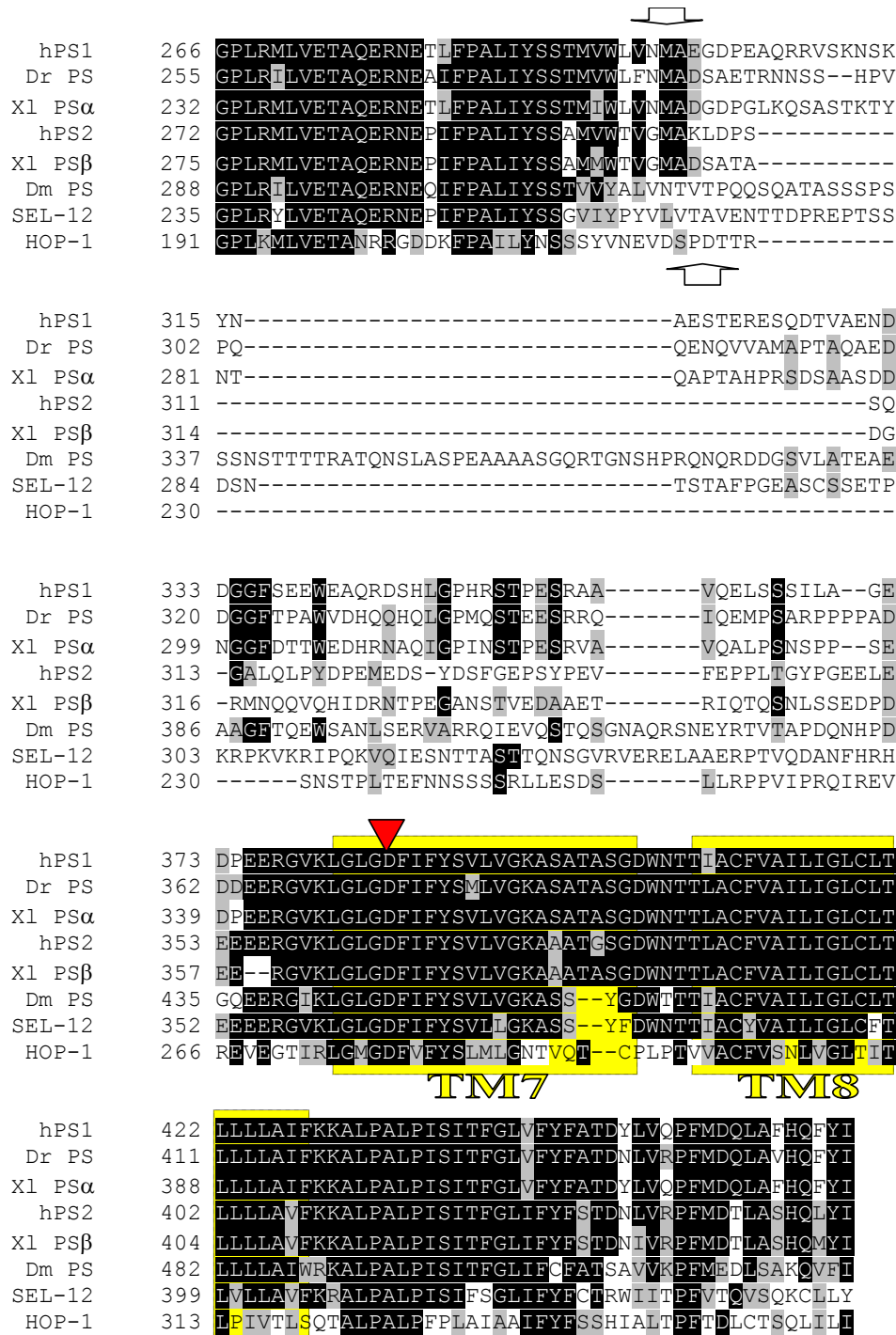


Figure 3: ClustalX alignment of the confirmed presenilin (PS) proteins from different organisms. The position of the invariant aspartate residues (red triangle) in the transmembrane domains (TM)6 and 7 are marked along with the sites of endoproteolysis (arrows) at the beginning of the large cytoplasmic loop. Identical residues are highlighted in black, similar residues in grey. [SEL-12 (accession number AF171064) and HOP-1 (AF021905); human PS1 (AH004968) and PS2 (NM012486); *Xenopus laevis* PS α (D84427) and PS β (D84428); *Drosophila melanogaster* PS (U78084); *Danio rerio* PS (AJ132931);]

second gene similar to presenilin 1 (PS1) was also responsible for a minor proportion of FAD cases and was called Presenilin 2 (PS2) (Table 1)(Price et al., 1998; Renbaum and Levy-Lahad, 1998). PS1 and PS2 encode highly conserved polytopic transmembrane proteins (Figure 3)(Hutton and Hardy, 1997). Similarly to APP, Presenilins are broadly expressed, but are predominantly present in neurons and, to a lesser extent, also in glia cells (Lee et al., 1996). Furthermore, like APP mutations, FAD mutations in PS1 and PS2 also increase the $A\beta_{42}/A\beta_{40}$ ratio by producing more $A\beta_{42}$ (Borchelt et al., 1996; Citron et al., 1997). The same effects were observed in transgenic mice expressing APP and FAD mutants of PS1 (Borchelt et al., 1997; Price et al., 2000). This indicates that the presenilins affect the γ -secretase processing of APP, suggesting that the presenilins are involved in the cleavage process. Even though more than 150 mutations in PS1 and PS2 have been identified in FAD patients, only missense mutations or small in frame deletions were found. This suggests that presenilins activity may be required for viability (Czech et al., 2000).

The Amyloid Hypothesis Model of Alzheimer's Disease progression

Although the FAD mutations found in APP, PS1 and PS2 account for only 30-50% of the autosomal dominant AD cases (Cruts et al., 1996), and these only represent a minor fraction of all AD cases, their value for our understanding of the disease progression is enormous. Furthermore, the disease phenotype in the majority of the FAD cases is indistinguishable from that of sporadic AD. Analysis of the amyloid plaques and of the effects of FAD mutations on APP processing have suggested that the β -amyloid peptide is one of the key players in AD. The model that summarises the pathogenic step leading to AD, with $A\beta$ aggregation as the initial pathogenic step, is widely known and accepted as the "Amyloid Cascade Hypothesis" (Hardy and Selkoe, 2002). According to this theory, increased production of $A\beta_{42}$, due to FAD mutations or increased gene dosage in the case of Down's syndrome, leads to a higher probability of $A\beta_{42}$ aggregation and to the nucleation of plaques (Figure 4).

Once an extracellular seed is formed, it works like a dump or sink for other proteins and for the large amounts of secreted $A\beta_{40}$ to aggregate also to it. This process, although it is considered to be nearly irreversible, is time-consuming, if not favoured by pathogenic predisposition. This may explain the late onset for sporadic AD.

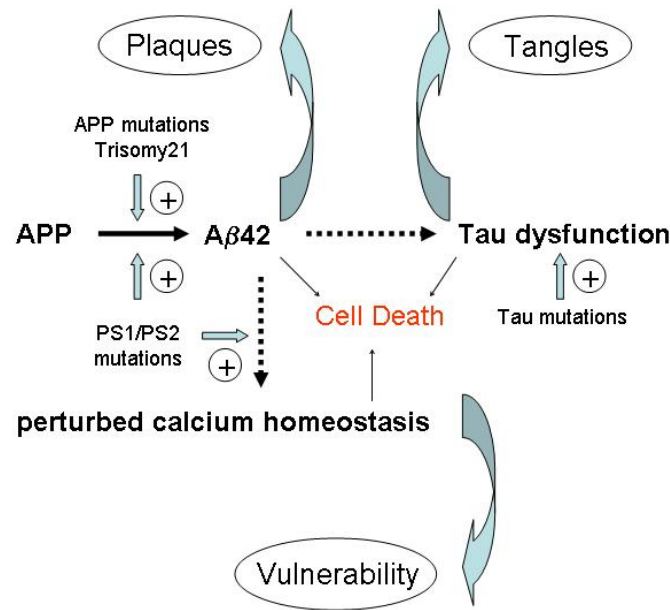


Figure 4: Representation of the widely accepted model of the development of Alzheimer's disease. The processes that have an enhancing effect on the disease progression are marked by arrows.

It is not the deposition of A β alone that causes AD, since A β also triggers a chain of events eventually resulting in the dysregulation and death of neuronal cells: Once a diffuse A β plaque has formed, microglial cells are activated in the vicinity of the plaque and initiate an inflammatory response by releasing cytokines (Selkoe, 2001). Subsequently, astrocytosis starts and, in this phase, large amounts of proteins are released, which are prone to accumulate in those plaques. Furthermore, the growing plaques and the increasing inflammatory response progressively lead to neuronal injury and dysfunction around the plaques. Moreover, there is evidence that already the A β protofibrils, which precede the amyloid plaque formation, are neurotoxic (Hartley et al., 1999; Lambert et al., 1998). Similarly, mice over-expressing APP exhibit functional alterations in the brains long before diffuse A β_{42} plaques are detectable (Hsia et al., 1999).

Therefore, aggregated A β_{42} already seems to be sufficient to disrupt neuronal metabolism and ionic homeostasis even without the appearance of plaques (Figure 4). It has been shown that the neuronal calcium homeostasis is strongly disturbed in AD (LaFerla, 2002; Mattson et al., 2001). Most notably, alterations in calcium signaling are detectable before extracellular A β pathology becomes visible (Guo et al., 1999; Larson et al., 1999; Leissring et al., 2000). This imbalance sensitises the cell and renders it vulnerable to oxidative injury, which increases with age. Therefore, A β deposition might affect cell ion homeostasis, which in turn increases the vulnerability of the cell to the toxic effects of A β resulting in a deadly cycle.

Besides A β 's effect on calcium homeostasis of the cell, it may also affect other cellular processes. A hallmark of the AD pathology in the brain is not only the appearance of amyloid plaques, but also the formation of neurofibrillary tangles within neurons. The fibrillar aggregates of hyperphosphorylated Tau protein are also thought to lead to cell injury and death. It is well established that the appearance of tangles follows the formation of amyloid plaques (Hardy et al., 1998). Therefore, it is likely that the cellular changes induced by the A β aggregates also disrupt the association of Tau with microtubules due to the hyperphosphorylation of the Tau protein and its subsequent aggregation (Figure 4). Evidence that A β deposition and Tau aggregation influence each other also comes from transgenic mice. Recently, it has been shown that mice over-expressing APP and a mutant form of the Tau protein exhibit a strongly increased neurofibrillary tangle pathology whereas the appearance of the A β deposits was unaffected (Lewis et al., 2001). Similarly, Tau mutant mice that have been injected with A β_{42} protofibrils directly into the hippocampus also show an increased tangle formation (Gotz et al., 2001). This further supports the view that A β deposition results in dysregulation of Tau function, which leads to intraneuronal tangle formation (Figure 4).

Eventually, these events lead to the death of neurons, which could be detected in AD, culminating in the clinical behavioural abnormalities and ultimately the death of the patient. Therefore, AD is clearly a multi-factorial disease rather than a monocausal disease, since all pathogenic events potentiate and affect each other. However, the initial lesion that triggers most of the subsequent events is most likely to be caused by A β_{42} deposition. Therefore, the biggest risk factor for AD is increased age and the concomitant decline in cellular integrity with age. Thus, the fight against Alzheimer's disease is ultimately connected to a fight against ageing, which is even more complex than the processes outlined above.

Biological functions of presenilins

Despite of our knowledge about the effects of pathogenic mutations in PS1 and PS2 on A β processing, the biological function of presenilins is less well understood. Presenilins are polytopic transmembrane proteins. Hydropathy analysis reveals the existence of up to ten hydrophobic clusters that could serve as transmembrane domains. *In vivo* topology studies suggest the existence of eight transmembrane domains (Figure 5) (Doan et al., 1996; Li and Greenwald, 1996; Li and Greenwald, 1998) although other topologies are discussed

(Lehmann et al., 1997; Nakai et al., 1999). Presenilins contain no obvious signal peptide and the N- and C-termini are presumably located in the cytoplasm (De Strooper et al., 1997; Doan et al., 1996; Li and Greenwald, 1996) (Figure 5).

Early studies based on over-expression have localized the presenilins mainly in the endoplasmic reticulum (ER) and Golgi subcellular compartments (De Strooper et al., 1997; Kovacs et al., 1996; Walter et al., 1996). Since these overexpression studies may overinterpret the accumulation of unfolded presenilin proteins in the ER/Golgi system, localization of the endogenous presenilins was necessary. Subcellular fractionation experiments and confocal microscopy confirmed that, in neurons, presenilins are indeed mainly found in the ER/Golgi system and in the nuclear membrane (Annaert et al., 1999; Kim et al., 2000; Li et al., 1997).

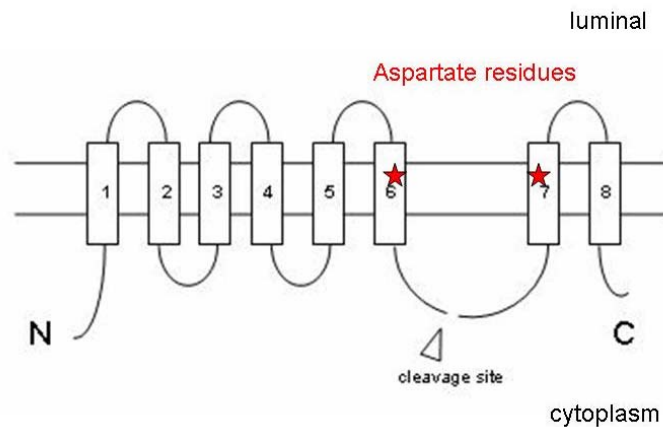


Figure 5: Schematic representation of the topology of the presenilin protein. The amino (N) and carboxy (C) terminus reside in the cytoplasm. The large cytoplasmic loop between the transmembrane domains (TM) 6 and 7 is cleaved endoproteolytically. The position of the invariant aspartate residues in TM6 and 7 are marked by asterisks.

However, recent experiments also suggest that presenilins are localized to the plasma membrane presented at the cell surface of human cells (Kaether et al., 2002; Ray et al., 1999) and *Drosophila* (Nowotny et al., 2000). Furthermore, endogenous presenilins were also detected in early endosomes (Lah and Levey, 2000). The abundance of presenilins in the secretory and endocytic pathways may reflect its involvement in the trafficking, maturation and processing of other proteins that enter the secretory pathway and that are delivered to the plasma membrane.

Presenilins are synthesised as a precursor which is endoproteolytically cleaved and forms a stable heterodimer (Figure 5) (Podlisny et al., 1997; Thinakaran et al., 1996). Endoproteolysis is rapid and, as a result, *in vivo* only very little holoprotein can be detected. This endoproteolysis of presenilins has been shown to be conserved between humans,

Drosophila (Nowotny et al., 2000) and *C. elegans* (Li and Greenwald, 1996; Okochi et al., 2000). Endoproteolytic processing greatly enhances the stability of the presenilins. Mutations that prevent the endoproteolysis result in very unstable proteins which are rapidly degraded (Moriyama et al., 2000; Wolfe et al., 1999). Furthermore, the amino terminal- and carboxy terminal- presenilin fragments have been shown to form a functional protein when expressed separately in *C. elegans* (Levitan et al., 2001a). In cells only the N- and C-terminal fragments can be detected with a half life of over 24 hours (Dewji et al., 1997; Ratovitski et al., 1997; Weihl et al., 1999; Zhang et al., 1998). Accordingly, it is difficult to overexpress presenilins in cell culture (Steiner et al., 1998). When presenilins are over-expressed in transfected cells, or in PS1 transgenic mice, only little full length holoprotein can be detected (Czech et al., 2000; Thinakaran et al., 1996). This suggests that the endoproteolysis of presenilins is a step during its maturation (Thinakaran, 2001). The presenilin cleavage products remain closely associated in high molecular weight (HMW) complexes (Capell et al., 1998; Edbauer et al., 2002; Li et al., 2000a; Seeger et al., 1997; Yu et al., 1998). Therefore, it is likely that the proteolytic processing of presenilins is a sign of their incorporation into the HMW complexes. Once assembled the complex components are stabilized. The fact that excess presenilins are degraded rapidly, suggests that other complex components are limiting (Thinakaran, 2001).

Presenilin containing complexes exhibit proteolytic activity and have been shown to be required for APP cleavage at the γ -secretase site (Figure 6) (De Strooper et al., 1998). A prerequisite for this so called γ -secretase cleavage event is the preceding proteolytic processing at either the α - or β -secretase site of APP (Figure 6).

Elimination of PS1 in mice leads to a strong reduction in the production of both $A\beta_{40}$ and $A\beta_{42}$ (De Strooper et al., 1998). On the other hand, deletion of both PS1 and PS2 completely abolishes the production of $A\beta$ (Herreman et al., 2000). The blockage of the γ -secretase leads to an accumulation of α - or β -secretase cleaved C-terminal stubs of APP (Figure 6). Genetic and biochemical studies in *C. elegans* and *Drosophila* revealed that presenilins are also involved in the proteolytic processing of other transmembrane proteins, most notably the LIN-12/Notch receptors (Fortini, 2001; Levitan and Greenwald, 1995; Struhl and Greenwald, 1999; Struhl and Greenwald, 2001; Ye et al., 1999).

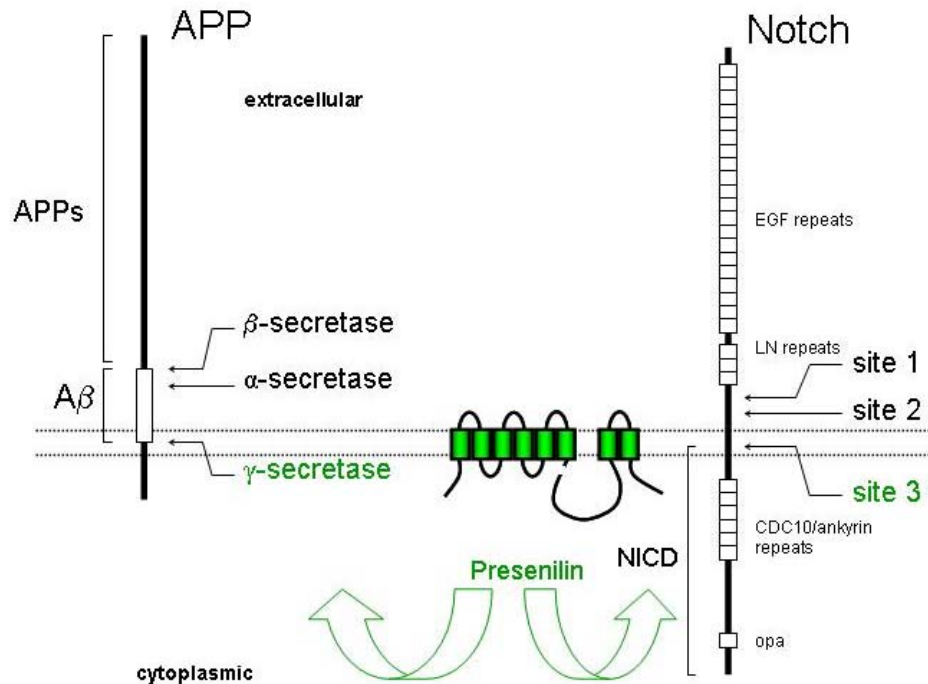


Figure 6: Comparison of the proteolytic processing events in the amyloid precursor protein (APP) and the Notch receptor. The sites corresponding to the different cleavage events are marked by arrows. Functional domains are annotated. The presenilin molecule is shown which is required for γ -secretase and site 3 cleavage releasing the β -amyloid peptide ($A\beta$) and the Notch intracellular domain (NICD), respectively.

In *C. elegans* it was shown that mutations in *sel-12*, one of the two somatic presenilins, lead to a reduction of LIN-12/Notch signaling (Levitan and Greenwald, 1995). Furthermore, additional removal of the second presenilin, *hop-1*, completely abolishes signaling by the two *C. elegans* Notch receptors, LIN-12 and GLP-1 (Li and Greenwald, 1997; Westlund et al., 1999). Null mutations in the single *Drosophila* presenilin lead to Notch like phenotypes and lethality (Struhl and Greenwald, 1999; Ye et al., 1999). The studies were supported by the finding that PS1 deficient mammalian cells show a dramatic decrease in the γ -secretase like site 3 cleavage of the Notch receptor (De Strooper et al., 1999). The dependence of Notch signaling on presenilin activity is further demonstrated by the fact that mice lacking PS1 and PS2 also show a Notch like phenotype. Presenilin knock-out mice display abnormal somitogenesis and axial skeletal development with shortened body length, as well as cerebral haemorrhages (Shen et al., 1997; Wong et al., 1997). PS1^{-/-} mice die at birth and exhibit an abnormal embryonic neurodevelopment in the forebrain characterised by a premature loss of neuronal precursors (Shen et al., 1997). The early embryonic lethality of PS1^{-/-}PS2^{-/-} mice (Herreman et al., 1999) is similar to that seen in mice that either carry a deletion of the Notch1 locus (Conlon et al., 1995; Swiatek et al., 1994), or express a site 2 cleavage defective Notch1 receptor (Huppert et al., 2000).

The proteolytic processing of Notch resembles, in many aspects, the processing of APP (Kopan and Goate, 2000; Sastre et al., 2001). Notch is cleaved by a furin-type protease at the site 1 while it passages through the Golgi system (Figure 6). The resulting two fragments are thought to be either covalently held together by a disulfide bond or by calcium ions (Rand et al, 2001). This heterodimeric Notch receptor is now activated and competent to be bound by its ligand when presented at the cell surface. The binding of the ligand stimulates a second cleavage of the Notch receptor the site 2 (Figure 6) by a TACE type or Kuzbanian type protease. This processing step liberates the membrane bound Notch C-terminus which then becomes a substrate for a presenilin dependent γ -secretase. Subsequently the Notch carboxy- terminal fragment is cleaved within its transmembrane domain at site 3 releasing the Notch intracellular domain (NICD). The NICD translocates to the nucleus where it interacts with other proteins to form an transcriptional activating complex (Mumm and Kopan, 2000; Struhl and Adachi, 1998). The presenilin dependent site 3 cleavage and release of the NICD have been shown to be absolutely required for the activation of genes downstream of Notch (Struhl and Adachi, 2000; Struhl and Greenwald, 1999; Struhl and Greenwald, 2001). This site 3 cleavage of the Notch receptor is analogous to the γ -secretase cleavage of APP and strictly dependent on presenilin activity (De Strooper et al., 1999; Kopan and Goate, 2000; Sastre et al., 2001).

Do presenilins belong to a novel type of transmembrane proteases?

It is well established that presenilin activity is absolutely required for the γ -secretase activity that cleaves the Notch receptors and APP (De Strooper et al., 1999; De Strooper et al., 1998). However, no direct evidence has been presented that presenilins may be involved directly in proteolysis. Therefore, it was very informative that γ -secretase inhibitors that mimic the transition state of the transmembrane domain cleavage are able to specifically target crosslinking reagents to the presenilins (Beher et al., 2001; Evin et al., 2001; Li et al., 2000b; Shearman et al., 2000). It was shown that both of the endoproteolytically derived N- and C-terminal fragments of the presenilins could be crosslinked, providing further evidence that these are the active subunits of presenilins. Further analysis of the presenilins revealed that they contain two invariant aspartate residues in the transmembrane domains (TM) 6 and 7

(Figure 3). These aspartates were thought to be the active site of unusual aspartyl protease (reviewed in Steiner and Haass, 2002).

Mutagenesis of either of the aspartates in TM6 and TM7 results in a loss of γ -secretase activity (Berezovska et al., 2000; Cervantes et al., 2001; Wolfe et al., 1999). This is accompanied by the accumulation of the membrane bound and uncleaved C-termini of APP and Notch receptors. Furthermore, loss of γ -secretase activity by mutations in one of the conserved aspartate residues also inhibits the endoproteolysis of the presenilin molecules within the large cytoplasmic loop (Figure 5)(Cervantes et al., 2001). Additionally, presenilin mutants that contain a mutation in one of the aspartate residues also behave like dominant negative molecules, interfering with the function of wild type presenilins (Wolfe et al., 1999). These data suggest that presenilins may be the long elusive γ -secretase and are proteolytically active by themselves. This would also explain why the aspartyl protease inhibitors specifically bind to presenilins and why some of the identified γ -secretase inhibitors also inhibit the autoproteolysis of the presenilin molecules.

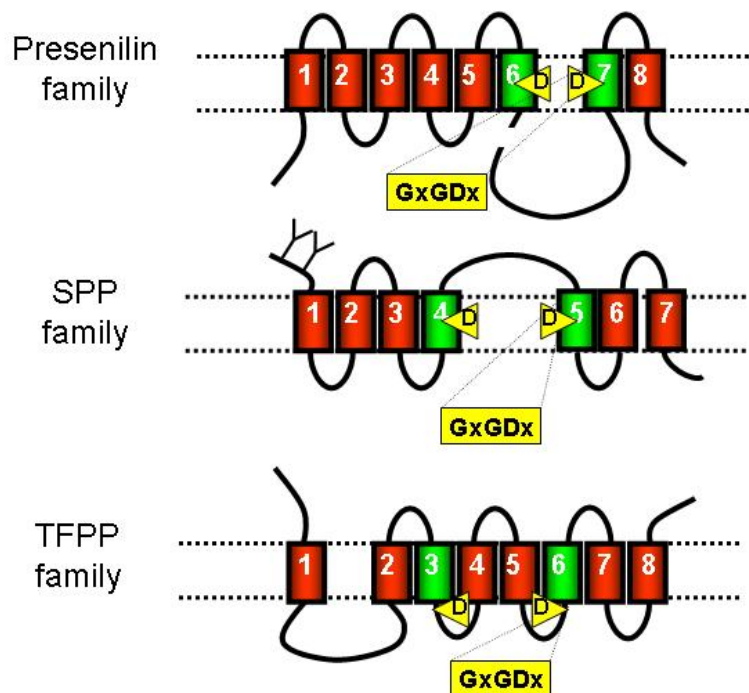


Figure 7: Presenilins belong to a family of polytopic aspartyl proteases. The common consensus motive GxGDx surrounding one of the active site aspartates (yellow triangles) is shown. TFPP are type 4 prepilin peptidases and SPP are signal peptide peptidases.

However, although it is very tempting to speculate that presenilin may resemble aspartyl proteases they do not show similarity to classical aspartyl proteases which contain a D(T/S)G(T/S) signature motif at their active center. Instead, presenilins do contain a highly

conserved GxGDx motif (x are variable amino acids) in TM7 in which one of the conserved aspartates is located (Figure 3). Database searches revealed that the same motif is also present in the active site of bacterial TFFPs (type 4 prepilin peptidases) (Steiner et al., 2000). These bacterial aspartyl proteases have been shown to remove the leader peptides of type 4 prepilins (Darzins and Russell, 1997; Lory and Strom, 1997). Therefore, the GxGDx motive may represent a new signature motif for a novel family of polytopic transmembrane proteases (Figure 7)(LaPointe and Taylor, 2000; Steiner et al., 2000). This notion has been supported by the recent finding that signal peptide peptidases (SPP) that remove signal peptides from the ER membrane after they have been cleaved off the secreted protein also share the same GxGDx motive (Weihofen et al., 2002). Furthermore, SPP proteases are also polytopic transmembrane proteins with the active site aspartates in their transmembrane domains (Figure 7). They also cleave their substrate within the transmembrane domain (Lemberg and Martoglio, 2002). In contrast to the presenilins, the SPP proteases show catalytic activity when isolated without binding partners.

Therefore, even though presenilins, TFPP and SPP proteases share only minimal sequence similarity and no substrate conservation, they may all share a similar mode of action. They are all embedded within the membrane and cleave their substrates within, or very close to, the membrane, although their topology and the position of the active site aspartate residues within the molecules vary (Figure 7). However, it is likely that during evolution a common mechanism has been adapted to the different needs of substrates and biological functions.

The Presenilin complex

Although there is growing evidence that the presenilins might be the active protease for the intramembrane cleavage, they have no detectable enzymatic activity on their own. Presenilins are only active as part of high molecular weight (HMW) complexes that control the cleavage of transmembrane domains (Capell et al., 1998; Edbauer et al., 2002; Li et al., 2000a; Seeger et al., 1997; Yu et al., 1998). It is obvious that such a rather non-sequence specific proteolytic activity has to be tightly regulated. It has been demonstrated that the cell surface display of the proteolytically active complex is controlled at the level of complex assembly and trafficking. All presenilin complex components are necessary for assembly and trafficking

(Chung and Struhl, 2001; Edbauer et al., 2002; Francis et al., 2002; Goutte et al., 2002; Steiner et al., 2002).

Although it has long been known that presenilins are integral components of high molecular weight (HMW) complexes (Capell et al., 1998; Seeger et al., 1997; Yu et al., 1998), the biochemical purification of the different additional complex components proved to be rather difficult. Again, the use of genetic screens in *C. elegans* and *Drosophila* has helped to identify new presenilin complex components which may resemble the core complex required for activity. Those screens were based on the assumption that the complex components that are required for its proteolytic activity should give the same phenotype as the elimination of presenilins or the different LIN-12/Notch receptors. Indeed, these screens uncovered new members of the presenilin complex: APH-1, APH-2/nicastrin, and PEN-2 (Chung and Struhl, 2001; Francis et al., 2002; Goutte et al., 2000; Goutte et al., 2002; Hu et al., 2002; Lopez-Schier and St Johnston, 2002).

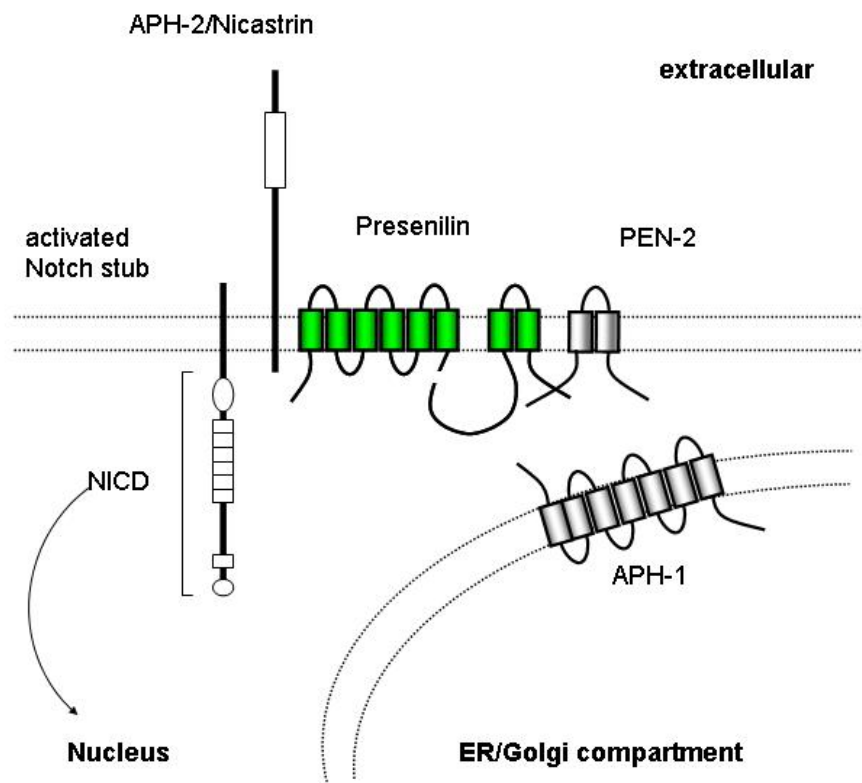


Figure 8: Schematic representation of the known presenilin complex components. APH-2/nicastrin and PEN-2 are present together with presenilins in the high molecular weight (HMW) complex. APH-1 might also be present in this complex at the plasma membrane. The presenilin complex cleaves pre-cleaved type I transmembrane domain proteins within their transmembrane domain, releasing them out off/from the membrane. In the case of the activated (site 2 cleaved) Notch receptor, the Notch intracellular domain (NICD) is released and translocates to the nucleus where it activates transcription of target genes.

APH-2/nicastrin

In a screen for mutants with a *glp-1* like phenotype, APH-2 was discovered and it was subsequently demonstrated to act in the same pathway as the presenilins (Goutte et al., 2000; Levitan et al., 2001b). At about the same time, a homologous type I transmembrane protein was isolated in the co-immunoprecipitates of presenilins from human cells and subsequently called APH-2/nicastrin (Yu et al., 2000). Furthermore, APH-2/nicastrin was also co-purified with presenilins using inhibitors directed against the active site of the γ -secretase (Esler et al., 2002) which specifically bind to presenilins (Esler et al., 2000). APH-2/nicastrin contains a large extracellular domain, which is highly glycosylated during the transport through the ER/Golgi system (Arawaka et al., 2002; Kimberly et al., 2002; Tomita et al., 2002; Yang et al., 2002). Except for the transmembrane domain, there are no other clearly recognisable domains present and the sequence conservation between the different species is very low (Yu et al., 2000).

It was shown that APH-2/nicastrin binds the membrane-tethered Notch receptor after site 2 cleavage (Chen et al., 2001). Furthermore, APH-2/nicastrin has been proven to be an essential component of the γ -secretase complex and is necessary for the intramembraneous cleavage (site 3) of the activated Notch receptors (Figure 7) (Chung and Struhl, 2001; Hu et al., 2002; Lopez-Schier and St Johnston, 2002). Consistently, mutations in APH-2/nicastrin in mice have also been shown to negatively influence the presenilin dependent site 3 cleavage of the Notch receptor (Rozmahel et al., 2002). Reducing the protein levels of APH-2/nicastrin in mammalian cells by RNA interference (RNAi) not only results in a loss of γ -secretase activity, but also in a destabilization of the presenilin molecules (Edbauer et al., 2002). In addition, the absence of presenilins also destabilizes APH-2/nicastrin to some extent and prevents its maturation, as indicated by glycosylation (Edbauer et al., 2002; Tomita et al., 2002). This suggests that presenilins and APH-2/nicastrin stabilize each other by complex formation and that the concentrations of the binding partner is the limiting factor during formation of the HMW complex (Tomita et al., 2002).

The lack of APH-2/nicastrin maturation and transport in the absence of presenilins also suggests that cell surface display of the HMW complexes is tightly controlled (Kimberly et al., 2002; Kopan and Goate, 2002). Therefore, a quality control mechanism seems to exist that assesses the functionality of the presenilin complexes, prior to export from the ER compartment. It is likely that the endoproteolysis, and thus the stabilization of the presenilins after their incorporation into the complexes, might serve as one of the check points. Similarly,

presenilins might also affect the cell surface transport of some its substrates (Leem et al., 2002).

APH-1 and PEN-2

In addition to APH-2/nicastrin, other presenilin complex components have been isolated in similar genetic screens for the absence of Notch signaling in *C. elegans* (Goutte, 2002). APH-1 and PEN-2 (presenilin enhancer) are also strictly required for γ -secretase activity and site 3 cleavage of the Notch receptors (Francis et al., 2002; Goutte et al., 2002). APH-1 and PEN-2 are conserved multipass transmembrane proteins. APH1 is predicted to span the membrane seven times (Figure 8) (Goutte et al., 2002), whereas PEN-2 contains two predicted transmembrane domains (Francis et al., 2002). The orientation within the membrane for PEN-2 appears to be similar to that of the presenilins, with the N- and C-terminus facing towards the cytoplasm (Francis et al., 2002). The APH-1 C-terminus is luminal, whereas the C-terminus may reside inside the cytosol (Francis et al., 2002; Goutte et al., 2002).

PEN-2 and APH-1 have also been reported to be integral components of the HMW presenilin complexes (Steiner et al., 2002) together with APH-2/nicastrin (Figure 8). However, for APH-1 no cell surface presentation has been demonstrated so far, although in mammalian cells APH-1 interacts with presenilins and APH-2/nicastrin and is required for proteolytic activity (Lee et al., 2002). Therefore, it is also likely that APH-1 may associate with presenilin complexes during their assembly and/or transport through the ER/Golgi system (Figure 8). APH-1 might be an assembly factor controlling the functionality of the presenilin complexes. Consistent with this view, in *aph-1* mutants APH-2/nicastrin is not transported to the cell surface any more, but stays trapped within the ER system (Goutte et al., 2002). The APH-2/nicastrin localisation is similarly affected in *sel-12; hop-1* double mutants lacking all presenilin activity in *C. elegans* (Goutte et al., 2002). Therefore, a lack of transport to the cell surface might just reflect the lack of functionality of the assembled complex which is then excluded from further export. Again, the fact that if one complex component is missing the stability of the other components are affected, may reflect an additional mode of regulation of presenilin complexes (Edbauer et al., 2002; Steiner et al., 2002).

The notion that all complex components act at the same step during Notch processing is further supported by the observation that in *C. elegans* all of the presumptive complex

components are able to block the signaling induced by an hyperactive LIN-12/Notch receptor but are not able to block the signaling induced by the expression of a constitutively active NICD fragment (Francis et al., 2002; Levitan and Greenwald, 1995; Levitan et al., 2001b). In addition, all presenilin complex components are broadly expressed in nearly all somatic cells of *C. elegans*, making it likely that these complexes are general and integral components of all cells (Baumeister et al., 1997; Francis et al., 2002; Goutte et al., 2000; Goutte et al., 2002; Levitan and Greenwald, 1995). This may also indicate that this proteolytically active complex is required more generally for basic cell function, and may be necessary to clear the plasma membrane from transmembrane stubs.

Notch signaling in *C. elegans*

If presenilins play a rather global role in clearing the plasma membrane from transmembrane stubs, this would explain why there seems to be no sequence specificity. However, some signaling pathway may have recruited these unspecific proteases for their signaling purposes to liberate active molecules from the membrane. One of the signaling pathways that has been shown to use presenilin activity is the Notch pathway. In Notch signaling, ligand binding leads to site 2 cleavage of the Notch receptor (Figure 6) to generate a membrane bound stub with a short extracellular domain. This stub serves as a substrate for presenilins and is subsequently cleaved at its site 3 (Figure 6), a cleavage that releases the Notch intracellular domain (NICD) from the plasma membrane. The liberated NICD then translocates to the nucleus to activate Notch target genes. The site 3 cleavage and the nuclear access of the NICD have been shown to be dependent on presenilin activity.

In *C. elegans* there are two Notch type receptors, LIN-12 and GLP-1. Both receptors are found within an interval of 0.02 centi Morgan (cM) on chromosome III, which suggests that they have arisen from a recent gene duplication (Rudel and Kimble, 2002). Both *C. elegans* Notch type receptors are similar in their domain structure and share 48% sequence identity over the entire length of the molecules (Rudel and Kimble, 2001; Yochem and Greenwald, 1989). Genetic data suggest that *lin-12* and *glp-1* are largely co-expressed and are partially redundant, although each receptor has acquired more specialised and separate functions during development (Austin and Kimble, 1989; Fitzgerald et al., 1993; Mango et al., 1991; Sundaram and Greenwald, 1993b). *glp-1* is required very early in development at the 4 and 12 cell stage of the *C. elegans* embryo. In the adult animal, *glp-1* is also needed for the induction of germline proliferation. In contrast, *lin-12* is involved in postembryonic cell fate decisions in the somatic gonad and in the sex muscle lineage. Furthermore, it is also required for the patterning of the hermaphrodite vulva.

Blastomere specification in the early embryo

As zygotic transcription starts at about the 12 cell stage, *glp-1* mRNA is supplied as a maternal component to the embryo (Moskowitz and Rothman, 1996). During the first few divisions GLP-1 signaling is used to induce different cell fates in formerly equal cells by cell-

cell interactions. At the 4 cell stage, the P2 blastomere induces the posterior AB blastomere (ABp) to adopt a fate distinct from its anterior sibling ABa (Bowerman et al., 1992; Hutter and Schnabel, 1994; Hutter and Schnabel, 1995; Mango et al., 1994; Mello et al., 1994; Moskowitz et al., 1994). This is achieved by restricting the cell-cell contacts of P2 to the ABp blastomere (Figure 9A). Although both the ABa and ABp blastomere expose the GLP-1/Notch-receptor at their cell surface, only ABp contacts the P2 blastomere, which selectively expresses APX-1, a GLP-1/Notch-receptor ligand (Mango et al., 1994; Mello et al., 1994; Mickey et al., 1996). Therefore, GLP-1/Notch-signaling is activated only in the ABp blastomere. This induces a cell fate in ABp that is different from that of ABa.

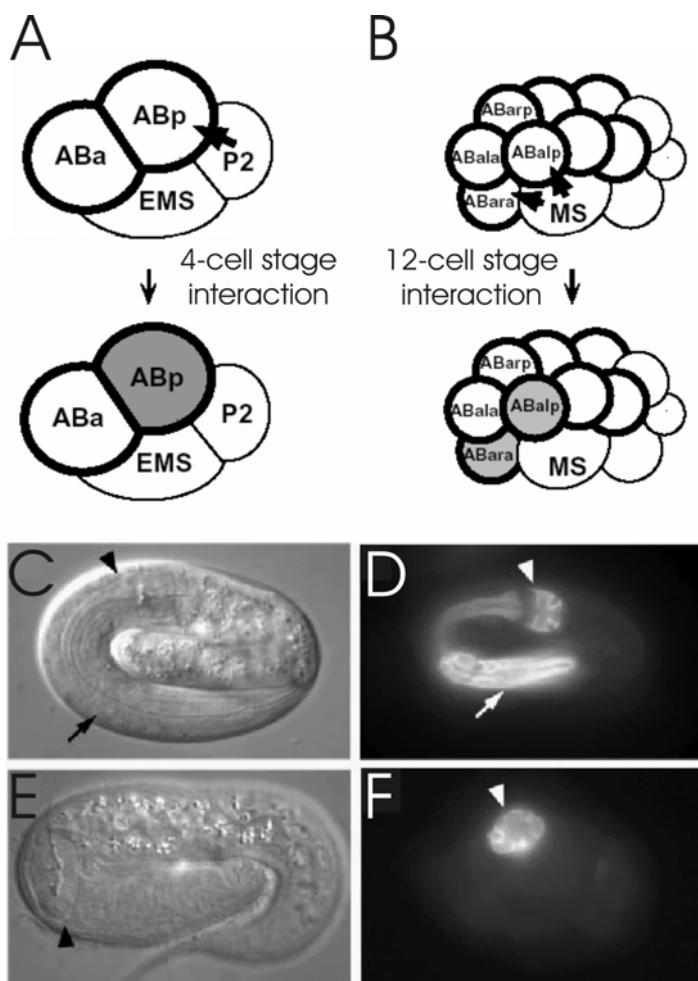


Figure 9: GLP-1 mediated blastomere specifications in the early embryo. (A) At the 4-cell stage the ABp blastomere receives GLP-1 signaling from the P2 blastomere and (B) at the 12-cell stage the ABa descendants ABalp and ABara are specified through GLP-1 signaling by interacting with the MS cell. (C) DIC view of a living wild type embryo; the arrow indicates the anterior half of the pharynx and the arrowhead the posterior half. (D) Immuno-stained pharyngeal cell in wild type embryo. (E) DIC view of *aph-1* mutant embryo in which GLP-1 signaling is impaired and (F) immunostaining of pharyngeal cells in an *aph-1* embryo reveals that the anterior pharynx is missing while the posterior pharynx is present (arrowhead) (Goutte et al, 2001).

A similar process occurs at the 12 cell stage, where the MS blastomere induces two descendants of ABa, ABalp, and ABara to generate pharyngeal tissue (Figure 9B)(Priess, 1994; Priess et al., 1987). This signaling event is also executed through GLP-1 signaling. All of the descendants of ABa still contain the cell surface exposed GLP-1 receptor, but only ABalp and ABara contact the MS blastomere (Figure 9B). MS provides the GLP-1/Notch-

receptor ligand necessary to induce GLP-1 signaling in ABalp and ABara. However, the identity of the ligand present on the MS cell is not known, but it is not APX-1 (Evans et al., 1994; Priess et al., 1987). Since the tissue that gives rise to the anterior part of the pharynx is generated from ABalp and ABara descendants, the anterior pharynx is missing in mutants defective in these early *glp-1* dependent signaling events (Figure 9E and F).

Induction of germline mitosis

The second developmental step that is dependent on GLP-1 signaling is the induction of mitosis in the germline of *C. elegans*. A somatic gonad cell, called the distal tip cell (DTC), signals the neighbouring germline to divide mitotically (Figure 10) (Kimble and White, 1981). This proliferative signal induces growth of the germline during larval development and maintains a population of germline stem cells in the adult. Furthermore, the localisation of the distal tip cell at the tip of the germline also establishes the polarity of the germline tissue (Figure 10).

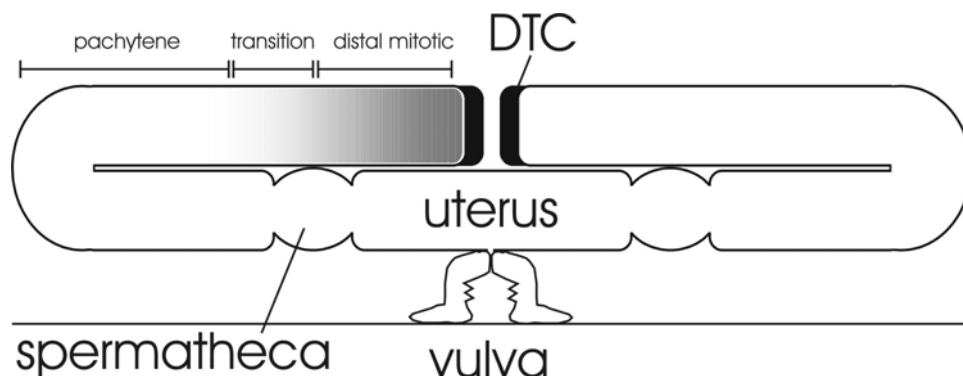


Figure 10: Gonad structure of an adult hermaphrodite of *C. elegans*. The distal tip cells (DTC) lie at the tips of the gonad arms. Adjacent to the DTCs are the distal mitotic regions of the gonad followed by a transition zone and the meiotic zone (pachytene). The GLP-1 protein (shaded in grey) is spatially restricted to the distal mitotic zone of the two gonad arms.

Signaling by the distal tip cell is required continually during larval development and adulthood for growth of the germline (Lambie, 2002). In its absence, germline nuclei enter meiosis and complete gametogenesis. The inductive signal from the distal tip cell is the expression of LAG-2, a Notch receptor ligand (Henderson et al., 1994; Lambie and Kimble, 1991; Tax et al., 1994). This signal is received by the germ nuclei through the GLP-1/Notch-receptor (Austin and Kimble, 1987; Christensen et al., 1996; Crittenden et al., 1994; Lambie and Kimble, 1991; Yochem and Greenwald, 1989). GLP-1 activation therefore promotes proliferation and blocks the entry into the meiotic pathway. By localizing the source of the

ligand LAG-2 to the distal end of the gonad, GLP-1 activation is spatially restricted (Henderson et al., 1994). In mutants carrying a constitutively active GLP-1 receptor the germ nuclei never exit mitosis and the animals therefore display a tumorous germline (Berry et al., 1997).

The AC/VU decision in the somatic gonad

Although there are functional redundancies between *glp-1* and *lin-12* in most of their signaling events, *lin-12* may have acquired a more specialised function during postembryonic development in *C. elegans*. The somatic gonad of *C. elegans* not only gives rise to the germline, but also to tissue that forms the uterus and induces the development of the vulva (Sulston and Horvitz, 1977). Two cells of the somatic gonad, Z1.ppp and Z4.aaa, that have an initially equivalent developmental potential, interact with another to select two opposite fates in each of the cells. One cell will become the anchor cell (AC) while the other will become a ventral uterine cell (VU) (Greenwald, 1998; Kimble, 1981). A rather stochastic event determines which of the cells will acquire which of the two fates (Figure 11). At the beginning of the L2 larval stage Z1.ppp and Z4.aaa are in close contact to each other. Both cells initially express the *lin-12*/Notch-receptor and *lag-2*, which encodes a membrane anchored ligand for the LIN-12/Notch-receptor (Figure 11A) (Wilkinson et al., 1994). The coexpression of *lin-12* and *lag-2* is unstable and the expression levels of receptor and ligand may differ slightly between the two adjacent cells. Therefore, one of the cells will receive a little bit more LIN-12 signaling than the other. This stochastically resolves in a situation in that *lag-2* expression becomes restricted either to Z1.ppp or Z4.aaa (Wilkinson et al., 1994). Since the expression of *lin-12* and *lag-2* are controlled reciprocally by transcriptional control through a feedback loop, this leads to a favoured down regulation of *lag-2* in the cell with more LIN-12 signaling and upregulation of *lag-2* in its neighbour (Figure 11B) (Wilkinson et al., 1994). As both cells are in contact they will negatively influence each other until they reach a stable state.

The cell to which *lin-12* expression becomes restricted will execute the VU fate, whereas the cell to which *lag-2* expression becomes restricted will adopt the AC fate (Figure 11). The contact between the AC/VU precursor cells is therefore essential, since in mutants where cell movement is affected, so that Z1.ppp and Z4.aaa fail to meet, both cells adopt the

AC fate as a default (Hedgecock et al., 1990). Similarly, in *lin-12* loss of function mutants 2ACs are generated (Greenwald et al., 1983).

However, the opposite cell fate transformation is observed in *lin-12* gain-of-function mutants. In mutants which produce an constantly active LIN-12/Notch receptor that does not require ligand binding both cells adopt the VU fate (Greenwald and Seydoux, 1990).

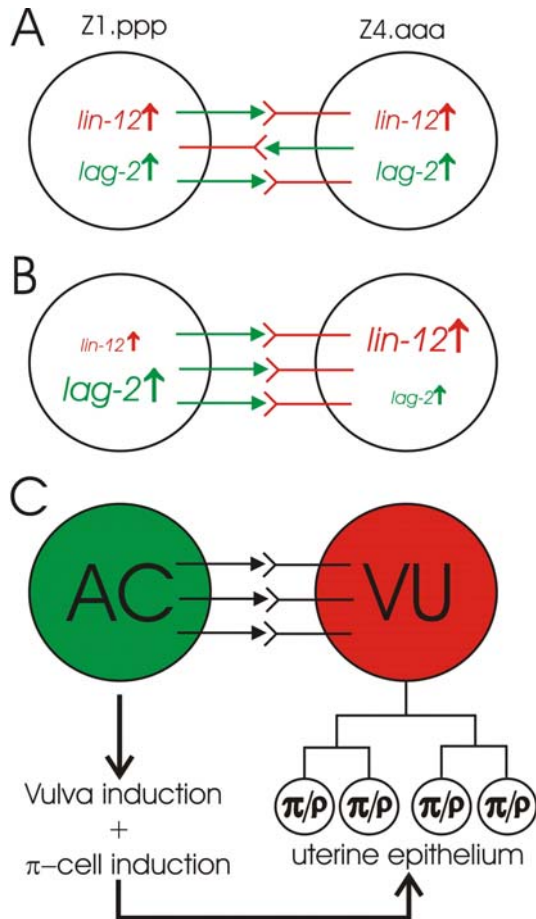


Figure 11: Diagram of the AC/VU cell fate decision. (A) Two cells of the somatic gonad, Z1.ppp and Z4.aaa, with the same developmental potential initially express both *lin-12* and *lag-2*. However the expression levels are slightly different. (B) Through the action of a feedback mechanism those initial differences are amplified and stabilised. (C) The cell that acquires strong *lag-2* expression becomes the anchor cell (AC) while the cell that expresses *lin-12* adopts the ventral uterine (VU) fate. The AC induces vulva pattern formation and π -cells while the VU gives rise to the uterine epithelium that connects vulva and uterus.

In wild type hermaphrodites, the cell that adopts the VU fate divides further to give rise to cells of the ventral uterine epithelium (Figure 11C) that connects the uterus and the vulva (Kimble, 1981; Newman and Sternberg, 1996). In contrast, the AC already has adopted its terminally differentiated stage and remains without any further division until it fuses to the uterine epithelium (Newman et al., 1996). Before its fusion the AC plays a key role both in the induction of vulva development and in the induction of a specialized set of the VU descendants that are necessary for the formation of a proper vulva-uterine connection (Figure 11C) (Greenwald et al., 1983; Newman et al., 1995).

Induction of vulva precursor cell fate patterning

During the L1 larval stage a set of hypodermal cells, P1.p to P12.p, are competent to adopt different cell fates (Figure 12). The so called vulval equivalence group, P3.p to P8.p, are able to generate the vulva. They are therefore also called vulva precursor cells (VPCs) (Greenwald, 1998; Kornfeld, 1997). The VPCs can adopt three different cell fates known as the 1°, 2°, and 3° cell fate. All VPCs are equally competent to adopt all of the possible vulval fates. The specific fate that they execute is dependent on an inductive signal from the anchor cell (AC). In wild type hermaphrodites only three of the VPCs, P5.p, P6.p and P7.p, receive an inductive signal from the AC and generate the cells that form the vulva (Figure 12). The other VPCs that are not induced receive an inhibitory signal from the hypodermis and fuse to the hypodermal syncytium (the 3° cell fate, Figure 12)(Herman and Hedgecock, 1990). The three VPCs that are induced lie beneath the somatic gonad with P6.p being centred under the AC (Figure 12). The anchor cell (AC) secretes LIN-3, a member of the EGF family of growth factors (Hill and Sternberg, 1992). This inductive signal is primarily sensed by the VPCs that are closest to the AC through the presence of the EGF-receptor tyrosine kinase *let-23* on their cell surface (Aroian et al., 1990; Ferguson and Horvitz, 1985). Thus, P6.p which is closest to the AC receives the strongest induction by the AC and is primed to adopt the so called 1° fate, while its neighbours P5.p and P7.p receive less inductive signal and are primed to adopt the 2° fate (Figure 12) (Sternberg and Horvitz, 1986; Sulston and White, 1980). This predisposition to acquire a specific cell fate is further stabilised through specific lateral signaling of the neighbouring VPCs. This lateral signaling event, which also involves LIN-12/Notch-signaling, is known as lateral inhibition (Figure 12)(Sternberg, 1988). In P6.p, the inductive signal from the AC leads to a strong activation of the Ras pathway. This has recently been shown to result in an active down-regulation of the LIN-12/Notch receptor specifically in P6.p through endocytosis (Shaye and Greenwald, 2002). As a consequence of the reduction in LIN-12 signaling, the expression of the ligand for the LIN-12/Notch-receptor is up-regulated in P6.p. The opposite happens in the neighbouring VPCs, P5.p and P7.p. In these cells, the Ras pathway is actively suppressed through the action of the MAP kinase phosphatase, *lip-1* (Berset et al., 2001). The expression of the phosphatase *lip-1* is activated by LIN-12/Notch signaling. Therefore, P6.p functions as an organiser: it induces LIN-12/Notch-signaling in the neighbouring cells, which in response then down-regulate their Ras-signaling that would otherwise antagonise the *lin-12* expression in these cells. As a consequence, *lin-12* expression

is stabilised in P5.p and P7.p and this further down-regulates LIN-12 signaling in P6.p by a feedback mechanism.

Therefore, through the action of an inductive signal and the subsequent lateral signaling, initially equal cells adopt the different cell fates that are required to give rise to 22 cells that form a proper vulva (Figure 12) (Sternberg and Horvitz, 1989).

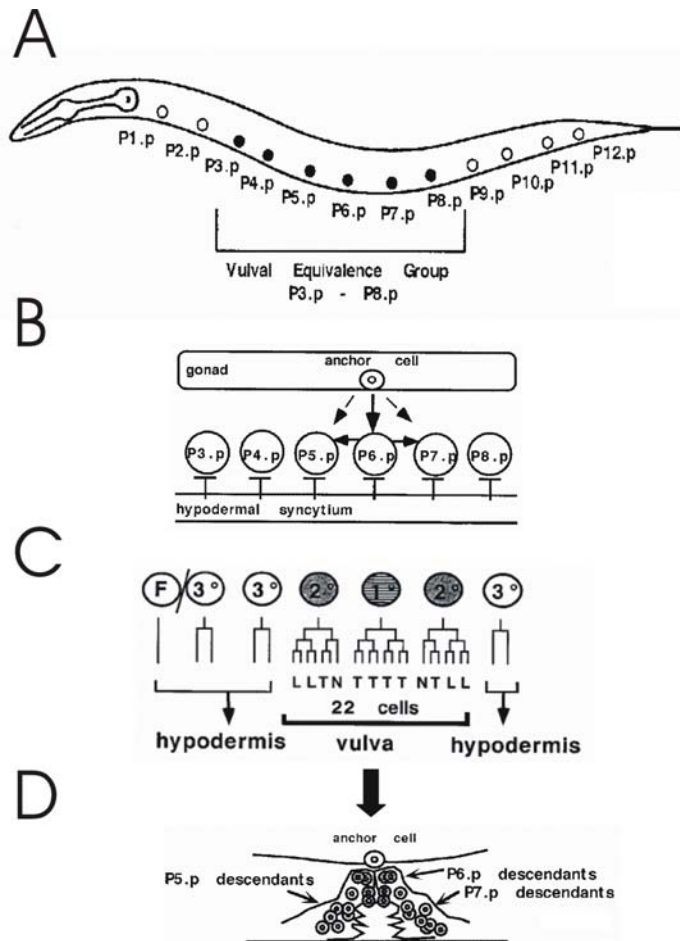


Figure 12: Pattern formation during *C. elegans* vulva development. (A) During the L1 stage the P1.p-P12.p cells are generated. P3.p-P8.p are all competent to generate vulval tissue and are therefore also called vulva precursor cells (VPCs). The remaining Pn.p cells fuse with the hypodermis during the L1 stage (the 3° fate). (B) In the L2 stage the anchor cell (AC) is generated and is centered above P6.p. Through an inductive signal coming from the AC P5.p and P7.p are induced to adopt the vulva fate, while the remaining VPCs receive an inhibitory signal from the hypodermis and subsequently fuse with it. After the induction of P5.p-P7.p by the AC, these cells are further specified by lateral signaling to adopt different vulval fates. (C) The P6.p adopts the 1° fate, while P5.p and P7.p adopt the 2° fate. The remaining non-induced VPCs that fuse to the hypodermal syncytium adopt the 3° fate. The induced VPCs P5.p-P7.p divide in a specific pattern according to their cell fate to generate the 22 cells that form the vulva (D) (modified from Eisenman and Kim, 2000).

Induction of the π -cell fate necessary for the formation of a proper vulva-uterine connection

The anchor cell (AC) not only induces the patterning of the vulva precursor cells (VPCs) but also induces some ventral uterine cells to adopt the π -cell fate (Figure 11) (Newman and Sternberg, 1996). The induction of the π -cell fate is required for the formation of a functional vulva-uterine connection that is necessary for proper egg-laying behavior in *C. elegans*. At the beginning of the L3 larval stage, after the AC/VU decision has been executed, the three vulva uterine (VU) cells are still in close proximity to the AC. Each of the three VU cells generate four intermediate precursors during the L3 stage (Kimble and Hirsh, 1979;

Newman et al., 1995; Newman et al., 1996). These precursors are competent to adopt two different cell fates, the ρ and π cell fates (Newman et al., 1995). These two cell fates differ in the number of cell divisions they subsequently execute and the orientation of these divisions. The ρ cell fate seems to be the default state, while the π cell fate has to be induced by the AC (Figure 13) (Newman et al., 1995).

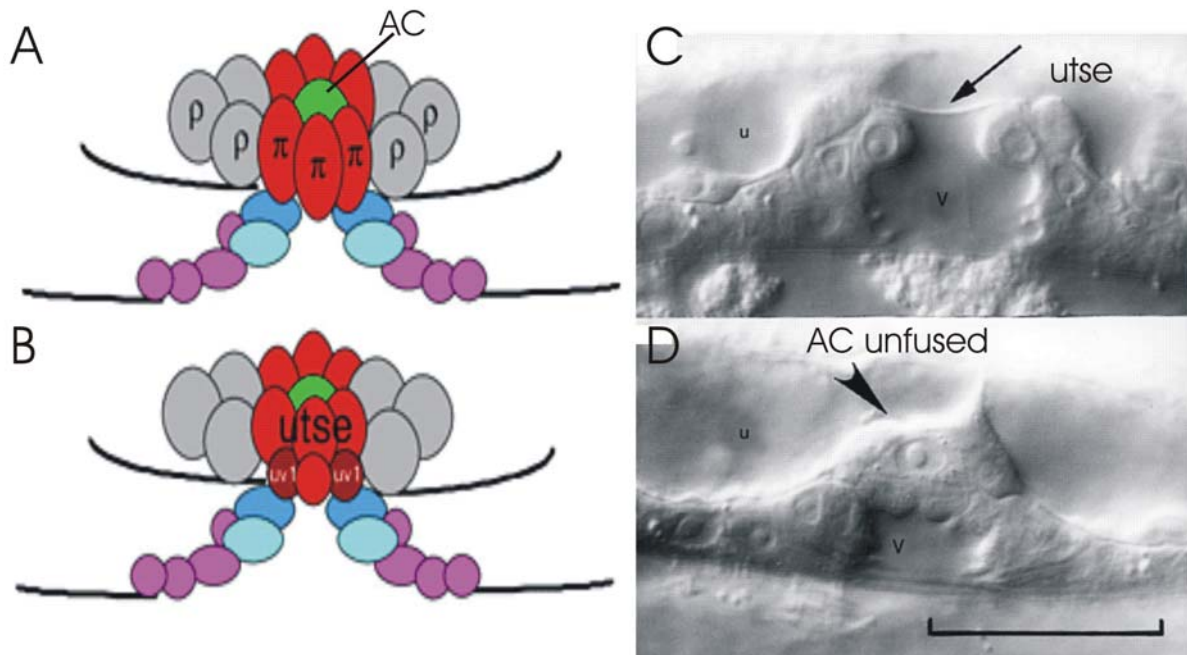


Figure 13: Cells of the vulva-uterine-seam cell connection. (A) To develop a proper vulva-uterine connection the π -cell fate has to be induced by the anchor cell (AC, green) during the late L3 stage. (B) After induction the π -cells give rise to uterine seam cell (utse) and to the uv1 cells. Both uterine cell types are required for the connection of the uterus to the vulva tissue. A DIC image of a mid L4 hermaphrodite vulva in wild type (C), and in mutants with an abnormal vulva-uterine connection due to a lack of π -cell induction (D). Note that instead of a thin lamina process of the utse in wild type (C), a thick layer of cells is separating the vulval (v) and uterine (u) lumen in *lin-12* mutants (D). As a consequence of the π -cell misspecification, the AC often remains unfused on top of the cell layer (D). The scale bar represents 20 μ m. (Pictures were modified from Newman et al, 2000).

Due to the close proximity, six out of the 12 VU descendants surrounding the AC are in contact with the AC (Figure 13). Since all VU cells express the LIN-12 receptor, all of their descendants also expose the LIN-12/Notch-receptor at the cell surface (Figure 11). Therefore, the six VU descendants that are contacting the AC will receive LIN-12 signaling as the AC expresses the LIN-12/Notch ligand LAG-2 (Figure 11). The maintenance of *lag-2* expression by the AC requires the zinc-finger transcription factor *lin-29* (Newman et al., 2000). In *lin-29* mutants, the AC is generated and initially expresses *lag-2* which is sufficient to induce the vulva structures. However, since *lag-2* expression is rapidly downregulated in the AC, the π cell fate is not induced, subsequently resulting in a defective vulva-uterine connection. Normally, in wild type hermaphrodites those VU descendants that are induced by LIN-12 signaling will adopt the π cell fate. However, in mutants that lack LIN-12 activity all VU

descendants adopt the ρ -fate, while in LIN-12 gain-of-function mutants all VU descendants adopt the π cell fate (Cinar et al., 2001; Newman et al., 1995). The π cells fate give rise to the uterine seam cell (utse) and the uv1 cells (Newman et al., 1996). These two uterine cell types connect the uterus to the vulva. The utse is a multinucleate cell that forms a thin laminar process that separates the vulval and uterine lumen. The utse is normally destroyed by the first egg passing through the vulva. In loss of function mutants of *lin-12*, *sel-12*, or *aph-2*, the π cell fate is not, or only partially, induced. This leads to the incomplete induction of the π cell fate and of the appearance of a thick layer of cells rather than the thin laminar utse cell (Figure 13) (Cinar et al., 2001; Levitan et al., 2001b; Newman et al., 1995). This layer of cells represents a sterical blockage of the vulva uterine connection and the mutant hermaphrodites are egg-laying defective (Egl). One of the hallmarks of this vulva-uterine connectivity defect is the appearance of a protruding vulva (Pvl) phenotype in the adult stage (Eimer et al., 2002).

The sex-myoblast/coelomocyte cell fate decision

In *C. elegans*, some mesodermal tissues are formed embryonically and some develop post-embryonically (Sulston and Horvitz, 1977; Sulston et al., 1983). The mesodermal tissue that is formed postembryonically is derived from a single mesoblast, M, which gives rise to six cell types: striated body-wall muscles, coelomocytes, which are non muscle cells, and four classes of nonstriated sex-muscles (Figure 14). The hermaphrodite sex-muscles are the eight vulva muscles (four vm1s and four vm2s) and the eight uterine muscles (four um1s and four um2s). All undifferentiated cells of the M lineage have in common that they express the *C. elegans* twist ortholog *hlh-8* (Corsi et al., 2000; Harfe and Fire, 1998; Harfe et al., 1998b). The M mesoblast is born in the posterior part of the animal at the end of the embryonic stage at the beginning of the L1 stage, just prior to hatching (Sulston and Horvitz, 1977). After three rounds of cell divisions, the ventrally located descendants of M give rise to the two sex-myoblast (SM) cells from which the sex-muscles are derived (Figure 14). From the mid L2 stage to the mid L3 stage the SMs migrate anteriorly to the middle of the animal where they reside at the position of the developing vulva. After three cell divisions the SM descendants differentiate into the different sex muscle types, the vulval and uterine muscles, involved in egg-laying.

The two coelomocytes which are generated in the dorsal part of the M lineage (Figure 14) are scavenger cells that non-specifically endocytose fluid from the pseudocoelom (body

cavity) of the worm (Fares and Greenwald, 2001a; Fares and Greenwald, 2001b). The adult hermaphrodite has six coelomocytes in total with the four additional coelomocytes that are derived from the embryonic mesoderm. All coelomocytes are dispensable for viability. However, coelomocytes are thought to be part of a simple immune system in the worm.

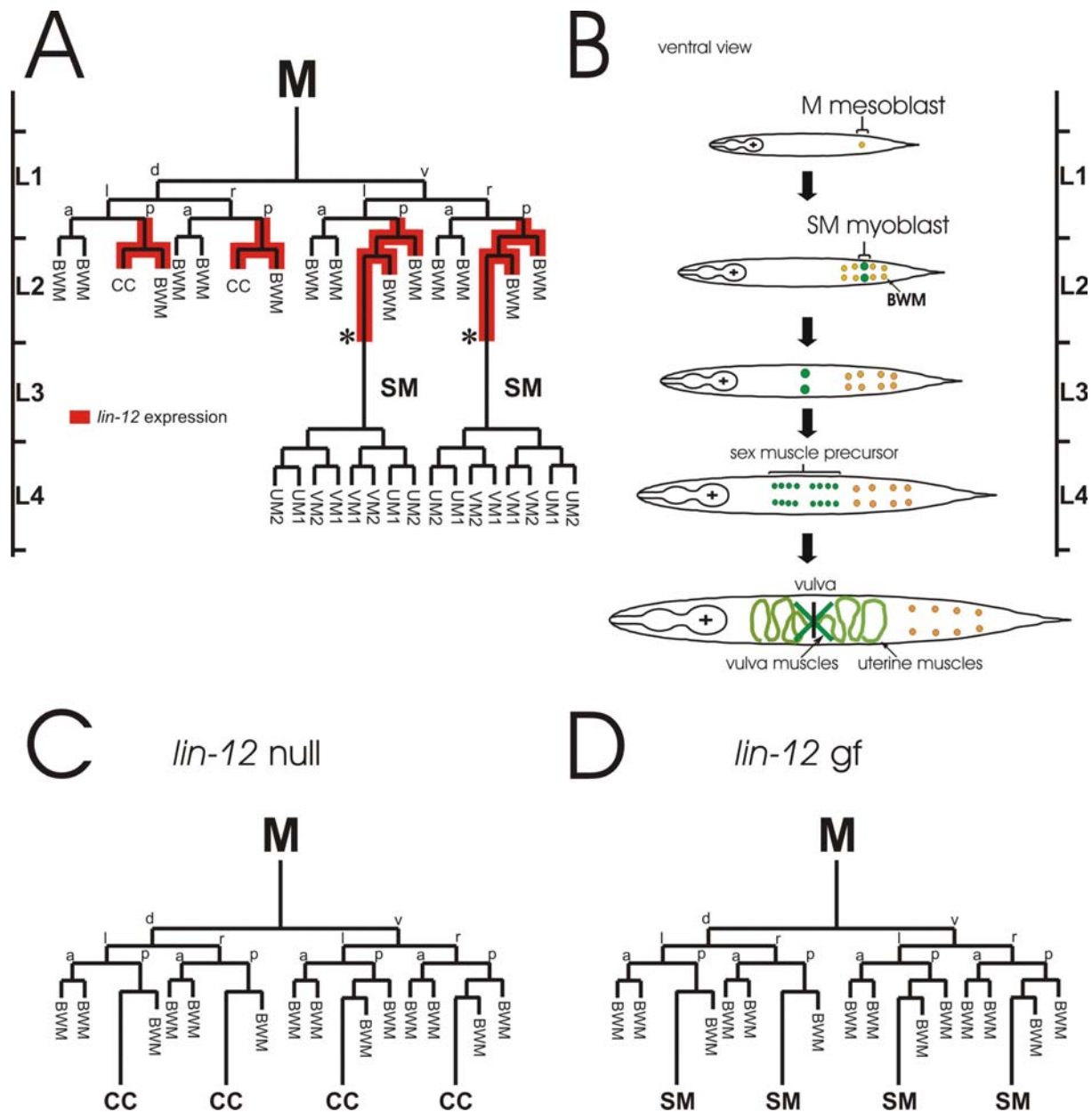


Figure 14: Representation of the hermaphrodite specific post-embryonic M lineage (Sulston and Horvitz, 1977). (A) The M mesoblast is born at the beginning of the L1 stage. Through subsequent divisions it gives rise to 14 striated body wall muscles (BWM), 16 non-striated sex muscles, and 2 coelomocytes (CC), which are non-muscle cells. The expression of *lin-12* in the M-lineage is shown (Wilkinson and Greenwald, 1995). This was only followed until the generation of the SM myoblasts (asterisks). (B) Schematic ventral view of the M lineage cells and their positions within the animal throughout development. (C) SM to CC cell fate transformations seen in *lin-12* null mutants and (D) CC to SM cell fate transformations present in *lin-12* gain-of-function (gf) mutants (Greenwald et al, 1983). [abbreviations: SM, sex myoblast; UM, uterine muscle; VM, vulva muscle; d, dorsal; v, ventral; l, left; r, right; a, anterior; p, posterior;]

The *lin-12*/Notch receptor has been shown to be expressed in the M lineage prior to the generation of the coelomocytes (CCs) and sex-myoblasts (SMs) (Figure 14) (Wilkinson and Greenwald, 1995). Furthermore, LIN-12 signaling has been directly implicated in the CC and SM decisions. Loss-of-function mutations in the *lin-12*/Notch receptor result in a conversion of the SMs into CCs whereas gain-of-function mutations lead to the inverse transformation of CCs into SMs and the generation of additional sex muscles (Figure 14) (Greenwald et al., 1983; Harfe et al., 1998a). Therefore, LIN-12/Notch signaling activity is required to generate sex muscles and it is likely that LIN-12/Notch signaling is thereby antagonizing the action of MyoD. Loss-of-function mutants in the *C. elegans* MyoD ortholog, *hll-1*, exhibit a CC to SM transformation which is partially suppressed in *lin-12*; *hll-1* double mutants (Harfe et al., 1998a; Krause et al., 1990). Similar inhibitory interactions between other basic helix-loop-helix transcription factors and the LIN-12/Notch signaling pathway have been reported in vertebrate myogenesis (Kopan et al., 1994; Nye et al., 1994).

Sex muscle morphology and attachment

LIN-12/Notch-signaling is necessary for the cell fate decision that generates the sex myoblasts, but it also seems to be required at later stages during sex muscle differentiation. Recently it was shown that LIN-12/Notch-signaling is used during sex muscle differentiation to facilitate correct morphology and attachment of the vulva muscles (Eimer et al., 2002). Mutants carrying a temperature-sensitive hypomorphic *lin-12* mutation generate the correct number of sex muscles. However, the functionality of their sex muscles is impaired at the restrictive temperature. Subsequently these mutants exhibit a completely penetrant egg-laying defect (Egl). Temperature shift experiments suggest that the defects leading to the Egl phenotype occur late in development after the mid L3 stage (Sundaram and Greenwald, 1993a). At that time the sex muscle precursor cells undergo the final divisions and differentiate to adopt the different types of sex muscle fates (Figure 14). Laser cell ablation studies have shown that the vulva muscles are required for egg laying (M. Stern, personal communication). When the vulva muscles are deleted or missing due to misspecification, animals are completely Egl (Corsi et al., 2000). The fact that, upon reduction of LIN-12 signaling, the sex muscle defects and the π -cell specification defects are the most penetrant defects suggests that they are most sensitive to alterations in LIN-12 signaling (Cinar et al., 2001; Eimer et al., 2002; Levitan et al., 2001b).

Presenilins in *C. elegans*

The *C. elegans* genome contains three presenilin orthologs *sel-12*, *hop-1*, and *spe-4* (Levitan and Greenwald, 1995; L'Hernault and Arduengo, 1992; Li and Greenwald, 1997). SPE-4 is the most divergent member of this family with a sole role restricted to spermatogenesis. *spe-4* is expressed only during the L4 larval stage when sperm is produced (Lakowski et al, submitted). SPE-4 is localized to ER/Golgi derived organelles and loss of function mutations in *spe-4* lead sterility due to a lack of proper partitioning of the cytoplasm during sperm maturation (Arduengo et al., 1998). Accordingly, *spe-4* is not able to substitute one of the other presenilins when expressed ectopically (see Chapter VIII).

In contrast, the other two somatically expressed presenilins, *sel-12* and *hop-1*, are able to replace each other and are functionally conserved with the human presenilins (Baumeister et al., 1997; Levitan and Greenwald, 1995; Li and Greenwald, 1997). In *sel-12*; *hop-1* double mutants, signaling through the Notch receptors LIN-12 and GLP-1 is almost completely blocked (Li and Greenwald, 1997; Westlund et al., 1999). However, mutant animals carrying a deletion of *hop-1* do not display an obvious phenotype (Westlund et al., 1999). This is similar to the mammalian system, where a deletion of PS2 also leads to only minor defects, whereas PS1 and PS2 double mutants are embryonically lethal (Herreman et al., 1999).

Mutations in *sel-12* lead to a highly penetrant egg-laying defect (Egl) in combination with a protruding vulva phenotype (Pvl) (Eimer et al., 2002; Levitan and Greenwald, 1995). The defects have recently been shown to be caused by *sel-12* affecting two independent LIN-12 signaling events: *sel-12* mutants display sex muscle morphology and attachment defects similar to those found in *lin-12* hypomorphic mutants (Eimer et al., 2002). Furthermore, *sel-12* mutant animals fail to specify the π -cell fate correctly leading to the appearance of a thick tissue separating the vulval and uterine lumen (Cinar et al., 2001). This failure to form a proper vulva-uterine connection is most likely the cause of the Pvl defect (Eimer et al., 2002).

Therefore, both defects in combination lead to the highly penetrant Egl phenotype of *sel-12* mutants. However, the AC/VU and the SM/CC cell fate decisions and the VPC induction that also require LIN-12/Notch signaling are not affected in *sel-12* mutants (Eimer et al., 2002; Levitan and Greenwald, 1995). This suggests that these LIN-12 signaling events that involve feedback loops are more stable towards alterations in LIN-12 signaling.

Additionally, *sel-12* has been shown to be required for proper development of the male specific sex muscles and tail structures and also for neuronal signaling involved in thermotaxis (Eimer et al., 2002; Wittenburg et al., 2000). The neuronal defects can also be rescued by transgenic expression of the human PS1 and PS2 (Wittenburg et al., 2000).

References

- Andra, K., Abramowski, D., Duke, M., Probst, A., Wiederhold, K. H., Burki, K., Goedert, M., Sommer, B., and Staufenbiel, M. (1996). Expression of APP in transgenic mice: a comparison of neuron-specific promoters. *Neurobiol Aging* **17**, 183-90.
- Annaert, W. G., Levesque, L., Craessaerts, K., Dierinck, I., Snellings, G., Westaway, D., George-Hyslop, P. S., Cordell, B., Fraser, P., and De Strooper, B. (1999). Presenilin 1 controls gamma-secretase processing of amyloid precursor protein in pre-golgi compartments of hippocampal neurons. *J Cell Biol* **147**, 277-94.
- Arawaka, S., Hasegawa, H., Tandon, A., Janus, C., Chen, F., Yu, G., Kikuchi, K., Koyama, S., Kato, T., Fraser, P. E., and St George-Hyslop, P. (2002). The levels of mature glycosylated nicastrin are regulated and correlate with gamma-secretase processing of amyloid beta-precursor protein. *J Neurochem* **83**, 1065-1071.
- Arduengo, P. M., Appleberry, O. K., Chuang, P., and L'Hernault, S. W. (1998). The presenilin protein family member SPE-4 localizes to an ER/Golgi derived organelle and is required for proper cytoplasmic partitioning during *Caenorhabditis elegans* spermatogenesis. *J Cell Sci* **111**, 3645-54.
- Aroian, R. V., Koga, M., Mendel, J. E., Ohshima, Y., and Sternberg, P. W. (1990). The *let-23* gene necessary for *Caenorhabditis elegans* vulval induction encodes a tyrosine kinase of the EGF receptor subfamily. *Nature* **348**, 693-9.
- Austin, J., and Kimble, J. (1987). *glp-1* is required in the germ line for regulation of the decision between mitosis and meiosis in *C. elegans*. *Cell* **51**, 589-99.
- Austin, J., and Kimble, J. (1989). Transcript analysis of *glp-1* and *lin-12*, homologous genes required for cell interactions during development of *C. elegans*. *Cell* **58**, 565-71.
- Baumeister, R., Leimer, U., Zweckbronner, I., Jakubek, C., Grunberg, J., and Haass, C. (1997). Human presenilin-1, but not familial Alzheimer's disease (FAD) mutants, facilitate *Caenorhabditis elegans* Notch signalling independently of proteolytic processing. *Genes Funct* **1**, 149-59.
- Behr, D., Wrigley, J. D., Nadin, A., Evin, G., Masters, C. L., Harrison, T., Castro, J. L., and Shearman, M. S. (2001). Pharmacological knock-down of the presenilin 1 heterodimer by a novel gamma -secretase inhibitor: implications for presenilin biology. *J Biol Chem* **276**, 45394-402.
- Berezovska, O., Jack, C., McLean, P., Aster, J. C., Hicks, C., Xia, W., Wolfe, M. S., Kimberly, W. T., Weinmaster, G., Selkoe, D. J., and Hyman, B. T. (2000). Aspartate mutations in presenilin and gamma-secretase inhibitors both impair notch1 proteolysis and nuclear translocation with relative preservation of notch1 signaling. *J Neurochem* **75**, 583-93.
- Berry, L. W., Westlund, B., and Schedl, T. (1997). Germ-line tumor formation caused by activation of *glp-1*, a *Caenorhabditis elegans* member of the Notch family of receptors. *Development* **124**, 925-36.
- Berset, T., Hoier, E. F., Battu, G., Canevascini, S., and Hajnal, A. (2001). Notch inhibition of RAS signaling through MAP kinase phosphatase LIP-1 during *C. elegans* vulval development. *Science* **291**, 1055-8.
- Borchelt, D. R., Ratovitski, T., van Lare, J., Lee, M. K., Gonzales, V., Jenkins, N. A., Copeland, N. G., Price, D. L., and Sisodia, S. S. (1997). Accelerated amyloid deposition in the brains of transgenic mice coexpressing mutant presenilin 1 and amyloid precursor proteins. *Neuron* **19**, 939-45.
- Borchelt, D. R., Thinakaran, G., Eckman, C. B., Lee, M. K., Davenport, F., Ratovitsky, T., Prada, C. M., Kim, G., Seekins, S., Yager, D., Slunt, H. H., Wang, R., Seeger, M.,

- Levey, A. I., Gandy, S. E., Copeland, N. G., Jenkins, N. A., Price, D. L., Younkin, S. G., and Sisodia, S. S. (1996). Familial Alzheimer's disease-linked presenilin 1 variants elevate Abeta1-42/1-40 ratio in vitro and in vivo. *Neuron* **17**, 1005-13.
- Bowerman, B., Tax, F. E., Thomas, J. H., and Priess, J. R. (1992). Cell interactions involved in development of the bilaterally symmetrical intestinal valve cells during embryogenesis in *Caenorhabditis elegans*. *Development* **116**, 1113-22.
- Brendza, R. P., Bales, K. R., Paul, S. M., and Holtzman, D. M. (2002). Role of apoE/Abeta interactions in Alzheimer's disease: insights from transgenic mouse models. *Mol Psychiatry* **7**, 132-5.
- Calhoun, M. E., Burgermeister, P., Phinney, A. L., Stalder, M., Tolnay, M., Wiederhold, K. H., Abramowski, D., Sturchler-Pierrat, C., Sommer, B., Staufenbiel, M., and Jucker, M. (1999). Neuronal overexpression of mutant amyloid precursor protein results in prominent deposition of cerebrovascular amyloid. *Proc Natl Acad Sci U S A* **96**, 14088-93.
- Campion, D., Flaman, J. M., Brice, A., Hannequin, D., Dubois, B., Martin, C., Moreau, V., Charbonnier, F., Didierjean, O., Tardieu, S., and et al. (1995). Mutations of the presenilin I gene in families with early-onset Alzheimer's disease. *Hum Mol Genet* **4**, 2373-7.
- Capell, A., Grunberg, J., Pesold, B., Diehlmann, A., Citron, M., Nixon, R., Beyreuther, K., Selkoe, D. J., and Haass, C. (1998). The proteolytic fragments of the Alzheimer's disease-associated presenilin-1 form heterodimers and occur as a 100-150-kDa molecular mass complex. *J Biol Chem* **273**, 3205-11.
- Carlson, G. A., Borchelt, D. R., Dake, A., Turner, S., Danielson, V., Coffin, J. D., Eckman, C., Meiners, J., Nilsen, S. P., Younkin, S. G., and Hsiao, K. K. (1997). Genetic modification of the phenotypes produced by amyloid precursor protein overexpression in transgenic mice. *Hum Mol Genet* **6**, 1951-9.
- Cervantes, S., Gonzalez-Duarte, R., and Marfany, G. (2001). Homodimerization of presenilin N-terminal fragments is affected by mutations linked to Alzheimer's disease. *FEBS Lett* **505**, 81-6.
- Chen, F., Yu, G., Arawaka, S., Nishimura, M., Kawarai, T., Yu, H., Tandon, A., Supala, A., Song, Y. Q., Rogaeva, E., Milman, P., Sato, C., Yu, C., Janus, C., Lee, J., Song, L., Zhang, L., Fraser, P. E., and St George-Hyslop, P. H. (2001). Nicastrin binds to membrane-tethered Notch. *Nat Cell Biol* **3**, 751-4.
- Christensen, S., Kodoyianni, V., Bosenberg, M., Friedman, L., and Kimble, J. (1996). *lag-1*, a gene required for *lin-12* and *glp-1* signaling in *Caenorhabditis elegans*, is homologous to human CBF1 and *Drosophila* Su(H). *Development* **122**, 1373-83.
- Chung, H. M., and Struhl, G. (2001). Nicastrin is required for Presenilin-mediated transmembrane cleavage in *Drosophila*. *Nat Cell Biol* **3**, 1129-32.
- Cinar, H. N., Sweet, K. L., Hosemann, K. E., Earley, K., and Newman, A. P. (2001). The SEL-12 Presenilin Mediates Induction of the *Caenorhabditis elegans* Uterine pi Cell Fate. *Dev Biol* **237**, 173-82.
- Citron, M., Westaway, D., Xia, W., Carlson, G., Diehl, T., Levesque, G., Johnson-Wood, K., Lee, M., Seubert, P., Davis, A., Kholodenko, D., Motter, R., Sherrington, R., Perry, B., Yao, H., Strome, R., Lieberburg, I., Rommens, J., Kim, S., Schenk, D., Fraser, P., St George Hyslop, P., and Selkoe, D. J. (1997). Mutant presenilins of Alzheimer's disease increase production of 42-residue amyloid beta-protein in both transfected cells and transgenic mice. *Nat Med* **3**, 67-72.
- Conlon, R. A., Reaume, A. G., and Rossant, J. (1995). Notch1 is required for the coordinate segmentation of somites. *Development* **121**, 1533-45.

- Corsi, A. K., Kostas, S. A., Fire, A., and Krause, M. (2000). *Caenorhabditis elegans* twist plays an essential role in non-striated muscle development. *Development* **127**, 2041-51.
- Crittenden, S. L., Troemel, E. R., Evans, T. C., and Kimble, J. (1994). GLP-1 is localized to the mitotic region of the *C. elegans* germ line. *Development* **120**, 2901-11.
- Cruts, M., Hendriks, L., and Van Broeckhoven, C. (1996). The presenilin genes: a new gene family involved in Alzheimer disease pathology. *Hum Mol Genet* **5 Spec No**, 1449-55.
- Czech, C., Masters, C., and Beyreuther, K. (1994). Alzheimer's disease and transgenic mice. *J Neural Transm Suppl* **44**, 219-30.
- Czech, C., Tremp, G., and Pradier, L. (2000). Presenilins and Alzheimer's disease: biological functions and pathogenic mechanisms. *Prog Neurobiol* **60**, 363-84.
- Dal Forno, G., Carson, K. A., Brookmeyer, R., Troncoso, J., Kawas, C. H., and Brandt, J. (2002). APOE genotype and survival in men and women with Alzheimer's disease. *Neurology* **58**, 1045-50.
- Darzins, A., and Russell, M. A. (1997). Molecular genetic analysis of type-4 pilus biogenesis and twitching motility using *Pseudomonas aeruginosa* as a model system--a review. *Gene* **192**, 109-15.
- David, D. C., Layfield, R., Serpell, L., Narain, Y., Goedert, M., and Spillantini, M. G. (2002). Proteasomal degradation of tau protein. *J Neurochem* **83**, 176-85.
- De Strooper, B., Annaert, W., Cupers, P., Saftig, P., Craessaerts, K., Mumm, J. S., Schroeter, E. H., Schrijvers, V., Wolfe, M. S., Ray, W. J., Goate, A., and Kopan, R. (1999). A presenilin-1-dependent gamma-secretase-like protease mediates release of Notch intracellular domain. *Nature* **398**, 518-22.
- De Strooper, B., Beullens, M., Contreras, B., Levesque, L., Craessaerts, K., Cordell, B., Moechars, D., Bollen, M., Fraser, P., George-Hyslop, P. S., and Van Leuven, F. (1997). Phosphorylation, subcellular localization, and membrane orientation of the Alzheimer's disease-associated presenilins. *J Biol Chem* **272**, 3590-8.
- De Strooper, B., Saftig, P., Craessaerts, K., Vanderstichele, H., Guhde, G., Annaert, W., Von Figura, K., and Van Leuven, F. (1998). Deficiency of presenilin-1 inhibits the normal cleavage of amyloid precursor protein. *Nature* **391**, 387-90.
- Dewachter, I., Moechars, D., van Dorpe, J., Tesseur, I., Van den Haute, C., Spittaels, K., and Van Leuven, F. (2001). Modelling Alzheimer's disease in multiple transgenic mice. *Biochem Soc Symp*, 203-10.
- Dewji, N. N., Do, C., and Singer, S. J. (1997). On the spurious endoproteolytic processing of the presenilin proteins in cultured cells and tissues. *Proc Natl Acad Sci U S A* **94**, 14031-6.
- Doan, A., Thinakaran, G., Borchelt, D. R., Slunt, H. H., Ratovitsky, T., Podlisny, M., Selkoe, D. J., Seeger, M., Gandy, S. E., Price, D. L., and Sisodia, S. S. (1996). Protein topology of presenilin 1. *Neuron* **17**, 1023-30.
- Edbauer, D., Winkler, E., Haass, C., and Steiner, H. (2002). Presenilin and nicastrin regulate each other and determine amyloid beta -peptide production via complex formation. *Proc Natl Acad Sci U S A*.
- Eimer, S., Donhauser, R., and Baumeister, R. (2002). The *Caenorhabditis elegans* Presenilin *sel-12* Is Required for Mesodermal Patterning and Muscle Function. *Dev Biol* **251**, 178-92.
- Esler, W. P., Kimberly, W. T., Ostaszewski, B. L., Diehl, T. S., Moore, C. L., Tsai, J. Y., Rahmati, T., Xia, W., Selkoe, D. J., and Wolfe, M. S. (2000). Transition-state analogue inhibitors of gamma-secretase bind directly to presenilin-1. *Nat Cell Biol* **2**, 428-34.
- Esler, W. P., Kimberly, W. T., Ostaszewski, B. L., Ye, W., Diehl, T. S., Selkoe, D. J., and Wolfe, M. S. (2002). Activity-dependent isolation of the presenilin- gamma -secretase

- complex reveals nicastrin and a gamma substrate. *Proc Natl Acad Sci U S A* **99**, 2720-5.
- Evans, D. A., Funkenstein, H. H., Albert, M. S., Scherr, P. A., Cook, N. R., Chown, M. J., Hebert, L. E., Hennekens, C. H., and Taylor, J. O. (1989). Prevalence of Alzheimer's disease in a community population of older persons. Higher than previously reported. *Jama* **262**, 2551-6.
- Evans, T. C., Crittenden, S. L., Kodoyianni, V., and Kimble, J. (1994). Translational control of maternal *glp-1* mRNA establishes an asymmetry in the *C. elegans* embryo. *Cell* **77**, 183-94.
- Evin, G., Sharples, R. A., Weidemann, A., Reinhard, F. B., Carbone, V., Culvenor, J. G., Holsinger, R. M., Sernee, M. F., Beyreuther, K., and Masters, C. L. (2001). Aspartyl protease inhibitor pepstatin binds to the presenilins of Alzheimer's disease. *Biochemistry* **40**, 8359-68.
- Fares, H., and Greenwald, I. (2001a). Genetic Analysis of Endocytosis in *Caenorhabditis elegans*. Coelomocyte uptake defective mutants. *Genetics* **159**, 133-45.
- Fares, H., and Greenwald, I. (2001b). Regulation of endocytosis by CUP-5, the *Caenorhabditis elegans* mucolipin-1 homolog. *Nat Genet* **28**, 64-8.
- Fassbender, K., Simons, M., Bergmann, C., Stroick, M., Lutjohann, D., Keller, P., Runz, H., Kuhl, S., Bertsch, T., von Bergmann, K., Hennerici, M., Beyreuther, K., and Hartmann, T. (2001). Simvastatin strongly reduces levels of Alzheimer's disease beta-amyloid peptides Abeta 42 and Abeta 40 in vitro and in vivo. *Proc Natl Acad Sci U S A* **98**, 5856-61.
- Ferguson, E. L., and Horvitz, H. R. (1985). Identification and characterization of 22 genes that affect the vulval cell lineages of the nematode *Caenorhabditis elegans*. *Genetics* **110**, 17-72.
- Fitzgerald, K., Wilkinson, H. A., and Greenwald, I. (1993). *glp-1* can substitute for *lin-12* in specifying cell fate decisions in *Caenorhabditis elegans*. *Development* **119**, 1019-27.
- Fortini, M. E. (2001). Notch and presenilin: a proteolytic mechanism emerges. *Curr Opin Cell Biol* **13**, 627-34.
- Francis, R., McGrath, G., Zhang, J., Ruddy, D. A., Sym, M., Apfeld, J., Nicoll, M., Maxwell, M., Hai, B., Ellis, M. C., Parks, A. L., Xu, W., Li, J., Gurney, M., Myers, R. L., Himes, C. S., Hiesch, R., Ruble, C., Nye, J. S., and Curtis, D. (2002). *aph-1* and *pen-2* are required for Notch pathway signaling, gamma-secretase cleavage of betaAPP, and presenilin protein accumulation. *Dev Cell* **3**, 85-97.
- Frears, E. R., Stephens, D. J., Walters, C. E., Davies, H., and Austen, B. M. (1999). The role of cholesterol in the biosynthesis of beta-amyloid. *Neuroreport* **10**, 1699-705.
- Gotz, J., Chen, F., van Dorpe, J., and Nitsch, R. M. (2001). Formation of neurofibrillary tangles in P301 tau transgenic mice induced by Abeta 42 fibrils. *Science* **293**, 1491-5.
- Goutte, C. (2002). Genetics leads the way to the accomplices of presenilins. *Dev Cell* **3**, 6-7.
- Goutte, C., Hepler, W., Mickey, K. M., and Priess, J. R. (2000). *aph-2* encodes a novel extracellular protein required for GLP-1-mediated signaling. *Development* **127**, 2481-92.
- Goutte, C., Tsunozaki, M., Hale, V. A., and Priess, J. R. (2002). APH-1 is a multipass membrane protein essential for the Notch signaling pathway in *Caenorhabditis elegans* embryos. *Proc Natl Acad Sci U S A* **99**, 775-779.
- Greenwald, I. (1998). LIN-12/Notch signaling: lessons from worms and flies. *Genes Dev* **12**, 1751-62.
- Greenwald, I., and Seydoux, G. (1990). Analysis of gain-of-function mutations of the *lin-12* gene of *Caenorhabditis elegans*. *Nature* **346**, 197-9.
- Greenwald, I. S., Sternberg, P. W., and Horvitz, H. R. (1983). The *lin-12* locus specifies cell fates in *Caenorhabditis elegans*. *Cell* **34**, 435-44.

- Guo, Q., Fu, W., Sopher, B. L., Miller, M. W., Ware, C. B., Martin, G. M., and Mattson, M. P. (1999). Increased vulnerability of hippocampal neurons to excitotoxic necrosis in presenilin-1 mutant knock-in mice. *Nat Med* **5**, 101-6.
- Hardy, J. (1997). Amyloid, the presenilins and Alzheimer's disease. *Trends Neurosci* **20**, 154-9.
- Hardy, J., Duff, K., Hardy, K. G., Perez-Tur, J., and Hutton, M. (1998). Genetic dissection of Alzheimer's disease and related dementias: amyloid and its relationship to tau. *Nat Neurosci* **1**, 355-8.
- Hardy, J., and Selkoe, D. J. (2002). The amyloid hypothesis of Alzheimer's disease: progress and problems on the road to therapeutics. *Science* **297**, 353-6.
- Harfe, B. D., Branda, C. S., Krause, M., Stern, M. J., and Fire, A. (1998a). MyoD and the specification of muscle and non-muscle fates during postembryonic development of the *C. elegans* mesoderm. *Development* **125**, 2479-88.
- Harfe, B. D., and Fire, A. (1998). Muscle and nerve-specific regulation of a novel NK-2 class homeodomain factor in *Caenorhabditis elegans*. *Development* **125**, 421-9.
- Harfe, B. D., Vaz Gomes, A., Kenyon, C., Liu, J., Krause, M., and Fire, A. (1998b). Analysis of a *Caenorhabditis elegans* Twist homolog identifies conserved and divergent aspects of mesodermal patterning. *Genes Dev* **12**, 2623-35.
- Hartley, D. M., Walsh, D. M., Ye, C. P., Diehl, T., Vasquez, S., Vassilev, P. M., Teplow, D. B., and Selkoe, D. J. (1999). Protofibrillar intermediates of amyloid beta-protein induce acute electrophysiological changes and progressive neurotoxicity in cortical neurons. *J Neurosci* **19**, 8876-84.
- Hedgecock, E. M., Culotti, J. G., and Hall, D. H. (1990). The *unc-5*, *unc-6*, and *unc-40* genes guide circumferential migrations of pioneer axons and mesodermal cells on the epidermis in *C. elegans*. *Neuron* **4**, 61-85.
- Henderson, S. T., Gao, D., Lambie, E. J., and Kimble, J. (1994). *lag-2* may encode a signaling ligand for the GLP-1 and LIN-12 receptors of *C. elegans*. *Development* **120**, 2913-24.
- Herman, R. K., and Hedgecock, E. M. (1990). Limitation of the size of the vulval primordium of *Caenorhabditis elegans* by *lin-15* expression in surrounding hypodermis. *Nature* **348**, 169-71.
- Herreman, A., Hartmann, D., Annaert, W., Saftig, P., Craessaerts, K., Serneels, L., Umans, L., Schrijvers, V., Checler, F., Vanderstichele, H., Baekelandt, V., Dressel, R., Cupers, P., Huylebroeck, D., Zwijsen, A., Van Leuven, F., and De Strooper, B. (1999). Presenilin 2 deficiency causes a mild pulmonary phenotype and no changes in amyloid precursor protein processing but enhances the embryonic lethal phenotype of presenilin 1 deficiency. *Proc Natl Acad Sci U S A* **96**, 11872-7.
- Herreman, A., Serneels, L., Annaert, W., Collen, D., Schoonjans, L., and De Strooper, B. (2000). Total inactivation of gamma-secretase activity in presenilin-deficient embryonic stem cells. *Nat Cell Biol* **2**, 461-2.
- Hill, R. J., and Sternberg, P. W. (1992). The gene *lin-3* encodes an inductive signal for vulval development in *C. elegans*. *Nature* **358**, 470-6.
- Holtzman, D. M., Bales, K. R., Tenkova, T., Fagan, A. M., Parsadanian, M., Sartorius, L. J., Mackey, B., Olney, J., McKeel, D., Wozniak, D., and Paul, S. M. (2000). Apolipoprotein E isoform-dependent amyloid deposition and neuritic degeneration in a mouse model of Alzheimer's disease. *Proc Natl Acad Sci U S A* **97**, 2892-7.
- Hsia, A. Y., Masliah, E., McConlogue, L., Yu, G. Q., Tatsuno, G., Hu, K., Kholodenko, D., Malenka, R. C., Nicoll, R. A., and Mucke, L. (1999). Plaque-independent disruption of neural circuits in Alzheimer's disease mouse models. *Proc Natl Acad Sci U S A* **96**, 3228-33.
- Hu, Y., Ye, Y., and Fortini, M. E. (2002). Nicastrin is required for gamma-secretase cleavage of the *Drosophila* Notch receptor. *Dev Cell* **2**, 69-78.

- Huppert, S. S., Le, A., Schroeter, E. H., Mumm, J. S., Saxena, M. T., Milner, L. A., and Kopan, R. (2000). Embryonic lethality in mice homozygous for a processing-deficient allele of Notch1. *Nature* **405**, 966-70.
- Hutter, H., and Schnabel, R. (1994). *glp-1* and inductions establishing embryonic axes in *C. elegans*. *Development* **120**, 2051-64.
- Hutter, H., and Schnabel, R. (1995). Specification of anterior-posterior differences within the AB lineage in the *C. elegans* embryo: a polarising induction. *Development* **121**, 1559-68.
- Hutton, M., and Hardy, J. (1997). The presenilins and Alzheimer's disease. *Hum Mol Genet* **6**, 1639-46.
- Jarrett, J. T., Berger, E. P., and Lansbury, P. T., Jr. (1993a). The carboxy terminus of the beta amyloid protein is critical for the seeding of amyloid formation: implications for the pathogenesis of Alzheimer's disease. *Biochemistry* **32**, 4693-7.
- Jarrett, J. T., Berger, E. P., and Lansbury, P. T., Jr. (1993b). The C-terminus of the beta protein is critical in amyloidogenesis. *Ann N Y Acad Sci* **695**, 144-8.
- Johnson, G. V., and Hartigan, J. A. (1999). Tau Protein in Normal and Alzheimer's Disease Brain: An Update. *J Alzheimers Dis* **1**, 329-351.
- Kaether, C., Lammich, S., Edbauer, D., Ertl, M., Rietdorf, J., Capell, A., Steiner, H., and Haass, C. (2002). Presenilin-1 affects trafficking and processing of betaAPP and is targeted in a complex with nicastrin to the plasma membrane. *J Cell Biol* **158**, 551-61.
- Kawas, C., Gray, S., Brookmeyer, R., Fozard, J., and Zonderman, A. (2000). Age-specific incidence rates of Alzheimer's disease: the Baltimore Longitudinal Study of Aging. *Neurology* **54**, 2072-7.
- Kim, S. H., Lah, J. J., Thinakaran, G., Levey, A., and Sisodia, S. S. (2000). Subcellular localization of presenilins: association with a unique membrane pool in cultured cells. *Neurobiol Dis* **7**, 99-117.
- Kimberly, W. T., LaVoie, M. J., Ostaszewski, B. L., Ye, W., Wolfe, M. S., and Selkoe, D. J. (2002). Complex N-linked glycosylated nicastrin associates with active gamma-secretase and undergoes tight cellular regulation. *J Biol Chem* **277**, 35113-7.
- Kimble, J. (1981). Alterations in cell lineage following laser ablation of cells in the somatic gonad of *Caenorhabditis elegans*. *Dev Biol* **87**, 286-300.
- Kimble, J., and Hirsh, D. (1979). The postembryonic cell lineages of the hermaphrodite and male gonads in *Caenorhabditis elegans*. *Dev Biol* **70**, 396-417.
- Kimble, J. E., and White, J. G. (1981). On the control of germ cell development in *Caenorhabditis elegans*. *Dev Biol* **81**, 208-19.
- Koistinaho, M., Ort, M., Cimadevilla, J. M., Vondrous, R., Cordell, B., Koistinaho, J., Bures, J., and Higgins, L. S. (2001). Specific spatial learning deficits become severe with age in beta -amyloid precursor protein transgenic mice that harbor diffuse beta -amyloid deposits but do not form plaques. *Proc Natl Acad Sci U S A* **98**, 14675-80.
- Kopan, R., and Goate, A. (2000). A common enzyme connects notch signaling and Alzheimer's disease. *Genes Dev* **14**, 2799-806.
- Kopan, R., and Goate, A. (2002). Aph-2/Nicastrin: an essential component of gamma-secretase and regulator of Notch signaling and Presenilin localization. *Neuron* **33**, 321-4.
- Kopan, R., Nye, J. S., and Weintraub, H. (1994). The intracellular domain of mouse Notch: a constitutively activated repressor of myogenesis directed at the basic helix-loop-helix region of MyoD. *Development* **120**, 2385-96.
- Kornfeld, K. (1997). Vulval development in *Caenorhabditis elegans*. *Trends Genet* **13**, 55-61.
- Kovacs, D. M., Fausett, H. J., Page, K. J., Kim, T. W., Moir, R. D., Merriam, D. E., Hollister, R. D., Hallmark, O. G., Mancini, R., Felsenstein, K. M., Hyman, B. T., Tanzi, R. E., and Wasco, W. (1996). Alzheimer-associated presenilins 1 and 2: neuronal expression

- in brain and localization to intracellular membranes in mammalian cells. *Nat Med* **2**, 224-9.
- Krause, M., Fire, A., Harrison, S. W., Priess, J., and Weintraub, H. (1990). CeMyoD accumulation defines the body wall muscle cell fate during *C. elegans* embryogenesis. *Cell* **63**, 907-19.
- LaFerla, F. M. (2002). Calcium dyshomeostasis and intracellular signalling in alzheimer's disease. *Nat Rev Neurosci* **3**, 862-72.
- Lah, J. J., and Levey, A. I. (2000). Endogenous presenilin-1 targets to endocytic rather than biosynthetic compartments. *Mol Cell Neurosci* **16**, 111-26.
- Lambert, M. P., Barlow, A. K., Chromy, B. A., Edwards, C., Freed, R., Liosatos, M., Morgan, T. E., Rozovsky, I., Trommer, B., Viola, K. L., Wals, P., Zhang, C., Finch, C. E., Krafft, G. A., and Klein, W. L. (1998). Diffusible, nonfibrillar ligands derived from Abeta1-42 are potent central nervous system neurotoxins. *Proc Natl Acad Sci U S A* **95**, 6448-53.
- Lambie, E. J. (2002). Cell proliferation and growth in *C. elegans*. *Bioessays* **24**, 38-53.
- Lambie, E. J., and Kimble, J. (1991). Two homologous regulatory genes, *lin-12* and *glp-1*, have overlapping functions. *Development* **112**, 231-40.
- LaPointe, C. F., and Taylor, R. K. (2000). The type 4 prepilin peptidases comprise a novel family of aspartic acid proteases. *J Biol Chem* **275**, 1502-10.
- Larson, J., Lynch, G., Games, D., and Seubert, P. (1999). Alterations in synaptic transmission and long-term potentiation in hippocampal slices from young and aged PDAPP mice. *Brain Res* **840**, 23-35.
- Lee, M. K., Slunt, H. H., Martin, L. J., Thinakaran, G., Kim, G., Gandy, S. E., Seeger, M., Koo, E., Price, D. L., and Sisodia, S. S. (1996). Expression of presenilin 1 and 2 (PS1 and PS2) in human and murine tissues. *J Neurosci* **16**, 7513-25.
- Lee, S. F., Shah, S., Li, H., Yu, C., Han, W., and Yu, G. (2002). Mammalian APH-1 Interacts with Presenilin and Nicastrin and Is Required for Intramembrane Proteolysis of Amyloid-beta Precursor Protein and Notch. *J Biol Chem* **277**, 45013-9.
- Leem, J. Y., Saura, C. A., Pietrzik, C., Christianson, J., Wanamaker, C., King, L. T., Veselits, M. L., Tomita, T., Gasparini, L., Iwatsubo, T., Xu, H., Green, W. N., Koo, E. H., and Thinakaran, G. (2002). A role for presenilin 1 in regulating the delivery of amyloid precursor protein to the cell surface. *Neurobiol Dis* **11**, 64-82.
- Lehmann, S., Chiesa, R., and Harris, D. A. (1997). Evidence for a six-transmembrane domain structure of presenilin 1. *J Biol Chem* **272**, 12047-51.
- Leissring, M. A., Akbari, Y., Fanger, C. M., Cahalan, M. D., Mattson, M. P., and LaFerla, F. M. (2000). Capacitative calcium entry deficits and elevated luminal calcium content in mutant presenilin-1 knockin mice. *J Cell Biol* **149**, 793-8.
- Lemberg, M. K., and Martoglio, B. (2002). Requirements for signal Peptide peptidase-catalyzed intramembrane proteolysis. *Mol Cell* **10**, 735-44.
- Levitan, D., and Greenwald, I. (1995). Facilitation of *lin-12*-mediated signalling by *sel-12*, a *Caenorhabditis elegans* S182 Alzheimer's disease gene. *Nature* **377**, 351-4.
- Levitan, D., Lee, J., Song, L., Manning, R., Wong, G., Parker, E., and Zhang, L. (2001a). PS1 N- and C-terminal fragments form a complex that functions in APP processing and Notch signaling. *Proc Natl Acad Sci U S A* **98**, 12186-90.
- Levitan, D., Yu, G., St George Hyslop, P., and Goutte, C. (2001b). APH-2/nicastrin functions in LIN-12/Notch signaling in the *Caenorhabditis elegans* somatic gonad. *Dev Biol* **240**, 654-61.
- Lewis, J., Dickson, D. W., Lin, W. L., Chisholm, L., Corral, A., Jones, G., Yen, S. H., Sahara, N., Skipper, L., Yager, D., Eckman, C., Hardy, J., Hutton, M., and McGowan, E. (2001). Enhanced neurofibrillary degeneration in transgenic mice expressing mutant tau and APP. *Science* **293**, 1487-91.

- L'Hernault, S. W., and Arduengo, P. M. (1992). Mutation of a putative sperm membrane protein in *Caenorhabditis elegans* prevents sperm differentiation but not its associated meiotic divisions. *J Cell Biol* **119**, 55-68.
- Li, H. P., Liu, Z. M., and Nirenberg, M. (1997). Kinesin-73 in the nervous system of *Drosophila* embryos. *Proc Natl Acad Sci U S A* **94**, 1086-91.
- Li, X., and Greenwald, I. (1996). Membrane topology of the *C. elegans* SEL-12 presenilin. *Neuron* **17**, 1015-21.
- Li, X., and Greenwald, I. (1997). HOP-1, a *Caenorhabditis elegans* presenilin, appears to be functionally redundant with SEL-12 presenilin and to facilitate LIN-12 and GLP-1 signaling. *Proc Natl Acad Sci U S A* **94**, 12204-9.
- Li, X., and Greenwald, I. (1998). Additional evidence for an eight-transmembrane-domain topology for *Caenorhabditis elegans* and human presenilins. *Proc Natl Acad Sci U S A* **95**, 7109-14.
- Li, Y. M., Lai, M. T., Xu, M., Huang, Q., DiMuzio-Mower, J., Sardana, M. K., Shi, X. P., Yin, K. C., Shafer, J. A., and Gardell, S. J. (2000a). Presenilin 1 is linked with gamma-secretase activity in the detergent solubilized state. *Proc Natl Acad Sci U S A* **97**, 6138-43.
- Li, Y. M., Xu, M., Lai, M. T., Huang, Q., Castro, J. L., DiMuzio-Mower, J., Harrison, T., Lellis, C., Nadin, A., Neduveilil, J. G., Register, R. B., Sardana, M. K., Shearman, M. S., Smith, A. L., Shi, X. P., Yin, K. C., Shafer, J. A., and Gardell, S. J. (2000b). Photoactivated gamma-secretase inhibitors directed to the active site covalently label presenilin 1. *Nature* **405**, 689-94.
- Lopez-Schier, H., and St Johnston, D. (2002). *Drosophila* nicastrin is essential for the intramembranous cleavage of notch. *Dev Cell* **2**, 79-89.
- Lory, S., and Strom, M. S. (1997). Structure-function relationship of type-IV prepilin peptidase of *Pseudomonas aeruginosa*--a review. *Gene* **192**, 117-21.
- Mango, S. E., Maine, E. M., and Kimble, J. (1991). Carboxy-terminal truncation activates *glp-1* protein to specify vulval fates in *Caenorhabditis elegans*. *Nature* **352**, 811-5.
- Mango, S. E., Thorpe, C. J., Martin, P. R., Chamberlain, S. H., and Bowerman, B. (1994). Two maternal genes, *apx-1* and *pie-1*, are required to distinguish the fates of equivalent blastomeres in the early *Caenorhabditis elegans* embryo. *Development* **120**, 2305-15.
- Mattson, M. P., Chan, S. L., and Camandola, S. (2001). Presenilin mutations and calcium signaling defects in the nervous and immune systems. *Bioessays* **23**, 733-44.
- Mattson, M. P., Cheng, B., Culwell, A. R., Esch, F. S., Lieberburg, I., and Rydel, R. E. (1993). Evidence for excitoprotective and intraneuronal calcium-regulating roles for secreted forms of the beta-amyloid precursor protein. *Neuron* **10**, 243-54.
- Mello, C. C., Draper, B. W., and Priess, J. R. (1994). The maternal genes *apx-1* and *glp-1* and establishment of dorsal-ventral polarity in the early *C. elegans* embryo. *Cell* **77**, 95-106.
- Mickey, K. M., Mello, C. C., Montgomery, M. K., Fire, A., and Priess, J. R. (1996). An inductive interaction in 4-cell stage *C. elegans* embryos involves APX-1 expression in the signalling cell. *Development* **122**, 1791-8.
- Morihara, T., Katayama, T., Sato, N., Yoneda, T., Manabe, T., Hitomi, J., Abe, H., Imaizumi, K., and Tohyama, M. (2000). Absence of endoproteolysis but no effects on amyloid beta production by alternative splicing forms of presenilin-1, which lack exon 8 and replace D257A. *Brain Res Mol Brain Res* **85**, 85-90.
- Moskowitz, I. P., Gendreau, S. B., and Rothman, J. H. (1994). Combinatorial specification of blastomere identity by *glp-1*-dependent cellular interactions in the nematode *Caenorhabditis elegans*. *Development* **120**, 3325-38.

- Moskowitz, I. P., and Rothman, J. H. (1996). *lin-12* and *glp-1* are required zygotically for early embryonic cellular interactions and are regulated by maternal GLP-1 signaling in *Caenorhabditis elegans*. *Development* **122**, 4105-17.
- Mumm, J. S., and Kopan, R. (2000). Notch signaling: from the outside in. *Dev Biol* **228**, 151-65.
- Nakai, T., Yamasaki, A., Sakaguchi, M., Kosaka, K., Mihara, K., Amaya, Y., and Miura, S. (1999). Membrane topology of Alzheimer's disease-related presenilin 1. Evidence for the existence of a molecular species with a seven membrane-spanning and one membrane-embedded structure. *J Biol Chem* **274**, 23647-58.
- Newman, A. P., Inoue, T., Wang, M., and Sternberg, P. W. (2000). The *Caenorhabditis elegans* heterochronic gene *lin-29* coordinates the vulval-uterine-epidermal connections. *Curr Biol* **10**, 1479-88.
- Newman, A. P., and Sternberg, P. W. (1996). Coordinated morphogenesis of epithelia during development of the *Caenorhabditis elegans* uterine-vulval connection. *Proc Natl Acad Sci U S A* **93**, 9329-33.
- Newman, A. P., White, J. G., and Sternberg, P. W. (1995). The *Caenorhabditis elegans lin-12* gene mediates induction of ventral uterine specialization by the anchor cell. *Development* **121**, 263-71.
- Newman, A. P., White, J. G., and Sternberg, P. W. (1996). Morphogenesis of the *C. elegans* hermaphrodite uterus. *Development* **122**, 3617-26.
- Nowotny, P., Gorski, S. M., Han, S. W., Philips, K., Ray, W. J., Nowotny, V., Jones, C. J., Clark, R. F., Cagan, R. L., and Goate, A. M. (2000). Posttranslational modification and plasma membrane localization of the *Drosophila melanogaster* presenilin. *Mol Cell Neurosci* **15**, 88-98.
- Nye, J. S., Kopan, R., and Axel, R. (1994). An activated Notch suppresses neurogenesis and myogenesis but not gliogenesis in mammalian cells. *Development* **120**, 2421-30.
- Okochi, M., Eimer, S., Bottcher, A., Baumeister, R., Romig, H., Walter, J., Capell, A., Steiner, H., and Haass, C. (2000). A loss of function mutant of the presenilin homologue SEL-12 undergoes aberrant endoproteolysis in *Caenorhabditis elegans* and increases abeta 42 generation in human cells. *J Biol Chem* **275**, 40925-32.
- Okochi, M., Steiner, H., Fukumori, A., Tanii, H., Tomita, T., Tanaka, T., Iwatsubo, T., Kudo, T., Takeda, M., and Haass, C. (2002). Presenilins mediate a dual intramembranous gamma-secretase cleavage of Notch-1. *Embo J* **21**, 5408-16.
- Perez, R. G., Zheng, H., Van der Ploeg, L. H., and Koo, E. H. (1997). The beta-amyloid precursor protein of Alzheimer's disease enhances neuron viability and modulates neuronal polarity. *J Neurosci* **17**, 9407-14.
- Podlisny, M. B., Citron, M., Amarante, P., Sherrington, R., Xia, W., Zhang, J., Diehl, T., Levesque, G., Fraser, P., Haass, C., Koo, E. H., Seubert, P., St George-Hyslop, P., Teplow, D. B., and Selkoe, D. J. (1997). Presenilin proteins undergo heterogeneous endoproteolysis between Thr291 and Ala299 and occur as stable N- and C-terminal fragments in normal and Alzheimer brain tissue. *Neurobiol Dis* **3**, 325-37.
- Poirier, J. (2000). Apolipoprotein E and Alzheimer's disease. A role in amyloid catabolism. *Ann N Y Acad Sci* **924**, 81-90.
- Price, D. L., Tanzi, R. E., Borchelt, D. R., and Sisodia, S. S. (1998). Alzheimer's disease: genetic studies and transgenic models. *Annu Rev Genet* **32**, 461-93.
- Price, D. L., Wong, P. C., Markowska, A. L., Lee, M. K., Thinakaran, G., Cleveland, D. W., Sisodia, S. S., and Borchelt, D. R. (2000). The value of transgenic models for the study of neurodegenerative diseases. *Ann N Y Acad Sci* **920**, 179-91.
- Priess, J. R. (1994). Establishment of initial asymmetry in early *Caenorhabditis elegans* embryos. *Curr Opin Genet Dev* **4**, 563-8.

- Priess, J. R., Schnabel, H., and Schnabel, R. (1987). The *glp-1* locus and cellular interactions in early *C. elegans* embryos. *Cell* **51**, 601-11.
- Ratovitski, T., Slunt, H. H., Thinakaran, G., Price, D. L., Sisodia, S. S., and Borchelt, D. R. (1997). Endoproteolytic processing and stabilization of wild-type and mutant presenilin. *J Biol Chem* **272**, 24536-41.
- Ray, W. J., Yao, M., Mumm, J., Schroeter, E. H., Saftig, P., Wolfe, M., Selkoe, D. J., Kopan, R., and Goate, A. M. (1999). Cell surface presenilin-1 participates in the gamma-secretase-like proteolysis of Notch. *J Biol Chem* **274**, 36801-7.
- Renbaum, P., and Levy-Lahad, E. (1998). Monogenic determinants of familial Alzheimer's disease: presenilin-2 mutations. *Cell Mol Life Sci* **54**, 910-9.
- Rozmahel, R., Mount, H. T., Chen, F., Nguyen, V., Huang, J., Erdebil, S., Liauw, J., Yu, G., Hasegawa, H., Gu, Y., Song, Y. Q., Schmidt, S. D., Nixon, R. A., Mathews, P. M., Bergeron, C., Fraser, P., Westaway, D., and St George-Hyslop, P. (2002). Alleles at the Nicastrin locus modify presenilin 1- deficiency phenotype. *Proc Natl Acad Sci U S A* **99**, 14452-7.
- Rudel, D., and Kimble, J. (2001). Conservation of *glp-1* regulation and function in nematodes. *Genetics* **157**, 639-54.
- Rudel, D., and Kimble, J. (2002). Evolution of discrete Notch-like receptors from a distant gene duplication in *Caenorhabditis*. *Evol Dev* **4**, 319-33.
- Sastre, M., Steiner, H., Fuchs, K., Capell, A., Multhaup, G., Condron, M. M., Teplow, D. B., and Haass, C. (2001). Presenilin-dependent gamma-secretase processing of beta-amyloid precursor protein at a site corresponding to the S3 cleavage of Notch. *EMBO Rep* **2**, 835-41.
- Seeger, M., Nordstedt, C., Petanceska, S., Kovacs, D. M., Gouras, G. K., Hahne, S., Fraser, P., Levesque, L., Czernik, A. J., George-Hyslop, P. S., Sisodia, S. S., Thinakaran, G., Tanzi, R. E., Greengard, P., and Gandy, S. (1997). Evidence for phosphorylation and oligomeric assembly of presenilin 1. *Proc Natl Acad Sci U S A* **94**, 5090-4.
- Selkoe, D. J. (2001). Alzheimer's disease: genes, proteins, and therapy. *Physiol Rev* **81**, 741-66.
- Shaye, D. D., and Greenwald, I. (2002). Endocytosis-mediated downregulation of LIN-12/Notch upon Ras activation in *Caenorhabditis elegans*. *Nature* **420**, 686-90.
- Shearman, M. S., Beher, D., Clarke, E. E., Lewis, H. D., Harrison, T., Hunt, P., Nadin, A., Smith, A. L., Stevenson, G., and Castro, J. L. (2000). L-685,458, an aspartyl protease transition state mimic, is a potent inhibitor of amyloid beta-protein precursor gamma-secretase activity. *Biochemistry* **39**, 8698-704.
- Shen, J., Bronson, R. T., Chen, D. F., Xia, W., Selkoe, D. J., and Tonegawa, S. (1997). Skeletal and CNS defects in Presenilin-1-deficient mice. *Cell* **89**, 629-39.
- Simons, M., Keller, P., De Strooper, B., Beyreuther, K., Dotti, C. G., and Simons, K. (1998). Cholesterol depletion inhibits the generation of beta-amyloid in hippocampal neurons. *Proc Natl Acad Sci U S A* **95**, 6460-4.
- Sisodia, S. S., Koo, E. H., Hoffman, P. N., Perry, G., and Price, D. L. (1993). Identification and transport of full-length amyloid precursor proteins in rat peripheral nervous system. *J Neurosci* **13**, 3136-42.
- Smith-Swintosky, V. L., Pettigrew, L. C., Craddock, S. D., Culwell, A. R., Rydel, R. E., and Mattson, M. P. (1994). Secreted forms of beta-amyloid precursor protein protect against ischemic brain injury. *J Neurochem* **63**, 781-4.
- Steinbach, J. P., Muller, U., Leist, M., Li, Z. W., Nicotera, P., and Aguzzi, A. (1998). Hypersensitivity to seizures in beta-amyloid precursor protein deficient mice. *Cell Death Differ* **5**, 858-66.
- Steiner, H., Capell, A., Pesold, B., Citron, M., Kloetzl, P. M., Selkoe, D. J., Romig, H., Mendla, K., and Haass, C. (1998). Expression of Alzheimer's disease-associated

- presenilin-1 is controlled by proteolytic degradation and complex formation. *J Biol Chem* **273**, 32322-31.
- Steiner, H., Kostka, M., Romig, H., Basset, G., Pesold, B., Hardy, J., Capell, A., Meyn, L., Grim, M. L., Baumeister, R., Fichtler, K., and Haass, C. (2000). Glycine 384 is required for presenilin-1 function and is conserved in bacterial polytopic aspartyl proteases. *Nat Cell Biol* **2**, 848-51.
- Steiner, H., Winkler, E., Edbauer, D., Prokop, S., Basset, G., Yamasaki, A., Kostka, M., and Haass, C. (2002). PEN-2 is an integral component of the gamma-secretase complex required for coordinated expression of presenilin and nicastrin. *J Biol Chem* **277**, 39062-5.
- Sternberg, P. W. (1988). Lateral inhibition during vulval induction in *Caenorhabditis elegans*. *Nature* **335**, 551-4.
- Sternberg, P. W., and Horvitz, H. R. (1986). Pattern formation during vulval development in *C. elegans*. *Cell* **44**, 761-72.
- Sternberg, P. W., and Horvitz, H. R. (1989). The combined action of two intercellular signaling pathways specifies three cell fates during vulval induction in *C. elegans*. *Cell* **58**, 679-93.
- Strittmatter, W. J., Saunders, A. M., Schmechel, D., Pericak-Vance, M., Enghild, J., Salvesen, G. S., and Roses, A. D. (1993). Apolipoprotein E: high-avidity binding to beta-amyloid and increased frequency of type 4 allele in late-onset familial Alzheimer disease. *Proc Natl Acad Sci U S A* **90**, 1977-81.
- Struhl, G., and Adachi, A. (1998). Nuclear access and action of notch in vivo. *Cell* **93**, 649-60.
- Struhl, G., and Adachi, A. (2000). Requirements for presenilin-dependent cleavage of notch and other transmembrane proteins. *Mol Cell* **6**, 625-36.
- Struhl, G., and Greenwald, I. (1999). Presenilin is required for activity and nuclear access of Notch in *Drosophila*. *Nature* **398**, 522-5.
- Struhl, G., and Greenwald, I. (2001). Presenilin-mediated transmembrane cleavage is required for Notch signal transduction in *Drosophila*. *Proc Natl Acad Sci U S A* **98**, 229-34.
- Sturchler-Pierrat, C., Abramowski, D., Duke, M., Wiederhold, K. H., Mistl, C., Rothacher, S., Ledermann, B., Burki, K., Frey, P., Paganetti, P. A., Waridel, C., Calhoun, M. E., Jucker, M., Probst, A., Staufenbiel, M., and Sommer, B. (1997). Two amyloid precursor protein transgenic mouse models with Alzheimer disease-like pathology. *Proc Natl Acad Sci U S A* **94**, 13287-92.
- Sulston, J. E., and Horvitz, H. R. (1977). Post-embryonic cell lineages of the nematode, *Caenorhabditis elegans*. *Dev Biol* **56**, 110-56.
- Sulston, J. E., Schierenberg, E., White, J. G., and Thomson, J. N. (1983). The embryonic cell lineage of the nematode *Caenorhabditis elegans*. *Dev Biol* **100**, 64-119.
- Sulston, J. E., and White, J. G. (1980). Regulation and cell autonomy during postembryonic development of *Caenorhabditis elegans*. *Dev Biol* **78**, 577-97.
- Sundaram, M., and Greenwald, I. (1993a). Genetic and phenotypic studies of hypomorphic *lin-12* mutants in *Caenorhabditis elegans*. *Genetics* **135**, 755-63.
- Sundaram, M., and Greenwald, I. (1993b). Suppressors of a *lin-12* hypomorph define genes that interact with both *lin-12* and *glp-1* in *Caenorhabditis elegans*. *Genetics* **135**, 765-83.
- Swiatek, P. J., Lindsell, C. E., del Amo, F. F., Weinmaster, G., and Gridley, T. (1994). Notch1 is essential for postimplantation development in mice. *Genes Dev* **8**, 707-19.
- Talbot, C., Lendon, C., Craddock, N., Shears, S., Morris, J. C., and Goate, A. (1994). Protection against Alzheimer's disease with apoE epsilon 2. *Lancet* **343**, 1432-3.
- Tanzi, R. E. (1999). A genetic dichotomy model for the inheritance of Alzheimer's disease and common age-related disorders. *J Clin Invest* **104**, 1175-9.

- Tax, F. E., Yeagers, J. J., and Thomas, J. H. (1994). Sequence of *C. elegans lag-2* reveals a cell-signalling domain shared with Delta and Serrate of *Drosophila*. *Nature* **368**, 150-4.
- Thinakaran, G. (2001). Metabolism of presenilins. *J Mol Neurosci* **17**, 183-92.
- Thinakaran, G., Borchelt, D. R., Lee, M. K., Slunt, H. H., Spitzer, L., Kim, G., Ratovitsky, T., Davenport, F., Nordstedt, C., Seeger, M., Hardy, J., Levey, A. I., Gandy, S. E., Jenkins, N. A., Copeland, N. G., Price, D. L., and Sisodia, S. S. (1996). Endoproteolysis of presenilin 1 and accumulation of processed derivatives in vivo. *Neuron* **17**, 181-90.
- Tomita, T., Katayama, R., Takikawa, R., and Iwatsubo, T. (2002). Complex N-glycosylated form of nicastrin is stabilized and selectively bound to presenilin fragments. *FEBS Lett* **520**, 117-21.
- Torroja, L., Chu, H., Kotovsky, I., and White, K. (1999). Neuronal overexpression of APPL, the *Drosophila* homologue of the amyloid precursor protein (APP), disrupts axonal transport. *Curr Biol* **9**, 489-92.
- Tschape, J. A., Hammerschmied, C., Muhlig-Versen, M., Athenstaedt, K., Daum, G., and Kretzschmar, D. (2002). The neurodegeneration mutant lochrig interferes with cholesterol homeostasis and Appl processing. *Embo J* **21**, 6367-6376.
- Walter, J., Capell, A., Grunberg, J., Pesold, B., Schindzielorz, A., Prior, R., Podlisny, M. B., Fraser, P., Hyslop, P. S., Selkoe, D. J., and Haass, C. (1996). The Alzheimer's disease-associated presenilins are differentially phosphorylated proteins located predominantly within the endoplasmic reticulum. *Mol Med* **2**, 673-91.
- Weihl, C. C., Ghadge, G. D., Miller, R. J., and Roos, R. P. (1999). Processing of wild-type and mutant familial Alzheimer's disease-associated presenilin-1 in cultured neurons. *J Neurochem* **73**, 31-40.
- Weihofen, A., Binns, K., Lemberg, M. K., Ashman, K., and Martoglio, B. (2002). Identification of signal peptide peptidase, a presenilin-type aspartic protease. *Science* **296**, 2215-8.
- Weisgraber, K. H., Roses, A. D., and Strittmatter, W. J. (1994). The role of apolipoprotein E in the nervous system. *Curr Opin Lipidol* **5**, 110-6.
- Westlund, B., Parry, D., Clover, R., Basson, M., and Johnson, C. D. (1999). Reverse genetic analysis of *Caenorhabditis elegans* presenilins reveals redundant but unequal roles for *sel-12* and *hop-1* in Notch-pathway signaling. *Proc Natl Acad Sci U S A* **96**, 2497-502.
- Wilkinson, H. A., Fitzgerald, K., and Greenwald, I. (1994). Reciprocal changes in expression of the receptor *lin-12* and its ligand *lag-2* prior to commitment in a *C. elegans* cell fate decision. *Cell* **79**, 1187-98.
- Wilkinson, H. A., and Greenwald, I. (1995). Spatial and temporal patterns of *lin-12* expression during *C. elegans* hermaphrodite development. *Genetics* **141**, 513-26.
- Wisniewski, T., Castano, E. M., Golabek, A., Vogel, T., and Frangione, B. (1994). Acceleration of Alzheimer's fibril formation by apolipoprotein E in vitro. *Am J Pathol* **145**, 1030-5.
- Wisniewski, T., Dowjat, W. K., Buxbaum, J. D., Khorkova, O., Efthimiopoulos, S., Kulczycki, J., Lojkowska, W., Wegiel, J., Wisniewski, H. M., and Frangione, B. (1998). A novel Polish presenilin-1 mutation (P117L) is associated with familial Alzheimer's disease and leads to death as early as the age of 28 years. *Neuroreport* **9**, 217-21.
- Wittenburg, N., Eimer, S., Lakowski, B., Rohrig, S., Rudolph, C., and Baumeister, R. (2000). Presenilin is required for proper morphology and function of neurons in *C. elegans*. *Nature* **406**, 306-9.

- Wolfe, M. S., Xia, W., Ostaszewski, B. L., Diehl, T. S., Kimberly, W. T., and Selkoe, D. J. (1999). Two transmembrane aspartates in presenilin-1 required for presenilin endoproteolysis and gamma-secretase activity. *Nature* **398**, 513-7.
- Wong, P. C., Zheng, H., Chen, H., Becher, M. W., Sirinathsinghji, D. J., Trumbauer, M. E., Chen, H. Y., Price, D. L., Van der Ploeg, L. H., and Sisodia, S. S. (1997). Presenilin 1 is required for Notch1 and DII1 expression in the paraxial mesoderm. *Nature* **387**, 288-92.
- Xie, H., Litersky, J. M., Hartigan, J. A., Jope, R. S., and Johnson, G. V. (1998). The interrelationship between selective tau phosphorylation and microtubule association. *Brain Res* **798**, 173-83.
- Yang, D. S., Tandon, A., Chen, F., Yu, G., Yu, H., Arawaka, S., Hasegawa, H., Duthie, M., Schmidt, S. D., Ramabhadran, T. V., Nixon, R. A., Mathews, P. M., Gandy, S. E., Mount, H. T., St George-Hyslop, P., and Fraser, P. E. (2002). Mature glycosylation and trafficking of nicastrin modulate its binding to presenilins. *J Biol Chem* **277**, 28135-42.
- Ye, Y., Lukinova, N., and Fortini, M. E. (1999). Neurogenic phenotypes and altered Notch processing in *Drosophila* Presenilin mutants. *Nature* **398**, 525-9.
- Yochem, J., and Greenwald, I. (1989). *glp-1* and *lin-12*, genes implicated in distinct cell-cell interactions in *C. elegans*, encode similar transmembrane proteins. *Cell* **58**, 553-63.
- Yu, G., Chen, F., Levesque, G., Nishimura, M., Zhang, D. M., Levesque, L., Rogaeva, E., Xu, D., Liang, Y., Duthie, M., St George-Hyslop, P. H., and Fraser, P. E. (1998). The presenilin 1 protein is a component of a high molecular weight intracellular complex that contains beta-catenin. *J Biol Chem* **273**, 16470-5.
- Yu, G., Nishimura, M., Arawaka, S., Levitan, D., Zhang, L., Tandon, A., Song, Y. Q., Rogaeva, E., Chen, F., Kawarai, T., Supala, A., Levesque, L., Yu, H., Yang, D. S., Holmes, E., Milman, P., Liang, Y., Zhang, D. M., Xu, D. H., Sato, C., Rogaeva, E., Smith, M., Janus, C., Zhang, Y., Aebbersold, R., Farrer, L. S., Sorbi, S., Bruni, A., Fraser, P., and St George-Hyslop, P. (2000). Nicastrin modulates presenilin-mediated notch/*glp-1* signal transduction and betaAPP processing. *Nature* **407**, 48-54.
- Zhang, J., Kang, D. E., Xia, W., Okochi, M., Mori, H., Selkoe, D. J., and Koo, E. H. (1998). Subcellular distribution and turnover of presenilins in transfected cells. *J Biol Chem* **273**, 12436-42.
- Zheng, H., Jiang, M., Trumbauer, M. E., Hopkins, R., Sirinathsinghji, D. J., Stevens, K. A., Conner, M. W., Slunt, H. H., Sisodia, S. S., Chen, H. Y., and Van der Ploeg, L. H. (1996). Mice deficient for the amyloid precursor protein gene. *Ann N Y Acad Sci* **777**, 421-6.

CHAPTER II

Amyloid Aggregates, Presenilins, and Alzheimer's Disease

published as:

Baumeister R and **Eimer S** (1998)

Amyloid Aggregates, Presenilins, and Alzheimer's Disease

Angew. Chem. Int. Ed. **37** (21): 2978-2982.

Amyloid Aggregates, Presenilins, and Alzheimer's Disease

Ralf Baumeister* and Stefan Eimer

Alzheimer's disease is today the most common cause of neurodegenerative death in the western world. The disease is characterized by two fundamental events, the accumulation of insoluble fibrillar aggregates of β -amyloid peptide ($A\beta$) and the degeneration and death of neurons in the brain regions that are concerned with learning and memory processes. Abnormal protein deposition is also a shared characteristic of other age-related neurodegenerative diseases, such as Parkinson's disease, Huntington's disease, and the Prion diseases. There is increasing evidence that the mechanism of this aggregation may be similar in each of these diseases.^[1] Several recent studies have advanced our understanding considerably of the molecular and cellular mechanisms that cause the disease. The purpose of this article is to summarize recent results.

The Biochemistry of APP Processing and Amyloid Aggregation

The central role in the pathogenesis of Alzheimer's disease is played by a small, 40–42 amino acid long, four kDa peptide called $A\beta$. $A\beta$ is derived from the 695–770 amino acid long amyloid precursor protein (APP) by various proteolytic steps that are thought to take place in several intracellular compartments^[2] (Figure 1). The detailed mechanism of $A\beta$ production from APP, the exact localization of the three proteases involved, and the functions of $A\beta$ and APP are

not yet understood (for review articles see refs. [3, 4]). The 40 amino acid peptide $A\beta_{40}$ is the predominant form that is produced during the metabolism of APP. Under pathological conditions the production of a 42 amino acid variant ($A\beta_{42}$), normally a minor product, is enhanced.

$A\beta_{40}$ is kinetically inert for several days in solution. In the disease state it is converted into a fibrous form, which is relatively resistant to chemical denaturing or proteolytic digestion.^[5] This conversion is mediated by a change in the three-dimensional structure of $A\beta_{40}$ and results in an increase in the hydrophobicity of the peptide. The peptide then aggregates and forms an ordered fibrillar morphology. The structural properties of the $A\beta$ aggregates suggest that, in contrast to amorphous precipitates, their formation is seeded and involves polymerization from a nucleus.^[1, 6] This process is very slow because of the high entropy of intermolecular interactions.^[6] For this reason, the sporadic forms of Alzheimer's disease, which comprise the fast majority of clinical cases, occur late in life (usually between the ages of 75 and 85), although $A\beta$ can be detected much earlier. Another $A\beta$ variant, $A\beta_{42}$, is more hydrophobic and may produce the pathogenic seed in the development of the disease.^[6] $A\beta_{42}$ is highly aggregable and is the predominant form of $A\beta$ in senile plaques.^[2] Overexpression of APP increases the amount of $A\beta_{40}$ and $A\beta_{42}$ and results in faster aggregation.^[7] It is in this context interesting to note that patients with Down's syndrome, who have an additional copy of chromosome 21 on which the APP gene is located, invariably develop symptoms of Alzheimer's disease and develop them significantly earlier.^[3]

[*] Dr. R. Baumeister, Dipl.-Biochem. S. Eimer
Genzentrum der Ludwigs-Maximilians-Universität
Feodor-Lynen-Strasse 25, D-81377 Munich (Germany)
Fax: (+49) 89-7401-7314
E-mail: bmeister@lmb.uni-muenchen.de

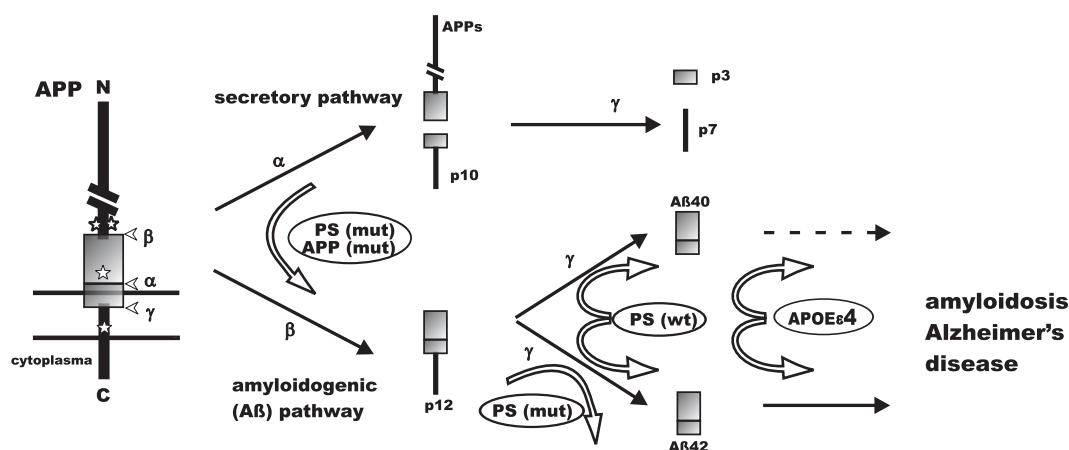


Figure 1. Flowchart of APP metabolism. The factors that affect the processing of APP and the onset of the disease are shown. Left: Schematic representation of APP with the relative positions of mutations indicated by asterisks. The position of the $A\beta$ region is shown by a box. p3, p7, p10, p12 = APP cleavage products with molecular weights of 3, 7, 10, and 12 kDa size, respectively; α , β , γ = secretases involved in the cleavages; mut: mutation; wt = normal type.

Modulators of Aggregation

The first susceptibility gene identified for the common, sporadic form of Alzheimer's disease was the *apoe* gene, which encodes a protein involved in cholesterol transport.^[8] People with a particular variant of the APOE protein (the $\epsilon 4$ isoform), have an increased risk of developing sporadic late-onset Alzheimer's disease.

Convincing evidence that the *apoe* gene directly affects $A\beta$ deposition was provided by Paul's research group.^[9] They crossed transgenic mice overexpressing a human APP variant, which exhibits strong $A\beta$ and amyloid deposition, with *apoe*-knock-out mice. The progeny from this cross showed a dramatic reduction of $A\beta$ deposits, which indicates that the main contribution of the APOE protein is to promote $A\beta$ fibril formation. Another recent report suggests that other polymorphisms in the transcriptional regulatory region of the *apoe* gene might also be associated with an increased risk of Alzheimer dementia, even in the absence of the $\epsilon 4$ isoform.^[10]

The APOE protein may be considered a modifier of Alzheimer's disease since APOE variants do not result in an earlier onset of the disease but promote the late stages of the disease. In contrast, mutations in the three identified loci on chromosomes 2, 14, and 21 cause an heritable form of the disease (FAD, familial Alzheimer's disease) that generally leads to an earlier onset and faster progression of the disease relative to the sporadic cases. All mutations have been shown to promote the seeding of amyloid aggregates. The first gene identified encodes APP itself.^[2,11] The various mutations affect the overproduction of $A\beta 42$ or an overall increase in $A\beta$ secretion. However, these mutations are rare and were found only in a small patient group worldwide. The vast majority of FAD cases correlate with two genes, which encode transmembrane proteins, which been designated presenilin-1 (PS1) and presenilin-2 (PS2). Mutations in PS1 and PS2 are responsible for the most aggressive clinical forms of Alzheimer's disease, with a mean age of onset of approximately 45 and 52 years, respectively. Recent research on the function

of the presenilins provides an important clue to understanding the mechanism of the disease.

Presenilin Mutants and Amyloid Formation

PS1 and PS2 encode proteins of 467 and 448 amino acids, respectively, which are about 67 % identical in their primary sequence.^[12] The presenilins are highly conserved in evolution, and have been identified in nematodes (*Caenorhabditis elegans*), fruit flies (*Drosophila*), clawed frogs (*Xenopus*), Zebrafish, and mammals.^[13] Several research groups have recently analyzed the topology of PS1^[14,15] and its *C. elegans* homologue SEL-12.^[16] The amino and carboxy termini of both proteins have a cytoplasmic localization and is followed by six transmembrane (TM) domains and a large, hydrophilic loop, which again protrudes into the cytoplasm of the cell (Figure 2). It is very likely that the other presenilins adopt similar structures based on the sequence conservation.

The phenotypes associated with mutations in the presenilin genes are most informative for understanding their function in the nervous system. To date, more than 35 mutations in the PS1 gene and two mutations in the PS2 gene have been isolated from FAD patients, which supports the key role of the presenilins in the mechanism of the disease.

With the noteworthy exception of PS1 $\Delta 10$, a splice variant which eliminates exon 10 (but results in a mutation of a highly conserved serine to cysteine at the splice site in TM6), all mutations that have been isolated from patients are single amino substitutions. No mutations have so far been isolated from FAD patients that result in frameshifts or premature translational stops and cause truncations of the carboxy terminal. This suggests that severe structural or functional defects cannot be tolerated in the presenilins. The embryonic lethality of presenilin-knock-out mice supports this view. One plausible explanation would be that the FAD mutations cause subtle defects, since they do not have embryonic phenotypes. More than 80 % of the mutations occur in amino acids that are conserved in presenilins of different species.^[17] The local-

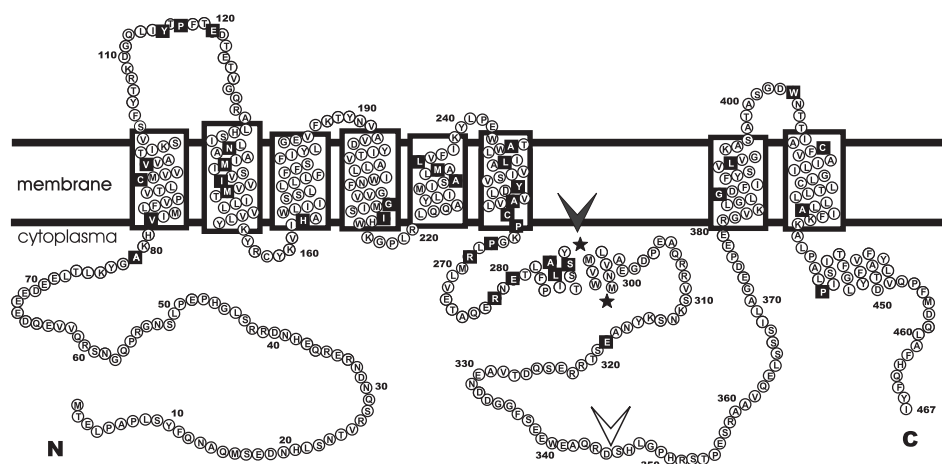


Figure 2. The structure of PS1. The eight transmembrane domain model of PS1 structure is depicted as suggested by Li et al.^[16] Putative TM domains are boxed. Sites of proteolytic cleavage by presenilinase (black arrowhead, exact position: black asterisk) and caspase (white arrowhead) are indicated. Positions of FAD mutations in PS1 are boxed.

ization of these mutations suggests that TM2 and the two large hydrophilic loops are most critical for PS1 function.

Proteolytic Processing of Presenilins

Only a minor amount of the endogenous presenilin proteins can be isolated as full-length proteins. The most abundant fragments identified are an approximately 27–28 kDa amino-terminal fragment (NTF) and an approximately 18–20 kDa carboxy-terminal fragment (CTF).^[12] PS2 is proteolytically cleaved into two stable cellular polypeptides of about 20 kDa and 34 kDa.^[18] The cleavage in the large cytoplasmic loop is obviously tightly regulated, since overproduction of PS results in the accumulation of the full-length protein, but not of the proteolytic fragments. The resulting fragments are very stable and interact with one another. Since they are found in complexes with a higher molecular weight, they probably bind other currently unidentified proteins as well. Considerable effort was made to identify whether presenilinase cleavage is a functional requirement,^[19] a stable degradation intermediate,^[20, 21] or even a preparation artifact.^[22] This question has not yet been fully resolved. Lack of cleavage is probably not a central feature of pathogenesis in FAD patients, since little, if any, full-length PS1 is observed in brain tissue of patients carrying PS1 mutations.^[23]

The presenilins PS1 and PS2 are also proteolytically processed by proteases of the caspase superfamily (proteins that take part in programmed cell death, apoptosis).^[18] This process generates a larger NTF and a smaller CTF if full-length presenilin is the substrate, or only a smaller CTF if the conventional CTF is the substrate (Figure 2). There was a lot of excitement last year when Tanzi's research group reported that the PS2 mutation N141I enhances the intracellular concentration of the alternative CTF derived by caspase-cleavage.^[24] It was postulated that apoptosis-mediated cleavage may be required for the effect of mutant PS proteins on abnormal A β processing. Indeed, a functional involvement of PS in apoptosis had been reported before. However, a combined effort of three research groups showed recently that the inhibition of caspase cleavage does not affect A β

generation. Moreover, mutation of the caspase cleavage site prevented the apoptotic proteolysis, but did not affect the biological activity of human PS1 and PS2 in *C. elegans*.^[25]

Presenilins and the Metabolism of APP

Mutant presenilin proteins, like mutant APP itself, affect proteolytic processing of APP (Figure 1). Mutations in all three genes enhance the processing pathway that results in an increased production of the 42 amino acid variant A β 42, whereas A β 40 levels are not affected.^[12] Since this variant aggregates much faster than A β 40, these results strongly support the model of A β 42 being the key component involved in the disease mechanism. All PS1 and PS2 mutations analyzed to date increase the A β 42 levels significantly. These results strongly support the central role of A β formation and presenilin function in the disease mechanism.

How are the presenilins involved in the proteolytic processing of APP? It has long been thought that proteolysis of APP mostly occurs at or near the cytoplasmic membrane (the non-amyloidogenic or secretory pathway, upper part in Figure 1) or during reinternalization (A β generating pathway, lower part in Figure 1).^[26] In contrast, the presenilins are located mostly in the membranes of the endoplasmic reticulum (ER) and the early Golgi apparatus. However, last year several research groups identified intracellular A β formation and showed that the ER is the first compartment where A β 42 accumulates.^[27–29] These results also suggest that the proteolytic cleavage at the carboxy terminus of A β 40 and A β 42 are accomplished by different enzymes and/or by a different intracellular localization of the enzyme(s) involved. These data provoked an exciting new model that explained how the presenilin can affect APP processing. The localization of the presenilin in the ER and Golgi membranes suggests that they are in a perfect position to control the transport and/or trafficking of APP. There is indeed support for such a role: the presenilin SPE-4 in the nematode *C. elegans* controls the sorting and protein trafficking in specialized organelles.^[30] In addition, several recent publications report that there may be direct binding of PS1 and PS2 to the immature form of APP in

the ER.^[31, 32] Although these interactions, identified through co-immunoprecipitation studies and in the yeast-two-hybrid system, nicely fit into this model, attempts to reproduce these results in other research groups have failed.^[33] Nevertheless, the generally observed increase in A β 42 production in the presence of presenilin mutants indicates that APP and presenilins at least interfere functionally.^[34] It came as a big surprise that in cells of PS1-knock-out mice the A β 40 and A β 42 levels dropped by 80%, whereas neurons in FAD patients have increased levels of A β 42.^[35] Although the subcellular localization of these fragments could not be determined, the most obvious interpretation is that the presenilins themselves have protease (γ -secretase, see Figure 1) activity or may regulate the activity of this protease. However, these results are also compatible with PS1 having a role in the intracellular compartmental transport of membrane proteins. In accordance with the latter model a lack of PS1 could redirect APP sorting and transport from the ER through compartments that lack γ -secretase activities. It is puzzling to see that both A β 40 and A β 42 are equally affected by PS mutants. Additional work is clearly required to solve these discrepancies, and eventually the presenilins might even serve as a therapeutic target for Alzheimer's disease. A significant decrease of presenilin activity, accomplished by either reducing the expression levels or by interfering with the processing, is suggested to reduce the A β production and, thus, the aggregation of plaque formation in the brain.

Biological Function of Presenilins

To fully understand the role of presenilins in Alzheimer's disease it is essential to know more about their biological function. The few data we have are derived from work carried out on the nematode *C. elegans* and in mice. The SEL-12 mutants *C. elegans* suggest that the presenilins play a role in the signal transduction of the Notch transmembrane receptor, a pathway through which adjacent cells communicate.^[36] The human presenilins are also linked to the Notch pathway, since human PS1 and PS2 are functional in *C. elegans*^[20, 21] and Notch activity is strongly reduced in PS1-knock-out mice.^[37, 38] It is not clear, at this point, whether the PS proteins function in the signaling pathway or activity of Notch, or, at an earlier step, in the sorting and transport of Notch from the ER to the membrane. Since SEL-12 mutations seem to influence the function of other secreted transmembrane proteins as well,^[39] which supports the latter model, we suggest that the PS proteins play a more general role in the cell.

Outlook

Significant progress has been made in the past couple of years to understand the molecular and genetic basis of Alzheimer's disease and FAD. The fundamental importance of A β 42 and the presenilins as key players in the disease mechanism has been substantiated. Work in the following years will most likely concentrate on the identification of new genes and interactors to close the remaining gaps in the story. The nematode *C. elegans* model as a biological assay system to identify additional components required for presenilin function, and the availability of several mouse models for A β

aggregation will provide additional clues and maybe targets for therapeutic intervention in the near future.

German version: *Angew. Chem.* **1998**, *110*, 3148–3152

Keywords: Alzheimer's disease • amyloids • presenilin • protein structures

- [1] P. T. Lansbury, Jr., *Neuron* **1997**, *19*, 1151–1154.
- [2] R. E. Tanzi, D. M. Kovacs, T. W. Kim, R. D. Moir, S. Y. Guenette, W. Wasco, *Neurobiol. Disease* **1996**, *3*, 159–168.
- [3] D. J. Selkoe, *J. Biol. Chem.* **1996**, *271*, 18295–18298.
- [4] D. J. Selkoe, *Science* **1997**, *275*, 630–631.
- [5] J. T. Jarrett, E. P. Berger, P. T. Lansbury, Jr., *Ann. N.Y. Acad. Sci.* **1993**, *695*, 144–148.
- [6] J. D. Harper, C. M. Lieber, P. T. Lansbury, Jr., *Chem. Biol.* **1997**, *4*, 951–959.
- [7] K. Hsiao, P. Chapman, S. Nilsen, C. Eckman, Y. Harigaya, S. G. Younkin, F. Yang, G. Cole, *Science* **1996**, *274*, 99–102.
- [8] W. J. Strittmatter, A. D. Roses, *Proc. Natl. Acad. Sci. USA* **1995**, *92*, 4725–4727.
- [9] K. R. Bales, T. Verina, R. C. Dodel, Y. Du, L. Altstiel, M. Bender, P. Hyslop, E. M. Johnstone, S. P. Little, D. J. Cummins, P. Piccardo, B. Ghetti, S. M. Paul, *Nature Genet.* **1997**, *17*, 263–264.
- [10] M. J. Bullido, M. J. Artiga, M. Recuero, I. Sastre, M. A. Garcia, J. Aldudo, C. Lendon, S. W. Han, J. C. Morris, A. Frank, J. Vazquez, A. Goate, F. Valdivieso, *Nature Genet.* **1998**, *18*, 69–71.
- [11] A. Goate, M. C. Chartier-Harlin, M. Mullan, J. Brown, F. Crawford, L. Fidani, L. Giuffra, A. Haynes, N. Irving, L. James, R. Mant, P. Newton, K. Rooke, P. Roques, C. Talbot, M. Pericak-Vance, A. Roses, R. Williamson, M. Rossor, M. Owen, J. Hardy, *Nature* **1991**, *349*, 704–706.
- [12] C. Haass, *Neuron* **1997**, *18*, 687–690.
- [13] R. Baumeister, C. Haass in *The Molecular Biology of Alzheimer's Disease* (Ed.: C. Haass), Harwood Academic Publishers, Chur, **1998**, in print.
- [14] A. Doan, G. Thinakaran, D. R. Borchelt, H. H. Slunt, T. Ratovitsky, M. Podlisny, D. J. Selkoe, M. Seeger, S. E. Gandy, D. L. Price, S. S. Sisodia, *Neuron* **1996**, *17*, 1023–1030.
- [15] S. Lehmann, R. Chiesa, D. A. Harris, *J. Biol. Chem.* **1997**, *272*, 12047–12051.
- [16] X. Li, I. Greenwald, *Neuron* **1996**, *17*, 1015–1021.
- [17] R. E. Tanzi, D. M. Kovacs, T.-W. Kim, R. D. Moir, S. Y. Guenette, W. Wasco, *Alzheimer's Disease Review* **1996**, *1*, 90–98.
- [18] T.-W. Kim, W. H. Pettingell, O. Hallmark, R. D. Moir, W. Wasco, R. E. Tanzi, *J. Biol. Chem.* **1997**, *272*, 11006–11010.
- [19] G. Thinakaran, D. R. Borchelt, M. K. Lee, H. H. Slunt, L. Spitzer, G. Kim, T. Ratovitsky, F. Davenport, C. Norderstedt, M. Seeger, J. Hardy, A. I. Levey, S. E. Gandy, N. A. Jenkins, N. G. Copeland, D. L. Price, S. S. Sisodia, *Neuron* **1996**, *17*, 181–190.
- [20] D. Levitan, T. G. Doyle, D. Brousseau, M. K. Lee, G. Thinakaran, H. H. Slunt, S. S. Sisodia, I. Greenwald, *Proc. Natl. Acad. Sci. USA* **1996**, *93*, 14940–14944.
- [21] R. Baumeister, U. Leimer, I. Zweckbronner, C. Jakubek, J. Grünberg, C. Haass, *Genes Funct.* **1997**, *1*, 149–159.
- [22] N. N. Dewji, C. Do, S. J. Singer, *Proc. Natl. Acad. Sci. USA* **1997**, *94*, 14031–14036.
- [23] L. Hendriks, G. Thinakaran, C. L. Harris, C. D. Jonghe, J.-J. Martin, S. S. Sisodia, C. V. Broeckhoven, *NeuroReport* **1997**, *8*, 1717–1721.
- [24] T. W. Kim, W. H. Pettingell, Y. K. Jung, D. M. Kovacs, R. E. Tanzi, *Science* **1997**, *277*, 373–376.
- [25] M. Brockhaus, J. Grünberg, S. Röhrig, H. Loetscher, N. Wittenburg, R. Baumeister, H. Jacobsen, C. Haass, *NeuroReport* **1998**, *9*, 1481–1486.
- [26] D. J. Selkoe, *Cold Spring Harbor Symp. Quant. Biol.* **1996**, *61*, 587–596.
- [27] C. Wild-Bode, T. Yamazaki, A. Capell, U. Leimer, H. Steiner, Y. Ihara, C. Haass, *J. Biol. Chem.* **1997**, *272*, 16085–16088.
- [28] T. Hartmann, S. C. Bieger, B. Bruhl, P. J. Tienari, N. Ida, D. Allsop, G. W. Roberts, C. L. Masters, C. G. Dotti, K. Unsicker, K. Beyreuther, *Nature Med.* **1997**, *3*, 1016–1020.

HIGHLIGHTS

- [29] D. G. Cook, M. S. Forman, J. C. Sung, S. Leight, D. L. Kolson, T. Iwatsubo, V. M. Lee, R. W. Doms, *Nature Med.* **1997**, *3*, 1021–1023.
- [30] S. W. L. Hernault, G. M. Benian, R. B. Emmons, *Genetics* **1993**, *134*, 769–780.
- [31] A. Weidemann, K. Paliga, U. Dürrwang, C. Czech, G. Evin, C. L. Masters, K. Beyreuther, *Nature Med.* **1997**, *3*, 328–332.
- [32] W. Xia, J. Zhang, R. Perez, E. H. Koo, D. J. Selkoe, *Proc. Natl. Acad. Sci. USA* **1997**, *94*, 8208–8213.
- [33] S. S. Sisodia, G. Thinakaran, H. H. Slunt, P. C. Wong, D. R. Borchelt, S. Naruse, H. Zheng, D. L. Price, *J. Neurochem.* **1998**, *70*, Suppl. 1, S3.
- [34] L. Holcomb, M. N. Gordon, E. McGowan, X. Yu, S. Benkovic, P. Jantzen, K. Wright, I. Saad, R. Mueller, D. Morgan, S. Sanders, C. Zehr, K. O'Campo, J. Hardy, C. M. Prada, C. Eckman, S. Younkin, K. Hsiao, K. Duff, *Nature Med.* **1998**, *4*, 97–100.
- [35] B. De Strooper, P. Saftig, K. Craessaerts, H. Vanderstichele, G. Guhde, W. Annaert, K. von Figura, F. Van Leuven, *Nature* **1998**, *391*, 387–390.
- [36] D. Levitan, I. Greenwald, *Nature* **1995**, *377*, 351–354.
- [37] J. Shen, R. T. Bronson, D. F. Chen, W. Xia, D. J. Selkoe, S. Tonegawa, *Cell* **1997**, *89*, 629–639.
- [38] P. C. Wong, H. Zheng, H. Chen, M. W. Becher, D. J. S. Sirinathsinghji, M. E. Trumbauer, H. Y. Chen, D. L. Price, L. H. T. Van der Pleog, S. S. Sisodia, *Nature* **1997**, *387*, 288–292.
- [39] R. Baumeister, unpublished results.
-

CHAPTER III

A loss of function mutant of the presenilin homologue SEL-12 undergoes aberrant endoproteolysis in *Caenorhabditis elegans* and increased A β 42 generation in human cells

published as:

Okochi M, **Eimer S**, Bottcher A, Baumeister R, Romig H, Walter J, Capell A, Steiner H, Haass C. (2000)

A loss of function mutant of the presenilin homologue *sel-12* undergoes aberrant endoproteolysis in *Caenorhabditis elegans* and increased A β 42 generation in human cells. J Biol Chem **275**: 40925-40932.

A Loss of Function Mutant of the Presenilin Homologue SEL-12 Undergoes Aberrant Endoproteolysis in *Caenorhabditis elegans* and Increases A β 42 Generation in Human Cells*

Received for publication, June 16, 2000, and in revised form, September 25, 2000
Published, JBC Papers in Press, September 29, 2000, DOI 10.1074/jbc.M005254200

Masayasu Okochi[‡], Stefan Eimer[§], Andreas Böttcher[§], Ralf Baumeister[¶]¶, Helmut Romig^{||},
Jochen Walter[‡], Anja Capell[‡], Harald Steiner[‡], and Christian Haass[‡] **

From the [‡]Adolf Butenandt-Institute, Department of Biochemistry, Laboratory for Alzheimer's Disease Research, Ludwig-Maximilians-University, 80336 Munich, Germany, the [§]Genzentrum, Ludwig-Maximilians-University, 81377 Munich, Germany, and the ^{||}Boehringer Ingelheim KG, CNS Research, 55216 Ingelheim, Germany

The familial Alzheimer's disease-associated presenilins (PSs) occur as a dimeric complex of proteolytically generated fragments, which functionally supports endoproteolysis of Notch and the β -amyloid precursor protein (β APP). A homologous gene, *sel-12*, has been identified in *Caenorhabditis elegans*. We now demonstrate that wild-type (wt) SEL-12 undergoes endoproteolytic cleavage in *C. elegans* similar to the PSs in human tissue. In contrast, SEL-12 C60S protein expressed from the *sel-12(ar131)* allele is miscleaved in *C. elegans*, resulting in a larger mutant N-terminal fragment. Neither SEL-12 wt nor C60S undergo endoproteolytic processing upon expression in human cells, suggesting that SEL-12 is cleaved by a *C. elegans*-specific endoproteolytic activity. The loss of function of *sel-12* in *C. elegans* is not associated with a dominant negative activity in human cells, because SEL-12 C60S and the corresponding PS1 C92S mutation do not interfere with Notch1 cleavage. Moreover, both mutant variants increase the aberrant production of the highly amyloidogenic 42-amino acid version of amyloid β -peptide similar to familial Alzheimer's disease-associated human PS mutants. Our data therefore demonstrate that the C60S mutation in SEL-12 is associated with aberrant endoproteolysis and a loss of function in *C. elegans*, whereas a gain of misfunction is observed upon expression in human cells.

Senile plaques composed of amyloid β -peptide (A β)¹ are an

* This work was supported by grants from the European Community (to C. H.) and from the Deutsche Forschungsgemeinschaft (to R. B.). The costs of publication of this article were defrayed in part by the payment of page charges. This article must therefore be hereby marked "advertisement" in accordance with 18 U.S.C. Section 1734 solely to indicate this fact.

** To whom correspondence may be addressed: Adolf-Butenandt-Institute, Ludwig-Maximilians-University Munich, Dept. of Biochemistry; Schillerstrasse 44, Munich D-80336, Germany. Tel.: 49-89-5996-471/472; Fax: 49-89-5996-415; E-mail: chaass@pbm.med.uni-muenchen.de.

¶ To whom correspondence may be addressed: Genzentrum, Feodor-Lynen-Strasse 25, Munich D-81377, Germany. Tel.: 49-89-2180-6938; Fax: 49-89-2180-6946, E-mail: bmeister@lmb.uni-muenchen.de.

¹ The abbreviations used are: A β , amyloid β -peptide; PS, presenilin; AD, Alzheimer's disease; FAD, familial Alzheimer's disease; β APP, β -amyloid precursor protein; HEK 293, human embryonic kidney 293; CTF, C-terminal fragment; NTF, N-terminal fragment; NICD, Notch intracellular cytoplasmic domain; TM, transmembrane; STS, staurosporine; ALLN, *N*-acetyl-leucyl-leucyl-norleucinal; wt, wild-type; Bicine, *N,N*-bis(2-hydroxyethyl)glycine; Tricine, *N*-[2-hydroxy-1,1-bis(hydroxymethyl)ethyl]glycine; PBS, phosphate-buffered saline; CHAPS, 3-[(3-cholamidopropyl)dimethylammonio]-1-propanesulfonic acid.

invariant pathological hallmark of Alzheimer's disease (AD). A β is generated by proteolytic processing from the β -amyloid precursor protein (β APP) (1). β -Secretase, a recently identified aspartyl protease, mediates the N-terminal cleavage (2–5), whereas γ -secretase performs the putative intramembranous C-terminal cut (1). These two sequential cleavages result in the physiological generation and secretion of A β (1).

Familial Alzheimer's disease (FAD) is frequently caused by mutations in the *presenilin* (PS) genes *PS1* and *PS2* (6). PSs are membrane proteins with 7 or 8 transmembrane (TM) domains (7–10). PSs undergo endoproteolysis (11), which results in the formation of a ~30-kDa N-terminal fragment (NTF) and a ~20-kDa C-terminal fragment (CTF). These fragments bind to each other and form a high molecular weight complex (12–15). Fragment formation is highly regulated allowing a limited level of expression (16, 17), which can only be slightly elevated upon transfection (11). Interestingly, ectopic overexpression of PSs results in the displacement of the endogenous PS1 and PS2 molecules (11, 16, 18).

FAD-associated PS mutations are thought to gain a pathological misfunction in the endoproteolytic processing of β APP. Similar to the β APP mutations, PS mutations result in the enhanced production of the highly amyloidogenic 42-amino acid variant of amyloid β -peptide (A β 42) (6).

PSs are not only involved in the aberrant A β production in rare FAD cases but are also required for physiological A β production. A *PS1* gene knock-out inhibits A β production and results in the accumulation of C-terminal β APP fragments, which are thought to be the immediate precursors for the γ -secretase cleavage (19). The inhibition of γ -secretase cleavage indicates that PSs are directly involved in endoproteolysis of β APP. This is supported by the finding that two aspartate residues located within the putative TM domains 6 and/or 7 of PS1 and PS2 are critically required for A β production (20–24). Moreover, Wolfe *et al.* (25) hypothesized that PSs are aspartyl proteases and therefore identical to the γ -secretase, which is strongly supported by the photoaffinity labeling of PS1 and PS2 (26, 27).

PSs do not only support the γ -secretase cleavage of β APP but also a similar cleavage of Notch (28–30) and Ire1 (31). FAD-associated mutations (32) as well as mutagenesis of residue 286 of PS1 to charged amino acids (33) and mutations of the aspartates located in TM6 and TM7 severely reduce endoproteolysis of Notch (21, 34, 35). Further evidence for a function of PSs in Notch signaling is also provided by a knock-out of the *PS1* gene (28, 36, 37), which results in a developmental phenotype similar to the *Notch* knock-out. Moreover, genetic evidence indicates that the PS homologous gene *sel-12* of the nematode

Caenorhabditis elegans is also directly involved in Notch signaling, because two mutations in *sel-12* reduce the activity of a hyperactive allele of *lin-12*, the *C. elegans* Notch homologue (38). These *sel-12* alleles result in an egg-laying defect (38) and a functional defect of two neurons involved in the animal's temperature memory (39). The additional deletion of the second *C. elegans* PS homologue, *hop-1*, strongly enhances the *sel-12* phenotype and results in sterility or early embryonic lethality, depending on the maternal contributions of either *hop-1* or *sel-12* (39–41). This is similar to the finding in mice where the additional ablation of the PS2 gene leads to a full Notch phenotype (42, 43). Both the egg-laying phenotype and the neuronal defects in *C. elegans* can be fully rescued by overexpression of wild-type (wt) PS1 and PS2 (44–47). However, FAD-associated PS1 or PS2 mutants exhibit only a weak activity in this genetic background, suggesting that human FAD mutations exhibit a reduced function rather than a dominant negative function (39, 44, 45). On the other hand, FAD-associated PS1 mutations fully rescue the developmental deficits of the PS1 $-/-$ mice (48, 49).

Although *sel-12* function is genetically well understood (38, 39, 41, 44, 45, 50), little is known about the biochemical abnormalities, which on the molecular level interfere with *sel-12* activity. We therefore analyzed SEL-12 expression and investigated its endoproteolysis as well as its function in proteolytic processing of β APP and Notch. Our data indicate that a loss of *sel-12* function is associated either with a severe truncation of the resulting protein (*sel-12(ar171)*) or a defect in endoproteolysis (*sel-12(ar131)*). Moreover, the *sel-12* loss of function mutation *sel-12 C605* causes a gain of misfunction upon expression in human cells by increasing aberrant A β 42 generation.

MATERIALS AND METHODS

Cell Culture and Cell Lines—Human embryonic kidney 293 (HEK 293) cells were cultured in Dulbecco's modified Eagle's medium supplemented with 10% fetal bovine serum, 1% penicillin/streptomycin, 200 μ g/ml G418 (to select for β APP expression), and 200 μ g/ml zeocin (to select for PS1/SEL-12 expression), as well as 100 μ g/ml hygromycin (to select for Notch Δ E expression). HEK 293 cells stably expressing PS1 D385A were generated as described previously (35).

Construction of cDNAs—The cDNAs encoding PS1 C92S and *sel-12 C60S* were constructed by polymerase chain reaction mediated mutagenesis of codon 92 of PS1 cDNA and codon 60 of *sel-12* cDNA (GeneBank AF171064) using appropriate primers (51). The mutant cDNAs were cloned into the expression vector pcDNA3.1/zeo(+) (Invitrogen) and sequenced to verify successful mutagenesis.

Antibodies—The polyclonal SEL-12 antibody SA6848 was raised against amino acids 297–313 of SEL-12. Antibody 322 to amino acids 226–364 of SEL-12 was raised against a thioredoxin-SEL-12 fusion protein. The polyclonal/monoclonal antibodies 3027/BI.3D7 to PS1 hydrophilic loop and 3711/BI.HF5c to PS2 hydrophilic loop were described previously (47). Antibody 2953 and PS1N (gift from Dr. R. Nixon) against PS1 N terminus were described before (17). Antibody 3926 was raised against synthetic A β and detects both A β 40 and A β 42 (52). The monoclonal antibody 9E10 against *c-myc* was obtained from Developmental Studies Hybridoma Bank (Iowa City, IA) (53).

Preparation of Protein Extracts from Cultured Cells and *C. elegans* Hermaphrodites—Cells were lysed in 10 \times radioimmune precipitation buffer containing 10% Triton X-100, 5% deoxycholic acid (Sigma), and 1% SDS, and diluted 10-fold by PBS containing a protease inhibitor mix (Sigma). 150 mg of frozen worms were resuspended in 300 μ l of 10 \times radioimmune precipitation buffer. The suspension was sonicated for 15 s \times 3 times on ice. Upon sonication, 600 μ l of PBS supplemented with protease inhibitors and 600 mg of glass beads (B. Braun, Melsungen, Germany) were added, and the suspension was incubated for 30 min under constant agitation at 1000 rpm/4 $^{\circ}$ C. After removal of the glass beads, the lysate was sonicated again for 10 s \times 2 times on ice. Insoluble material was removed by centrifugation (15,000 \times g at 4 $^{\circ}$ C). Then, 2.1 ml of PBS containing protease inhibitors was added to the lysate, and SEL-12 was immunoprecipitated as described (51).

Combined Immunoprecipitation/Western Blotting—Cell lysates or worm extracts were immunoprecipitated using the indicated antibodies. Following gel electrophoresis, immunoprecipitated SEL-12 deriva-

tives were identified by immunoblotting using antibody SA6848. Human PSs were identified by immunoblotting using the monoclonal antibody PS1N (to detect the PS1 NTF), BI.3D7 (to detect the PS1 CTF), or BI.HF5c (to detect the PS2 CTF). Bound antibodies were detected by enhanced chemiluminescence using standard procedures (ECL, Amersham Pharmacia Biotech).

CNBr Digest—Proteolytic fragments of PS1 or SEL-12 were purified by immunoprecipitation. Immunoprecipitated SEL-12 and PS derivatives were identified by immunoblotting. Adjacent bands were excised from the gel and incubated in 70% (v/v) formic acid with or without 500 μ l of 80 mg/ml cyanogen bromide (CNBr) overnight at 4 $^{\circ}$ C (54). The solution was dried in a Speed-Vac, redissolved in 50 μ l of H₂O, and dried again. The dried peptides were dissolved in SDS sample buffer and separated by SDS-polyacrylamide gel electrophoresis. SEL-12 fragments were identified by immunoblotting.

In Vitro Cleavage by Caspase-3—PS1 and SEL-12 derivatives were immunoprecipitated from cell lysates and incubated for 4 h at 37 $^{\circ}$ C in 25 μ l of caspase assay buffer (20 mM Hepes/100 mM sodium chloride/10 mM dithiothreitol/10 mM magnesium chloride/1 mM EDTA/0.1% CHAPS/10% sucrose, pH 7.2) in the presence or absence of 20 ng of recombinant active caspase-3 (PharMingen) (55). Fragments were separated by SDS-polyacrylamide gel electrophoresis and identified by immunoblotting.

Induction of Apoptosis—Apoptosis was induced by treating HEK 293 cells with 1 μ M staurosporine (STS) for 6 h as described (62). To protect caspase-generated fragments from degradation, 50 μ M *N*-acetyl-leucyl-leucyl-norleucinal (ALLN) was added to the incubation media (55).

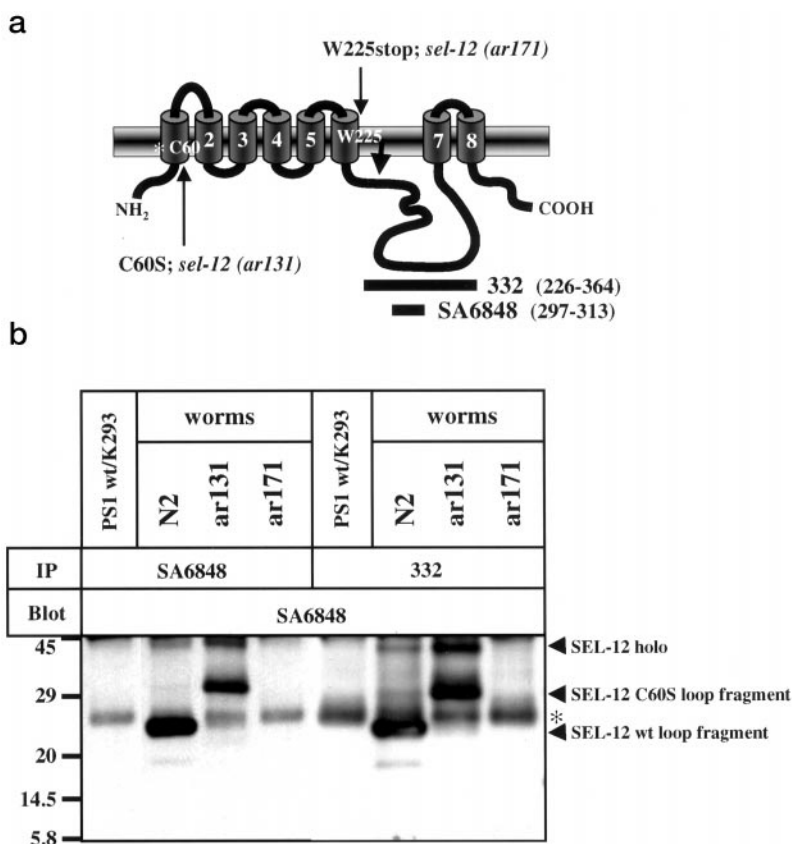
Analysis of β APP Metabolites—Stably transfected HEK 293 cell lines were grown to confluence. For the analysis of A β and p3 in conditioned media, cells were metabolically labeled with 300 μ Ci of [³⁵S]methionine (Promix, Amersham Pharmacia Biotech) as indicated. A β species and p3 were immunoprecipitated from conditioned media with antibody 3926 (52). A β 1–40 and A β 1–42 were separated on previously described Tris-Bicine gels (56).

Analysis of Notch1 Endoproteolysis—cDNAs encoding the myc-tagged Notch Δ E (53) were stably transfected into HEK 293 cells expressing the indicated SEL-12 or PS derivatives. Endoproteolysis of Notch1 Δ E was investigated as described (21).

RESULTS

Aberrant Endoproteolysis of SEL-12 C60S in *C. elegans*—So far, the expression and endoproteolysis of SEL-12 in the nematode *C. elegans* has not been studied in detail. We therefore first analyzed endoproteolysis of wt SEL-12 in the nematode. Protein extracts from wt worms (N2) were prepared and SEL-12 derivatives were isolated by immunoprecipitation using two independent polyclonal antibodies (SA6848 and 322), which were raised against the large cytoplasmic loop of SEL-12 (Fig. 1a). Precipitated SEL-12 derivatives were identified by immunoblotting using antibody SA6848. As a negative control we also analyzed protein extracts from HEK 293 cells transfected with human PS1 as well as worms expressing the *sel-12(ar171)* allele, which results in a premature stop of *sel-12* translation (W225stop) and should therefore not give rise to any specific translation product detected by the antibodies used. Although, indeed, no specific *sel-12* translation products were identified in *C. elegans* expressing the *sel-12(ar171)* allele (Fig. 1b), we detected an approximately 24-kDa CTF in the wt worms (N2) (Fig. 1b). Endoproteolysis of SEL-12 is consistent with the findings that PSs from all other species analyzed, including mice (11), zebrafish (18), and *Drosophila* (57, 58), are proteolytically processed as well. When we analyzed protein extracts derived from worms expressing the *sel-12(ar131)* allele (SEL-12 C60S), we surprisingly did not detect SEL-12 C-terminal fragments of similar molecular weight as observed in the wt worms. Instead of the ~24-kDa CTF obtained in the wt N2 worms, a novel fragment of ~32 kDa was observed (Fig. 1b). In parallel the holoprotein appeared to accumulate as well. This indicates that SEL-12 C60S is not efficiently processed in the worm and that an alternative processing activity leads to an aberrant cleavage.

FIG. 1. Endoproteolysis of SEL-12.
a, schematic diagram of SEL-12 and the antigens (*bars*) used to generate the worm-specific antibodies. The *arrow* denotes the expected conventional cleavage site (8, 9). *b*, expression and endoproteolysis of SEL-12 in *C. elegans*. Lysates from wt PS1-transfected HEK 293 cells or worms (N2, Bristol Strain N2; ar131, *sel-12 C60S*; ar171, *sel-12 W225stop*) (38) were subjected to immunoprecipitation/Western blotting with the indicated antibodies. Lysates from wt PS1-overexpressing cells did not show any specific bands, demonstrating no cross-reaction of SEL-12-specific antibodies with human PS1. Lysates from the *sel-12(ar171)* worms showed no significant SEL-12 derivatives consistent with a premature translational stop at W225. The corresponding NTF cannot be recognized by the antibody SA6848 (see "Discussion"). Note that immunoprecipitation with two independent antibodies, SA6848 and 332, obtained very similar results. The *asterisk* corresponds to IgG light chains.



Alternative Cleavage of SEL-12 C60S Occurs Close to TM7—
 Based on the findings described in Fig. 1*b*, it was difficult to predict the site of alternative cleavage. Alternative cleavage could either occur further C-terminal producing a larger NTF or further N-terminal producing a larger CTF. In both cases the epitopes for antibodies SA6848 and 332 would be retained in the novel proteolytic product. To discriminate between these two possibilities, we performed a cyanogen bromide (CNBr) digest of isolated SEL-12 fragments. Because no methionine residues are observed within the cytoplasmic loop, we predicted that CNBr should not further digest the wt SEL-12 CTF but may result in additional cleavage products upon incubation with the larger SEL-12 C60S fragment (Fig. 2*a*). If the miscleavage would produce a larger NTF due to a C-terminal cleavage close to TM7, CNBr treatment would create a ~17-kDa fragment (corresponding to a peptide between Ala-203 and TM7). In contrast, a larger fragment would be produced by CNBr digestion (between Ala-203 and the C terminus of SEL-12) if endoproteolysis of SEL-12 C60S would occur further N-terminal (Fig. 2*a*).

SEL-12 loop fragments derived from the wt gene as well as from the *sel-12(ar131)* allele were isolated by immunoprecipitation (Fig. 2*b*), separated on Tris-Tricine gels and visualized by immunoblotting using antibody SA6848. Bands of interest were cut out of the gel and subsequently digested with CNBr. Similar experiments were carried out with isolated NTF and CTF of human PS1 (Fig. 2*b*). As shown in Fig. 2*b*, CNBr treatment did not reveal additional fragments, when SEL-12 fragment from the wt N2 worm was digested. This was fully confirmed by CNBr digestion of the human PS1 CTF, whereas the human PS1 NTF was sensitive to CNBr as expected (Fig. 2*b*). In contrast, the alternative SEL-12 proteolytic fragment gave rise to an ~17-kDa species (Fig. 2*b*), which was completely absent upon digestion of the SEL-12 fragment derived from the wt gene (Fig. 2*b*). Based on its molecular mass, the 17-kDa

peptide may correspond to a CNBr fragment starting at Ala-203 within the predicted TM5 (Fig. 2*a*). These results demonstrate that the alternative SEL-12 fragment in mutant *sel-12(ar131)* worms is generated by a cleavage further C-terminal to the physiological cleavage site thus giving rise to a larger N-terminal fragment (Fig. 2*c*).

The Alternative Cleavage Is Not Produced by Caspases—
 It was previously shown that caspases can mediate alternative cleavage of PS1 and PS2 (59–62). SEL-12 indeed contains three potential caspase cleavage sites after the aspartate residues 276, 284, and 345 in the large cytoplasmic loop (Fig. 3*a*). Furthermore, FAD-associated mutations may induce apoptosis (63), and the SEL-12 C60S mutation behaves very similar to FAD mutations (see below). We therefore investigated whether caspases could generate the alternative fragment observed in the SEL-12 C60S worms. If SEL-12 is cleaved at Asp-345, an *in vitro* digest of isolated SEL-12 holoprotein could generate a fragment co-migrating with the alternative fragments observed in the *sel-12(ar131)* worms (Fig. 3*a*). On the other hand, if SEL-12 C60S is cleaved at Asp-276 or Asp-284, the SEL-12 loop antibodies should recognize a caspase-generated CTF, which migrates considerably faster than the regular CTF of SEL-12 (Fig. 3*a*). Based on previous findings (55, 59–61) caspase-3 was chosen for the *in vitro* assay. As substrates we used the wt SEL-12 and the SEL-12 C60S holoproteins isolated from HEK 293 stably transfected with the *sel-12* cDNA (see next paragraph). As shown in Fig. 3 (*b* and *c*), cleavage of wt SEL-12 as well as SEL-12 C60S by caspase-3 resulted in an alternative CTF with a lower molecular mass than the CTF derived from wt worms. Therefore, these data suggest that caspase-3 cleavage of SEL-12 occurs after either Asp-276 or Asp-284 (see Fig. 3*e*). To confirm this finding under *in vivo* conditions, we induced apoptosis in HEK 293 expressing PS1 or SEL-12 with 1 μ M staurosporine (STS). To control STS-induced apoptosis we also monitored the production of the previously described (62)

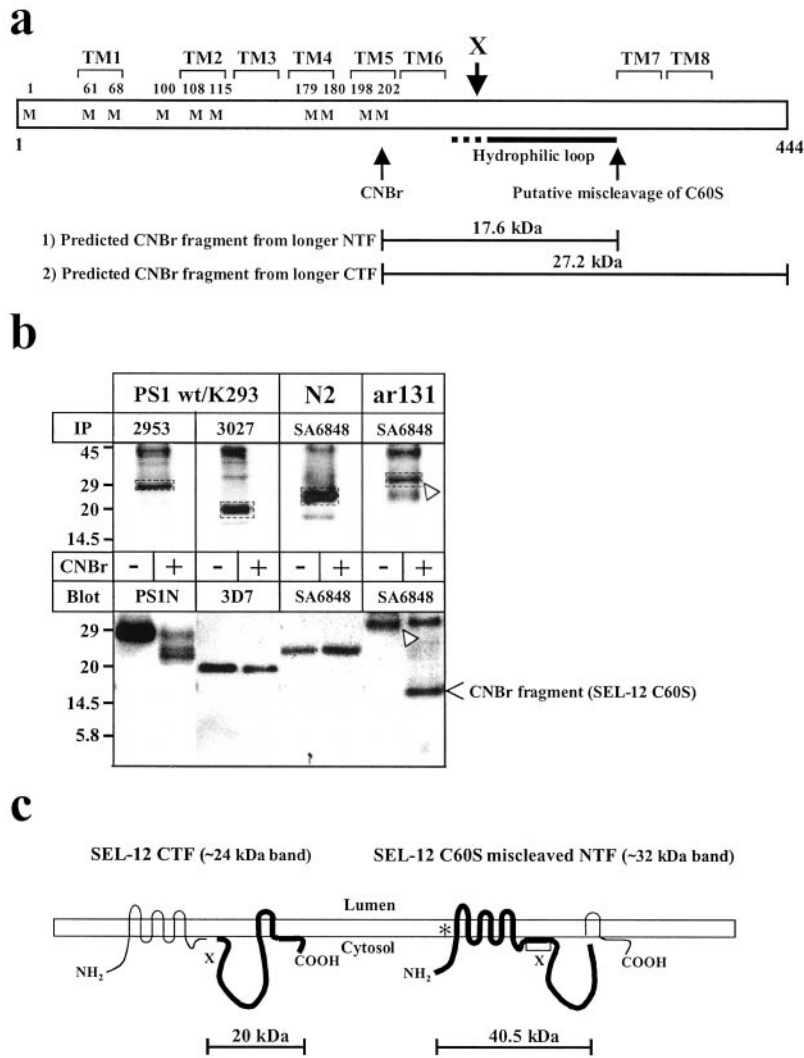


FIG. 2. CNBr digestion of SEL-12 C60S miscleaved fragment. *a*, schematic representation of SEL-12. *M* and *X* denote methionine residues and the predicted conventional cleavage site, respectively. Note that no methionine residues occur in the SEL-12 CTF. *b*, CNBr digestion of PS1 and SEL-12 fragments. Lysates from the indicated cells/worms were immunoprecipitated with the indicated antibodies (*upper panel*). Bands of interest were recovered and incubated in the absence (–) or presence (+) of CNBr. CNBr-sensitive/resistant bands were recovered by Western blotting using the indicated antibodies (*lower panel*). As expected, the PS1 NTF was sensitive to CNBr. However, only limited digestion was observed, which may be due to aggregation of the highly hydrophobic cleavage products. In contrast, the PS1 CTF is largely resistant to CNBr digestion. Note that the PS1 CTF contains 1 to 3 methionine residues depending on its cleavage site at Met-292, Met-298, or Met-457 (69, 73). Because these residues are either very close to the N or C termini, CNBr cleavage at these sites will not substantially affect the molecular mass of the remaining peptide. The SEL-12 CTF is resistant to CNBr digestion as expected. Note that a ~15-kDa fragment was generated by CNBr treatment from the mutant SEL-12 C60S peptide, which is not observed upon digestion of the wt SEL-12 CTF. *Arrowheads* denote the bands which co-migrate with the original band cut out from polyacrylamide gels. *c*, schematic diagram of endoproteolysis of wt SEL-12 and SEL-12 C60S. The *asterisk* indicates the C60S mutation.

alternative CTF of PS1 (Fig. 3*d*, *lower panel*). Under conditions where STS-induced apoptosis led to the generation of the caspase-generated alternative PS1 CTF, a prominent approximately 20-kDa CTF occurred in HEK 293 cells expressing SEL-12. This fragment co-migrated with a SEL-12-derived CTF, which was generated by caspase cleavage *in vitro* (Fig. 3*d*, *upper panel*). These results are consistent with previous results on caspase-generated CTFs of human PSs (59, 62–64). Because the caspase-generated fragment identified by antibody SA6848 exhibits a considerably different molecular mass as the alternative fragments observed in the *sel-12(ar131)* worms (Fig. 3*c*), these data demonstrate that the alternative cleavage in the worm is not mediated by caspases induced during apoptosis (Fig. 3*e*; see also Fig. 2*c*). (Note that only the caspase cleavage of SEL-12 is observed in human cells; see next paragraph.)

Lack of Endoproteolysis of SEL-12 in Human Cells—To test if the miscleavage of SEL-12 can be observed upon expression

in human cells, the wt *sel-12* cDNA as well as the cDNA encoding *sel-12 C60S* were stably transfected into HEK 293 cells. This cell line was previously used in many studies (*i.e.* Refs. 21, 33, 35, 65) to investigate endoproteolysis of PSs as well as their function in Notch and β APP endoproteolysis. To mimic the SEL-12 C60S mutation in human PS1, we introduced the corresponding mutation at the conserved codon 92 (*PS1 C92S*; Fig. 4*a*) and generated cell lines stably expressing this cDNA construct.

PS1 and SEL-12 derivatives were identified by a combined immunoprecipitation/Western blotting protocol. Surprisingly, this revealed no detectable endoproteolysis of SEL-12 (wt or C60S) in human cells, although high levels of the holoprotein were observed (Fig. 4*b*, *first panel*). Because worms are grown at 15–25 °C, the lack of SEL-12 endoproteolysis may be due to aberrant folding of SEL-12 at 37 °C. To test if that could be the case, HEK 293 cells were grown at 25 °C for 24 h. However, under these conditions endoproteolysis of SEL-12 was still not

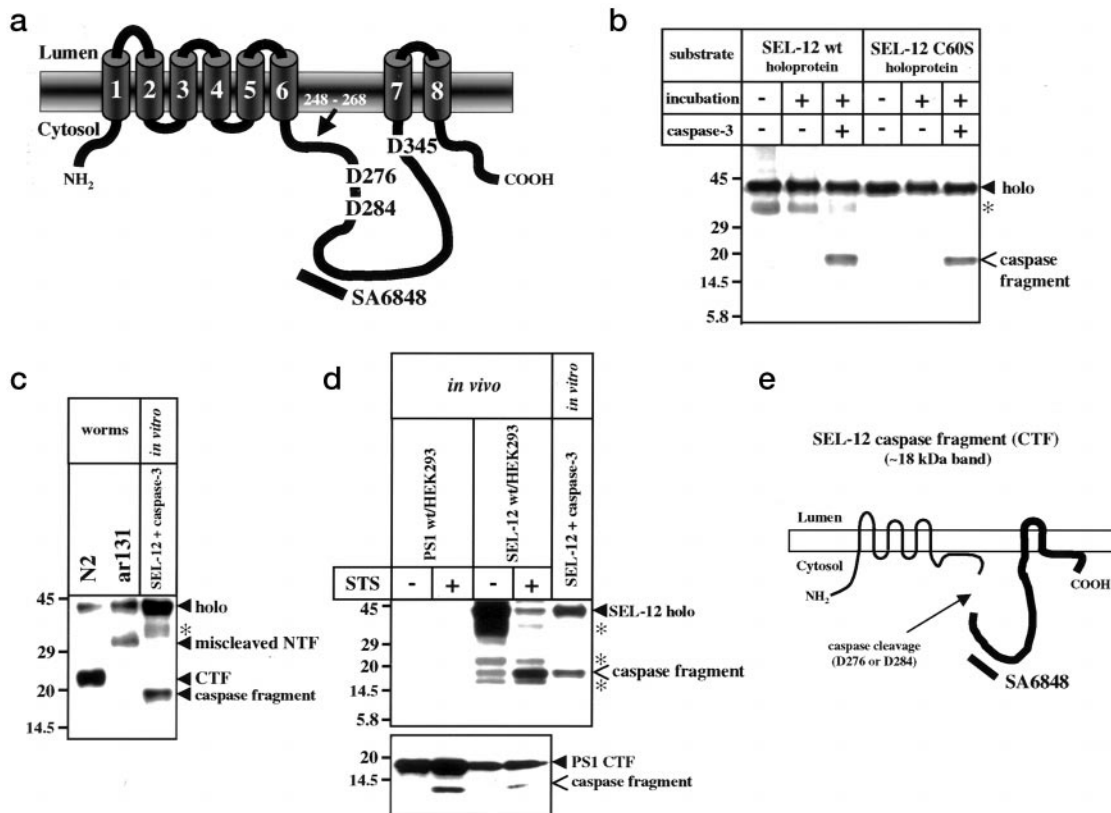


FIG. 3. Caspase cleavage of wt SEL-12 and SEL-12 C60S. *a*, schematic diagram of SEL-12 and the aspartic residues within and close to the hydrophilic loop. Three candidate aspartic residues for caspase cleavage were identified, which may give rise to the alternative cleavage product. *b*, *in vitro* digestion of wt SEL-12 and SEL-12 C60S by caspase-3. Lysates of cells expressing wt SEL-12 or SEL-12 C60S (see also Fig. 4) were immunoprecipitated with SA6848 to isolate SEL-12 holoproteins. Immunoprecipitates were incubated with (+) or without (-) caspase-3. Following proteolytic digestion, the fragments were detected by immunoblotting using the same antibody. Successful digestion by caspase-3 was monitored by the generation of PS1 caspase fragment from PS1 CTF (55) (data not shown). *c*, the SEL-12 caspase fragment does not co-migrate with the alternative fragment observed in *sel-12(ar131)* worms. Caspase-3-digested SEL-12 as well as lysates from *sel-12(ar131)* mutant or wt worms were immunoprecipitated with antibody SA6848. Precipitated SEL-12 derivatives were identified by immunoblotting. *d*, *in vivo* and *in vitro* produced SEL-12 fragments co-migrated. HEK 293 cells expressing wt PS1 or SEL-12 were treated with (+) and without (-) 1 μ M STS to induce apoptosis. SEL-12 derivatives were identified by immunoprecipitation/immunoblotting. As a control, SEL-12 was digested with caspase-3 *in vitro*. Under the same conditions STS treatment resulted in the production of the previously described (62) alternative PS1 CTF (*lower panel*). *e*, schematic diagram of caspase-mediated cleavage of SEL-12. Compare with Fig. 2c. Asterisks indicate degradation products stabilized by ALLN treatment.

observed (Fig. 4b, *second panel*). In contrast, human PS1 did undergo sufficient endoproteolysis under these conditions (Fig. 4b, *third panel*). This suggests that SEL-12 undergoes worm-specific endoproteolysis and indicates that human cells lack a component required for SEL-12 cleavage. Furthermore, introduction of the corresponding C92S mutation into human PS1 led to the generation of a C-terminal fragment co-migrating with PS1 CTFs derived from the wt cDNA (Fig. 4c). This also indicates that the failure in the endoproteolysis of mutant SEL-12 is worm-specific and can not be observed upon expression of the corresponding PS1 mutation in human cells.

We also analyzed whether ectopic expression of SEL-12 results in the replacement of endogenous PS fragments. Replacement of endogenous PS fragments is a widely observed phenomenon and thought to be an indication of a stable expression of the ectopic PS variant (11, 16). We observed that SEL-12 could at least partially replace endogenous PS1 and PS2 fragments, because derivatives of both endogenous PSs are reduced (Fig. 4c; see also Fig. 4b, *lower panel*). However, *sel-12*-mediated replacement of endogenous PSs is not as efficient as the replacement caused by ectopic PS expression (Fig. 4c).

SEL-12 C60S and PS1 C92S Facilitate Notch1 Endoproteolysis in Human Cells—Because SEL-12 C60S results in reduced Notch signaling in the *sel-12(ar131)* allele, we next analyzed whether SEL-12 C60S or the corresponding human PS1 C92S mutation interfere with Notch1 endoproteolysis in hu-

man cells in a dominant negative manner. Cells expressing wt SEL-12, SEL-12 C60S, endogenous PSs, PS1 C92S, or the FAD-associated PS1 L286V were co-transfected with the Notch1 ΔE derivative described previously (21, 28, 33, 35, 53). In pulse-chase experiments we then followed the production of the Notch1 intracellular cytoplasmic domain (NICD). Cells were metabolically labeled for 15 min with [³⁵S]methionine and chased for 60 min in the presence of excess amounts of unlabeled methionine. A 60-min cold chase was chosen, because we and others previously found efficient NICD formation at this time point (21, 33, 66). Interestingly, SEL-12 C60S as well as PS1 C92S efficiently supported NICD formation like all other PS derivatives (Fig. 5; *left panel*). From these results we conclude that, in contrast to the loss of function caused by the active site mutation (Fig. 5; *right panel*), the cysteine to serine mutations in TM1 do not interfere with Notch1 endoproteolysis in human cells. Moreover, neither accumulation of β APP CTFs nor decreased secretion of A β was observed in cells expressing SEL-12 C60S or PS1 C92S (data not shown). Therefore, these mutations do not interfere with Notch1 and β APP endoproteolysis in a dominant negative manner.

A Gain of Misfunction in Human Cells—The C60S mutation occurs at a highly conserved amino acid residue (Fig. 4a). This point mutation is therefore very similar to almost all FAD-associated point mutations, which also occur at evolutionary conserved residues and involve chemically rather subtle amino

acid exchanges (67). We therefore investigated whether the PS1 C92S mutation, which corresponds to the C60S mutation of the worm (see above) exhibits a pathological function in terms of increased A β 42 generation. Conditioned media from metabolically labeled cells stably transfected with wt PS1, the FAD-associated PS1 L286V mutation, and the PS1 C92S mutation were collected and immunoprecipitated with antibody 3926. This antibody immunoprecipitates all A β species, including A β 40 and A β 42 (47). Immunoprecipitates were separated on a previously described gel system, which allowed the specific

detection and quantitation of both A β species (56). Consistent with previous results (33, 68) this revealed that the FAD-associated PS1 L286V mutation increased the A β 42/A β 40 levels (Fig. 6a). Interestingly, the PS1 C92S mutation caused the production of very high levels of A β 42. Quantitation revealed an increase of approximately 3-fold (Fig. 6a). The data were further confirmed by a previously described enzyme-linked immunosorbent assay (17, 18, 21, 33, 35, 47, 69) (data not shown). Therefore, the C60S homologous mutation in human PS1 behaves like a FAD-associated mutation. We next analyzed whether wt SEL-12 or the SEL-12 C60S mutation affects A β 42 generation in human cells. Interestingly, an increased level of A β 42 was observed upon expression of the wt cDNA. This was further elevated upon the expression of the C60S mutation (Fig. 6a). Increased A β 42 production driven by wt SEL-12 indicated that wt SEL-12 has a pathological activity in human cells. Similar to our work on zebrafish PS1 (18), this appears to be due to several different amino acids within SEL-12 protein at positions corresponding to previously identified FAD-associated point mutations (Fig. 6b).

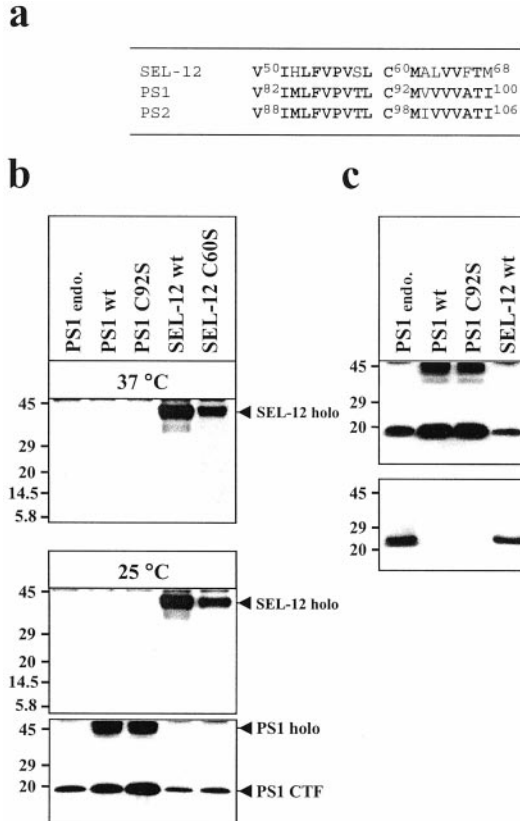


FIG. 4. Expression and endoproteolysis of PS1 C92S, wt SEL-12 and SEL-12 C60S in human cells. *a*, sequence alignment of the TM1 region of SEL-12 and PS1/PS2. Based on the significant sequence similarity, Cys-60 of SEL-12 corresponds to Cys-92 of human PS1. **Boldface letters** denote conserved sequences. *b*, expression and endoproteolysis of wt SEL-12 and SEL-12 C60S in HEK 293 cells. Cells were grown at 37 °C (*first panel*) or 25 °C (*second and third panel*). Aliquots of the lysates were subjected to immunoprecipitation/Western blotting with SA6848 to detect SEL-12 derivatives (*first and second panel*). To identify human PS1 derivatives, cell lysates were immunoprecipitated with antibody 3027 and immunoblotted with BI.3D7 (*third panel*). *c*, replacement of endogenous PSs by overexpressed SEL-12. PS1 derivatives were identified by a combined immunoprecipitation/immunoblotting protocol using antibodies 3027/BI.3D7 (*upper panel*). PS2 derivatives were identified by a combined immunoprecipitation/immunoblotting protocol using antibodies 3711/BI.HF5c (*lower panel*). Note that overexpression of SEL-12 reduces expression of endogenous PS1 and PS2.

DISCUSSION

Experiments to rescue the egg-laying phenotype of *C. elegans* (*sel-12(ar131)*, *sel-12(ar171)*) are now frequently used to test the biological activity of human PSs (44, 45, 47, 50). However, very little is known about the molecular mechanisms of the *sel-12* mutant alleles. Specifically, endoproteolysis of SEL-12, the PS homologue in the worm has so far not been investigated. Because endoproteolysis of human PS proteins appears to be an indication for functional expression and complex formation (11, 13, 14, 17, 70), we now studied the expression of wt SEL-12, SEL-12 C60S (*sel-12(ar131)*) and SEL-12 W225stop (*sel-12(ar171)*) in *C. elegans*.

SEL-12 undergoes endoproteolysis in *C. elegans* very similar to presenilin homologues of other species (18, 57, 58). As observed in other species, we found high levels of a SEL-12 CTF and only low amounts of the corresponding holoprotein. Expression of the *sel-12(ar171)* allele, which results in a premature translational stop at W225 in TM6, produces a truncated derivative that corresponds to a truncated NTF as suggested before (38). Because we and others have shown previously that such a fragment is unstable and biologically inactive, the W225stop mutation may correspond to a functional knock-out (17, 71, 72). In contrast the *sel-12(ar131)* allele is robustly expressed. However, we surprisingly found that the C60S mutation inhibited endoproteolysis at the wt cleavage site. We identified a larger NTF, which suggests that the aberrant endoproteolytic cleavage occurs much further C-terminal to the conventional cleavage site, most likely close to TM7. We had sequenced the *sel-12* coding region in *sel-12(ar131)* worms and tested the correct mRNA length by reverse transcription-polymerase chain reaction (data not shown). Therefore, the aberrant fragment is not due to additional mutations that may result in alternative mRNA splicing. In addition, the *sel-12(ar131)* worms had been backcrossed extensively to remove

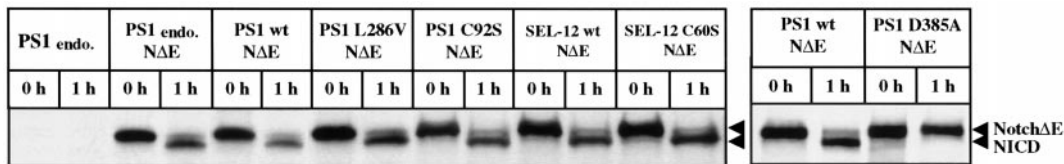


FIG. 5. Notch endoproteolysis is supported by PS1 C92S-, wt SEL-12-, and SEL-12 C60S-expressing cells. *Notch1* ΔE was co-transfected into the cell lines stably expressing wt PS1, PS1 L286V, PS1 C92S, PS1 D385A, wt SEL-12, and SEL-12 C60S. To analyze Notch1 endoproteolysis, cells were pulse-labeled with [³⁵S]methionine and chased for 60 min. Lysates were immunoprecipitated with antibody 9E10 to the *c-myc* tag (53). Only the previously described dominant negative PS1 D385A mutation blocked Notch1 endoproteolysis in a dominant negative manner, whereas all other PS1/SEL-12 derivatives supported Notch1 cleavage. N ΔE denotes Notch1 ΔE .

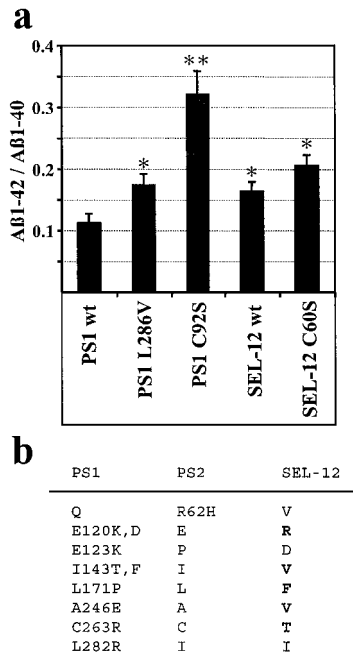


FIG. 6. The pathological function of PS1 C92S, wt SEL-12, and SEL-12 C60S. *a*, quantitation of the A β 1-42/A β 1-40 ratio. Conditioned media from metabolically labeled cells were immunoprecipitated with antibody 3926 to detect all species of A β . A β 1-40 and A β 1-42 were identified on a previously described Tris-Bicine gel system (56). Quantitation of the A β 1-42/A β 1-40 ratio was performed by phosphorimaging. Bars represent the mean \pm S.E. of three independent experiments. Asterisks (*) and (**) correspond to statistical significance (* p < 0.01; Student's t test) and (** p < 0.001; Student's t test), respectively. *b*, amino acid exchanges of SEL-12 at sites corresponding to FAD mutations in human PS1 and PS2. **Boldface letters** indicate SEL-12-specific amino acid exchanges at positions, which are conserved in human PS1 and PS2.

Putative cleavage site		
SEL-12	²⁵⁵ LIYSSG V IY PYVL VT AVE ²⁷²	
PS1 human	²⁸⁶ LIYSS T ↓ M VV LVM J A E GDP ³⁰³	
PS2 mouse	²⁹² LIYSSA M ↓ V V T VGM AK↓LDP ³⁰⁹	

FIG. 7. Alignment of the SEL-12 and PS1/PS2 cleavage sites. Cleavage of human PS1 and PS2 is heterogeneous and appears to occur at three different sites. Arrows denote reported cleavage sites (69, 74, 75, 77). **Boldface letters** indicate conserved amino acids. All three cleavage sites are not conserved in SEL-12.

background mutations in other genes.

The alternative cleavage is remarkable, because the SEL-12 C60S mutation occurs far away from the site of endoproteolytic processing. This suggests that the mutation affects the structure of SEL-12, thus blocking the conventional cleavage site but making a secondary alternative site available for aberrant proteolytic processing. Interestingly, a very similar phenomenon was observed for an envelope protein of spleen necrosis virus (73). Several independent loss-of-function mutations located N-terminal from the conserved retroviral cleavage site of the protein induce aberrant endoproteolysis at a secondary site.

When *sel-12* cDNAs were expressed in human cells, we did not observe any detectable endoproteolysis. It should be emphasized that heterologous overexpression of zebrafish PS1 in human cells allowed normal endoproteolysis (18). Interestingly, the SEL-12 holoprotein was active in A β generation, because wt SEL-12 as well as SEL-12 C60S increased the levels of A β 42 generation very similar to the FAD-associated point mutation PS1 L286V. This is remarkable, because recently it

was claimed that the uncleaved holoprotein of PSs is a proteolytically inactive zymogene (26). However, together with previous findings (69, 76) this appears to be unlikely, because at least some uncleaved PS derivatives can support aberrant A β 42 generation and do not inhibit Notch endoproteolysis in a dominant negative manner like the active site mutations (35, 69, 23). The failure of SEL-12 to undergo endoproteolysis in human cells may be due to the lack of sequence conservation at the endoproteolytic cleavage site (Fig. 7; Refs. 69, 74, 75). This suggests that the endoproteolytic activity of human cells does not recognize SEL-12. However, because SEL-12 induces A β 42 generation in human cells (and is therefore pathologically active), our data suggest that endoproteolysis of PSs and γ -secretase activity are not necessarily correlated.

The C60S mutation occurs at a highly conserved position very similar to the FAD-associated PS1 mutation. Indeed, the introduction of the serine to cysteine mutation at the homologous position of human PS1 resulted in a significant increase of A β 42 generation, as it is observed in all FAD-associated PS mutations. One may therefore speculate that the PS1 C92S mutation could be found at some point in a family with early onset FAD. Strikingly, during the time this manuscript was under consideration, this mutation has been reported to occur in an Italian family (76).

Acknowledgments—We thank Dr. I. Greenwald for the *sel-12* alleles, Drs. D. Selkoe and R. Kopan for the PS1 D385A and the Notch ΔE cDNAs, respectively, and members of our laboratories for helpful discussions and technical assistance.

REFERENCES

- Haass, C., and Selkoe, D. J. (1993) *Cell* **75**, 1039–1042
- Vassar, R., Bennett, B. D., Babu-Khan, S., Kahn, S., Mendiaz, E. A., Denis, P., Teplow, D. B., Ross, S., Amarante, P., Loeloff, R., Luo, Y., Fisher, S., Fuller, J., Edenson, S., Lile, J., Jarosinski, M. A., Biere, A. L., Curran, E., Burgess, T., Louis, J. C., Collins, F., Treanor, J., Rogers, G., and Citron, M. (1999) *Science* **286**, 735–741
- Hussain, I., Powell, D., Howlett, D. R., Tew, D. G., Meek, T. D., Chapman, C., Gloger, I. S., Murphy, K. E., Southan, C. D., Ryan, D. M., Smith, T. S., Simmons, D. L., Walsh, F. S., Dingwall, C., and Christie, G. (1999) *Mol. Cell Neurosci.* **14**, 419–427
- Yan, R., Bienkowski, M. J., Shuck, M. E., Miao, H., Tory, M. C., Pauley, A. M., Brashier, J. R., Stratman, N. C., Mathews, W. R., Buhl, A. E., Carter, D. B., Tomasselli, A. G., Parodi, L. A., Heinrikson, R. L., and Gurney, M. E. (1999) *Nature* **402**, 533–537
- Sinha, S., Anderson, J. P., Barbour, R., Basi, G. S., Caccavello, R., Davis, D., Doan, M., Dovey, H. F., Frigon, N., Hong, J., Jacobson-Croak, K., Jewett, N., Keim, P., Knops, J., Lieberburg, I., Power, M., Tan, H., Tatsuno, G., Tung, J., Schenk, D., Seubert, P., Suomensaari, S. M., Wang, S., Walker, D., Zhao, J., Mconlogue, L., and John, V. (1999) *Nature* **402**, 537–540
- Selkoe, D. J. (1999) *Nature* **399**(Suppl), A23–A31
- Doan, A., Thinakaran, G., Borchelt, D. R., Slunt, H. H., Ratovitsky, T., Podlisny, M., Selkoe, D. J., Seeger, M., Gandy, S. E., Price, D. L., and Sisodia, S. S. (1996) *Neuron* **17**, 1023–1030
- Li, X., and Greenwald, I. (1996) *Neuron* **17**, 1015–1021
- Li, X., and Greenwald, I. (1998) *Proc. Natl. Acad. Sci. U. S. A.* **95**, 7109–7114
- Nakai, T., Yamasaki, A., Sakaguchi, M., Kosaka, K., Mihara, K., Amaya, Y., and Miura, S. (1999) *J. Biol. Chem.* **274**, 23647–23658
- Thinakaran, G., Borchelt, D. R., Lee, M. K., Slunt, H. H., Spitzer, L., Kim, G., Ratovitsky, T., Davenport, F., Nordstedt, C., Seeger, M., Hardy, J., Levey, A. I., Gandy, S. E., Jenkins, N. A., Copeland, N. G., Price, D. L., and Sisodia, S. S. (1996) *Neuron* **17**, 181–190
- Seeger, M., Nordstedt, C., Petanceska, S., Kovacs, D. M., Gouras, G. K., Hahne, S., Fraser, P., Levesque, L., Czernik, A. J., George-Hyslop, P. S., Sisodia, S. S., Thinakaran, G., Tanzi, R. E., Greengard, P., and Gandy, S. (1997) *Proc. Natl. Acad. Sci. U. S. A.* **94**, 5090–5094
- Capell, A., Grunberg, J., Pesold, B., Diehlmann, A., Citron, M., Nixon, R., Beyreuther, K., Selkoe, D. J., and Haass, C. (1998) *J. Biol. Chem.* **273**, 3205–3211
- Yu, G., Chen, F., Levesque, G., Nishimura, M., Zhang, D. M., Levesque, L., Rogaeva, E., Xu, D., Liang, Y., Duthie, M., St. George-Hyslop, P. H., and Fraser, P. E. (1998) *J. Biol. Chem.* **273**, 16470–16475
- Thinakaran, G., Regard, J. B., Bouton, C. M., Harris, C. L., Price, D. L., Borchelt, D. R., and Sisodia, S. S. (1998) *Neurobiol. Dis.* **4**, 438–453
- Thinakaran, G., Harris, C. L., Ratovitsky, T., Davenport, F., Slunt, H. H., Price, D. L., Borchelt, D. R., and Sisodia, S. S. (1997) *J. Biol. Chem.* **272**, 28415–28422
- Steiner, H., Capell, A., Pesold, B., Citron, M., Kloetzel, P. M., Selkoe, D. J., Romig, H., Mendla, K., and Haass, C. (1998) *J. Biol. Chem.* **273**, 32322–32331
- Leimer, U., Lun, K., Romig, H., Walter, J., Grunberg, J., Brand, M., and Haass, C. (1999) *Biochemistry* **38**, 13602–13609
- De Strooper, B., Saftig, P., Craessaerts, K., Vanderstichele, H., Guhde, G.,

- Annaert, W., Von Figura, K., and Van Leuven, F. (1998) *Nature* **391**, 387–390
20. Wolfe, M. S., Xia, W., Ostaszewski, B. L., Diehl, T. S., Kimberly, W. T., and Selkoe, D. J. (1999) *Nature* **398**, 513–517
21. Steiner, H., Duff, K., Capell, A., Romig, H., Grim, M. G., Lincoln, S., Hardy, J., Yu, X., Picciano, M., Fichtler, K., Citron, M., Kopan, R., Pesold, B., Keck, S., Baader, M., Tomita, T., Iwatsubo, T., Baumeister, R., and Haass, C. (1999) *J. Biol. Chem.* **274**, 28669–28673
22. Haass, C., and De Strooper, B. (1999) *Science* **286**, 916–919
23. Kimberly, W. T., Xia, W., Rahmati, T., Wolfe, M. S., and Selkoe, D. J. (2000) *J. Biol. Chem.* **275**, 3173–3178
24. Selkoe, D. J. (2000) *Curr. Opin. Neurobiol.* **10**, 50–57
25. Wolfe, M. S., De Los Angeles, J., Miller, D. D., Xia, W., and Selkoe, D. J. (1999) *Biochemistry* **38**, 11223–11230
26. Li, Y., Xu, M., Lai, M., Huang, Q., Castro, J. L., DiMuzio-Mower, J., Harrison, T., Lellis, C., Nadin, A., Neduvilil, J. G., Register, R. B., Sardana, M. K., Sheaman, M. S., Smith, A. L., Shi, X., Yin, K., Shafer, J. A., and Gardell, S. J. (2000) *Nature* **405**, 689–694
27. de Strooper, B. (2000) *Nature* **405**, 628–629
28. de Strooper, B., Annaert, W., Cupers, P., Saftig, P., Craessaerts, K., Mumm, J. S., Schroeter, E. H., Schrijvers, V., Wolfe, M. S., Ray, W. J., Goate, A., and Kopan, R. (1999) *Nature* **398**, 518–522
29. Ye, Y., Lukinova, N., and Fortini, M. E. (1999) *Nature* **398**, 525–529
30. Struhl, G., and Greenwald, I. (1999) *Nature* **398**, 522–525
31. Niwa, M., Sidrauski, C., Kaufman, R. J., and Walter, P. (1999) *Cell* **99**, 691–702
32. Song, W., Nadeau, P., Yuan, M., Yang, X., Shen, J., and Yankner, B. A. (1999) *Proc. Natl. Acad. Sci. U. S. A.* **96**, 6959–6963
33. Kulic, L., Walter, J., Multhaup, G., Teplow, D. B., Baumeister, R., Romig, H., Capell, A., Steiner, H., and Haass, C. (2000) *Proc. Natl. Acad. Sci. U. S. A.* **97**, 5913–5918
34. Ray, W. J., Yao, M., Nowotny, P., Mumm, J., Zhang, W., Wu, J. Y., Kopan, R., and Goate, A. M. (1999) *Proc. Natl. Acad. Sci. U. S. A.* **96**, 3263–3268
35. Capell, A., Steiner, H., Romig, H., Keck, S., Baader, M., Grim, M. G., Baumeister, R., and Haass, C. (2000) *Nat. Cell Biol.* **2**, 205–211
36. Wong, P. C., Zheng, H., Chen, H., Becher, M. W., Sirinathsinghji, D. J., Trumbauer, M. E., Chen, H. Y., Price, D. L., Van der Ploeg, L. H., and Sisodia, S. S. (1997) *Nature* **387**, 288–292
37. Shen, J., Bronson, R. T., Chen, D. F., Xia, W., Selkoe, D. J., and Tonegawa, S. (1997) *Cell* **89**, 629–639
38. Levitan, D., and Greenwald, I. (1995) *Nature* **377**, 351–354
39. Wittenburg, N., Eimer, S., Lakowski, B., Röhrig, S., and Baumeister, R. (2000) *Nature* **406**, 306–309
40. Li, X., and Greenwald, I. (1997) *Proc. Natl. Acad. Sci. U. S. A.* **94**, 12204–12209
41. Westlund, B., Parry, D., Clover, R., Basson, M., and Johnson, C. D. (1999) *Proc. Natl. Acad. Sci. U. S. A.* **96**, 2497–2502
42. Herreman, A., Hartmann, D., Annaert, W., Saftig, P., Craessaerts, K., Serneels, L., Umans, L., Schrijvers, V., Checler, F., Vanderstichele, H., Baekelandt, V., Dressler, R., Cupers, P., Huylebroeck, D., Zwijsen, A., Van Leuven, F., and De Strooper, B. (1999) *Proc. Natl. Acad. Sci. U. S. A.* **96**, 11872–11877
43. Donoviel, D. B., Hadjantonakis, A. K., Ikeda, M., Zheng, H., Hyslop, P. S., and Bernstein, A. (1999) *Genes Dev.* **13**, 2801–2810
44. Levitan, D., Doyle, T. G., Brousseau, D., Lee, M. K., Thinakaran, G., Slunt, H. H., Sisodia, S. S., and Greenwald, I. (1996) *Proc. Natl. Acad. Sci. U. S. A.* **93**, 14940–14944
45. Baumeister, R., Leimer, U., Zweckbronner, I., Jakubek, C., Grunberg, J., and Haass, C. (1997) *Genes Funct.* **1**, 149–159
46. Brockhaus, M., Grunberg, J., Rohrig, S., Loetscher, H., Wittenburg, N., Baumeister, R., Jacobsen, H., and Haass, C. (1998) *Neuroreport* **9**, 1481–1486
47. Steiner, H., Romig, H., Grim, M. G., Philipp, U., Pesold, B., Citron, M., Baumeister, R., and Haass, C. (1999) *J. Biol. Chem.* **274**, 7615–7618
48. Davis, J. A., Naruse, S., Chen, H., Eckman, C., Younkin, S., Price, D. L., Borchelt, D. R., Sisodia, S. S., and Wong, P. C. (1998) *Neuron* **20**, 603–609
49. Qian, S., Jiang, P., Guan, X. M., Singh, G., Trumbauer, M. E., Yu, H., Chen, H. Y., Van de Ploeg, L. H., and Zheng, H. (1998) *Neuron* **20**, 611–617
50. Levitan, D., and Greenwald, I. (1998) *Development* **125**, 3599–3606
51. Okochi, M., Walter, J., Koyama, A., Nakajo, S., Baba, M., Iwatsubo, T., Meijer, L., Kahle, P. J., and Haass, C. (2000) *J. Biol. Chem.* **275**, 390–397
52. Wild-Bode, C., Yamazaki, T., Capell, A., Leimer, U., Steiner, H., Ihara, Y., and Haass, C. (1997) *J. Biol. Chem.* **272**, 16085–16088
53. Schroeter, E. H., Kisslinger, J. A., and Kopan, R. (1998) *Nature* **393**, 382–386
54. Luo, K. X., Hurley, T. R., and Sefton, B. M. (1991) *Methods Enzymol.* **201**, 149–152
55. Walter, J., Schindzielorz, A., Grunberg, J., and Haass, C. (1999) *Proc. Natl. Acad. Sci. U. S. A.* **96**, 1391–1396
56. Wiltfang, J., Smirnov, A., Schnierstein, B., Kelemen, G., Matthies, U., Klafki, H. W., Staufenbiel, M., Huther, G., Ruther, E., and Kornhuber, J. (1997) *Electrophoresis* **18**, 527–532
57. Guo, Y., Livne-Bar, I., Zhou, L., and Boulianne, G. L. (1999) *J. Neurosci.* **19**, 8435–8442
58. Nowotny, P., Gorski, S. M., Han, S. W., Philips, K., Ray, W. J., Nowotny, V., Jones, C. J., Clark, R. F., Cagan, R. L., and Goate, A. M. (2000) *Mol. Cell Neurosci.* **15**, 88–98
59. Kim, T. W., Pettingell, W. H., Jung, Y. K., Kovacs, D. M., and Tanzi, R. E. (1997) *Science* **277**, 373–376
60. Vito, P., Ghayur, T., and D'Adamio, L. (1997) *J. Biol. Chem.* **272**, 28315–28320
61. Loetscher, H., Deuschle, U., Brockhaus, M., Reinhardt, D., Nelboeck, P., Mous, J., Grunberg, J., Haass, C., and Jacobsen, H. (1997) *J. Biol. Chem.* **272**, 20655–20659
62. Grunberg, J., Walter, J., Loetscher, H., Deuschle, U., Jacobsen, H., and Haass, C. (1998) *Biochemistry* **37**, 2263–2270
63. Wolozin, B., Iwasaki, K., Vito, P., Ganjei, J. K., Lacana, E., Sunderland, T., Zhao, B., Kusiak, J. W., Wasco, W., and D'Adamio, L. (1996) *Science* **274**, 1710–1713
64. Vito, P., Wolozin, B., Ganjei, J. K., Iwasaki, K., Lacana, E., and D'Adamio, L. (1996) *J. Biol. Chem.* **271**, 31025–31028
65. Citron, M., Westaway, D., Xia, W., Carlson, G., Diehl, T., Levesque, G., Johnson-Wood, K., Lee, M., Seubert, P., Davis, A., Kholodenko, D., Motter, R., Sherrington, R., Perry, B., Yao, H., Strome, R., Lieberburg, I., Rommens, J., Kim, S., Schenk, D., Fraser, P., St. George Hyslop, P., and Selkoe, D. J. (1997) *Nat. Med.* **3**, 67–72
66. Ray, W. J., Yao, M., Mumm, J., Schroeter, E. H., Saftig, P., Wolfe, M., Selkoe, D. J., Kopan, R., and Goate, A. M. (1999) *J. Biol. Chem.* **274**, 36801–36807
67. Haass, C. (1997) *Neuron* **18**, 687–690
68. Murayama, O., Tomita, T., Nihonmatsu, N., Murayama, M., Sun, X., Honda, T., Iwatsubo, T., and Takashima, A. (1999) *Neurosci. Lett.* **265**, 61–63
69. Steiner, H., Romig, H., Pesold, B., Philipp, U., Baader, M., Citron, M., Loetscher, H., Jacobsen, H., and Haass, C. (1999) *Biochemistry* **38**, 14600–14605
70. Ratovitsky, T., Slunt, H. H., Thinakaran, G., Price, D. L., Sisodia, S. S., and Borchelt, D. R. (1997) *J. Biol. Chem.* **272**, 24536–24541
71. Citron, M., Eckman, C. B., Diehl, T. S., Corcoran, C., Ostaszewski, B. L., Xia, W., Levesque, G., St. George Hyslop, P., Younkin, S. G., and Selkoe, D. J. (1998) *Neurobiol. Dis.* **5**, 107–116
72. Tomita, T., Tokuhito, S., Hashimoto, T., Aiba, K., Saido, T. C., Maruyama, K., and Iwatsubo, T. (1998) *J. Biol. Chem.* **273**, 21153–21160
73. Martinez, I., and Dornburg, R. (1996) *J. Virol.* **70**, 6036–6043
74. Podlisny, M. B., Citron, M., Amarante, P., Sherrington, R., Xia, W., Zhang, J., Diehl, T., Levesque, G., Fraser, P., Haass, C., Koo, E. H., Seubert, P., St. George-Hyslop, P., Teplow, D. B., and Selkoe, D. J. (1997) *Neurobiol. Dis.* **3**, 325–337
75. Jacobsen, H., Reinhardt, D., Brockhaus, M., Bur, D., Kocyba, C., Kurt, H., Grim, M. G., Baumeister, R., and Loetscher, H. (1999) *J. Biol. Chem.* **274**, 35233–35239
76. Terreni, L., Valeria, C., Calella, A. M., Gavazzi, A., Alberoni, M., Grimaldi, L. M., Mariani, C., and Forloni, G. (2000) *Neurobiol. Aging* **21**, S176–S177
77. Shirovani, K., Takahashi, K., Araki, W., Maruyama, K., and Tabira, T. (2000) *J. Biol. Chem.* **275**, 3681–3686

CHAPTER IV

Presenilin is required for proper morphology and function of neurons in *C. elegans*

published as:

Wittenburg N, **Eimer S**, Lakowski B, Rohrig S, Rudolph C, Baumeister R. (2000)
Presenilin is required for proper morphology and function of neurons in *C.elegans*.
Nature **406**: 306-309.

Presenilin is required for proper morphology and function of neurons in *C. elegans*

Nicole Wittenburg*, Stefan Eimer*, Bernard Lakowski*, Sascha Röhrig*, Claudia Rudolph† & Ralf Baumeister*

* Genzentrum, Ludwig-Maximilians-Universität, Feodor-Lynen-Strasse 25, D-81377 Munich, Germany

† EleGene GmbH, Am Klopferspitz 19, D-82152 Martinsried, Germany

Mutations in the human presenilin genes cause the most frequent and aggressive forms of familial Alzheimer's disease (FAD)¹. Here we show that in addition to its role in cell fate decisions in non-neuronal tissues^{2–4}, presenilin activity is required in terminally differentiated neurons *in vivo*. Mutations in the *Caenorhabditis elegans* presenilin genes *sel-12* and *hop-1* result in a defect in the temperature memory of the animals. This defect is caused by the loss of presenilin function in two cholinergic interneurons that display neurite morphology defects in presenilin mutants. The morphology and function of the affected neurons in *sel-12* mutant animals can be restored by expressing *sel-12* only in these cells. The wild-type human presenilin PS1, but not the FAD mutant PS1 A246E, can also rescue these morphological defects. As *lin-12* mutant animals display similar morphological and functional defects to presenilin mutants, we suggest that presenilins mediate their activity in postmitotic neurons by facilitating Notch signalling. These data indicate cell-autonomous and evolutionarily conserved control of neural morphology and function by presenilins.

To study the activity of presenilin genes in neurons, we focused on *C. elegans sel-12* as the detailed morphology and function of many neurons in *C. elegans* is known. Like presenilins in other species, *C. elegans sel-12* is strongly expressed in neurons. We tested the functional integrity of the nervous system of *sel-12* mutants by looking for defects in the execution of a variety of behaviours, such as movement and response to mechanical, chemical and thermal stimuli.

We found that *sel-12* mutants display a highly penetrant defect in

their ability to sense and/or memorize temperature. Wild-type *C. elegans* display strong preference for their growth temperature, and can memorize it and store the information for several hours, suggesting a neuronal plasticity⁵. This behaviour can be studied with a simple experimental model. When placed in a radial thermal gradient on the agar surface of a petri dish, wild-type animals migrate to their preferred temperature, and then move in isothermal circles (Table 1, Fig. 1a). In contrast, the *sel-12(ar131)* and *sel-12(ar171)* mutant animals have lost the ability to perform isothermal tracks. Most animals are non-responsive to the temperature gradient and moved randomly on the plate (athermotactic behaviour), and 10% of the remaining animals moved to colder temperatures than the wild-type (cryophilic behaviour). These results indicate that *sel-12* mutants may have defects in the neural circuit for thermotaxis.

The neurons necessary for thermotaxis have been studied extensively by mutational analyses and laser ablation studies⁶. Temperature input activates the two AFD sensory neurons, which synapse extensively onto the two AIY interneurons. Chemical signals from AIY and AIZ (synaptic partners that represent the four central integrating interneurons), in turn, regulate postsynaptic inter- and motor neurons that control the motor response. We carefully examined the morphology of the AFD, AIZ and AIY neurons in *sel-12* animals using green fluorescent protein (GFP) reporter constructs, and saw no obvious defects in AFD and AIZ neurons (data not shown). However, we identified defects in the morphology of AIY neurons (Table 2, Fig. 2). In wild-type animals, the processes of both AIY neurons extend anteriorly from the cell bodies along the ventral cord, run around the nerve ring and meet and terminate at the dorsal midline⁷ (Fig. 2e). In adult *sel-12* mutants the AIY cell bodies are correctly positioned in the head ganglion. However, the AIY axons often grow too far anteriorly before turning and fasciculating in the nerve ring (Fig. 2d), and/or do not stop growth at the dorsal side of the nerve ring, but turn posteriorly, sometimes extending up to the midbody region (Fig. 2b–d, classified as severe defects in Table 2). In addition, short extra neurites often emerge directly from the cell soma or branch off the primary process (Fig. 2a, classified as minor defects in Table 2). The number of animals showing these types of defects in AIY morphology was higher in *sel-12(ar171)* mutants (35% defects) than in *sel-12(ar131)* mutants (20% defects; Table 2). This is consistent with the severity of these mutations and their effect on egg-laying behaviour (*ar171* carries a nonsense mutation in *sel-12* and genetically represents a null allele, and *ar131* carries a missense mutation in *sel-12*)². Behavioural defects are far more penetrant than the morphological defects, indicating that *sel-12* animals may also have more subtle defects in the AIY neurons than can be visualized with GFP

Table 1 Rescue of the *sel-12* thermotaxis defect

Genotype	Transgene	Fraction showing isothermal tracks
Wild type*		41/46
<i>sel-12(ar131)</i>		1/42
<i>sel-12(ar171)</i>		3/38
<i>hop-1(g1501)</i>		0/44
<i>lin-12(n941)</i>		0/15
<i>hop-1(g1501);sel-12(ar131)</i>		0/31
<i>hop-1(g1501);sel-12(ar171)</i>		0/33
<i>sel-12(ar171);byIs101</i>	<i>sel-12::sel-12</i>	38/49
<i>sel-12(ar171);byIs100</i>	<i>sel-12::sel-12</i>	19/41
Wild type†		49/55
<i>sel-12(ar131)†</i>		3/40
<i>sel-12(ar171)†</i>		2/39
<i>sel-12(ar131); byEx103†</i>	<i>ttx-3::sel-12</i>	18/42
<i>sel-12(ar131); byEx115†</i>	<i>ttx-3::sel-12</i>	21/41
<i>sel-12(ar171); byEx115†</i>	<i>ttx-3::sel-12</i>	35/67
<i>sel-12(ar171); byEx115†</i>	<i>ttx-3::sel-12</i>	18/41

* Strain carries a *daf-6(e1377)* mutation that did not affect thermotaxis behaviour.

† Animals expressing *ttx-3::GFP*.

byIs100 and *byIs101* are independent chromosomally integrated arrays expressing *sel-12* cDNA from the *sel-12* promoter.

constructs. This is not unprecedented, because mutations in other axonal guidance genes often lead to highly penetrant behavioural defects with a much lower penetrance of morphological defects than is visible by light microscopy⁸.

To confirm that the defects we observed are due to a loss of *sel-12* activity, we transformed *sel-12* mutants with a *sel-12* complementary DNA under the control of the *sel-12* promoter. This construct rescued the egg-laying defect (data not shown), the thermotaxis behaviour of *sel-12(ar171)* and the neurite morphology defect (Tables 1 and 2). To determine whether *sel-12* activity is required cell-autonomously or non-cell-autonomously, we used the *ttx-3* promoter to express *sel-12* cDNA exclusively in AIY⁹. We analysed *sel-12(ar131)* and *sel-12(ar171)* mutants that expressed *ttx-3::sel-12* from an extra-chromosomal array. All transgenic animals still showed the fully penetrant egg-laying defect typical of *sel-12* mutants, but expression of *sel-12* solely in AIY restored isothermal tracking (Table 1, Fig. 1d). In addition, the morphology of the AIY neurons was indistinguishable from wild-type (Table 2). Together, our data indicate that SEL-12 activity in AIY is required cell-autonomously for correct neurite connectivity and for the only known function of this neuron.

A second somatically expressed presenilin, *hop-1*, exists in *C. elegans* and is thought to be largely redundant with *sel-12*. *hop-1* mutants were described to have no obvious phenotype on their own, but strongly enhance the developmental defect of *sel-12* mutants¹⁰; however, we find that *hop-1(lg1501)* mutants are also defective in their thermotaxis behaviour. None of the mutants that we tested performed isothermal tracking. Twenty-seven of the forty-four animals tested showed cryophilic behaviour similar to those animals in which both AIY neurons were ablated by microsurgery⁶, indicating that *hop-1* activity is required for AIY function (Fig. 1c). Like *sel-12* animals, *hop-1* animals displayed a weakly penetrant morphological defect in AIY (Table 2). We found that 91% of the *hop-1(lg1501);sel-12(ar131)* and 94% of the *hop-1(lg1501);sel-12(ar171)* double mutants showed abnormal AIY morphology. The severity of the defects was considerably stronger than that observed in the *hop-1(lg1501)*, *sel-12(ar131)* or *sel-12(ar171)* single mutants, indicating that the low penetrance of neuronal defects in *sel-12* mutants is due in part to the functional redundancy of *sel-12* and *hop-1*. These data also indicate that the activities of both presenilins are required for the function of the AIY interneurons and for their correct neurite morphology.

The vertebrate presenilin genes are strongly expressed in neurons and the protein has been detected in neurite growth cones and vesicles^{11–13}. This indicates that human presenilins may have a function in neurite outgrowth. To test whether human presenilins can functionally replace *sel-12* in the AIY neurons, we expressed the cDNAs of PS1 and the FAD mutant PS1 A246E under the control of a *sel-12* promoter in *sel-12* mutants. The neurite morphology in the strains expressing PS1 was completely rescued (Table 2). In contrast, rescue was reduced when we expressed PS1 A246E in *sel-12* mutants (Table 2). This is consistent with previous experiments showing that wild-type human presenilins, but not FAD mutants, can rescue the *sel-12* egg-laying defect^{3,4}. Our data indicate that human and *C. elegans* presenilin may have conserved functions in postmitotic neurons. We propose that in vertebrates, presenilins may also be required cell-autonomously to control neurite morphology.

As *sel-12* is expressed in most neurons in the *C. elegans* nervous system, we analysed the general neural anatomy of *sel-12* mutants using other GFP reporter genes, including a pan-neuronally expressed *unc-119::GFP* construct. The position and process morphology of most neurons appeared normal. However, irregular branching of neurites was sometimes observed in the BDU cells (a pair of interneurons of unknown function) and fasciculation and pathfinding defects were observed in neuronal processes in the ventral cord in 18% of the examined animals ($n = 103$). We also examined locomotion and tested many other behaviours (such as

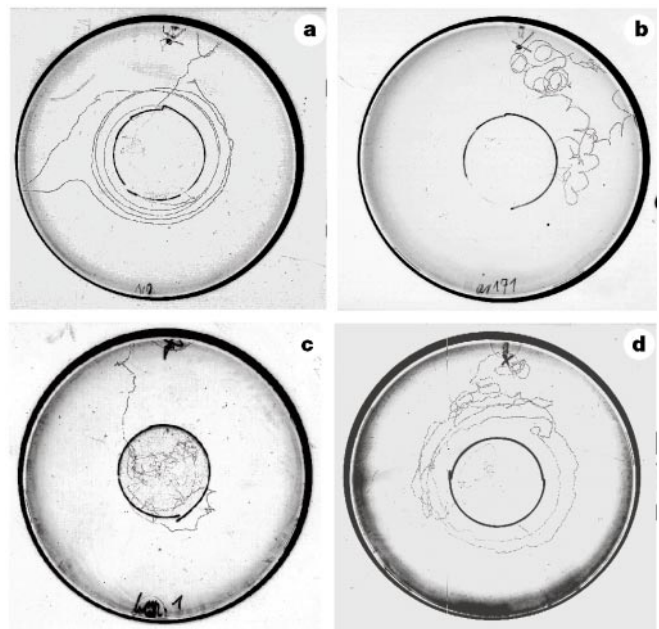


Figure 1 Tracking of animals on a radial temperature gradient. Animals raised at 20 °C were tested on a radial temperature gradient ranging from 17 °C (in the central circle) to room temperature at the edge. After the animals were transferred to the gradient (at the X-mark on top) they were given at least 1 hour to move freely on the plate. The tracks they left in the agar were photographed. A representative plate is shown for wild-type (a); *sel-12(ar171)* (b); *hop-1(lg1501)* animals (c); *sel-12(ar171)* animals expressing a *ttx-3::sel-12* transgene in AIY (d).

chemotaxis to food, foraging and mechanoperception of *sel-12* mutant animals) (data not shown), but could not identify any abnormalities in these behaviours. Accordingly, no anatomical defects were seen in the associated neurons. This indicates that, although *sel-12* is expressed in most or all neurons, it is absolutely required in only a subset of neurons.

Is the abnormal morphology of AIY a secondary consequence of abnormal AIY function? There is evidence that axon connectivity in *C. elegans* may not in all cases be determined by developmental outgrowth, but also can be refined by sensory activity¹⁴. To test whether AIY morphology may be affected by the lack of synaptic activity, we tested axon development in an *egl-19(n2368)* mutant that shows reduced neural transmission owing to a defective voltage-gated Ca²⁺-channel subunit^{14,15}. Whereas only 1 of 137 newly hatched L1 animals tested displayed a non-wild-type AIY morphology, 38% of the *egl-19* animals showed AIY defects as adults. This indicates that lack of synaptic activity may influence AIY morphology. We compared AIY morphology in *sel-12(ar131)* and *sel-12(ar171)* mutants shortly after hatching (L1) with that of adult animals. Sixteen percent of L1 ($n = 167$) and 20% of adult *ar131* mutants, and 26% of L1 ($n = 173$) and 35% of adult *ar171* mutants exhibited AIY defects. As the defects can be observed shortly after hatching, and therefore before a significant and biologically relevant sensory input, we suggest that the morphological defects of *sel-12* mutants are predominantly generated during axonal outgrowth in AIY and not as a consequence of a reduced activity of their neurons.

Results in a variety of model systems have shown that presenilin activity controls the function of several, obviously non-related transmembrane proteins. Presenilin activity is required for the proteolytic processing of the amyloid precursor protein involved in Alzheimer's disease¹, but also for the proteolysis of the Irf1 receptor¹⁶ and Notch receptor^{17–19}. In *C. elegans*, presenilins are required for Notch-mediated cell fate decisions in the vulval and uterine tissues². The *C. elegans* Notch homologues LIN-12 and GLP-1 affect neural development by controlling lineage identity, but

no expression or activity of *lin-12* or *glp-1* in the neurons involved in the circuitry required for thermotaxis has been reported.

To determine whether the consequences of reduced Notch activity in AIY are similar to those of mutations in *sel-12*, we examined the neural anatomy of AIY in *lin-12* and *glp-1* strong loss-of-function alleles. We observed a very weak AIY defect in *glp-1* alleles. However, there was a highly penetrant defective AIY morphology in *lin-12(n941)* mutants (61% defects, Table 1). The same morphological abnormalities were found as in *sel-12* mutant animals, including a failure of the AIY axon to terminate at the dorsal side of the nerve ring and a remarkable increase in neurite sprouting very similar to that seen in *sel-12* mutants (Fig. 2f). As with *sel-12* mutants, *lin-12* animals also display a thermotaxis defect. Although most of the *lin-12(n941)* animals displayed strongly impaired movement on a temperature gradient, 15 out of 44 animals did migrate. All of these animals moved to the centre of the radial temperature gradient and may be considered cryophilic (Fig. 1c). From these data we conclude that the reduction of LIN-12/Notch activity also results in a morphological and behavioural defect of AIY. The similarity of the observed phenotype indicates that presenilins may control AIY morphology and function through the activity of LIN-12/Notch. The defective motility of *lin-12(n941)* may also indicate additional neurogenic or myogenic roles for *lin-12* that have not been analysed in detail.

We have shown that the AIY defects in *sel-12* mutants can be fully rescued by human PS1, indicating that the neural function of presenilins is evolutionarily conserved. As we have suggested for *C. elegans*, presenilins in other organisms may control the connectivity and function of selected neurons by modulating Notch signalling in these cells. It has been shown that the *Drosophila* Notch is involved in specific regionally constricted guidance of neuronal outgrowth²⁰, although the cells that require Notch activity were not determined. Experiments in cell culture show that Notch signalling affects neurite growth^{21,22}, and that a functional interaction between human PS1 and Notch1 exists in postmitotic mammalian neurons²³. On the basis of cell-culture experiments, both autonomous and non-autonomous regulation of neurite development by Notch signalling have been suggested²⁴. Our results indicate a conserved function for presenilins in postmitotic neurons which is supported by data from cell-culture experiments. Owing to the lack of obvious other behavioural defects of *sel-12* mutants, it is likely that *sel-12* activity is only required in a subset of the neurons in *C. elegans*, despite the broad expression of *sel-12* in the nervous system. It is interesting to note that the AIY neurons produce the neurotransmitter acetylcholine (J. Duerr and J. Rand, personal communication) and that cholinergic neurons have an increased susceptibility to dysfunction in Alzheimer's disease²⁵. Mutations in the *C. elegans* choline acetyltransferase *cha-1* also affect AIY neurite

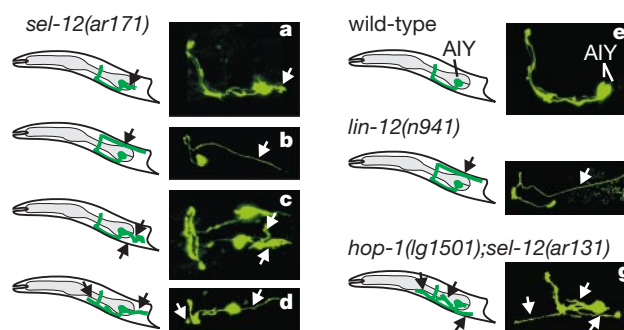


Figure 2 AIY interneuron morphology in *sel-12*, wild-type, *lin-12* and *hop-1;sel-12* mutant animals. Left, drawing of morphology of AIY interneurons (adapted from ref. 7). Right, expression of *tx-3::GFP* in AIY. Abnormal axonal projections are indicated by arrows. **a–d**, Defects seen in *sel-12* mutants. **a**, A posteriorly directed process sprouts from the cell soma. **b**, An axon does not terminate at dorsal mid-line but continues to grow posteriorly; in severe cases we saw extension to the midbody region. **c**, Rootlet-like projections extend from the cell somata in no defined direction. **d**, An axon leaves the fascicle when it turns into the nerve ring. Additional rootlet-like neurites project posteriorly from the cell soma. **e**, Wild-type morphology. AIY processes run anteriorly up the ventral cord, then enter the nerve ring and finally meet and terminate at the dorsal mid-line. **f**, Defects observed in *lin-12(n941)* animals resemble those seen in *sel-12* mutants. **g**, In *hop-1(lg1501);sel-12(ar131)* AIY defects also resemble the defects seen in the other mutants, but were more severe. Small axonal projections were scored as minor defects (**a**). All defects that lead to a gross change in AIY morphology are grouped as severe defects (**b–d, f, g**).

morphology (our unpublished results), and it has been reported that mutations in the human presenilins can reduce choline acetyltransferase activity that may contribute to the cognitive impairment in Alzheimer's disease²⁵. In the human brain, the neural structure whose function is most severely affected by presenilin mutations during the progression of FAD is the hippocampus, which is central to the perception and long-term storage of memory²⁶. Remarkably, the neurons most strongly affected in *C. elegans* by presenilin mutations are the AIY neurons that are involved in the only neural circuit for which synaptic plasticity has been suggested⁶.

Here we correlate behavioural and morphological assays to monitor presenilin function in a pair of *C. elegans* neurons. The detailed knowledge of the *C. elegans* neural anatomy and the conservation of presenilin function can now be exploited to analyse the molecular details leading to these defects. Understanding the role of presenilins in the nervous system may result in an understanding of the abnormal neurite pattern and neural deficits of Alzheimer's disease patients. □

Table 2 AIY morphology defects

Strain*	Transgene	No defects (%)	Minor defects (%)	Severe defects (%)	No. of animals
Wild type		97	3	0	113
<i>sel-12(ar131)</i>		80	16	4	159
<i>sel-12(ar171)</i>		65	12	23	145
<i>hop-1(lg1501)</i>		70	17	13	100
<i>lin-12(n941)</i>		39	43	18	108
<i>glp-1(e2144)</i>		90	6	4	220
<i>glp-1(q46)</i>		92	7	1	112
<i>hop-1(lg1501); sel-12(ar131)</i>		4	27	69	70
<i>hop-1(lg1501); sel-12(ar171)</i>		9	65	26	43
<i>sel-12(ar171)</i>	<i>sel-12::sel-12</i>	96	4	9	102
<i>sel-12(ar131)</i>	<i>tx-3::sel-12</i>	98.0 ± 2.0	1.0 ± 1.0	1.0 ± 1.0	337
<i>sel-12(ar171)</i>	<i>tx-3::sel-12</i>	98.0 ± 2.0	1.0 ± 1.0	1.0 ± 1.0	342
<i>sel-12(ar131)</i>	<i>sel-12::PS1</i>	98.5 ± 0.5	0.5 ± 0.5	1.0 ± 0.0	369
<i>sel-12(ar171)</i>	<i>sel-12::PS1</i>	94.5 ± 2.5	3.5 ± 1.5	2.0 ± 1.0	336
<i>sel-12(ar131)</i>	<i>sel-12::PS1 A246E</i>	78.0 ± 6.0	14.0 ± 6.0	8.0 ± 0.0	224
<i>sel-12(ar171)</i>	<i>sel-12::PS1 A246E</i>	74.5 ± 4.5	15.5 ± 6.5	10.0 ± 2.0	453

The neuronal and axonal morphology of AIY in *C. elegans* wild-type, presenilin, Notch and *sel-12* transgenic animals was examined. The percentage of animals displaying no defects, minor defects and severe defects (for definition see Fig. 2) are listed along with the total number of animals examined. All values for the transgenic lines are given as the mean percentage of two independent lines ± the standard deviation.

* Strains carry an extrachromosomal array containing *tx-3::GFP*.

Methods

General procedures

C. elegans strains were grown as described²⁷. *sel-12(ar171)* was separated from the marker mutation *unc-1(e538)* by standard techniques to allow analysis of thermotaxis. *sel-12(ar131)* and *sel-12(ar171)* were each backcrossed five times. XY1002 *hop-1(lg1501)* contains a 1,878-base-pair (bp) deletion in the gene. It eliminates bp 20,359–22,238 of cosmid C18E3 leading to a deletion of the carboxy-terminal exons 4–6 of *hop-1*.

Behavioural assays

We performed single animal thermotaxis assays⁵ and the results were scored⁶ as described.

Expression constructs and generation of transgenic animals

sel-12 cDNA was obtained by PCR from a *C. elegans* cDNA library (Genbank accession number AF171064). This cDNA was cloned under the control of a 2.8-kilobase (kb) fragment 5' of the translational start ATG of *sel-12* to generate pBY895. pBY478 contains a *Kpm1-SpeI* fragment of the *ttx-3* promoter⁹ that drives expression of the *sel-12* cDNA exclusively in the AIY neurons. The expression constructs for human PS1 (pBY140) and the FAD mutant PS1 A246E (pBY147) have been described⁴. pBY140, pBY147 and pBY478 were injected into *him-8(e1489)* with *ttx-3::GFP* as a transformation marker. Two independent lines per construct were crossed into *sel-12(ar131)* and *sel-12(ar171)*. pBY895 was directly injected into *sel-12(ar171)* using *tph-1::GFP* as a transformation marker. Two integrated lines were obtained after X-ray irradiation and subsequently outcrossed five times each (*byIs100* and *byIs101*).

Identification of neuroanatomy

The *unc-119::GFP* reporter construct is expressed in all neurons²⁸. To identify AFD, a cell-specific *gcy-8::GFP* was used²⁹. AIY morphology was observed by using *ttx-3::GFP*⁹. We generated seven independent transgenic lines by injecting different *ttx-3::GFP* concentrations (1–50 ng μl^{-1}). All lines displayed AIY morphology defects in a *sel-12(ar171)* background. Line *byEx116* was chosen for all subsequent analyses, and was crossed into the different genetic backgrounds. AIZ was identified by using *lin-11::GFP* as a marker³⁰. Additional GFP reporter genes used contain *mec-7*, *tph-1* and *sel-12* promoters, which drive GFP expression in different subsets of neurons. All GFP constructs were injected into wild-type animals and subsequently crossed into various mutant backgrounds. *lin-12(n941);byEx116* were obtained by crossing into MT1965 *lin-12(n941)/eT1 III; him-5(e1467)/eT1[him-5(e1476)]V*. Animals homozygous for *lin-12* were Pvl (protruding vulva phenotype 1) and sterile. Homozygous *glp-1(e2144) byEx116* animals were identified on the basis of their embryonic lethality at 25 °C. *byEx116* was also crossed into *hop-1(lg1501);sel-12(ar131)* and *hop-1(lg1501);sel-12(ar171)* strains. For this purpose, *hop-1(lg1501)* was balanced over *unc-73(e936)*. Double homozygous animals were identified as being sterile and Pvl (ref. 10). The neuronal and axonal morphology was studied at 630–1,000-fold magnification using a Zeiss Axioskop compound microscope. Abnormal axonal projections were documented using a Leica TCS NT confocal microscope.

Received 11 February; accepted 25 May 2000.

1. Haass, C. & De Strooper, B. The presenilins in Alzheimer's disease—proteolysis holds the key. *Science* **286**, 916–919 (1999).
2. Levitan, D. & Greenwald, I. Facilitation of *lin-12*-mediated signalling by *sel-12*, a *Caenorhabditis elegans* S182 Alzheimer's disease gene. *Nature* **377**, 351–354 (1995).
3. Levitan, D. *et al.* Assessment of normal and mutant human presenilin function in *Caenorhabditis elegans*. *Proc. Natl Acad. Sci. USA* **93**, 14940–14944 (1996).
4. Baumeister, R. *et al.* Human presenilin-1, but not familial Alzheimer's disease (FAD) mutants, facilitate *Caenorhabditis elegans* Notch signalling independently of proteolytic processing. *Genes Funct.* **1**, 149–159 (1997).
5. Hedgecock, E. M. & Russell, R. L. Normal and mutant thermotaxis in the nematode *Caenorhabditis elegans*. *Proc. Natl Acad. Sci. USA* **72**, 4061–4065 (1975).
6. Mori, I. & Ohshima, Y. Neural regulation of thermotaxis in *Caenorhabditis elegans*. *Nature* **376**, 344–348 (1995).
7. White, J. G., Southgate, E., Thomson, J. N. & Brenner, S. The structure of the nervous system of the nematode *Caenorhabditis elegans*. *Phil. Trans. R. Soc. Lond.* **314**, 1–340 (1986).
8. Hedgecock, E. M., Culotti, J. G., Thomson, J. N. & Perkins, L. A. Axonal guidance mutants of *Caenorhabditis elegans* identified by filling sensory neurons with fluorescent dyes. *Dev. Biol.* **111**, 158–170 (1985).
9. Hobert, O. *et al.* Regulation of interneuron function in the *C. elegans* thermoregulatory pathway by the *ttx-3* LIM homeobox gene. *Neuron* **19**, 345–357 (1997).
10. Westlund, B., Parry, D., Clover, R., Basson, M. & Johnson, C. D. Reverse genetic analysis of *Caenorhabditis elegans* presenilins reveals redundant but unequal roles for *sel-12* and *hop-1* in Notch pathway signaling. *Proc. Natl Acad. Sci. USA* **96**, 2497–2502 (1999).
11. Kovacs, D. M. *et al.* Alzheimer-associated presenilins 1 and 2: Neuronal expression in brain and localization to intracellular membranes in mammalian cells. *Nature Med.* **2**, 224–229 (1996).
12. Cook, D. G. *et al.* Expression and analysis of presenilin 1 in a human neuronal system: Localization in cell bodies and dendrites. *Proc. Natl Acad. Sci. USA* **93**, 9223–9228 (1996).
13. Lee, M. K. *et al.* Expression of Presenilin 1 and 2 (PS1 and PS2) in human and murine tissues. *J. Neurosci.* **16**, 7513–7525 (1996).
14. Peckol, E., Zallen, J., Yarrow, J. & Bargmann, C. Sensory activity affects sensory axon development in *C. elegans*. *Development* **126**, 1891–1902 (1999).
15. Lee, R., Lobel, L., Hengartner, M., Horvitz, H. & Avery, L. Mutations in the $\alpha 1$ subunit of an L-type voltage-activated Ca^{2+} channel cause myotonia in *Caenorhabditis elegans*. *EMBO J.* **16**, 6066–6076 (1997).

16. Katayama, T. *et al.* Presenilin-1 mutations downregulate the signalling pathway of the unfolded-protein response. *Nature Cell Biol.* **1**, 479–485 (1999).
17. Struhl, G. & Greenwald, I. Presenilin is required for activity and nuclear access of Notch in *Drosophila*. *Nature* **398**, 522–525 (1999).
18. Wolfe, M. S. *et al.* Two transmembrane aspartates in presenilin-1 required for presenilin endo-proteolysis and gamma-secretase activity. *Nature* **398**, 513–517 (1999).
19. Ye, Y., Lukinova, N. & Fortini, M. E. Neurogenic phenotypes and altered Notch processing in *Drosophila* presenilin mutants. *Nature* **398**, 525–529 (1999).
20. Giniger, E., Jan, L. & Jan, Y. Specifying the path of the intersegmental nerve of the *Drosophila* embryo: a role for Delta and Notch. *Development* **117**, 431–440 (1993).
21. Berezovska, O. *et al.* Notch1 inhibits neurite outgrowth in postmitotic primary neurons. *Neuroscience* **93**, 433–439 (1999).
22. Sestan, N., Artavanis-Tsakonas, S. & Rakic, P. Contact-dependent inhibition of cortical neurite growth mediated by Notch signaling. *Science* **286**, 741–746 (1999).
23. Berezovska, O. *et al.* The Alzheimer-related gene presenilin 1 facilitates notch 1 in primary mammalian neurons. *Brain Res. Mol. Brain Res.* **69**, 273–280 (1999).
24. Franklin, J. L. *et al.* Autonomous and non-autonomous regulation of mammalian neurite development by Notch1 and Delta. *Curr. Biol.* **9**, 1448–1457 (1999).
25. Pedersen, W. A., Guo, Q., Hartman, B. K. & Mattson, M. P. Nerve growth factor-independent reduction in choline acetyltransferase activity in PC12 cells expressing mutant presenilin-1. *J. Biol. Chem.* **272**, 22397–22400 (1997).
26. Mayford, M. & Kandel, E. R. Genetic approaches to memory storage. *Trends Genet.* **15**, 463–470 (1999).
27. Brenner, S. The genetics of *Caenorhabditis elegans*. *Genetics* **77**, 71–94 (1974).
28. Maduro, M. & Pilgrim, D. Identification and cloning of *unc-119*, a gene expressed in the *Caenorhabditis elegans* nervous system. *Genetics* **141**, 977–988 (1995).
29. Yu, S., Avery, L., Baude, E. & Garbers, D. Guanylyl cyclase expression in specific sensory neurons: a new family of chemosensory receptors. *Proc. Natl Acad. Sci. USA* **94**, 3384–3387 (1997).
30. Hobert, O., D'Alberti, T., Liu, X. & Ruvkun, G. Control of neural development and function in a thermoregulatory network by the LIM homeobox gene *lin-11*. *J. Neurosci.* **18**, 2084–2096 (1998).

Acknowledgements

Some strains used in this study were provided by the *Caenorhabditis* Genetics Center, which is funded by the NIH National Center for Research Resources. We thank I. Greenwald, E. Lambie and H. R. Horvitz for strains; R. Barstead for cDNA libraries; O. Hobert and A. Fire for plasmids and R. Donhauser and M. Grim for technical assistance. We also thank I. Mori and H. Kagoshima for their help with interpreting thermotaxis data, and C. Haass and the members of our lab for discussions and for critically reading the manuscript. Part of this work was supported by grants from the DFG to R.B. and from EMBO to B.L.

Correspondence and requests for materials should be addressed to R.B. (e-mail: bmeister@lmb.uni-muenchen.de).



CHAPTER V

The *C. elegans* presenilin *sel-12* is required for mesodermal patterning and muscle function

published as:

Eimer S., Donhauser R. and Baumeister R. (2002)

The *C. elegans* presenilin *sel-12* is required for mesodermal patterning and muscle function.
Dev Biol, **251**: 178-192.

The *Caenorhabditis elegans* Presenilin *sel-12* Is Required for Mesodermal Patterning and Muscle Function

Stefan Eimer, Roland Donhauser, and Ralf Baumeister¹

ABI, Department of Biochemistry, Laboratory of Molecular Neurogenetics, Ludwig-Maximilians-Universität Munich, Schillerstrasse 44, Munich D-80336, Germany

Mutations in presenilin genes impair Notch signalling and, in humans, have been implicated in the development of familial Alzheimer's disease. We show here that a reduction of the activity of the *Caenorhabditis elegans* presenilin *sel-12* results in a late defect during sex muscle development. The morphological abnormalities and functional deficits in the sex muscles contribute to the egg-laying defects seen in *sel-12* hermaphrodites and to the severely reduced mating efficiency of *sel-12* males. Both defects can be rescued by expressing *sel-12* from the *hlh-8* promoter that is active during the development of the sex muscle-specific M lineage, but not by expressing *sel-12* from late muscle-specific promoters. Both weak and strong *sel-12* mutations cause defects in the sex muscles that resemble the defects we found in *lin-12* hypomorphic alleles, suggesting a previously uncharacterised LIN-12 signalling event late in postembryonic mesoderm development. Together with a previous study indicating a role of *lin-12* and *sel-12* during the specification of the π cell lineage required for proper vulva-uterine connection, our data suggest that the failure of *sel-12* animals to lay eggs properly is caused by defects in at least two independent signalling events in different tissues during development. © 2002 Elsevier Science (USA)

Key Words: SEL-12; presenilin; LIN-12; Notch; *C. elegans*; Alzheimer's disease; sex muscle development.

INTRODUCTION

The presenilin genes encode multipass transmembrane proteins (Doan *et al.*, 1996; Li and Greenwald, 1996, 1998) that are found in all multicellular organisms. Mutations in the human presenilin genes (PS1 and PS2) cause aberrant processing of the amyloid precursor protein APP, resulting in early-onset familial Alzheimer's disease (FAD). In addition, presenilins positively influence *lin-12*/Notch signalling as has been shown by a number of genetic studies (Levitan and Greenwald, 1995; Struhl and Adachi, 2000; Struhl and Greenwald, 1999, 2001; Ye *et al.*, 1999). Presenilins are part of a high-molecular weight complex with nicastrin/APH-2 that directly or indirectly mediates the proteolytic release of the C terminus of Notch receptors. This cleavage is critical for nuclear transport and signaling of the Notch intracellular domain (Kidd *et al.*, 1998; Schroeter *et al.*, 1998; Struhl and Adachi, 1998; Struhl *et al.*, 1993). A similar complex also controls the proteolytic

cleavage of APP at the γ -secretase cleavage site (Yu *et al.*, 2000).

Targeted deletion of presenilins in different organisms results in pleiotropic defects. A loss-of-function mutation in the single *Drosophila* presenilin gene causes lethal Notch-like phenotypes, such as maternal neurogenic effects during embryogenesis, loss of lateral inhibition within proneural cell clusters, and absence of wing margin formation (Ye *et al.*, 1999). PS1-deficient mice die soon after birth from respiratory problems caused by a Notch-like developmental defect (Koizumi *et al.*, 2001; Shen *et al.*, 1997; Wong *et al.*, 1997), whereas deletion of PS2 causes only mild phenotypes (Herreman *et al.*, 1999). However, the simultaneous deletion of PS1 and PS2 results in an early embryonic lethality (Herreman *et al.*, 1999) strikingly resembling that of animals carrying a processing-deficient allele of Notch1 (Huppert *et al.*, 2000) or a deletion of the Notch1 receptor gene (Conlon *et al.*, 1995; Swiatek *et al.*, 1994).

The *Caenorhabditis elegans* genome harbours two Notch genes, *glp-1* and *lin-12*, and three presenilin orthologues, *sel-12*, *hop-1*, and *spe-4* (Levitan and Greenwald, 1995; L'Hernault and Arduengo, 1992; Li and Greenwald, 1997).

¹ To whom correspondence should be addressed. Fax: +49 (89) 5996 483. E-mail: ralf.baumeister@pbm.med.uni-muenchen.de.

spe-4 is a distant member of this family with a sole role during spermatogenesis. Accordingly, ectopic expression of *spe-4* does not rescue the *sel-12* mutant phenotype (S.E., unpublished data). However, both *sel-12* and *hop-1* genes can substitute for each other and are functionally conserved with the human presenilins (Baumeister *et al.*, 1997; Levitan *et al.*, 1996; Li and Greenwald, 1997). In *sel-12;hop-1* double mutant animals, *C. elegans* GLP-1 and LIN-12 Notch receptor signalling is almost completely inhibited (Li and Greenwald, 1997; Westlund *et al.*, 1999). The deletion of *hop-1*, analogous to that of the mammalian PS2, does not reveal an obvious phenotype (Westlund *et al.*, 1999), whereas mutations in *sel-12* alone reduce the activity of *lin-12* and *glp-1*, resulting in phenotypic effects (Levitan and Greenwald, 1995). *sel-12* mutant animals display neuronal defects (Wittenburg *et al.*, 2000) and a highly penetrant egg-laying defect (Levitan and Greenwald, 1995). Both defects can be rescued by transgenic expression of either *C. elegans* or human PS1 and PS2 (Baumeister *et al.*, 1997; Levitan *et al.*, 1996; Li and Greenwald, 1997; Wittenburg *et al.*, 2000). In addition, *sel-12* animals also display an incompletely penetrant, morphologically abnormal, protruding vulva phenotype (Pvl). The cellular nature of this defect is not known. The penetrance of the Pvl phenotype differs between *sel-12* alleles, but is fully penetrant in *sel-12;hop-1* double mutant animals (Westlund *et al.*, 1999; S.E. and R.B., unpublished observations).

The ability of *C. elegans* hermaphrodites to lay eggs is dependent on the integrity of multiple cell types derived from various lineages, including epidermal, neuronal, and muscle cells. Several developmental cell fate decisions necessary for proper egg laying require LIN-12/Notch signaling. Vulva formation is induced by a signal from the anchor cell (AC), whose fate is determined by cell-cell interactions involving LIN-12/Notch activity. A signal from AC then induces the vulva cell fates in a group of competent epithelial cells called vulva precursor cells (VPCs). After induction, VPCs are specified through a process called lateral inhibition, which again is dependent on LIN-12 signalling. LIN-12 activity is also required to generate the sex myoblasts (SM), the precursors of the vulva and uterine muscles. The vulva muscles, as well as the neurons that innervate them, are necessary for a proper egg laying behaviour (Corsi *et al.*, 2000; Trent *et al.*, 1983; White *et al.*, 1983; M. Stern, personal communication). Previous studies did not report any obvious morphological defects in the hermaphrodite-specific neurons (HSN), the sex-muscles, the vulva precursor cell lineage (VPC), or in the specification of the AC in *sel-12* mutants (Levitan and Greenwald, 1995). However, AC also induces a group of uterine cells to form a proper connection between the vulva and the uterus in a *lin-12*/Notch-dependent process (Hirsh *et al.*, 1976; Kimble and Hirsh, 1979; Newman *et al.*, 1995, 1996; Sulston and Horvitz, 1977; Thomas *et al.*, 1990). This inductive signalling is perturbed in *sel-12* null mutants and weak *lin-12* loss-of-function mutants (Cinar *et al.*, 2001). However, although all *sel-12* mutants have a highly pen-

etrant egg-laying defect, the π cell fate specification defect is only incompletely penetrant, suggesting another role of *sel-12* in egg-laying.

We show here that *sel-12* and *hop-1* presenilins are required late in the *C. elegans* hermaphrodite vulva muscle development to control their morphology and attachment to the vulva. Reduction of SEL-12 activity during sex muscle differentiation impairs egg-laying. Furthermore, we show that, in *sel-12* males, sex muscles are also defective, resulting in a reduced male mating efficiency. Similar sex muscle defects were also observed in hypomorphic *lin-12* mutant animals. Taken together, these results reveal a contribution of presenilin mediated Notch signalling not only in sex myoblast (SM) fate determination, as shown previously (Greenwald *et al.*, 1983; Harfe *et al.*, 1998a), but also an as yet uncharacterised role late during sex muscle development.

MATERIALS AND METHODS

C. elegans Strains and Culture

All strains were maintained and manipulated under standard conditions as described (Brenner, 1974). Unless otherwise noted, strains were kept and analysed at 20°C. The following mutants, and combinations thereof, were used in this work: LGI: *unc-73(e936)*, *hop-1(lg1501)* (Wittenburg *et al.*, 2000); LGII: *unc-4(e120)*; LGIII: *lin-12(n676n930)*, *lin-12(oz48)* (Sundaram and Greenwald, 1993); *oz48* was kindly provided by Tim Schedl), *unc-32(e189)*; LGIV: *him-8(e1489)*, *fem-1(hc17ts)* (Kimble *et al.*, 1984); LGV: *him-5(e1490)*; LGX: *sel-12(ar131)*, *sel-12(ar171)* (Levitan and Greenwald, 1995), *sel-12(lg1401)* (gift from EleGene AG, Martinsried), *sel-12(by125)* (this work). All *sel-12* and *hop-1* strains were outcrossed between 5 and 10 times with the *C. elegans* wild type strain N2 before phenotypic analysis.

NH2447(*ayIs2*)IV contains an *egl-15::gfp* fusion (kindly provided by C. Branda and M. Stern), PD4667(*ayIs7*)IV contains a *hlh-8::gfp* fusion (kindly provided by B. Harfe and A. Fire; Harfe *et al.*, 1998b) which shows GFP expression during the entire M lineage development. The *Nde-box::gfp* strain, PD4655(*ccIs4655*)II, is expressed in all eight vulva muscles and eight uterine muscles (Harfe and Fire, 1998) and was provided by B. Harfe and A. Fire. Strain PD4251 carries an integrated array, *ccIs4251*, which expresses GFP under the *myo-3* promoter in body wall muscle cells (Fire *et al.*, 1998).

To generate *sel-12;hop-1* double mutant animals, two strains were constructed: Both *hop-1(lg1501)/unc-73(e936)*; *sel-12(ar171)*; *ayIs2* and *hop-1(lg1501)*; *sel-12(ar171) unc-1(e538)/+*; *ayIs2* strains were maintained by picking non-Unc hermaphrodites that segregated Unc progeny.

Isolation of Additional *sel-12* Alleles

To screen for mutations that fail to complement the Egl defect of *sel-12(ar171)* mutant hermaphrodites, *sel-12(ar171) unc-1(e538)/dpy-3(m39)* hermaphrodites were mutagenised with 50 mM EMS and their Non-Dpy Non-Unc F₁ progeny were scored for the appearance of an Egl phenotype. After screening 12,000 haploid genomes, 2 novel *sel-12* alleles, *by125* and *by152*, were identified. To further characterise its phenotype, *sel-12(by125)* was outcrossed 7 times and unlinked from *dpy-3*.

Plasmid Constructs and Injections

To express *sel-12* in differentiated muscle cells, we constructed transcriptional fusions of the *sel-12* cDNA with the *myo-3* and *unc-54* promoters. The *sel-12* cDNA was amplified from a mixed stage cDNA library (kindly provided by Bob Barstead) by PCR using primers RB541 (5'-gaggtaccgggcaaaaaatgccttccacaaggagacaacagg-3') and RB542 (5'-gtgaattcggccgcttaataataaacttttgagagacttg-3') and subcloned into pBlueScriptIIKS (Stratagene) as a *KpnI/NotI* fragment leading to pBY453. The *sel-12* cDNA sequence was confirmed by sequencing (GenBank Accession No. AF171064). Subsequently, a *sel-12 KpnI/SacI* fragment was subcloned into pPD96.52 to generate pBY897 (*myo-3::sel-12*) and into pPD30.38 to create pBY896 (*unc-54::sel-12*). Each plasmid was injected at 20 ng/ μ l together with 20 ng/ μ l pBY218 (*ttx-3::gfp* fusion (Hobert *et al.*, 1997), as a cotransformation marker.

To rescue the sex muscle defects of *sel-12* animals, the *sel-12* cDNA was fused to the *hlh-8* promoter at the ATG translation start of *hlh-8*. The *sel-12* cDNA was amplified by using the PCR primers RB1098 (5'-atatgatttcacagatgccttccacaaggagaca-3') and RB1099 (5'-tctcctgtggaaggcatctgtgaaatcatattgaaatcg-3') and was cloned into pBH47.70 (gift of B. Harfe and A. Fire; Corsi *et al.*, 2000; Harfe *et al.*, 1998b) to replace GFP. The resulting vector pBY1224 expresses *sel-12* from the 1791-bp *hlh-8* promoter and was injected at a concentration of 20 ng/ μ l. To exclude any influence of the cotransformation marker on the Egl rescue, pBY1224 was injected with either pBY218 (*ttx-3::gfp* fusion; Hobert *et al.*, 1997) at 20 ng/ μ l, or with the dominant phenotypic marker *rol-6* (pRF4; Mello *et al.*, 1991) at 100 ng/ μ l. For π cell expression of *sel-12*, the plasmid cHCN2 (*cog-2::sel-12*) (Cinar *et al.*, 2001) was injected at 80 ng/ μ l together with pRF4 (*rol-6*) at 100 ng/ μ l as coinjection marker.

Drug Tests

The egg-laying behaviour in response to 5 mg/ml serotonin (Sigma), 0.75 mg/ml imipramine (Sigma), and/or 1 mg/ml chlorpromazine (Sigma) was scored in M9 according to previously published procedures (Trent *et al.*, 1983; Weinschenker *et al.*, 1995). Tests were conducted with synchronised adult hermaphrodites that contained on average 15 eggs in their uterus. Only those animals that did not show a Pvl phenotype were analysed in the drug tests (see Results).

Phenotypic Analysis

To analyse their brood size, hermaphrodites were picked as L2 or L3 larvae onto single plates. After they reached adulthood, animals were transferred to new plates daily until death, and the progeny were counted the following day. To quantify the Pvl phenotype, worms were singled as L2 and L3 and scored as young adults. To assess their muscle morphology, worms carrying the various GFP constructs were synchronised and analysed at different developmental stages by using a Zeiss Axioskop microscope. The appearance of a thick tissue separating the vulval and uterine lumen indicative of a π cell specification defect was scored in worms in mid-L4 as described (Cinar *et al.*, 2001).

Male Mating Test

Male mating efficiency tests were performed at 25°C according to Hodgkin (1980). Five young adult males were placed on 3.5-cm

NGM plates with five *fem-1(hc17ts)*; *unc-4(e120)* virgins. After 12 h, the males were removed from the plates and the hermaphrodites were transferred to new plates daily. As *fem-1(hc17ts)* mutants are unable to produce sperm at 25°C, all progeny on the plates must be cross progeny. To generate sufficient numbers of males for mating tests, we constructed double mutants of each *sel-12* allele with both *him-5(e1490)* and *him-8(e1489)*. Two different *him* genes were used to exclude any synthetic interaction between the *him* mutation and *sel-12*. The mating tests gave comparable results in both *him* genetic backgrounds.

Male Tail Curling Tests

Male tail curling tests were performed as described (Loer and Kenyon, 1993). Adult males were placed in M9 medium containing 20 mM serotonin, and their ability to curl their tails was scored after 10 min for a period of 10 s for each animal.

RESULTS

Molecular Characterisation of *sel-12* Mutants

Although both *sel-12(ar131)* and *sel-12(ar171)* alleles display a highly penetrant Egl defect, the exact phenotype differs. To determine the degree of variability, we compared the phenotypes of both alleles with those of two new *sel-12* alleles, *by125* and *lg1401*. *sel-12(by125)* contains a mutation in the eighth codon, changing a CAG into TAG, which converts a glutamine into a stop codon (Fig. 1). *sel-12(by1401)* harbours a 1028-bp deletion that extends from nucleotide 4766 to 5793 of cosmid F35H12, deleting 244 bp of promoter sequences, the ATG and the first three exons of *sel-12* that encode transmembrane domains 1 and 2. On a Northern blot, no *sel-12* mRNA was detectable from the *sel-12(lg1401)* allele, indicating that it is a null allele. The *sel-12* mRNA level from allele *sel-12(ar171)* was strongly reduced, whereas *sel-12(by125)* and *sel-12(ar131)* had mRNA levels comparable with wild type (data not shown).

All *sel-12* alleles tested display a similar egg-laying defect (Egl phenotype) to that described previously for *sel-12(ar131)* and *sel-12(ar171)* (Levitan and Greenwald, 1995) (Table 1). The presumptive null alleles *sel-12(ar171)* and *sel-12(lg1401)* almost never lay eggs, whereas *sel-12(by125)* animals occasionally lay a few eggs before retaining eggs as older adults. Most animals die of a bag-of-worms phenotype because the young larvae that hatch intrauterinely kill their mothers. On the other hand, many *sel-12(ar131)* animals lay a considerable number of eggs and not all animals become Egl. We conclude that the *sel-12* alleles *ar171*, *lg1401*, and *by125* have a comparably penetrant Egl defect, whereas *sel-12(ar131)* mutants are somewhat different and show a weaker Egl phenotype (Table 1).

sel-12 mutant animals also display an easily visible protruding vulva (Pvl) phenotype (Fig. 1) with a variable penetrance. The Pvl defect was observed in 80% of *sel-12(ar171)*, 62% of *sel-12(lg1401)*, and 60% of *sel-12(by125)* animals (Table 1). However, only 13% of the *sel-12(ar131)* adults became Pvl, suggesting that there is no strong

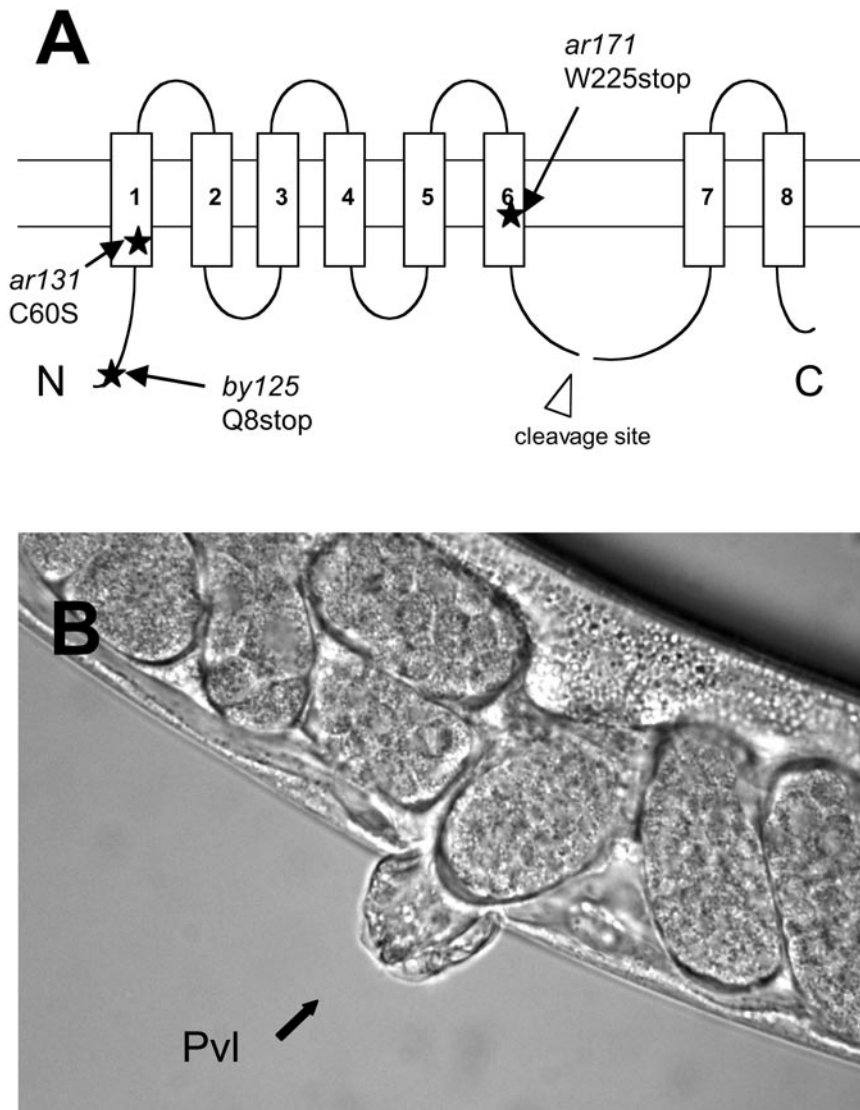


FIG. 1. (A) The SEL-12 topology as proposed (Doan *et al.*, 1996; Li and Greenwald, 1996, 1998). Positions of the mutations used here are indicated. The arrow marks the cleavage site of SEL-12 (Okochi *et al.*, 2000). *sel-12(lg1401)* is a 1.0-kb deletion of part of the promoter and the first three exons of *sel-12*. (B) Protruding vulva phenotype (Pvl) of a *sel-12(ar171)* mutant adult hermaphrodite.

correlation between the penetrance of the Pvl and Egl phenotypes.

It had been suggested previously that the egg-laying defect of *sel-12* mutant animals is caused by a misspecification of the π cell lineage that results in a failure of the vulva to connect to the uterine tissues (Cinar *et al.*, 2001). Indeed, we noticed that 79% of *sel-12(ar171)*, 73% of *sel-12(lg1401)*, and 66% of *sel-12(by125)* animals displayed the thick tissue separating the uterus and vulva that is typical for animals with the π cell defect (Table 1). However, only in a minority of *sel-12(ar131)* animals is the utse cell (uterine seam cell) thick, even though 88% of these animals developed an Egl phenotype (Table 1).

We concluded that a sterical blockage of the vulva opening as a consequence of a π cell misspecification is unlikely to be the only cause of the highly penetrant Egl defect seen in *sel-12(ar131)* hermaphrodites (see Table 1). This interpretation is also supported by the observation that most of the *sel-12(ar131)* hermaphrodites lay some eggs as young adults before they become Egl. In addition, since all *sel-12* strains tested so far can be mated, we conclude that, in all alleles, the vulva is open in at least some animals, allowing sperm entry. We also note that the penetrance of the π cell defect corresponds rather well to the penetrance of the Pvl defect. The penetrance of Pvl and egg-laying defects were also reflected in the brood size of the various alleles. All

TABLE 1Phenotypic Characterization of the Egg-Laying of Different *sel-12* Alleles

Allele	Phenotype ^a					<i>n</i>
	Thick tissue§ (%)	Pvl (%)	Egl (%)	Bagged (%)	Progeny ± SEM	
N2	0 (0/40)	0	0	0	316 ± 8	20
<i>sel-12(ar171)</i>	79 (33/42)	80	100	100	62 ± 5	25
<i>sel-12(lg1401)</i>	73 (44/60)	62	100	100	81 ± 6	29
<i>sel-12(by125)</i>	66 (42/64)	60	100	95	94 ± 6	57
<i>sel-12(ar131)</i>	20 (22/108)	13	88	83	100 ± 7	40

Note. *n*, number of animals characterised; SEM, standard error of the mean.

^a Pvl, protruding vulva; Egl, egg-laying defective; bagged, death due to internal hatching. *sel-12* molecular lesions are as follows: (*ar171*) W227stop; (*lg1401*) 1.0-kb deletion of part of the promoter and the first three exons of *sel-12*; (*by125*) Q8stop; and (*ar131*) C60S.

^b Thick tissue describes the defects in utse specification scored in mid L4, where a thick tissue rather than a thin laminar process separates the uterus and the vulva (Cinar *et al.*, 2001).

alleles that display a high percentage of Pvl have strongly reduced brood size. However, *sel-12(ar131)* animals produce, on average, a significantly higher number of progeny, and some animals even reach brood sizes in the range of the wild type (200 progeny and more).

***sel-12* Egg-Laying Does Not Respond to Neurotransmitter Stimulation**

Since most of the *sel-12(ar131)* animals lack obvious morphological abnormalities, we reasoned that the highly penetrant egg-laying defect of this allele cannot be explained by the Pvl or the π lineage defect. The egg-laying behaviour of *C. elegans* requires the intact anatomy and function of the uterus, the vulva, and their respective muscles, as well as neuronal input from the two HSN neurons and the six VC motor neurons (Corsi *et al.*, 2000; Li and Chalfie, 1990). The generation of the anchor cell (AC) (Kimble, 1981; Sulston and White, 1980; Thomas *et al.*, 1990; Trent *et al.*, 1983) that is critical for the induction of the vulva development is not affected in *sel-12* animals (Levitan and Greenwald, 1995) and there is no obvious defect in the epidermal portion of the vulva (Levitan and Greenwald, 1998). Since we have previously shown that neural function is affected in *sel-12* mutant animals (Wittenburg *et al.*, 2000), we reasoned that defective neuronal input into the sex muscles could be the cause of the Egl phenotype.

Neuronal signalling to the vulva muscles can be mimicked by a variety of drugs that stimulate the contraction of the vulva muscles, and therefore, egg-laying (Trent *et al.*, 1983; Weinshenker *et al.*, 1995). We exposed *sel-12* mutant

animals to the serotonin reuptake inhibitor imipramine, to the dopamine antagonist chlorpromazine, to serotonin (Table 2), and to the acetylcholine agonist levamisole (data not shown). Since we expected that the physical blockage of the vulva opening in Pvl animals would effectively prevent stimulation of egg-laying under any conditions, we only tested non-Pvl animals in our pharmacological assays. None of the *sel-12* alleles that we tested responded to any of the drugs. Since exogenous addition of serotonin, a strong, direct stimulator of the egg-laying muscles that is effective even if the innervating motorneurons HSN are absent (Trent *et al.*, 1983; Weinshenker *et al.*, 1995), could not induce egg-laying, our results suggest that *sel-12* mutants have a postsynaptic defect in the muscular structures of the vulva, or behave like muscle activation mutants (Mac (Reiner *et al.*, 1995; Trent *et al.*, 1983).

***sel-12* Mutant Animals Display Defects in Their Sex Muscles**

Two types of muscles control the expulsion of fertilised eggs in the *C. elegans* hermaphrodite: the uterine muscles (um1 and um2) and the vulva muscles (vm1 and vm2) (Corsi *et al.*, 2000; Sulston and Horvitz, 1977). Both types of sex muscles are derived from the sex myoblast (SM) cells in wild type. In the wild type, the SMs migrate during the second larval stage (L2) from their place of birth in the tail towards the midbody region, where the epidermal structures of the vulva are formed. At their final position near the vulva, they divide three times to generate the eight uterine and eight vulva muscles (Fig. 2). However, in *lin-12* null mutants, a cell fate transformation from SM to CC (coelomocytes) prevents the generation of all sex muscles.

In order to examine the generation of the SM lineage and the morphological integrity of the sex muscles in *sel-12* mutants, we visualised cells in the SM lineage using differ-

TABLE 2Pharmacological Egg-Laying Response of Wild Type and *sel-12* Mutant Animals

	Eggs layed per time interval in response to:			Animals tested
	Serotonin	Imipramine	Chlorpromazine	
N2	6.1 ± 0.9	11.8 ± 1.1	7.8 ± 2.0	30
<i>sel-12(ar171)</i>	0.5 ± 0.3	0.9 ± 0.3	0.2 ± 0.0	30 ^a
<i>sel-12(ar131)</i>	1.5 ± 0.3	1.8 ± 0.3	3.4 ± 0.7	30 ^a

Note. The egg laying response (±SEM) of wild type and *sel-12* mutant animals to 5 mg/ml serotonin, 1.0 mg/ml chlorpromazine (time intervals = 60 min), and 0.75 mg/ml imipramine (time interval = 90 min) was tested in liquid M9 medium as described (Trent *et al.*, 1983; Weinshenker *et al.*, 1995).

^a Only *sel-12* mutant animals without a Pvl were tested (see Material and Methods).

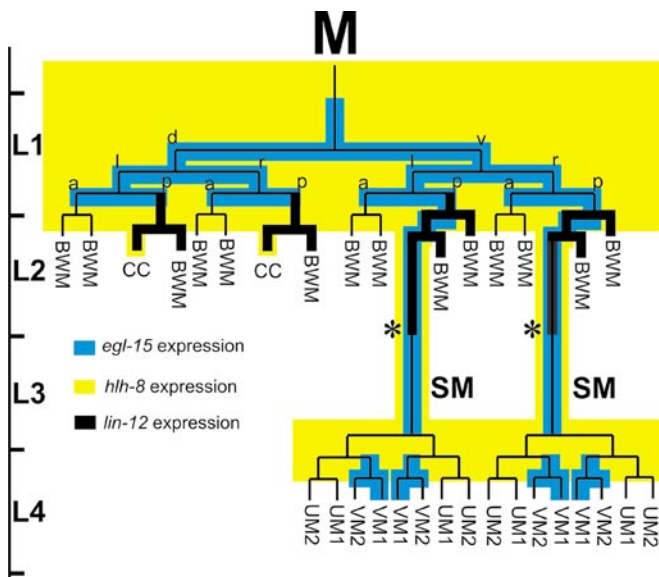


FIG. 2. Postembryonic mesodermal M lineage in *C. elegans* (lineage was redrawn from Harfe *et al.*, 1998a; Sulston and Horvitz, 1977). The M lineage gives rise to different cell types: BWM (body wall muscles), CC (coelomocytes), SM (sex myoblasts), UM (uterine muscles), and VM (vulva muscles). The M mesoblast is born shortly before hatching, and its descendants divide until the L4 stage. The expression patterns of *hlh-8* (Corsi *et al.*, 2000; Harfe *et al.*, 1998b), *egl-15* (Harfe *et al.*, 1998a), and *lin-12* (Wilkinson and Greenwald, 1995) within the M-lineage are shown. *, *lin-12* expression has only been followed until the birth of SM. There are no published expression data for the SM lineage in L3 and L4.

ent GFP reporter constructs. The *hlh-8::gfp* marker is active in all cells derived from the M lineage (Harfe *et al.*, 1998b). To examine whether a transformation of SM into CC fate occurs in *sel-12* mutants, we counted the number of GFP-positive cells at different stages of larval development in *sel-12* animals expressing *hlh-8::gfp*. In all *sel-12* alleles tested, we found 2 SMs that, after migration and divisions, gave rise to 16 *hlh-8::gfp*-positive cells (data not shown). From this, we conclude that *sel-12* null mutants, unlike *lin-12* null mutants, do not affect the SM/CC decision. However, the sex muscle cells displayed structural abnormalities that we further examined using other markers. To visualise the vulva muscles, we used an integrated GFP construct (*ayIs2*) expressed specifically in the vm1 muscles under the control of the *egl-15* promoter (Harfe *et al.*, 1998a). In a wild type background, more than 99% of the GFP-expressing vm1 cells in adult animals are symmetrically aligned around the vulva and show the typical X-shaped structure reported earlier (Harfe *et al.*, 1998a) (Fig. 3A). In *sel-12(ar171)* mutants, the migration of the SMs is only weakly affected. About 90% ($n = 30$) of the animals examined had the vm1 muscles positioned in the correct body region, and in only 10% of the animals, a SM descendant was positioned incorrectly in the posterior body re-

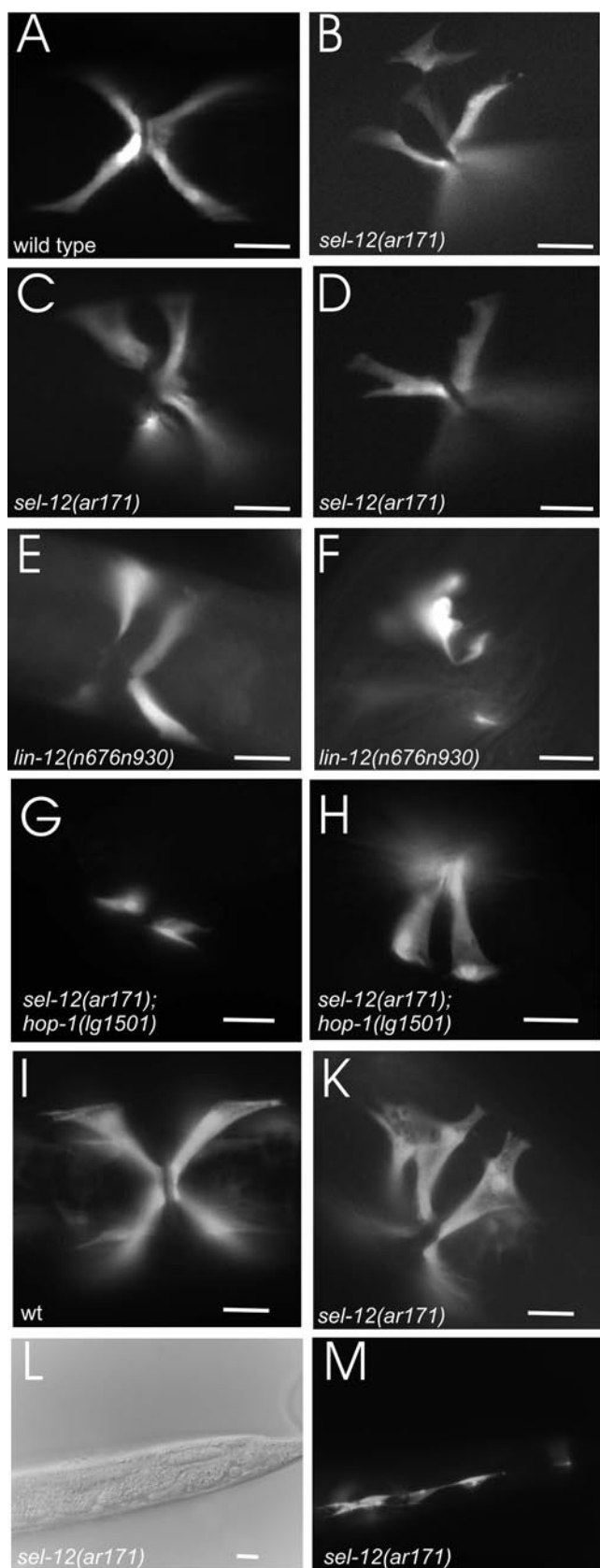
gion. These mismigrated vulva muscle cells still differentiated and acquired their vulva muscle-specific shape (see, e.g., Fig. 3M). Although the majority of vm1 cells were found at the correct place, 25 of 30 *sel-12(ar171)* non-Pv1 animals had visible defects in both their morphology and their attachment to the vulva opening (Figs. 3B–3D). The majority (89%) of animals with the weaker *sel-12(ar131)* allele also displayed vulva muscle defects. From these data, we conclude that *sel-12* is required for the correct morphogenesis of the sex muscles vm1.

In order to test whether *sel-12* mutations also affect the morphogenesis of vm2 muscles, we used an integrated array, *ccIs4656*, which contains the *Nde-box::gfp* gene (Harfe *et al.*, 1998a; Harfe and Fire, 1998). The *Nde-box* is derived from the *ceh-24* promoter, and in L4, this construct drives expression late in the development of all vulva muscles and the uterine muscles (Harfe and Fire, 1998). It is therefore considered to be a marker for differentiated sex muscles (Liu and Fire, 2000). The GFP-positive vm2 muscles in all *sel-12* alleles tested displayed morphological defects similar to those seen in the vm1 muscles (Figs. 3K and 3M). However, the expression levels of the *egl-15::gfp* and *Nde-box::gfp* markers were comparable with wild type, suggesting that the sex muscles are specified correctly and have differentiated into muscle cells. Their adoption of the correct cell fate is also indicated by their expression of *myo-3::gfp* (*ccIs4251*), a marker for terminally differentiated muscle cells.

In summary, mutations in *sel-12* affect the morphology and attachment of the sex muscles. However, the expression of at least three late markers suggests that parts of their terminal differentiation program that identifies them as sex muscle cells are executed correctly.

Expression of *sel-12* in the M Lineage Potentially Rescues the *Egl* Defect

Since *sel-12* is expressed in most, if not all, cells of the animals, the sex muscle defects seen in *sel-12* mutant animals could be caused by loss of *sel-12* activity in the differentiating muscle itself, in its precursor during its development, or in adjacent cells that provide signals for muscle orientation or attachment. To distinguish between these different possibilities, we tried to rescue the sex muscle defects of *sel-12* mutant animals by expressing the *sel-12* cDNA from different promoters. From previous experiments, we knew that the *sel-12* cDNA expressed from its own promoter is able to rescue all defects present in *sel-12* mutant animals (Baumeister *et al.*, 1997; Levitan *et al.*, 1996; Wittenburg *et al.*, 2000). Since the vulva muscles in *sel-12* mutants expressed a number of muscle-specific markers, we suspected that *sel-12* is required late in sex muscle development. Therefore, we first tested whether *sel-12* expression from the well-characterised muscle-specific myosin promoters *unc-54* and *myo-3* (Miller *et al.*, 1983) is sufficient to rescue the muscle defect. *unc-54* and *myo-3* are expressed in all body wall muscles as well as in



the vulva muscles (Miller *et al.*, 1983). We generated five independent transgenic lines for *unc-54::sel-12* and for *myo-3::sel-12*, respectively, but did not detect any rescuing activity in transgenic animals (between 21 and 63 transgenic animals analysed per line, 386 animals total). The functionality of these well characterised promoters had been tested before using GFP. Since the fluorescence levels of *unc-54::gfp* and *myo-3::gfp* transgenes containing the corresponding promoter elements are comparable or even stronger than that of *sel-12::gfp* (data not shown), we consider it unlikely that insufficient expression levels of *sel-12* are responsible for the lack of rescue.

In *C. elegans*, both *unc-54* and *myo-3* are expressed at a rather late stage in sex muscle differentiation, starting at the L4 stage (Liu and Fire, 2000). It is therefore possible that *sel-12* activity is needed at an earlier step during the differentiation of the sex muscles. To test this hypothesis, we expressed the *sel-12* cDNA under the control of the *hlh-8* promoter. This promoter is specific for the M lineage from which all postembryonic mesoderm is derived (Sulston and Horvitz, 1977). The *hlh-8* promoter is active at the time the M mesoblast is born and remains active until the vulval and uterine muscles are specified (Fig. 2). Its activity is lost only when cells have differentiated into body wall or sex muscles (Harfe *et al.*, 1998b). Expression of the *sel-12* cDNA from the *hlh-8* promoter rescued the Egl defect of 85% of the weaker *sel-12(ar131)* animals, whereas it was sufficient to rescue the Egl defect in 20% of the *sel-12(ar171)* animals (Table 3). However, in no case was the morphological defect leading to the Pvl phenotype rescued by transgenic *hlh-8::sel-12* expression (Table 3).

We suggest that the egg-laying defect in the majority of *sel-12(ar131)* animals and a smaller portion of the *sel-*

FIG. 3. Vulva muscle defects in presenilin and *lin-12*/Notch mutants visualised by *egl-15::gfp* (A–H) and *Nde-box::gfp* (I, K, M). (A) Wild-type (N2) hermaphrodite: ventral view of *egl-15::gfp* expression in the four vm1 vulva muscles. The vulva muscles are attached to the vulva epithelium in an X-shaped arrangement. (B–D) *sel-12(ar171)* animals (ventral view) exhibit disorganised and malformed vm1 vulva muscles. Similar sex muscle defects are also seen for the other *sel-12* alleles tested (data not shown). (E, F) *lin-12(n676n930)* mutant hermaphrodites grown at 23°C show the same kind of vulva muscle defects as *sel-12* mutant animals. The *lin-12(n676n930)* strain also contained a linked *unc-32(e189)* mutation which did not influence vulva muscle morphology. (G, H) *hop-1(lg1501); sel-12(ar171)* animals. Shown here are the sex muscle defects in two of the rare animals that did not display a significant Pvl. (I) Wild-type hermaphrodite, ventral view, transgenic for the *Nde-box::gfp* that is expressed in both vm1 and vm2 (compare with A). (K) *sel-12(ar171)* animal with multiple vm1 and vm2 attachment defects. (L, M) Migration defect of sex muscles in the tail of a *sel-12(ar171)* animal. Left side, Nomarski image. Wild type and *sel-12* mutant animals were raised at 20°C, whereas *lin-12(n676n930)* mutant animals were raised at 23°C. Each scale bar represents 10 μm.

TABLE 3
Expression of the *sel-12* cDNA in the M Lineage Can Rescue the Egg-Laying Defect of *sel-12* Mutant Animals

Genotype	Phenotype			Progeny: Mean ± SEM	n
	Pvl (%)	Egl (%)	Bagged (%)		
N2	0	0	0	316 ± 8	20
<i>sel-12(ar131)</i>	13	88	83	100 ± 7	40
<i>sel-12(ar131); byEx166^a</i>	9	16	16	240 ± 14	32
<i>sel-12(ar131); byEx167^a</i>	9	16	13	271 ± 8	32
<i>sel-12(ar171)</i>	80	100	100	62 ± 5	25
<i>sel-12(ar171); byEx166^a</i>	77	80	77	241 ± 9 ^b	128
<i>sel-12(ar171); byEx167^a</i>	78	82	81	212 ± 11 ^b	129

Note. n, The number of animals counted.

^a *byEx166* and *byEx167* are extrachromosomal arrays containing the *hlh-8::sel-12* rescue construct and the *ttx-3::gfp* as coinjections marker.

^b Note that these numbers contain only the non-Pvl animals. As shown in the text, the Pvl phenotype precludes rescue by *hlh-8::sel-12*.

12(ar171) animals is caused solely by a lack of *sel-12* expression during muscle differentiation. This phenotype can be rescued by expression of *sel-12* from the *hlh-8* promoter. The Egl rescue is very strong, since rescued animals not only display wild type egg-laying behaviour, but also have greatly increased brood sizes (241 ± 9) in the range of wild type (see Table 3). In addition, none of the transgenic *sel-12(ar171)* animals that we scored as rescued died of a bag-of-worms phenotype as compared with 100% of their nontransgenic siblings. However, those animals that cannot be rescued by *hlh-8* promoter driven *sel-12* expression had a pronounced Pvl phenotype. Only animals that did not have a steric blockage due to a π cell defect, and therefore do not develop a Pvl phenotype, could be rescued using this transgene. In summary, we conclude that, in addition to the defective vulva-uterine connection described for the strong *sel-12(ty11)* and *sel-12(ar171)* alleles (Cinar *et al.*, 2001), reduction of *sel-12* activity also causes a developmental defect in the sex muscles that is highly penetrant in all *sel-12* mutants, including the weaker *sel-12(ar131)* allele.

Since expression of *sel-12* from the *hlh-8* promoter did not rescue egg-laying in Pvl animals, we suspected that the protruding vulva is not the consequence of a defect occurring in the sex muscles. We wanted to investigate whether the π cell induction defect in the late L3 of *sel-12* mutant animals (Cinar *et al.*, 2001) is the cause of the later Pvl phenotype. Therefore, we scored the Pvl phenotype in two *sel-12(ar171)* lines transgenic for *cog-2::sel-12* (gift of A. Newman, Houston), a construct previously shown to rescue the π cell specification defect (Cinar *et al.*, 2001). This construct strongly rescued the Pvl defects, as only 3 and 5% ($n > 100$) of transgenic *sel-12(ar171)* animals became Pvl

compared with 80% of the nontransgenic control animals. To confirm this link between π cell defect and appearance of a Pvl, we scored how many of the *sel-12(by125)* animals that showed the presence of a thick tissue separating the vulval and uterine lumen at the L4 stage later developed a protruding vulva (Pvl). All animals ($n = 18$) with a Pvl defect also displayed a thick tissue. Furthermore, those animals ($n = 15$) that showed a thin utse cell (no π cell specification defect) never developed a Pvl.

We conclude that defective specification of the uterine π cells in L3 can lead to a Pvl phenotype in adult animals. This steric blockage of the vulva opening, in combination with defective sex-muscles, is sufficient to cause the highly penetrant egg-laying defect seen in *sel-12* animals.

***lin-12(n676n930)* and *sel-12* Mutants Display Similar Vulva Muscle Defects**

sel-12 mutants reduce, but do not eliminate, *lin-12* signalling and, therefore, *sel-12* animals have no obvious defects in AC/VU decision and in VPC specification (Levitani and Greenwald, 1995). Instead, *sel-12* mutants have a defect in the differentiation of the sex muscles, as shown here, and an additional defect associated with the fate specification of the π cells that control the uterus-vulva connection (Cinar *et al.*, 2001; Wen *et al.*, 2000). *lin-12* is also expressed in cells of the M lineage (Wilkinson and Greenwald, 1995), and in *lin-12* null mutants, the SM descendants of M are transformed to coelomocytes. As a consequence, no sex muscles are formed (Greenwald *et al.*, 1983). In contrast, animals with the weaker loss-of-function allele *lin-12(n676n930)* were shown to contain sex muscles that were positioned correctly. *lin-12(n676n930)* animals show wild type egg-laying at 15°C but become egg-laying defective when these are shifted to 25°C before their temperature-sensitive period (L3/L4) (Sundaram and Greenwald, 1993). A cause for this "late defect" could not be found (Sundaram and Greenwald, 1993). To see whether a *lin-12* loss-of-function mutant displays a similar sex muscle patterning defect to *sel-12* mutants, we examined the morphology of sex muscles in *lin-12(n676n930)* at different temperatures using the *ayIs2 (egl-15::gfp)* marker. Ninety-one percent of *lin-12(n676n930) unc-32(e189)* animals raised at 25°C, but only 3% of the *unc-32(e189)* animals raised at 25°C showed morphological abnormalities in the vm1 muscles (Figs. 3E and 3F). Like in the *sel-12* mutant animals, we detected defects in the attachment of the vm1 muscles to the vulval epidermis, aberrant orientation with respect to the vulva, and structural abnormalities. Similar defects were also detected in a second hypomorphic *lin-12* allele, *lin-12(oz48)* (data not shown). Like in *sel-12* animals, the differentiation of vm1 muscles does not seem to be affected in *lin-12(n676n930)* mutants, since the late sex muscle marker *Nde-Box::gfp* is expressed correctly (data not shown). When raised at the permissive temperature of 15°C, only 5% of the *lin-12(n676n930) unc-32(e189)* hermaphrodites exhibited abnormal vm1 muscles. The fact that *lin-*

TABLE 4The Male Tail Curling and Mating Efficiencies of *sel-12* Mutants Are Reduced

Genotype	Male mating efficiency ^a (%)	Cross progeny Mean \pm SEM	Plates scored (n)	Male tail curling efficiency (%)	Animals tested (n)
<i>sel-12</i> (+)	100	185 \pm 33	12	90	48
<i>sel-12(ar131)</i>	18	34 \pm 11	12	nd	nd
<i>sel-12(ar171)</i>	7	12 \pm 7	6	29	72
<i>sel-12(ar171); byEx166^b</i>	33	60 \pm 26	5	80	96
<i>sel-12(ar171); byEx167^b</i>	27	49 \pm 22	6	90	72

Note. All strains contain *him-5(e1490)*. Similar results were obtained with *sel-12;him-8(e1489)* double mutants. See Materials and Methods for the detailed experimental setup. nd, not determined.

^a Determined in the presence of 20 mM serotonin.

^b *byEx166* and *byEx167* are extrachromosomal arrays containing the *hlh-8::sel-12* rescue construct and the *ttx-3::gfp* as coinjection marker.

lin-2(n676n930) animals show the same range of vulva muscle defects as *sel-12* mutant animals suggests that *sel-12* functions by affecting the *lin-12* activity late during sex muscle development. This activity is different from the previously documented requirement of *lin-12* during specification of the SM fate (Greenwald *et al.*, 1983; Harfe *et al.*, 1998a). The SM/CC decision is executed correctly in both *sel-12* and *lin-12* hypomorphic strains since they develop sex muscles. This suggests a new mode of *sel-12* mediated *lin-12* signalling late in development, possibly to control cell morphology and attachment.

The Sex Muscle Defect Is Most Severe in the Absence of Presenilin Activity

sel-12 is functionally redundant with *hop-1*, another presenilin gene (Li and Greenwald, 1997; Westlund *et al.*, 1999). To test whether the activity of *hop-1* could be responsible for providing sufficient *lin-12* signalling activity in *sel-12* mutants to prevent an SM-to-CC cell fate transformation as seen in *lin-12* null mutants, we examined *hop-1;sel-12* double mutants. Since *sel-12;hop-1* double mutant animals lacking presenilin activity both maternally and zygotically have an embryonic lethal phenotype, we tested maternally rescued animals in which maternal contribution of either *sel-12* gene products (from *sel-12/+;hop-1* mothers) or *hop-1* gene products (from *sel-12;hop-1/+* mothers) allows the homozygous progeny to survive.

Surprisingly, 89% (91/102) of the *sel-12;hop-1* double mutant animals develop vulva muscle cells that express the *egl-15::gfp* marker, regardless of whether the maternally provided presenilin is *sel-12* or *hop-1*. The GFP-positive cells of the SM lineage migrate to their correct position at the vulva, although their terminal position and structure were highly aberrant in all GFP-positive animals ($n = 91$) (Figs. 3G and 3H). This indicates that the SM/CC decision, which occurs in the L2, is not affected in these animals, and that maternal *sel-12* or *hop-1* is sufficient to provide enough presenilin activity in the double mutant progeny to facilitate LIN-12 signalling at least until L2 (see Fig. 2).

Male-Specific *sel-12* Defects in Fan and Sex Muscles Result in Aberrant Male Mating Behaviour

Male mating behaviour requires the functional integrity of several male-specific tissues, including neurons and sex muscles. We found that, in *sel-12* males, the efficiency of mating is strongly impaired, as scored by their ability to fertilise a defined number of sperm-deficient *fem-1(hc17ts)* mutant virgins during a 12-h period (Table 4). Similar to the egg-laying behaviour, the male mating efficiency of *sel-12(ar171)* mutants was lower than that of *sel-12(ar131)* mutants.

One possible cause of the reduced male mating efficiency could be morphological defects in the male tail structures. We therefore inspected the male tails by differential interference contrast (DIC) microscopy. A significant portion of *sel-12(ar171)* animals displayed defects in the structural components of the tail. In 31% of the animals, the fan was strongly affected, being either reduced in size or completely absent (Fig. 4), a phenotype that had also been reported for *lin-12(0)* mutant males (Horvitz *et al.*, 1983). A portion of *sel-12* animals also displayed a notched fan phenotype not described before (as shown in Figs. 4C and 4D). In addition to the malformation in the fan structures in some *sel-12* mutant males, we also noted animals that had a variably abnormal tail tip containing extra tissue (Figs. 4B and 4D). As a consequence, the male tail appears enlarged and flat. In males in which the fan was visible, the number and position of the tail rays were not obviously affected (compare Fig. 4).

Since the morphological defects in the tail structures of *sel-12* males would most likely be sufficient to strongly impair mating success, we tried to directly assess the functionality of the sex muscles in *sel-12* males. A male-specific behaviour that is dependent on functional sex muscles is the ability of wild type males to curl their tail in response to 20 mM serotonin (Loer and Kenyon, 1993). We found that only 29% of the *sel-12(ar171)* males responded to serotonin compared with 90% of the control males tested (Table 4). This tail curling defect could be rescued by

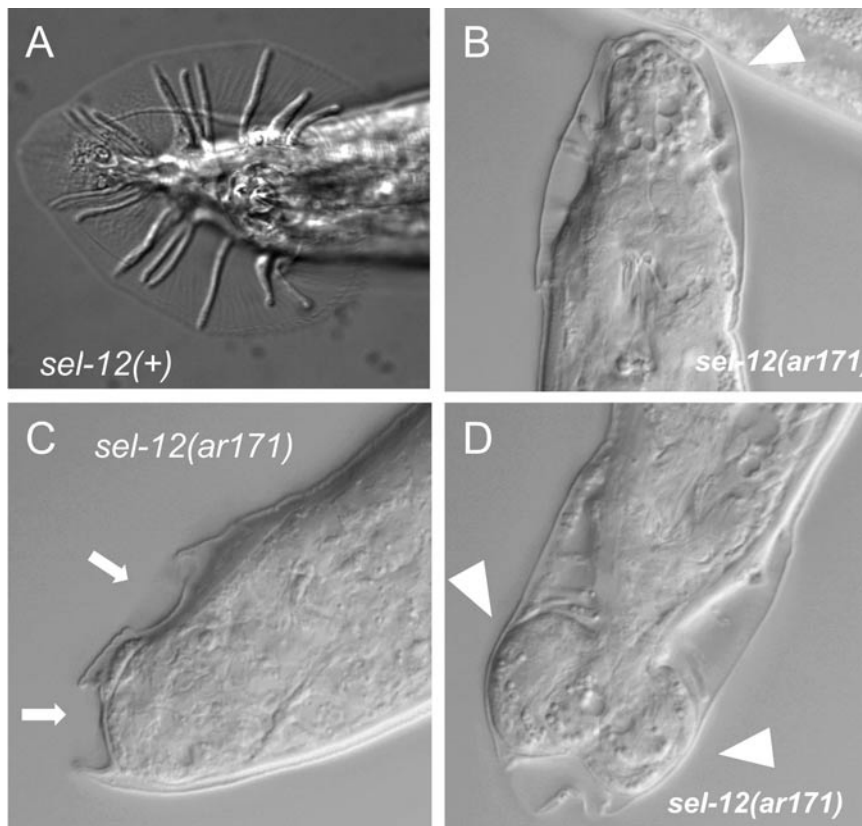


FIG. 4. Nomarski photomicrographs showing the morphological defects in the tails of *sel-12* mutant males. (A) Wild type-like adult male tail of *him-5(e1490)* mutant animals (ventral view). (B–D) *sel-12(ar171);him-5(e1490)* adult male tails exhibiting defects in the fan and tail structures (side views). Arrows, Notched fan structures. Arrowheads, epithelial protrusions never seen in wild type animals. The scale bar represents 20 μm .

expressing *sel-12* specifically in the male sex muscles under the control of the *hlh-8* promoter. In 80% (90%) of the *sel-12* males transgenic for *hlh-8::sel-12*, male tail curling was indistinguishable from *him-5* animals, suggesting a robust rescue of the defect (Table 4). To confirm these results, we also tested the execution of yet another critical step during the male mating behaviour that has also been shown to require the function of the male sex muscles: the turning step (Loer and Kenyon, 1993). The quality of the male turning can be classified as either a good turn, a sloppy turn, or a missed turn. A good turn occurs when the male tail remains in contact with the hermaphrodite throughout the turn. A turn is considered sloppy if the male tail briefly loses contact but then makes contact again on the opposite side of the hermaphrodite. Missed turns occur if the male tail loses and does not regain contact with the hermaphroditic cuticle. By these criteria, the *sel-12* males showed a significant increase in the number of missed and sloppy turns for all *sel-12* alleles tested (Fig. 5). Again, this defect in the male turning behaviour could be rescued by the *hlh-8::sel-12* construct (Fig. 5), indicating that *sel-12* activity is also needed in the male-specific M-lineage.

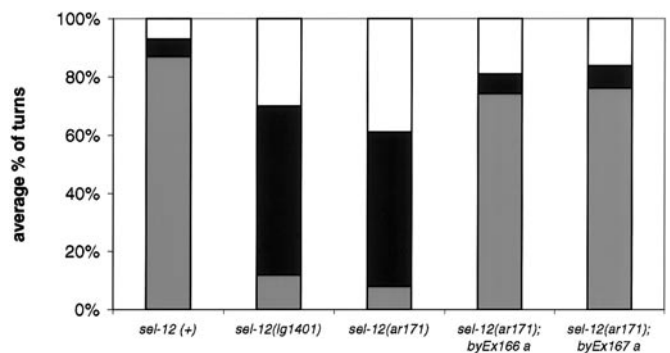


FIG. 5. The male turning ability is reduced in *sel-12* mutant males and can be rescued by expression of the *sel-12* cDNA in the male-specific M-lineage. The y-axis indicates the percentage of turns we characterised as good (light grey), sloppy (dark grey), and missed (white) according to the standards of Loer and Kenyon (1993) (see Material and Methods). *byEx166* and *byEx167* are extrachromosomal arrays containing the *hlh-8::sel-12* rescuing construct as well as the *ttx-3::gfp* coinjection marker. All males used in this analysis also contain *him-5(e1490)*.

However, the overall efficiency of mating by *sel-12* mutant males was only slightly improved by the *hlh-8::sel-12* construct (Table 4), suggesting that additional defects are still present. Consistent with this, only the sex muscle-specific defect could be rescued by the *hlh-8::sel-12* construct and not the aberrant tail structures (data not shown). We conclude that the defects in the sex muscles can be clearly separated from the morphological defects in the tail structures in *sel-12* males. This resembles the situation found in *sel-12* hermaphrodites, where the egg laying is caused by independent defects in both the π cell specification and in the sex muscles.

DISCUSSION

Different Defects Contribute to the *sel-12* Egg-Laying Phenotype

We characterised the developmental defect resulting in the failure of both hypomorphic and null alleles of *sel-12* to lay eggs. Cinar *et al.* (2001) have shown recently that 77% of *sel-12* null mutants display a defect in the *lin-12*-dependent inductive signalling from the AC to the π cell lineage. This signalling is necessary to generate a proper connection between the vulva and uterus (Newman *et al.*, 1995). By expressing *sel-12* in the π cell precursors, the Egl defect of *sel-12(0)* animals could be partially rescued. Our results suggest that a cell specification defect in the π lineage is not the only cause of the Egl phenotype in *sel-12* animals. First, both weak and strong *sel-12* allelic animals display morphological and functional defects in their sex muscles. The absence of functional sex muscles has been shown to be sufficient to cause a completely penetrant Egl defect (Corsi *et al.*, 2000). Second, between 21 and 34% of the *sel-12(0)* animals have the thin process of the utse typical of a correct π cell specification. These animals are not Pvl, but display a fully penetrant Egl phenotype. Third, although only a minority (20%) of the weaker *sel-12(ar131)* animals display the thick tissue characteristic of a defective vulva-uterine interface and only 13% are Pvl, 88% eventually become Egl. Moreover, most of the *sel-12(ar131)* animals initially lay some eggs, which suggests that the connection between the vulval and uterine lumen is not blocked.

We can rescue the majority of the egg-laying defective animals that do not display a Pvl phenotype by cell-autonomous expression of *sel-12* in the M lineage, from which the sex muscles are derived. These animals lack muscle patterning defects (data not shown) and have strongly increased brood sizes within the range of wild type. Efficient behavioural rescue was obtained for all animals that did not display a π cell specification defect. For example, the Egl defect was rescued in 82% of the *sel-12(ar131)* animals, while in 20% of the animals, the steric blockage that is the consequence of the π cell specification defect prevented rescue. Sterical blockage of the vulva is more penetrant in the presumptive *sel-12(0)* alleles, as

approximately 80% of the animals display these defects. However, those *sel-12(0)* animals that did not show vulval blockage were also efficiently rescued by *sel-12* expression in the differentiating sex muscles (Table 3). This suggests that mutations in *sel-12* result in defects in both the vulva-uterine connection and in the sex muscles, and together they cause the highly penetrant Egl phenotype.

In addition to the defects in π cell specification and sex muscle function, *sel-12* animals are also Pvl. We noticed that neither the π cell specification defect nor the Pvl phenotype could be rescued by expressing *sel-12* from the M-lineage-specific *hlh-8* promoter. We also show that only those animals in which the thick tissue separating the vulva and uterine lumen (characteristic for a π lineage defect) was observed in mid-L4 later developed a Pvl phenotype, whereas animals with a thin utse cell (characteristic for wild type) never became Pvl. The progeny of the π cells normally gives rise to two cell types, the utse and the uv1 cells. Both cell types are required for a proper connection between vulva and uterus, the utse cell also has to attach to the seam to prevent vulva eversion (Newman *et al.*, 1996, 2000). The fact that we could rescue the Pvl defect by expressing *sel-12* from the *cog-2* promoter, which is active in π cell precursors (Hanna-Rose and Han, 1999), suggests that the Pvl phenotype results from a defective vulva-uterine connection.

Taken together, our data indicate that different levels of *sel-12* activity are required in the π cell lineage and the M lineage to enable wild type egg-laying. The missense mutation, *sel-12(ar131)*, partially reduces *sel-12* activity and predominantly affects only the M lineage patterning with only very weakly penetrant defects in the π cell lineage, whereas the *sel-12(0)* mutations cause both highly penetrant M lineage and π lineage defects.

Reduced *sel-12* Activity Affects Male Tail Structures

Sex muscle function itself can be assessed more directly in the male tail than in the hermaphrodite egg-laying system. We show here that *sel-12* males also display defects in sex muscle function. Both male tail curling in response to exogenous serotonin and male turning behaviour during mating depend on functional sex muscles and both are impaired in *sel-12* males. Consistently, the expression of a *sel-12* transgene in the male M lineage is sufficient to completely rescue these defects. However, the reduced mating efficiency of *sel-12* males can only be rescued partially by *hlh-8::sel-12* expression. We suggest that the failure to rescue the male mating defect completely is due to additional defects in tail structures in *sel-12* males. The fan defects in mutant males may also reflect defects in *lin-12* signalling since males carrying *lin-12(0)* alleles have been reported to have defective tail structures (Horvitz *et al.*, 1983). We conclude that *sel-12* is required in males for sex muscle function, but has additional roles in other tissues of the male tail that may require *lin-12* signalling activity.

sel-12 Affects LIN-12 Signalling in the Sex Muscles Late in Their Development

The *C. elegans* Notch gene, *lin-12*, is expressed in the M lineage that generates the vulva muscles (Wilkinson and Greenwald, 1995). Null mutations in *lin-12* prevent the generation of the SM precursor cells and result in extra coelomocytes (CC), a cell fate decision that occurs in the early L2 larval stage (Greenwald *et al.*, 1983; Harfe *et al.*, 1998a). Neither *lin-12* expression has been reported in the daughter cells of the SM/CC mothers nor have defects in this lineage after the SM/CC decision that result from the reduction of Notch activity. However, the vulva muscle defects we observed in animals carrying the hypomorphic allele *lin-12(n676n930)* are strikingly similar to those we have seen in *sel-12* mutants. Interestingly, the temperature-sensitive period of this *lin-12* allele extends from the L2 to the mid-L4 stage, long after the SM/CC decision was made (Sundaram and Greenwald, 1993), indicating a late defect in this allele. A late defect in this allele had already been suspected before, but no cellular cause could be determined (Sundaram and Greenwald, 1993). We show here that both *sel-12* and *lin-12(n676n930)* animals have morphologically abnormal vulva muscles and that the attachment of the vulval muscles to the surrounding epidermal tissue does not occur properly.

When are *sel-12* and *lin-12* activities required in the sex muscles and which program is affected by the mutants? Sex muscle cells are generated in both *sel-12* and *lin-12(n676n930)*, since most L4 larvae have *hlh-8::gfp*-expressing SM descendants flanking the developing vulva (Corsi *et al.*, 2000; Harfe *et al.*, 1998b). Therefore, it is unlikely that the SM/CC cell fate decision is strongly affected in *sel-12* and in *lin-12(n676n930)* mutants raised at 25°C. Based on the expression of late sex muscle-specific markers, like *ceh-24::gfp*, *egl-15::gfp*, as well as on the marker for terminally differentiated muscles, *myo-3::gfp* (GFP under the control of the myosin promoter), the sex muscle specification is also probably not affected. We therefore conclude that *sel-12*-mediated *lin-12* signalling is required for sex muscle morphogenesis and attachment rather than for the execution of sex muscle fate. However, *sel-12* has to be active prior to terminal differentiation in the sex muscles, since *unc-54::sel-12* and *myo-3::sel-12* transgenes, which are only expressed in terminally differentiated muscles, were not able to rescue the egg-laying defect in *sel-12* mutants. This is further corroborated by the fact that the promoter we used for efficient rescue, *hlh-8*, is switched off once the uterine and vulval muscles are differentiated (Harfe *et al.*, 1998b).

The *lin-12* null mutant animals have fully penetrant cell specification defects in the SM/CC and the AC/VU decision. *sel-12* null mutants have been shown to reduce *lin-12* signalling. It has been proposed that *hop-1;sel-12* double null mutants have two ACs, indicative of a defective AC/VU decision. Maternal contribution of *hop-1* is not sufficient to rescue the AC/VU defect (Berry *et al.*, 1997; Li

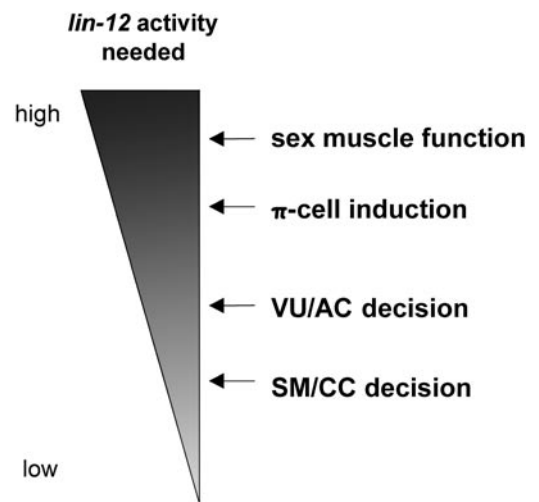


FIG. 6. Distinct signalling events require different levels of *lin-12* activity. Different developmental decisions discussed in the text are ordered according to their sensitivity towards alterations (reductions) in *lin-12* activity. The criterion for the order given is the penetrance of defects in *lin-12*, *sel-12*, and *aph-2* (Levitani *et al.*, 2001) null alleles and in *lin-12* and *sel-12* hypomorphic alleles. VPC specification is not included, since it is not affected in *sel-12* mutants (Levitani and Greenwald, 1995), but probably requires similar levels of *lin-12* signalling as the AC/VU decision.

and Greenwald, 1997; Westlund *et al.*, 1999). In contrast, we show here that either maternally contributed *hop-1* or *sel-12* is sufficient to generate SMs, indicated by the presence of the correct numbers of cells that express an *hlh-8::gfp* marker gene. However, neither the sex muscle patterning defects nor the π cell defects, that are both 100% penetrant in the double mutants, can be rescued maternally.

We therefore suggest that there exist two types of LIN-12 signalling events that require different amounts of *sel-12/hop-1* presenilin and *lin-12* activity. One type of LIN-12 signalling allows two initially equipotent cells to acquire different fates, a well-understood function termed lateral inhibition (Greenwald, 1998; Greenwald and Rubin, 1992). This type of LIN-12 signalling requires initially a small difference in LIN-12 activity in the opposing cells, which is then magnified and stabilised through feedback loops. For such feedback mechanisms, the initial total amount of LIN-12 signalling in both cells involved should be less important than the fact that a small difference can be generated. Both the AC/VU and the SM/CC cell fate decisions belong to this category of LIN-12 cell-cell signalling, explaining why they are rather insensitive to an overall reduction in *lin-12* (and *sel-12*) activity (Fig. 6). The fact that there is a higher amount of *lin-12* (and *sel-12*) activity required for proper π cell induction and sex muscle morphology/attachment suggests that this mode of LIN-12 signalling, unlike the lateral inhibition required in AC and VPC, is unidirectional and inductive (Newman *et al.*, 1995).

Based on the analysis of the *sel-12* Egl defect, we conclude that sex muscle morphology and attachment are the most sensitive events that respond to changes in LIN-12 signaling activity.

Many aspects of presenilin and Notch functions are conserved in evolution, and evidence is accumulating that presenilins may have a similar role in muscle development in vertebrates. Both the presenilins and at least three different Notch receptor genes are expressed in the vascular smooth muscle cells (VSMC) (Krebs *et al.*, 2000). Furthermore, Notch activity in these cells is most likely also required postembryonically, since the receptors and some of their downstream effector genes are constitutively expressed in adult VSMC (Wang *et al.*, 2002). In addition, PS1 is involved in mesodermal patterning in vertebrates, and PS1-deficient mice develop multiple hemorrhages (Shen *et al.*, 1997). Given the striking conservation of the Notch pathways in nonvertebrates and vertebrates, we suggest that *C. elegans* offers an animal model in which we can study in detail both the genetics and the cellular consequences on myogenesis of mutations in the Notch/presenilin pathway.

ACKNOWLEDGMENTS

We thank Brian Harfe, Andy Fire, Michael Stern, and Bernard Lakowski for helpful discussions and comments. We thank Iva Greenwald and Tim Schedl for strains; Brian Harfe, Andy Fire, Catherine Branda, and Michael Stern for GFP reporter constructs; and A. Newman for the *cog-2::sel-12* construct. The *sel-12(lg1401)* deletion allele was kindly provided by Elegene AG, Martinsried, Germany. Some nematode strains used in this work were provided by the *Caenorhabditis* Genetic Stock Center, which is funded by the NIH National Center for research Resources (NCRR). R.B. is supported by grants from the Deutsche Forschungsgemeinschaft, the European Community, and the VERUM Foundation.

REFERENCES

Baumeister, R., Leimer, U., Zweckbronner, I., Jakubek, C., Grunberg, J., and Haass, C. (1997). Human presenilin-1, but not familial Alzheimer's disease (FAD) mutants, facilitate *Caenorhabditis elegans* Notch signalling independently of proteolytic processing. *Genes Funct.* **1**, 149–159.

Berry, L. W., Westlund, B., and Schedl, T. (1997). Germ-line tumor formation caused by activation of *glp-1*, a *Caenorhabditis elegans* member of the Notch family of receptors. *Development* **124**, 925–936.

Brenner, S. (1974). The genetics of *Caenorhabditis elegans*. *Genetics* **77**, 71–94.

Cinar, H. N., Sweet, K. L., Hosemann, K. E., Earley, K., and Newman, A. P. (2001). The SEL-12 presenilin mediates induction of the *Caenorhabditis elegans* uterine π cell fate. *Dev. Biol.* **237**, 173–182.

Conlon, R. A., Reaume, A. G., and Rossant, J. (1995). Notch1 is required for the coordinate segmentation of somites. *Development* **121**, 1533–1545.

Corsi, A. K., Kostas, S. A., Fire, A., and Krause, M. (2000). *Caenorhabditis elegans* twist plays an essential role in non-striated muscle development. *Development* **127**, 2041–2051.

Doan, A., Thinakaran, G., Borchelt, D. R., Slunt, H. H., Ratovitsky, T., Podlisny, M., Selkoe, D. J., Seeger, M., Gandy, S. E., Price, D. L., and Sisodia, S. S. (1996). Protein topology of presenilin 1. *Neuron* **17**, 1023–1030.

Fire, A., Xu, S., Montgomery, M. K., Kostas, S. A., Driver, S. E., and Mello, C. C. (1998). Potent and specific genetic interference by double-stranded RNA in *Caenorhabditis elegans*. *Nature* **391**, 806–811.

Greenwald, I. (1998). LIN-12/Notch signaling: Lessons from worms and flies. *Genes Dev.* **12**, 1751–1762.

Greenwald, I., and Rubin, G. M. (1992). Making a difference: The role of cell–cell interactions in establishing separate identities for equivalent cells. *Cell* **68**, 271–281.

Greenwald, I. S., Sternberg, P. W., and Horvitz, H. R. (1983). The *lin-12* locus specifies cell fates in *Caenorhabditis elegans*. *Cell* **34**, 435–444.

Hanna-Rose, W., and Han, M. (1999). COG-2, a sox domain protein necessary for establishing a functional vulval–uterine connection in *Caenorhabditis elegans*. *Development* **126**, 169–179.

Harfe, B. D., Branda, C. S., Krause, M., Stern, M. J., and Fire, A. (1998a). MyoD and the specification of muscle and non-muscle fates during postembryonic development of the *C. elegans* mesoderm. *Development* **125**, 2479–2488.

Harfe, B. D., and Fire, A. (1998). Muscle and nerve-specific regulation of a novel NK-2 class homeodomain factor in *Caenorhabditis elegans*. *Development* **125**, 421–429.

Harfe, B. D., Vaz Gomes, A., Kenyon, C., Liu, J., Krause, M., and Fire, A. (1998b). Analysis of a *Caenorhabditis elegans* Twist homolog identifies conserved and divergent aspects of mesodermal patterning. *Genes Dev.* **12**, 2623–2635.

Herreman, A., Hartmann, D., Annaert, W., Saftig, P., Craessaerts, K., Serneels, L., Umans, L., Schrijvers, V., Checler, F., Vanderschichele, H., Baekelandt, V., Dressel, R., Cupers, P., Huylebroeck, D., Zwijsen, A., Van Leuven, F., and De Strooper, B. (1999). Presenilin 2 deficiency causes a mild pulmonary phenotype and no changes in amyloid precursor protein processing but enhances the embryonic lethal phenotype of presenilin 1 deficiency. *Proc. Natl. Acad. Sci. USA* **96**, 11872–11877.

Hirsh, D., Oppenheim, D., and Klass, M. (1976). Development of the reproductive system of *Caenorhabditis elegans*. *Dev. Biol.* **49**, 200–219.

Hobert, O., Mori, I., Yamashita, Y., Honda, H., Ohshima, Y., Liu, Y., and Ruvkun, G. (1997). Regulation of interneuron function in the *C. elegans* thermoregulatory pathway by the *txx-3* LIM homeobox gene. *Neuron* **19**, 345–357.

Hodgkin, J. (1980) More sex-determination mutants of *Caenorhabditis elegans*. *Genetics* **96**, 649–664.

Horvitz, H. R., Sternberg, P. W., Greenwald, I. S., Fixsen, W., and Ellis, H. M. (1983). Mutations that affect neural cell lineages and cell fates during the development of the nematode *Caenorhabditis elegans*. *Cold Spring Harbor Symp. Quant. Biol.* **48**, 453–463.

Huppert, S. S., Le, A., Schroeter, E. H., Mumm, J. S., Saxena, M. T., Milner, L. A., and Kopan, R. (2000). Embryonic lethality in mice homozygous for a processing-deficient allele of Notch1. *Nature* **405**, 966–970.

Kidd, S., Lieber, T., and Young, M. W. (1998). Ligand-induced cleavage and regulation of nuclear entry of Notch in *Drosophila melanogaster* embryos. *Genes Dev.* **12**, 3728–3740.

- Kimble, J. (1981). Alterations in cell lineage following laser ablation of cells in the somatic gonad of *Caenorhabditis elegans*. *Dev. Biol.* **87**, 286–300.
- Kimble, J., Edgar, L., and Hirsh, D. (1984). Specification of male development in *Caenorhabditis elegans*: The fem genes. *Dev. Biol.* **105**, 234–239.
- Kimble, J., and Hirsh, D. (1979). The postembryonic cell lineages of the hermaphrodite and male gonads in *Caenorhabditis elegans*. *Dev. Biol.* **70**, 396–417.
- Koizumi, K., Nakajima, M., Yuasa, S., Saga, Y., Sakai, T., Kuriyama, T., Shirasawa, T., and Koseki, H. (2001). The role of presenilin 1 during somite segmentation. *Development* **128**, 1391–1402.
- Krebs, L. T., Xue, Y., Norton, C. R., Shutter, J. R., Maguire, M., Sundberg, J. P., Gallahan, D., Closson, V., Kitajewski, J., Callahan, R., Smith, G. H., Stark, K. L., and Gridley, T. (2000). Notch signaling is essential for vascular morphogenesis in mice. *Genes Dev.* **14**, 1343–1352.
- Levitán, D., Doyle, T. G., Brousseau, D., Lee, M. K., Thinakaran, G., Slunt, H. H., Sisodia, S. S., and Greenwald, I. (1996). Assessment of normal and mutant human presenilin function in *Caenorhabditis elegans*. *Proc. Natl. Acad. Sci. USA* **93**, 14940–14944.
- Levitán, D., and Greenwald, I. (1995). Facilitation of *lin-12*-mediated signalling by *sel-12*, a *Caenorhabditis elegans* S182 Alzheimer's disease gene. *Nature* **377**, 351–354.
- Levitán, D., and Greenwald, I. (1998). Effects of SEL-12 presenilin on LIN-12 localization and function in *Caenorhabditis elegans*. *Development* **125**, 3599–3606.
- Levitán, D., Yu, G., St George Hyslop, P., and Goutte, C. (2001). APH-2/nicastrin functions in LIN-12/Notch signaling in the *Caenorhabditis elegans* somatic gonad. *Dev. Biol.* **240**, 654–661.
- L'Hernault, S. W., and Arduengo, P. M. (1992). Mutation of a putative sperm membrane protein in *Caenorhabditis elegans* prevents sperm differentiation but not its associated meiotic divisions. *J. Cell Biol.* **119**, 55–68.
- Li, C., and Chalfie, M. (1990). Organogenesis in *C. elegans*: Positioning of neurons and muscles in the egg-laying system. *Neuron* **4**, 681–695.
- Li, X., and Greenwald, I. (1996). Membrane topology of the *C. elegans* SEL-12 presenilin. *Neuron* **17**, 1015–1021.
- Li, X., and Greenwald, I. (1997). HOP-1, a *Caenorhabditis elegans* presenilin, appears to be functionally redundant with SEL-12 presenilin and to facilitate LIN-12 and GLP-1 signaling. *Proc. Natl. Acad. Sci. USA* **94**, 12204–12209.
- Li, X., and Greenwald, I. (1998). Additional evidence for an eight-transmembrane-domain topology for *Caenorhabditis elegans* and human presenilins. *Proc. Natl. Acad. Sci. USA* **95**, 7109–7114.
- Liu, J., and Fire, A. (2000). Overlapping roles of two Hox genes and the exd ortholog *ceh-20* in diversification of the *C. elegans* postembryonic mesoderm. *Development* **127**, 5179–5190.
- Loer, C. M., and Kenyon, C. J. (1993). Serotonin-deficient mutants and male mating behavior in the nematode *Caenorhabditis elegans*. *J. Neurosci.* **13**, 5407–5417.
- Mello, C. C., Kramer, J. M., Stinchcomb, D., and Ambros, V. (1991). Efficient gene transfer in *C. elegans*: Extrachromosomal maintenance and integration of transforming sequences. *EMBO J.* **10**, 3959–3970.
- Miller, D. M., 3rd, Ortiz, I., Berliner, G. C., and Epstein, H. F. (1983). Differential localization of two myosins within nematode thick filaments. *Cell* **34**, 477–490.
- Newman, A. P., Inoue, T., Wang, M., and Sternberg, P. W. (2000). The *Caenorhabditis elegans* heterochronic gene *lin-29* coordinates the vulval–uterine–epidermal connections. *Curr. Biol.* **10**, 1479–1488.
- Newman, A. P., White, J. G., and Sternberg, P. W. (1995). The *Caenorhabditis elegans lin-12* gene mediates induction of ventral uterine specialization by the anchor cell. *Development* **121**, 263–271.
- Newman, A. P., White, J. G., and Sternberg, P. W. (1996). Morphogenesis of the *C. elegans* hermaphrodite uterus. *Development* **122**, 3617–3626.
- Okochi, M., Eimer, S., Bottcher, A., Baumeister, R., Romig, H., Walter, J., Capell, A., Steiner, H., and Haass, C. (2000). A loss of function mutant of the presenilin homologue SEL-12 undergoes aberrant endoproteolysis in *Caenorhabditis elegans* and increases aβ42 generation in human cells. *J. Biol. Chem.* **275**, 40925–40932.
- Reiner, D. J., Weinschenker, D., and Thomas, J. H. (1995). Analysis of dominant mutations affecting muscle excitation in *Caenorhabditis elegans*. *Genetics* **141**, 961–976.
- Schroeter, E. H., Kisslinger, J. A., and Kopan, R. (1998). Notch-1 signalling requires ligand-induced proteolytic release of intracellular domain. *Nature* **393**, 382–386.
- Shen, J., Bronson, R. T., Chen, D. F., Xia, W., Selkoe, D. J., and Tonegawa, S. (1997). Skeletal and CNS defects in Presenilin-1-deficient mice. *Cell* **89**, 629–639.
- Struhl, G., and Adachi, A. (1998). Nuclear access and action of notch in vivo. *Cell* **93**, 649–660.
- Struhl, G., and Adachi, A. (2000). Requirements for presenilin-dependent cleavage of notch and other transmembrane proteins. *Mol. Cell* **6**, 625–636.
- Struhl, G., Fitzgerald, K., and Greenwald, I. (1993). Intrinsic activity of the Lin-12 and Notch intracellular domains in vivo. *Cell* **74**, 331–345.
- Struhl, G., and Greenwald, I. (1999). Presenilin is required for activity and nuclear access of Notch in *Drosophila*. *Nature* **398**, 522–525.
- Struhl, G., and Greenwald, I. (2001). Presenilin-mediated transmembrane cleavage is required for Notch signal transduction in *Drosophila*. *Proc. Natl. Acad. Sci. USA* **98**, 229–234.
- Sulston, J. E., and Horvitz, H. R. (1977). Post-embryonic cell lineages of the nematode, *Caenorhabditis elegans*. *Dev. Biol.* **56**, 110–156.
- Sulston, J. E., and White, J. G. (1980). Regulation and cell autonomy during postembryonic development of *Caenorhabditis elegans*. *Dev. Biol.* **78**, 577–597.
- Sundaram, M., and Greenwald, I. (1993). Genetic and phenotypic studies of hypomorphic *lin-12* mutants in *Caenorhabditis elegans*. *Genetics* **135**, 755–763.
- Swiatek, P. J., Lindsell, C. E., del Amo, F. F., Weinmaster, G., and Gridley, T. (1994). Notch1 is essential for postimplantation development in mice. *Genes Dev.* **8**, 707–719.
- Thomas, J. H., Stern, M. J., and Horvitz, H. R. (1990). Cell interactions coordinate the development of the *C. elegans* egg-laying system. *Cell* **62**, 1041–1052.
- Trent, C., Tsung, N., and Horvitz, H. R. (1983). Egg-laying defective mutants of the nematode *C. elegans*. *Genetics* **104**, 619–647.
- Wang, W., Campos, A. H., Prince, C., Mou, M., and Pollman, M. J. (2002). Coordinate notch3-hairy-related transcription factor pathway regulation in response to arterial injury: Mediator role of PDGF and ERK. *J. Biol. Chem.* **277**, 23165–23171.

- Weinshenker, D., Garriga, G., and Thomas, J. H. (1995). Genetic and pharmacological analysis of neurotransmitters controlling egg laying in *C. elegans*. *J. Neurosci.* **15**, 6975–6985.
- Wen, C., Levitan, D., Li, X., and Greenwald, I. (2000). *spr-2*, a suppressor of the egg-laying defect caused by loss of *sel-12* presenilin in *Caenorhabditis elegans*, is a member of the SET protein subfamily. *Proc. Natl. Acad. Sci. USA* **97**, 14524–14529.
- Westlund, B., Parry, D., Clover, R., Basson, M., and Johnson, C. D. (1999). Reverse genetic analysis of *Caenorhabditis elegans* presenilins reveals redundant but unequal roles for *sel-12* and *hop-1* in Notch-pathway signaling. *Proc. Natl. Acad. Sci. USA* **96**, 2497–2502.
- White, J. G., Southgate, E., Thomson, J. N., and Brenner, S. (1983). Factors that determine connectivity in the nervous system of *Caenorhabditis elegans*. *Cold Spring Harbor Symp. Quant. Biol.* **48**, 633–640.
- Wilkinson, H. A., and Greenwald, I. (1995). Spatial and temporal patterns of *lin-12* expression during *C. elegans* hermaphrodite development. *Genetics* **141**, 513–526.
- Wittenburg, N., Eimer, S., Lakowski, B., Rohrig, S., Rudolph, C., and Baumeister, R. (2000). Presenilin is required for proper morphology and function of neurons in *C. elegans*. *Nature* **406**, 306–309.
- Wong, P. C., Zheng, H., Chen, H., Becher, M. W., Sirinathsinghji, D. J., Trumbauer, M. E., Chen, H. Y., Price, D. L., Van der Ploeg, L. H., and Sisodia, S. S. (1997). Presenilin 1 is required for Notch1 and Dll1 expression in the paraxial mesoderm. *Nature* **387**, 288–292.
- Ye, Y., Lukinova, N., and Fortini, M. E. (1999). Neurogenic phenotypes and altered Notch processing in *Drosophila* Presenilin mutants. *Nature* **398**, 525–529.
- Yu, G., Nishimura, M., Arawaka, S., Levitan, D., Zhang, L., Tandon, A., Song, Y. Q., Rogava, E., Chen, F., Kawarai, T., Supala, A., Levesque, L., Yu, H., Yang, D. S., Holmes, E., Milman, P., Liang, Y., Zhang, D. M., Xu, D. H., Sato, C., Rogava, E., Smith, M., Janus, C., Zhang, Y., Aebbersold, R., Farrer, L. S., Sorbi, S., Bruni, A., Fraser, P., and St. George-Hyslop, P. (2000). Nicastrin modulates presenilin-mediated notch/glp-1 signal transduction and β APP processing. *Nature* **407**, 48–54.

Received for publication March 14, 2002

Revised July 8, 2002

Accepted July 8, 2002

Published online

CHAPTER VI

**Loss of *spr-5* bypasses the requirement for the presenilin *sel-12*
by stage-specific derepression of *hop-1***

published as:

Eimer S., Lakowski B, Donhauser R. and Baumeister R. (2002)

Loss of *spr-5* bypasses the requirement for the presenilin *sel-12* by stage-specific derepression of *hop-1*.

EMBO Journal **21**: 5787-5796.

Loss of *spr-5* bypasses the requirement for the *C.elegans* presenilin *sel-12* by derepressing *hop-1*

S.Eimer, B.Lakowski¹, R.Donhauser and R.Baumeister²

ABI, Department of Biochemistry, Laboratory of Molecular Neurogenetics, Ludwig-Maximilians-Universität Munich, Schillerstraße 44, D-80336 Munich, Germany

¹Present address: Department of Neuroscience, Pasteur Institute, Paris, France

²Corresponding author
e-mail: ralf.baumeister@pbm.med.uni-muenchen.de

Presenilins are part of a protease complex that is responsible for the intramembraneous cleavage of the amyloid precursor protein involved in Alzheimer's disease and of Notch receptors. In *Caenorhabditis elegans*, mutations in the presenilin *sel-12* result in a highly penetrant egg-laying defect. *spr-5* was identified as an extragenic suppressor of the *sel-12* mutant phenotype. The SPR-5 protein has similarity to the human polyamine oxidase-like protein encoded by KIAA0601 that is part of the HDAC–CoREST co-repressor complex. Suppression of *sel-12* by *spr-5* requires the activity of HOP-1, the second somatic presenilin in *C.elegans*. *spr-5* mutants derepress *hop-1* expression 20- to 30-fold in the early larval stages when *hop-1* normally is almost undetectable. SPR-1, a *C.elegans* homologue of CoREST, physically interacts with SPR-5. Moreover, down-regulation of SPR-1 by mutation or RNA interference also bypasses the need for *sel-12*. These data strongly suggest that SPR-5 and SPR-1 are part of a CoREST-like co-repressor complex in *C.elegans*. This complex might be recruited to the *hop-1* locus controlling its expression during development.

Keywords: Alzheimer's disease/*C.elegans*/Notch/presenilins/suppressor genetics

Introduction

Mutations in the presenilins PS1 and PS2 account for the majority of early-onset familial Alzheimer's disease (Selkoe, 2001). These mutations lead to the aberrant processing of the amyloid precursor protein (APP) and the generation of increasing amounts of the highly amyloidogenic form of A β , the amyloid β -peptide. A β is the predominant component of the plaques found in the brains of Alzheimer's patients. Presenilins are polytopic transmembrane proteins that are part of the proteolytic γ -secretase complex that liberates A β . Apart from their role in APP processing, presenilins are also required for proteolytic processing of the Notch receptors in their transmembrane domain. Ligand-induced cleavage and release of the intracellular domain of the Notch receptor (NICD) are crucial for nuclear Notch signalling (Struhl

and Adachi, 1998). In agreement with these results, in all organisms tested so far, the loss of presenilin activity leads to phenotypes that resemble that of Notch loss-of-function mutants (Fortini, 2001).

Similarly to humans, *Caenorhabditis elegans* has two somatically expressed presenilin genes, *hop-1* and *sel-12* (Levitan and Greenwald, 1995; Li and Greenwald, 1997). *hop-1* and *sel-12*, like PS1 and PS2, show redundant activities since only double mutants display phenotypes associated with a complete loss of Notch signalling in *C.elegans* (Li and Greenwald, 1997; Westlund *et al.*, 1999). A *sel-12* null mutant can be rescued by transgenic expression of *hop-1* (as well as either of the human PS1 or PS2). *sel-12* is expressed rather uniformly at all developmental stages, while *hop-1* expression is very weak and could not be detected by reporter gene fusions (Westlund *et al.*, 1999). Probably as a consequence of these different levels of expression, *hop-1* mutants are viable with no obvious phenotype, whereas *sel-12* mutants display, along with other more subtle defects, an egg-laying (Egl) defect. The *sel-12* Egl phenotype is caused by reduced LIN-12/Notch signalling, resulting in the failure to form a proper vulva–uterine connection (Cinar *et al.*, 2001) and in sex-muscle patterning defects (Eimer *et al.*, 2002).

One approach to identify new molecules involved in the regulation of presenilin activity or molecules that are able to bypass the need for presenilin activity is to perform genetic screens for suppressors of the Egl defect of *sel-12* mutant animals. Two *sel-12* suppressors have been described already. Mutations in the *C.elegans* gene *sel-10* directly influence LIN-12/Notch signalling by enhancing the half-life of the intracellular signalling domain of LIN-12 (Wu *et al.*, 1998). The F-box/WD40 repeat protein SEL-10 is part of a ubiquitin ligase complex that mediates the ubiquitylation and degradation of the activated nuclear NICD (Lai, 2002). In contrast, the suppressor mutant *spr-2* does not influence LIN-12/Notch signalling directly but requires HOP-1 activity in a manner that has not been characterized (Wen *et al.*, 2000) but obviously does not affect the level of its transcription. SPR-2 belongs to a family of nuclear assembly proteins (NAPs) which have been implicated in chromatin remodelling and cell cycle control. The different modes of action of *sel-10* and *spr-2* function suggest that there exist distinct mechanisms to suppress *sel-12*.

The functional conservation of presenilins suggests that a third possible mechanism to suppress the *sel-12* mutant phenotype could involve transcriptional up-regulation of the expression of the second presenilin, in this case *hop-1*. Therefore, second site suppressors of *sel-12* could include mutations in transcriptional activators that render them hyperactive, or mutations in repressors or repressor complexes that eliminate the down-regulation of *hop-1*.

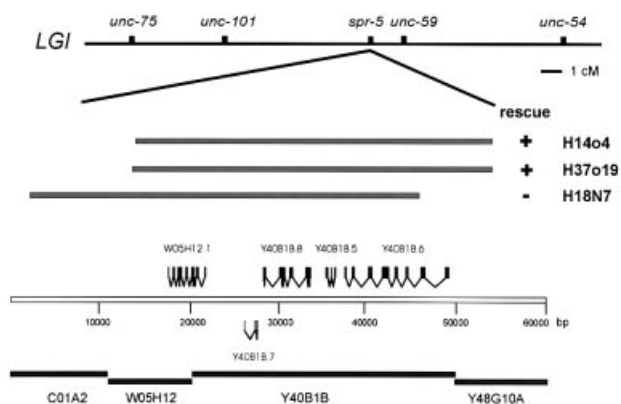


Fig. 1. Physical map of the *spr-5* region on LGI. The location and the extension of the fosmid H14o4, H37o19 and H18N7 relative to the Y40B1B locus, as well as their rescuing activity, are indicated. The scale bar below represents base pairs.

It is becoming increasingly obvious that histone deacetylase (HDAC)-containing repressor complexes are required for both transient and persistent transcriptional silencing of selected genes. Notably, HDAC complexes play an important role in the Notch-mediated transcriptional silencing of downstream genes (reviewed in Mumm and Kopan, 2000). HDACs associate with several distinct complexes, including the Sin-associated protein (SAP) complex and the nucleosome remodelling and histone deacetylation (NURD) complex, which exhibits ATP-dependent chromatin-remodelling activity (Jepsen and Rosenfeld, 2002). Recently, yet another HDAC complex was identified containing the transcriptional co-repressor CoREST and protein KIAA0601, which is a putative flavin-adenine dinucleotide (FAD)-dependent enzyme of still unknown function.

We report here the identification of two new suppressors of the Egl defect of *sel-12* mutant *C.elegans* animals, *spr-5* and *spr-1*. The analysis of *spr-5* revealed that it acts by depression of *hop-1* expression in developmental stages where *hop-1* normally is not expressed. Therefore, *sel-12* presenilin activity is replaced by *hop-1* activity. SPR-5 exhibits homology to the human polyamine oxidase (PAO)-like protein KIAA0601, which is an integral component of the CoREST co-repressor complex. Our screens also identified *by133*, an *spr-1* allele that, like RNA interference (RNAi) inhibition of a *C.elegans* homologue of CoREST, phenocopies the *spr-5* suppressor function. Furthermore, we show that D1014.8/SPR-1 forms a complex with SPR-5. We suggest that a CoREST-like co-repressor complex also exists in *C.elegans* and participates in the transcriptional repression of the presenilin *hop-1* during development.

Results

spr-5 suppresses the *sel-12* Egl phenotype in a non-allele-specific way

In a screen using the mutator strain *sel-12(ar171) unc-1(e538); mut-7(pk204)*, we recovered a mutation on chromosome I, *by101*, that suppressed the Egl defect of *sel-12(ar171)* hermaphrodites. Genetic mapping of the mutant loci placed the suppressor in the interval between

Table I. *spr-5* bypasses the need for *sel-12* in a non-allele-specific way

Genotype	Pvl (%)	Egl (%)	Brood size	n
Wild-type N2	0	0	316 ± 8	20
<i>sel-12(ar171)</i>	80	100	62 ± 7	25
<i>sel-12(ar171); spr-5(by113)</i>	0	5	188 ± 15	20
<i>sel-12(ar171); spr-5(by128)</i>	10	15	230 ± 20	20
<i>sel-12(ar171); spr-5(by134)</i>	10	10	219 ± 12	20
<i>sel-12(ar171); spr-5(by101)</i>	5	10	208 ± 15	40
<i>sel-12(lg1401); spr-5(by101)</i>	0	5	214 ± 12	19
<i>sel-12(ar131); spr-5(by101)</i>	0	5	231 ± 17	20
<i>spr-5(by101)</i>	0	0	276 ± 12	27

unc-101 and *unc-59* close to *unc-59* (Figure 1; for details see Materials and methods). As it complements the previously mapped but not yet cloned presenilin suppressor *spr-4(ar208)* on LGI (Wen et al., 2000), the mutant locus we found corresponds to a new gene, which we will refer to as *spr-5*. Subsequently, we identified five additional alleles of *spr-5* in similar screens using chemical mutagens (details of the experimental procedures will be published elsewhere; B.Lakowski and R.Baumeister, unpublished data).

All *spr-5* mutants result in a very strong suppression of all aspects of the *sel-12* Egl defect. Eighty-five to 95% of all *spr-5; sel-12* animals are non-Pvl and non-Egl (Table I). Furthermore, the brood size of these animals is much larger than that of *sel-12* and is in the range of that of the wild type (Table I). *spr-5* mutations suppress all *sel-12* alleles tested (Table I): *ar171*, a truncation after the fifth transmembrane domain (W225stop); *ar131*, a C60S missense mutation (Levitan and Greenwald, 1995); and *lg1401*, a deletion of *sel-12* and part of the promoter that is a clear null allele (Eimer et al., 2002; Table I). This indicates that the mechanism of suppression is not allele specific and does not depend on the presence of SEL-12 protein.

In addition, as opposed to *sel-12* animals, *spr-5; sel-12* hermaphrodites also lay eggs in response to the drugs serotonin and imipramine, suggesting that they have a functional egg-laying system that can be stimulated pharmacologically (Trent et al., 1983). *spr-5* mutations also restore male mating that is defective in *sel-12* males (Eimer et al., 2002). Therefore, *spr-5* rescues not only the structural defects of the egg-laying system of *sel-12* animals, but also the functional defects.

When genetically separated from *sel-12* alleles, *spr-5* mutants alone display no obvious phenotype, suggesting that *spr-5* is a specific suppressor of *sel-12*. Neither egg-laying, egg motility nor other behaviours were different from those of wild-type animals under the conditions tested (data not shown). In addition, the brood size of all *spr-5* alleles is in the range of wild type (Table I).

spr-5 mutants do not enhance LIN-12/Notch signalling directly

In order to determine the mechanism of suppression, we first tested whether *lin-12* is the prime target of *spr-5* genetic interactions. Since *sel-12* mutations reduce LIN-12 signalling, *spr-5* mutations might act by increasing LIN-12 expression or activity. From other experiments not

Table II. Genetic interactions of *spr-5* with *lin-12* and *hop-1*

sel-12 suppression by *spr-5* is dependent on *hop-1*

Genotype	No. of sterile/total (%)
<i>sel-12(ar171); hop-1(lg1501)^a</i>	36/36 (100%)
<i>sel-12(ar171); hop-1(lg1501) spr-5(by101)^a</i>	43/43 (100%)
<i>sel-12(ar171); hop-1(lg1501)^b</i>	No. of Egl/total (%)
<i>sel-12(ar171); hop-1(lg1501) spr-5(by101)^b</i>	50/50 (100%)
	48/49 (98%) ^c

No effect on the 0 AC defect caused by elevating *lin-12* activity

Genotype	No. of Egl/total (%)
<i>lin-12(n302)/ unc-32(e189)</i>	40/79 (51%)
<i>lin-12(n302)/ unc-32(e189); spr-5(by101)</i>	77/141 (55%)

No enhancement of a *lin-12* hypomorphic mutation

Relevant genotype	No. of Egl/total (%) at 25°C
<i>lin-12(n676n930)^d</i>	50/50 (100%)
<i>lin-12(n676n930)^d; spr-5(by101)</i>	50/50 (100%)

^aThese animals segregated from *sel-12(ar171); hop-1(lg1501)/unc-73(e936)* or *sel-12(ar171); hop-1(lg1501) spr-5(by101)/unc-73(e936) spr-5(by101)* mothers. The genotype is therefore: *sel-12 m⁻ z⁻; hop-1 m⁺ z⁻*.

^bThese animals segregated from *sel-12(ar171) unc-1(e538)/++;* *hop-1(lg1501)* or *sel-12(ar171) unc-1(e538)/++;* *hop-1(lg1501) spr-5(by101)* mothers. The genotype is therefore: *sel-12 m⁺ z⁻; hop-1 m⁻ z⁻*.

^cOne animal was sterile.

^dThis strain also carries an *unc-32(e189)* mutation that is linked to *lin-12*. The Egl phenotype was scored with animals raised at 25°C.

reported here, we had concluded that mRNA levels expressed from both *C.elegans* Notch genes, *lin-12* and *glp-1*, did not differ between wild type and the *spr* mutants we had recovered in our screens (B.Lakowski and R.Baumeister, unpublished data). Therefore, it is unlikely that *spr-5* mutants act by transcriptional up-regulation of Notch expression. The *lin-12(n676n930)* reduction of function allele displays a temperature-sensitive Egl defect (Sundaram and Greenwald, 1993), which is similar to the *sel-12* Egl phenotype (Eimer *et al.*, 2002). Therefore, we wondered whether *spr-5* might suppress the Egl defect of *lin-12(n676n930)* at 25°C. However, *spr-5* did not rescue any aspect of the *lin-12(n676n930)* Egl defect (Table II). We also tested whether *spr-5* is able to enhance another well-characterized process that is defective in *lin-12* mutants, the AC/VU decision (Greenwald *et al.*, 1983). In the AC/VU decision, two initially equipotent cells of the somatic gonad adopt different cell fates through a LIN-12-dependent process called lateral inhibition. The *lin-12(n302)* gain-of-function allele is vulva-less and therefore Egl, because it develops two VU cells at the expense of an AC (Greenwald *et al.*, 1983). As the *lin-12(n302)* mutation is semi-dominant, 50% of the heterozygote animals are Egl. *spr-5* mutants show no increase in the 0 AC phenotype in heterozygotes, indicating that the LIN-12-dependent lateral inhibition is also not affected in *spr-5* mutants (Table II). From these results, we conclude that *spr-5* does not directly influence any of the characterized modes of LIN-12 signalling. Therefore, we consider it unlikely that *spr-5* suppresses *sel-12* by directly up-regulating LIN-12 signalling.

The suppressor activity of *spr-5* requires functional HOP-1 presenilin

To determine whether *spr-5* bypasses the need for functional presenilins in LIN-12 signalling or may act

through modulating the activity of the second presenilin *hop-1*, we constructed *hop-1 spr-5; sel-12* triple mutants. Both *sel-12* and *hop-1* have partial maternal effects, so the phenotype of *hop-1; sel-12* double mutants depends on how they are constructed. Double mutant animals that have maternally supplied *hop-1* are sterile, whereas, if *sel-12* is provided maternally, *hop-1; sel-12* mutants become Egl, with embryos that do not hatch (Westlund *et al.*, 1999). *hop-1 spr-5; sel-12* triple mutants, with maternally supplied *sel-12*, are also Egl (Table II) and only produce dead embryos. Furthermore, triple mutants with maternally supplied *hop-1* are sterile like the similarly constructed *sel-12; hop-1* double mutants (Table II). We therefore conclude that *spr-5* mutants require *hop-1* activity for *sel-12* suppression.

Molecular cloning of *spr-5*

Initially, *spr-5* was mapped near *unc-59* on the right arm of chromosome I (Figure 1). A Tc3 transposon was found to co-segregate with the suppression phenotype in *spr-5(by101)* (for details see Materials and methods). Sequencing of the genomic DNA flanking the transposon revealed that the Tc3 had inserted into the seventh exon in codon 606 of the predicted reading frame Y40B1B.6 (Figure 1). When injected into *sel-12; spr-5* animals, fosmids H14o4 (four out of four transgenic lines) and H37o19 (five out of six transgenic lines) that contain the entire coding region of Y40B1B.6 rescued the *spr-5* mutant phenotype, and restored a *sel-12* phenotype (Egl). In contrast, fosmid H18N7 that terminates after the sixth exon of Y40B1B.6 was not able to rescue the suppression by *spr-5* (none out of three transgenic lines), suggesting that Y40B1B.6 indeed corresponds to *spr-5* (Figure 1).

Further analysis of the genomic organization of the open reading frames (ORFs) on Y40B1B indicated that the genes Y40B1B.8, Y40B1B.5 and Y40B1B.6/*spr-5* belong

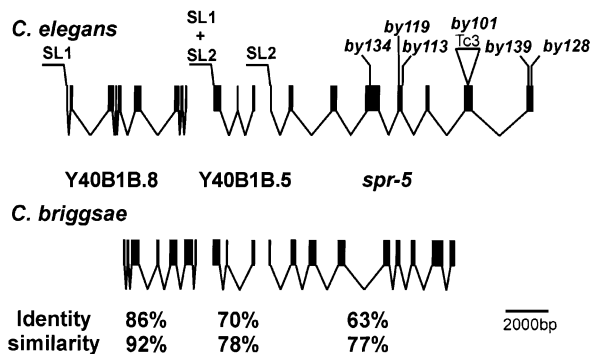


Fig. 2. Exon–intron structure of the *spr-5* operon on LGI. The specific splice leader and the locations of the mutations in the different *spr-5* alleles are shown. In addition, the organization of the homologous operon in *C. briggsae* is included, along with the identity and similarity scores of the *C. elegans* and *C. briggsae* proteins.

to an operon consisting of three genes (Figure 2). In operons, the downstream genes are *trans*-spliced to a 22 nucleotide splice leader SL2 (Spieth *et al.*, 1993), whereas the most upstream gene is *trans*-spliced to an SL1 splice leader. We used RT–PCR with SL1 and SL2 primers to determine the 5' ends of all three putative ORFs. We found that Y40B1B.8 is spliced exclusively to SL1, Y40B1B.5 is *trans*-spliced to a mixture of SL1 and SL2, and Y40B1B.6/*spr-5* is spliced primarily to SL2 (Figure 2). The existence of a three-gene operon containing *spr-5* is supported further by DNA array data (Blumenthal *et al.*, 2002). Based both on their orientation and their encoded amino acid sequence, these three genes are highly conserved in the related nematode *Caenorhabditis briggsae*, consistent with being in an operon. However, the exon–intron structure of the *C. elegans* and *C. briggsae* genes differs to some extent (Figure 2). Although the genes are highly conserved on a protein level, Y40B1B.8 contains seven exons in *C. elegans* compared with nine in *C. briggsae*, and the fourth exon of Y40B1B.6/*spr-5* is represented by two exons in *C. briggsae* (Figure 2).

We examined in all *spr-5* alleles the expression of the two downstream reading frames of the operon. On a mixed stage northern blot, most *spr-5* alleles show clear alterations in either the size and/or the intensity of bands detected with an Y40B1B.6 probe, and no obvious differences in the transcript of Y40B1B.5 (Figure 3). To support this notion further, we performed RNAi experiments against each of the three genes in this operon by bacterial feeding of double-stranded RNA (dsRNA) (Timmons and Fire, 1998; Timmons *et al.*, 2001). Although it has been reported that RNAi may also target the pre-mRNA (Bosher *et al.*, 1999), only the dsRNAi against *spr-5*/Y40B1B.6 led to suppression of the Egl defect of *sel-12* animals that is typical for the different *spr-5* alleles (Table III). dsRNAi against any of the upstream genes was not able to suppress the Egl defect of *sel-12* (Table III). Therefore, we conclude that *spr-5* is Y40B1B.6. Subsequently, we confirmed the genomic structure predicted in Wormbase by sequencing. Y40B1B.6/*spr-5* encodes a protein of 770 amino acids (Figure 4A). The positions of all mutations and alterations found in the various *spr-5* alleles are shown in Figures 2 and 4A.

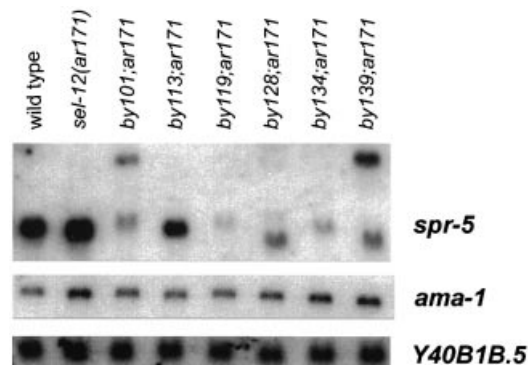


Fig. 3. Northern blot of mixed staged total RNA from the different alleles probed with *spr-5*, Y40B1B.5, and *ama-1* as a loading control.

***spr-5* is homologous to amine oxidases found in transcriptional repressor complexes**

SPR-5 exhibits strong similarity to a large class of FAD-dependent amine oxidases. SPR-5 is most similar to the class of FAD-dependent PAOs (Figure 4). The PAOs are found in all organisms from bacteria to mammals and plants, and catalyse the oxidation of secondary amine groups of straight chain aminoalkanes (Sebela *et al.*, 2001). Despite the differences in the site of action on the secondary amine group between plants and mammals, PAOs are monomeric soluble enzymes with non-covalently bound FAD cofactor (Seiler, 1995). All PAOs have a two-domain organization, with one domain binding the FAD cofactor while the other binds the substrate (Binda *et al.*, 1999, 2001). Even though they only share 20–30% identity, the maize PAO has the same three-dimensional structure as the vertebrate monoamine oxidase, known to act on primary amines (Binda *et al.*, 2002). SPR-5 and the maize PAO share the same FAD-binding signature motif (Dailey and Dailey, 1998), and the residues known to bind the FAD cofactor in maize PAO are conserved (Binda *et al.*, 1999), while those residues that recognize the substrate are not conserved (Binda *et al.*, 2001). Therefore, we conclude that it is likely that SPR-5 binds FAD as a cofactor while the substrate specificity may have diverged.

SPR-5 defines a subfamily of the PAOs along with a second *C. elegans* protein T08D10.2, the *Drosophila melanogaster* protein encoded by expressed sequence tag (EST) CG17149 and the human protein encoded by EST KIAA0601 (Nagase *et al.*, 1998). Members of this subfamily of proteins are more similar to each other than to the maize PAO (Figure 4A and B). SPR-5 has 27% amino acid identity (45% similarity) to hKIAA0601 and Dm CG17149, whereas it has 44% identity (62% similarity) to the *C. elegans* paralogue. The protein that corresponds to KIAA0601 was co-purified as an integral component of the human CoREST–HDAC complex (Tong *et al.*, 1998; Humphrey *et al.*, 2001; You *et al.*, 2001). The CoREST complex was shown to be a functional co-repressor that is required for REST-mediated repression of neuronal genes in non-neuronal cells (Andres *et al.*, 1999; Ballas *et al.*, 2001; Griffith *et al.*, 2001). Additional components of the human CoREST complex are HDACs 1 and 2 and the SANT domain protein CoREST (Humphrey *et al.*, 2001; You *et al.*,

Table III. Summary of dsRNAi feeding experiments

RNAi construct	RNAi phenotype in strains		
	Wild type	<i>sel-12(ar171)</i>	<i>sel-12(ar131)</i>
–	wt (15/15)	Egl (10/10)	Egl (10/10)
<i>spr-5</i>	wt (10/10)	Non-Egl (39/40) ^a	Non-Egl (20/20)
Y40B1B.5	wt (10/10)	Egl (20/20)	Egl (20/20)
Y40B1B.8	wt (10/10) ^b	Egl (20/20) ^b	Egl (20/20) ^b
T08D10.2	wt (11/11)	Egl (20/20)	Egl (20/20)
D1014.8	wt (10/10)	Non-Egl (30/30)	ND
Y74C9A.4	wt (10/10)	Egl (30/30)	ND

^aOne animal was sterile.

^bThere were sick worms on the plates at a low penetrance.

2001), which binds to the zinc finger factor REST (Andres *et al.*, 1999; Ballas *et al.*, 2001). REST recruits the CoREST complex to specific DNA sites, suggesting that the complex may regulate individual genes.

Loss of *spr-5* leads to derepression of *hop-1* expression

Due to the sequence similarity of SPR-5 to a member of a complex involved in transcriptional repression, it is possible that SPR-5 may have a similar function in *C.elegans*. Thus, we searched for candidate target genes in the Notch signalling pathway that may be regulated by *spr-5*. The suppression of *sel-12* by *spr-5* was shown not to up-regulate LIN-12/Notch signalling but was dependent on *hop-1* activity. Since *hop-1* and *sel-12* are functionally redundant, *hop-1* was an attractive candidate for *spr-5*-mediated transcriptional regulation. Therefore, we analysed the stage-specific transcriptional regulation of *hop-1* by northern blot analysis. *sel-12* is ubiquitously expressed at high levels throughout all developmental stages (Baumeister *et al.*, 1997). In contrast, *hop-1* expression dramatically changes throughout development. *hop-1* is almost undetectable in the L1 and L2 larvae and its expression gradually increases throughout further development and reaches a maximum at the adult stage (B.Lakowski and R.Baumeister, unpublished data). As a consequence of the high expression levels in the adult stage, probably a high level of *hop-1* mRNA is supplied to the embryo maternally. In *sel-12* mutant animals, *hop-1* expression levels are indistinguishable from wild-type levels, suggesting that *sel-12* does not control *hop-1* expression at the transcriptional level. Next, we investigated *hop-1* expression in *spr-5*; *sel-12* suppressor strains. *hop-1* expression was detectable already in the L1 stage, while it is almost absent in wild-type L1 animals (Figure 6). The up-regulation of *hop-1* expression was between 20- and 30-fold depending on the *spr-5* allele tested and independent of the presence of *sel-12* (data not shown). *spr-5* is expressed in all stages at nearly the same level, indicating that it may act as a general co-repressor (Figure 5).

These data suggest that *spr-5* is required to repress *hop-1* expression in the first larval stages and that loss of *spr-5* leads to a derepression of *hop-1* in these stages. Derepression of *hop-1* expression is sufficient to replace the lack of *sel-12* activity and, therefore, suppresses the Egl phenotype of the *sel-12* mutants.

A CoREST-like complex might be involved in transcriptional repression of *hop-1*

If SPR-5 functions in a HDAC–CoREST complex of transcriptional regulation, then one might assume that manipulating the expression of other members of this complex should result in a phenotype similar to that of *spr-5* mutants. We identified two predicted open reading frames, D1014.8 and Y74C9A.4, encoding proteins with similarity to CoREST. dsRNAi experiments were performed for both genes in a *sel-12* mutant background (Table III). RNAi against Y74C9A.4 did not reveal any novel phenotype in a *sel-12* background. Strikingly, however, dsRNAi against D1014.8 suppressed the *sel-12* Egl defect as strongly as *spr-5* (Table III). D1014.8 maps to a genomic region on LGV where another *sel-12* suppressor, *spr-1*, was mapped previously (Wen *et al.*, 2000), suggesting that D1014.8 corresponds to *spr-1*.

In our screens for *sel-12* suppressors, we had identified a mutant with properties similar to *spr-5* alleles. We had mapped this suppressor allele, *by133*, close to D1014.8, suggesting that it might encode an allele of *spr-1*. To determine if *by133* is an allele of *spr-1*, we performed rescue experiments with the cosmid D1014 using an *spr-1(by133)*; *sel-12(ar171)* strain. Seven of seven transgenic F₂ lines clearly and profoundly rescued the *spr-1(by133)*-mediated suppression of *sel-12*. Subsequently, we sequenced the coding region of the *by133* mRNA and found that it contains a T→A mutation at position +905, converting a TTA (leucine) to TAA (stop). This mutation truncates the protein at amino acid 301 after the first SANT domain, but before the second SANT domain. Thus, mutations in two members of the CoREST complex suppress the presenilin defect in *C.elegans*.

RNAi against the three *C.elegans* class I HDACs *hda-1*, *hda-2* and *hda-3*, alone or in combination, resulted in a pleiotropic phenotype that was difficult to interpret. This result was not unexpected since it had been shown before that these HDACs in *C.elegans* are involved in a variety of different functions in different cell types (Dufourcq *et al.*, 2002). Interestingly, RNAi against *hda-1/gon-10* resulted in multiple defects affecting the egg-laying system, but also in sterility, which prevented the monitoring of *sel-12* suppression.

Complex formation is one prerequisite of the concerted activity of PAO and CoREST in human cells. Although our genetic data already strongly suggest a similar function for *C.elegans* SPR-1/CoREST and SPR-5/PAO, we tested whether both proteins are able to interact physically. A GST–MYC–SPR-5 protein fusion was used to probe protein interaction with SPR-1/CoREST by co-immunoprecipitation experiments. For this purpose, GST–SPR-5 expressed in Sf9 insect cells, immobilized on glutathione–Sepharose and incubated with ³⁵S-labelled SPR-1 was *in vitro* translated in a reticulocyte lysate system. Protein binding was analysed by SDS–PAGE and western blots (Figure 7). Our results demonstrate that SPR-5/PAO binds specifically to SPR-1/CoREST, corroborating previous results (obtained with the human factors) that both proteins are components of the same protein complex. Interaction was subsequently confirmed by yeast two-hybrid experiments (S.Eimer, data not shown).

(B.Lakowski and R.Baumeister, unpublished data). In contrast, *sel-12* is ubiquitously expressed at all stages. Most of the known LIN-12/Notch signalling events take place during the L2 to late L3 stage, including the AC/VU specification, the π -cell specification for a proper vulva-uterine connection, and sex-muscle morphogenesis (Li and Chalfie, 1990; Newman *et al.*, 1995; Greenwald, 1998; Sharma-Kishore *et al.*, 1999). Therefore, loss of *sel-12* activity during L2 and L3 is most critical and is the cause of the Egl phenotype. Why do *sel-12* mutants not show a *lin-12* null phenotype, including a defective AC/VU decision? This is probably because different thresholds for the amount of LIN-12/Notch signalling are required for each developmental decision (Eimer *et al.*, 2002). The AC/VU cell fate decision most probably needs less LIN-12/Notch activity than π -cell induction and sex-muscle morphogenesis and, therefore, the low *hop-1* expression levels during larval stages, or the maternally supplied *hop-1*, are sufficient to maintain LIN-12 activity.

As shown here, loss of *spr-5* function leads to a 20- to 30-fold increase in *hop-1* expression in the first larval stages (Figure 6) most probably due to a removal of a repression of *hop-1* expression in those stages. Therefore, *hop-1* derepression occurs at precisely those stages at which lack of *sel-12* presenilin activity would be most critical. We do not know why derepression is most significant in L1–L3, although *spr-5* obviously is expressed at all developmental stages. Probably the timing of *spr-5* dependent derepression is regulated by other, not yet identified factors.

The mechanism of the derepression is not clear, but might affect chromatin structure and remodelling. Another

known suppressor of the *sel-12* Egl defect, *spr-2*, encodes a protein with similarity to the Set/TAF- $\text{I}\beta$ oncoprotein found in the INHAT (inhibitor of acetyltransferase) complex which is able to inhibit histone acetyltransferase (HAT) activities by p300/CBP and PCAF through histone masking (Seo *et al.*, 2001). Genetically, *spr-2* behaves similarly to *spr-5* and was also shown to be dependent on *hop-1* activity (Wen *et al.*, 2000). However, in *spr-2* mutants, *hop-1* transcription does not increase, suggesting that *spr-2* and *spr-5* function through separate mechanisms. Interestingly, both proteins might be associated with chromatin complexes.

The proteins that are most similar to SPR-5, except for T08D10.2, a *C.elegans* paralogue, are the human KIAA0601/p110b and a predicted protein from *D.melanogaster* encoded by CG17149. All those proteins share regions of similarity with FAD-dependent PAOs. The mutation in *spr-5*(*by113*) results in an exchange of a conserved glycine residue to arginine at position 423. This allele is phenotypically indistinguishable from the deletion alleles, suggesting that the G423R point mutation interferes with an essential function of the protein. Interestingly, in the maize PAO crystal structure, this position is located in the FAD-binding domain, close to the FAD-binding pocket (Binda *et al.*, 1999). The human KIAA0601 protein was found to be an integral component of the CoREST co-repressor complex (Tong *et al.*, 1998; Humphrey *et al.*, 2001; You *et al.*, 2001). This may indicate that the mutation interferes with an enzymatic function of SPR-5 required for the repressor activity of such a complex.

In addition to the PAO, other HDAC–CoREST complex components are HDAC1, HDAC2 and the SANT domain protein CoREST (Humphrey *et al.*, 2001; You *et al.*, 2001; Figure 8). CoREST, together with REST/NRSF (RE1 silencing transcription factor/neural-restrictive silencing

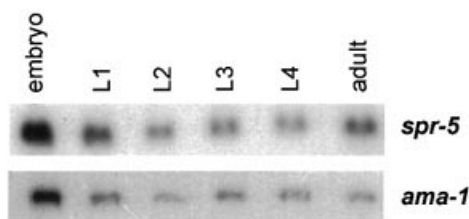


Fig. 5. Stage-specific northern blot of wild-type total RNA probed with *spr-5*, and *ama-1* as a loading control.

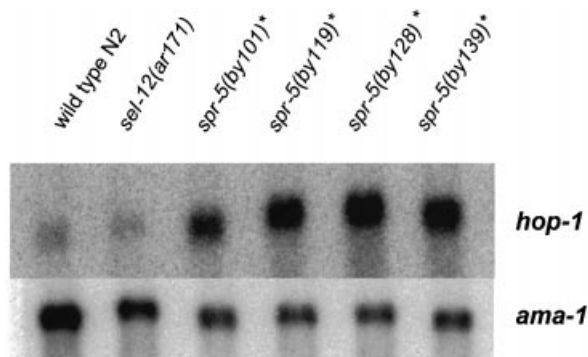


Fig. 6. Northern blot of L1-specific total RNA N2, *sel-12*(*ar171*) and different *sel-12*(*ar171*); *spr-5* double mutants probed with *hop-1*- and *ama-1*-specific probes. *Every *spr-5* allele was in a *sel-12*(*ar171*) mutant background.

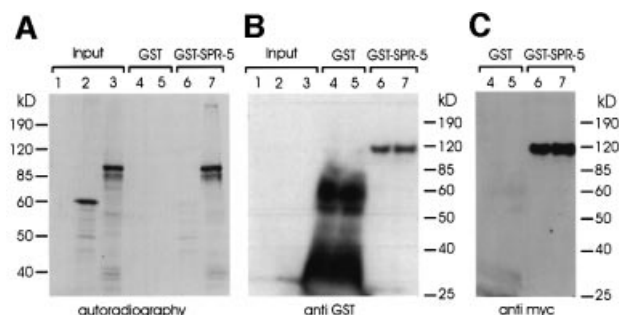


Fig. 7. SPR-5 and D1014.8/SPR-1 interact *in vitro*. (A) Autoradiography of 10% SDS-PAGE. Lanes 1–3 are input controls of ^{35}S -labelled *in vitro* translation reactions: empty vector (lane 1), luciferase (lane 2; 61 kDa), D1014.8/SPR-1 (lane 3; 68 kDa). ^{35}S -labelled luciferase and SPR-1 were incubated with GST (lanes 4 and 5), or with GST–SPR-5 (lanes 6 and 7), respectively and analysed for binding by SDS-PAGE and autoradiography as described in Materials and methods. Lanes 1–3 represent 12% of the input, and lanes 4 and 5, and lanes 6 and 7 represent 25%, each, of the binding reaction. (B) Detection of GST proteins on a western blot. The lanes are as described in (A). The blot was probed with an anti-GST antibody. Note that excess GST protein (100 μg ; lanes 4 and 5) was used for the binding reaction compared with GST–SPR-5 (4 μg ; lanes 6 and 7). (C) Detection of GST–SPR-5 fusion protein on a western blot. Since the GST–SPR-5 (115 kDa) fusion protein also contains a myc epitope tag, the blot was probed in addition with an anti-myc tag antibody. The lanes are as described in (A).

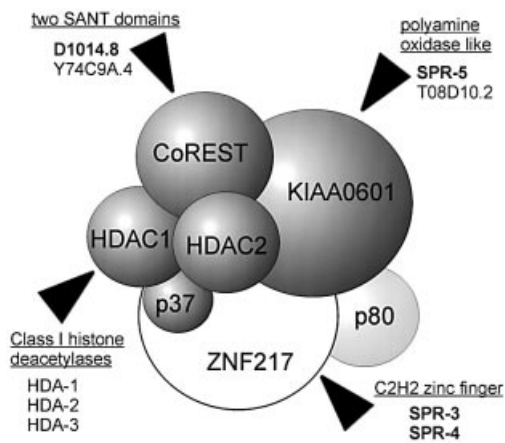


Fig. 8. Schematic representation of the human CoREST complexes as proposed (Humphrey *et al.*, 2001). The components that are overlapping in both purifications are highlighted in grey. The molecular identities of the different proteins and the homologues found in *C.elegans* are indicated. The *C.elegans* proteins involved in *sel-12* suppression are highlighted in bold. SPR-3 and SPR-4 will be described elsewhere.

factor), acts to repress neuronally expressed genes in non-neuronal cells (Andres *et al.*, 1999; Ballas *et al.*, 2001). However, REST can act through multiple deacetylase complexes, only one of them being CoREST (Griffith *et al.*, 2001). The existence of a CoREST complex in *C.elegans* is corroborated further by the fact that our screens also identified a mutant of *spr-1*/CoREST. The similar phenotypes of *spr-5* and *spr-1* suggest a similar function of both encoded proteins in the repression of early *hop-1* transcription. Our co-immunoprecipitation experiments also strongly indicate that SPR-1 and SPR-5 proteins interact in *C.elegans*, as was shown previously for their human homologues. Furthermore, in additional screens not reported here, we have identified two other *sel-12* suppressors, *spr-3* and *spr-4*, whose closest human homologue is REST (B.Lakowski and R.Baumeister, unpublished data). Therefore, mutations in at least four proteins similar to components of the CoREST–HDAC complex are able to suppress *sel-12* by up-regulating the activity of the second presenilin, *hop-1*.

The fact that there exist two reading frames encoding proteins with obvious homology to KIAA0601 (SPR-5 and T08D10.2) and CoREST protein (D1014.8 and Y74C9A.4), respectively, indicates that at least two independent CoREST complexes might exist in *C.elegans* that have different roles. Only one of them is involved in the regulation of *hop-1*.

What is the mechanism of *hop-1* de-repression by *spr-5*?

The FAD-binding motif of SPR-5 is well conserved and places SPR-5 into the superfamily of FAD-dependent oxidases (Dailey and Dailey, 1998). It is probably inactive in the *spr-5*(*by113*) mutant (see above). The amino acid sequence identities between different members of this superfamily are normally quite low and range between 20 and 30% (Binda *et al.*, 1999). In contrast to the FAD domain, the substrate recognition domain is not conserved among various members of this family and, therefore, different oxidative reactions are catalysed by individual amine oxidases. Although different substrates are bound,

the overall three-dimensional structures of the substrate recognition domains of PAOs are strikingly similar to those of monoamine oxidases (Binda *et al.*, 1999, 2002). It is possible, therefore, that despite its divergent substrate recognition domain, SPR-5 might have retained a comparable enzymatic activity. However, in the absence of functional data, one can only speculate about a function for this class of PAO.

A number of different proteins with enzymatic activities have been identified recently in HDAC complexes regulating transcriptional repression. For example, both HAT and HDAC complexes are involved in controlling transcriptional regulation mediated by the Notch intracellular domain (reviewed in Mumm and Kopan, 2000). However, our data clearly show that SPR-1 and SPR-5 do not regulate *lin-12*/Notch signalling directly. A recently discovered family of co-repressor proteins, the C-terminal binding proteins (CtBPs), exhibits similarity to dehydrogenase enzymes (Chinnadurai, 2002). CtBP adopts different conformations dependent on the cofactor bound (NAD⁺ or NADH), modulating its affinity for partner proteins and, thus, the level of repression (Zhang *et al.*, 2002). It is possible that, upon FAD binding, a similar mechanism is induced in the SPR-5/PAO in the CoREST complexes. It has been suggested that KIAA0601 could, in principle, have an enzymatic activity that involves the oxidation of amines or amino groups, such as for example the methylation of lysine or arginine side chains on modified histone tails (Chinenov, 2002). The methylation of lysine residues in the histone tails has been shown to modulate the interaction of repressor complexes with specific regulatory sequences tails (Zegerman *et al.*, 2002).

In summary, our data strongly indicate that *spr-5* encodes a PAO-like factor that is part of a transcriptional repressor complex similar to the human CoREST complex. We describe for the first time a target gene that is controlled genetically by a CoREST-associated PAO. *Caenorhabditis elegans* SPR-5, most probably in a complex with CoREST/SPR-1, regulates the repression of *hop-1* presenilin at early developmental stages. The presence of two homologous proteins of each component of the CoREST complex in *C.elegans* indicates that there may exist more co-repressor complexes of this type in the nematode, only one of them being involved in *hop-1* regulation. Based on the dsRNAi experiment, it is possible that additional CoREST complexes might function in other regulatory processes not related to *hop-1*.

Materials and methods

Strains, plasmids and molecular techniques

All strains and mutants were maintained at 20°C according to standard procedures, if not stated otherwise. LGX, *sel-12*(*ar171*), *sel-12*(*ar131*), *sel-12*(*lg1401*); LGI, *hop-1*(*lg1501*), *unc-73*(*e936*), *glp-4*(*bn2ts*); LGII, *unc-4*(*e120*); LGIII, *mut-7*(*pk204*) (Ketting *et al.*, 1999), *lin-12*(*n676n930*) *unc-32*(*e189*), *unc-32*(*e189*), *lin-12*(*n302*); LGIV, *fem-1*(*hc17ts*); LGVI, *him-5*(*e1489*).

Sequences of oligonucleotides and details on plasmid constructions are listed in the Supplementary data available at *The EMBO Journal* Online.

Screens for extragenic suppressors of the *sel-12*(*ar171*) Egl phenotype

A *sel-12*(*ar171*) *unc-1*(*e538*); *mut-7*(*pk204*) strain was constructed and was maintained at 15°C and for mutagenesis shifted to 20–23°C. The

strain was tested for the appearance of an Egl and Him phenotype and sterility at 25°C, as described previously (Ketting *et al.*, 1999). During the mutagenesis, single worms were transferred to 3.5 cm plates and kept at 20°C for two generations. The F₂ progeny were transferred to 9 cm plates and screened for the appearance of eggs on the plate. The eggs or their non-Egl, Unc mothers were picked to new plates and tested for the inheritance of the non-Egl phenotype. Two independent mutations were discovered in a screen corresponding to ~9600 haploid genomes. *spr-3(by110)* X will be described elsewhere (B.Lakowski and R.Baumeister, unpublished data); *spr-5(by101)* I was outcrossed with N2 and subsequently was analysed.

Transposon display and cloning of *spr-5*

The spontaneous mutants that showed a heritable suppression of the *sel-12* Egl defect were outcrossed with N2 six times. The remaining transposons with their flanking sequences were displayed by PCR as described previously (Wicks *et al.*, 2000). Genomic DNA from the *sel-12(ar171)* and *sel-12(ar171)*; *spr-5(by101)* strains was prepared and digested with *Sau3A*. The digested DNA was ligated to an adaptor, and transposons were displayed following the Transposon Insertion Display protocol (<http://genomics.niob.knaw.nl/>) and identified Y40B1B.6 as the insertion locus of the transposon. To isolate a fosmid including Y40B1B.6, we hybridized a fosmid filter grid (kindly provided by Alan Coulson, Cambridge) with Y40B1B.6-specific radioactively labelled PCR products. Three positive fosmids were found that contain the identical genomic region except for differences around Y40B1B.6. H1404 and H37019 contain the whole coding region of Y40B1B.6 (DDBJ/EMBL/GenBank accession No. AY152852), whereas H18N7 terminates after the sixth exon of Y40B1B.6 (Figure 1).

Transgenic lines and rescue

As there was only one yeast artificial chromosome, Y40B1, available containing the genomic region of *spr-5*, we screened a *C.elegans* fosmid filter grid kindly provided by Alan Coulson for fosmids including *spr-5*. For that purpose, the filter grid was probed with two PCR products corresponding to the 5' (RB927/RB928) and 3' end (RB828/RB944) of the *spr-5* cDNA. Two fosmids, H1404 and H37019, were found to hybridize to both probes, whereas H18N7 was only positive for the 5'-specific probe. To determine whether the *spr-5*-containing fosmids are able to revert the Egl suppression by *sel-1(ar171)*; *spr-5(by101)* double mutants, they were injected individually at 10 ng/μl along with the *rol-6(d)* co-injection marker pRF4, at 100 ng/μl, using standard transformation techniques (Mello *et al.*, 1991).

Identification of *spr-1*

Genetic mapping confirmed that *by133* is an allele of *spr-1* (Wen *et al.*, 2000; S.Jarriault and I.Greenwald, personal communication). To rescue *spr-1*, we injected a *spr-1(by133)*; *sel-12(ar171)* strain with the cosmid D1014 at 20 ng/μl with 100 ng/μl pRF4 as a co-transformation marker. We screened the transgenic progeny for appearance of Egl-defective animals indicating solid rescue of the *spr-1*-mediated Egl suppression.

Northern blotting

RNA was isolated from mixed stage plates or staged plates, and prepared with an RNeasy kit (Qiagen) according to the manufacturer's instructions. For most northern blots, 5 μg of total RNA per lane was denatured at 65°C for 5 min and then loaded onto a 0.8% agarose RNA gel. The gel was run overnight to separate fragments and blotted onto Hybond N+ membranes according to the protocol of Sambrook *et al.* (1989). For the L1 northern blots, 20 μg of total RNA was used per lane. Probes were labelled with [α -³²P]dCTP using a Megaprime labelling kit according to the manufacturer's instructions (Amersham, Freiburg, Germany). Blots were hybridized and washed according to the procedure of Church and Gilbert (1984) at 65°C. As a loading control, all northern blots were probed with an *ama-1*-specific probe using the PCR primers RB1186/RB1187 (Johnstone and Barry, 1996).

dsRNAi by feeding

Genes were transiently inactivated by RNAi through feeding of the *Escherichia coli* strain HT115(DE3) expressing dsRNA of the gene of interest (Timmons and Fire, 1998; Timmons *et al.*, 2001). The dsRNA expression was induced as described previously (Kamath *et al.*, 2000) and the worms were transferred as L4 larvae onto seeded plates containing 50 μg/ml ampicillin and 1 mM isopropyl-β-D-thiogalactopyranoside (IPTG), and kept at 20°C. The progeny were scored for the ability to lay eggs. A plate was scored as non-Egl if the majority of the progeny showed

no protruding vulva (Pvl), solid egg-laying over 3 days and did not die with a bag of worm phenotype.

GST purification of the GST-SPR-5 fusion protein

Sf9 lysates from GST- and GST-SPR-5-expressing cells, respectively, were incubated with glutathione-Sepharose beads (Pharmacia, Freiburg) for 2 h at room temperature and washed with IP buffer (25 mM HEPES pH 7.6, 100 mM NaCl, 1 mM MgCl₂, 0.1% NP-40, 10% glycerol, 1 mM dithiothreitol, 0.5 mM EDTA, 30 μM FAD) twice. Incubation with ³⁵S-labelled SPR-1 produced *in vitro* using the TNT Coupled Reticulocyte Lysate System (Promega, Mannheim) was carried out for 2 h at room temperature. Subsequently, GST beads were collected by centrifugation and washed three times with 1 ml of IP buffer, resuspended in 40 μl of Laemmli sample buffer, and analysed by SDS-PAGE, western blotting and autoradiography.

Supplementary data

Supplementary data are available at *The EMBO Journal* Online.

Acknowledgements

We would like to thank past and present members of the Baumeister lab for discussions and support. We are particularly grateful to Henri van Luenen and Ronald Plasterk for their help with the transposon display. We also thank Peter Becker and his lab for help and suggestions, Iva Greenwald and EleGene AG for strains, Tom Blumenthal and Iva Greenwald for providing unpublished results, Alan Coulson for the fosmid grid and fosmid clones, Yuji Kohara for providing EST clones, and Bob Barstead for the cDNA library. Some strains used in this work were provided by the *Caenorhabditis* Genetics Center. B.L. was supported by an EMBO fellowship, and R.B. was supported by grants from the EC (DIADEM), the DFG and the BMBF (NGFN network).

References

- Andres,M.E., Burger,C., Peral-Rubio,M.J., Battaglioli,E., Anderson, M.E., Grimes,J., Dallman,J., Ballas,N. and Mandel,G. (1999) CoREST: a functional corepressor required for regulation of neuronal-specific gene expression. *Proc. Natl Acad. Sci. USA*, **96**, 9873–9878.
- Ballas,N. *et al.* (2001) Regulation of neuronal traits by a novel transcriptional complex. *Neuron*, **31**, 353–365.
- Baumeister,R., Leimer,U., Zweckbronner,I., Jakubek,C., Grunberg,J. and Haass,C. (1997) Human presenilin-1, but not familial Alzheimer's disease (FAD) mutants, facilitate *Caenorhabditis elegans* Notch signalling independently of proteolytic processing. *Genes Funct.*, **1**, 149–159.
- Binda,C., Coda,A., Angelini,R., Federico,R., Ascenzi,P. and Mattevi,A. (1999) A 30-Ångstrom-long U-shaped catalytic tunnel in the crystal structure of polyamine oxidase. *Struct. Fold. Design*, **7**, 265–276.
- Binda,C., Angelini,R., Federico,R., Ascenzi,P. and Mattevi,A. (2001) Structural bases for inhibitor binding and catalysis in polyamine oxidase. *Biochemistry*, **40**, 2766–2776.
- Binda,C., Newton-Vinson,P., Hubalek,F., Edmondson,D.E. and Mattevi,A. (2002) Structure of human monoamine oxidase B, a drug target for the treatment of neurological disorders. *Nat. Struct. Biol.*, **9**, 22–26.
- Blumenthal,T. *et al.* (2002) A global analysis of *Caenorhabditis elegans* operons. *Nature*, **417**, 851–854.
- Bosher,J.M., Dufourcq,P., Sookhareea,S. and Labouesse,M. (1999) RNA interference can target pre-mRNA: consequences for gene expression in a *Caenorhabditis elegans* operon. *Genetics*, **153**, 1245–1256.
- Chinenov,Y. (2002) A second catalytic domain in the Elp3 histone acetyltransferases: a candidate for histone demethylase activity? *Trends Biochem. Sci.*, **27**, 115–117.
- Chinnadurai,G. (2002) CtBP, an unconventional transcriptional corepressor in development and oncogenesis. *Mol. Cell*, **9**, 213–224.
- Church,G.M. and Gilbert,W. (1984) Genomic sequencing. *Proc. Natl Acad. Sci. USA*, **81**, 1991–1995.
- Cinar,H.N., Sweet,K.L., Hosemann,K.E., Earley,K. and Newman,A.P. (2001) The SEL-12 presenilin mediates induction of the *Caenorhabditis elegans* uterine π cell fate. *Dev. Biol.*, **237**, 173–182.
- Dailey,T.A. and Dailey,H.A. (1998) Identification of an FAD superfamily containing protoporphyrinogen oxidases, monoamine oxidases and phytoene desaturase. Expression and characterization

- of phytoene desaturase of *Myxococcus xanthus*. *J. Biol. Chem.*, **273**, 13658–13662.
- Dufourcq,P., Victor,M., Gay,F., Calvo,D., Hodgkin,J. and Shi,Y. (2002) Functional requirement for histone deacetylase 1 in *Caenorhabditis elegans* gonadogenesis. *Mol. Cell. Biol.*, **22**, 3024–3034.
- Eimer,S., Donhauser,R. and Baumeister,R. (2002) The *C.elegans* presenilin *sel-12* is required for mesodermal patterning and muscle function. *Dev. Biol.*, in press.
- Fortini,M.E. (2001) Notch and presenilin: a proteolytic mechanism emerges. *Curr. Opin. Cell Biol.*, **13**, 627–634.
- Greenwald,I. (1998) LIN-12/Notch signaling: lessons from worms and flies. *Genes Dev.*, **12**, 1751–1762.
- Greenwald,I.S., Sternberg,P.W. and Horvitz,H.R. (1983) The *lin-12* locus specifies cell fates in *Caenorhabditis elegans*. *Cell*, **34**, 435–444.
- Griffith,E.C., Cowan,C.W. and Greenberg,M.E. (2001) REST acts through multiple deacetylase complexes. *Neuron*, **31**, 339–340.
- Humphrey,G.W., Wang,Y., Russanova,V.R., Hirai,T., Qin,J., Nakatani,Y. and Howard,B.H. (2001) Stable histone deacetylase complexes distinguished by the presence of SANT domain proteins CoREST/kiaa0071 and Mta-L1. *J. Biol. Chem.*, **276**, 6817–6824.
- Jepsen,K. and Rosenfeld,M.G. (2002) Biological roles and mechanistic actions of co-repressor complexes. *J. Cell Sci.*, **115**, 689–698.
- Johnstone,I.L. and Barry,J.D. (1996) Temporal reiteration of a precise gene expression pattern during nematode development. *EMBO J.*, **15**, 3633–3639.
- Kamath,R.S., Martinez-Campos,M., Zipperlen,P., Fraser,A.G. and Ahringer,J. (2000) Effectiveness of specific RNA-mediated interference through ingested double-stranded RNA in *Caenorhabditis elegans*. *Genome Biol.*, **2**, 1–10.
- Ketting,R.F., Haverkamp,T.H., van Luenen,H.G. and Plasterk,R.H. (1999) Mut-7 of *C.elegans*, required for transposon silencing and RNA interference, is a homolog of Werner syndrome helicase and RNaseD. *Cell*, **99**, 133–141.
- Lai,E.C. (2002) Protein degradation: four e3s for the notch pathway. *Curr. Biol.*, **12**, R74–R78.
- Levitani,D. and Greenwald,I. (1995) Facilitation of *lin-12*-mediated signalling by *sel-12*, a *Caenorhabditis elegans* S182 Alzheimer's disease gene. *Nature*, **377**, 351–354.
- Li,C. and Chalfie,M. (1990) Organogenesis in *C.elegans*: positioning of neurons and muscles in the egg-laying system. *Neuron*, **4**, 681–695.
- Li,X. and Greenwald,I. (1997) HOP-1, a *Caenorhabditis elegans* presenilin, appears to be functionally redundant with SEL-12 presenilin and to facilitate LIN-12 and GLP-1 signaling. *Proc. Natl Acad. Sci. USA*, **94**, 12204–12209.
- Mello,C.C., Kramer,J.M., Stinchcomb,D. and Ambros,V. (1991) Efficient gene transfer in *C.elegans*: extrachromosomal maintenance and integration of transforming sequences. *EMBO J.*, **10**, 3959–3970.
- Mumm,J.S. and Kopan,R. (2000) Notch signaling: from the outside in. *Dev. Biol.*, **228**, 151–165.
- Nagase,T., Ishikawa,K., Miyajima,N., Tanaka,A., Kotani,H., Nomura,N. and Ohara,O. (1998) Prediction of the coding sequences of unidentified human genes. IX. The complete sequences of 100 new cDNA clones from brain which can code for large proteins *in vitro*. *DNA Res.*, **5**, 31–39.
- Newman,A.P., White,J.G. and Sternberg,P.W. (1995) The *Caenorhabditis elegans lin-12* gene mediates induction of ventral uterine specialization by the anchor cell. *Development*, **121**, 263–271.
- Sambrook,J., Fritsch,E.F. and Maniatis,T. (1989) *Molecular Cloning: A Laboratory Manual*. Cold Spring Harbor Laboratory Press, Cold Spring Harbor, NY.
- Sebela,M., Radova,A., Angelini,R., Tavladoraki,P., Frebort,I.I. and Pec,P. (2001) FAD-containing polyamine oxidases: a timely challenge for researchers in biochemistry and physiology of plants. *Plant Sci.*, **160**, 197–207.
- Seiler,N. (1995) Polyamine oxidase, properties and functions. *Prog. Brain Res.*, **106**, 333–344.
- Selkoe,D.J. (2001) Alzheimer's disease: genes, proteins and therapy. *Physiol. Rev.*, **81**, 741–766.
- Seo,S.B., McNamara,P., Heo,S., Turner,A., Lane,W.S. and Chakravarti,D. (2001) Regulation of histone acetylation and transcription by INHAT, a human cellular complex containing the set oncoprotein. *Cell*, **104**, 119–130.
- Sharma-Kishore,R., White,J.G., Southgate,E. and Podbilewicz,B. (1999) Formation of the vulva in *Caenorhabditis elegans*: a paradigm for organogenesis. *Development*, **126**, 691–699.
- Spith,J., Brooke,G., Kuersten,S., Lea,K. and Blumenthal,T. (1993) Operons in *C.elegans*: polycistronic mRNA precursors are processed by trans-splicing of SL2 to downstream coding regions. *Cell*, **73**, 521–532.
- Struhl,G. and Adachi,A. (1998) Nuclear access and action of notch *in vivo*. *Cell*, **93**, 649–660.
- Sundaram,M. and Greenwald,I. (1993) Genetic and phenotypic studies of hypomorphic *lin-12* mutants in *Caenorhabditis elegans*. *Genetics*, **135**, 755–763.
- Timmons,L. and Fire,A. (1998) Specific interference by ingested dsRNA. *Nature*, **395**, 854.
- Timmons,L., Court,D.L. and Fire,A. (2001) Ingestion of bacterially expressed dsRNAs can produce specific and potent genetic interference in *Caenorhabditis elegans*. *Gene*, **263**, 103–112.
- Tong,J.K., Hassig,C.A., Schnitzler,G.R., Kingston,R.E. and Schreiber,S.L. (1998) Chromatin deacetylation by an ATP-dependent nucleosome remodelling complex. *Nature*, **395**, 917–921.
- Trent,C., Tsung,N. and Horvitz,H.R. (1983) Egg-laying defective mutants of the nematode *C.elegans*. *Genetics*, **104**, 619–647.
- Wen,C., Levitan,D., Li,X. and Greenwald,I. (2000) *spr-2*, a suppressor of the egg-laying defect caused by loss of *sel-12* presenilin in *Caenorhabditis elegans*, is a member of the SET protein subfamily. *Proc. Natl Acad. Sci. USA*, **97**, 14524–14529.
- Westlund,B., Parry,D., Clover,R., Basson,M. and Johnson,C.D. (1999) Reverse genetic analysis of *Caenorhabditis elegans* presenilins reveals redundant but unequal roles for *sel-12* and *hop-1* in Notch-pathway signaling. *Proc. Natl Acad. Sci. USA*, **96**, 2497–2502.
- Wicks,S.R., de Vries,C.J., van Luenen,H.G. and Plasterk,R.H. (2000) CHE-3, a cytosolic dynein heavy chain, is required for sensory cilia structure and function in *Caenorhabditis elegans*. *Dev. Biol.*, **221**, 295–307.
- Wu,G., Hubbard,E.J., Kitajewski,J.K. and Greenwald,I. (1998) Evidence for functional and physical association between *Caenorhabditis elegans* SEL-10, a Cdc4p-related protein and SEL-12 presenilin. *Proc. Natl Acad. Sci. USA*, **95**, 15787–15791.
- You,A., Tong,J.K., Grozinger,C.M. and Schreiber,S.L. (2001) CoREST is an integral component of the CoREST–human histone deacetylase complex. *Proc. Natl Acad. Sci. USA*, **98**, 1454–1458.
- Zegerman,P., Canas,B., Pappin,D. and Kouzarides,T. (2002) Histone H3 lysine 4 methylation disrupts the binding of the nucleosome remodelling and deacetylase (NuRD) repressor complex. *J. Biol. Chem.*, **277**, 11621–11624.
- Zhang,Q., Piston,D.W. and Goodman,R.H. (2002) Regulation of corepressor function by nuclear NADH. *Science*, **295**, 1895–1897.

Received May 10, 2002; revised August 19, 2002;
accepted September 2, 2002

CHAPTER VII

**Two suppressors of *sel-12* encode C2H2 zinc finger proteins
that regulate presenilin transcription in *C. elegans***

published as:

Lakowski B., Eimer S., Göbel C., Böttcher A., Wagler B. and Baumeister R.

Two suppressors of *sel-12* encode C2H2 zinc finger proteins that regulate presenilin transcription in *C. elegans*.

Development **130**: 2117-2128.

Summary

Mutations in presenilin genes are associated with Familial Alzheimer's Disease in humans and affect LIN-12/Notch signaling in all organisms tested so far. Loss of *sel-12* presenilin activity in *Caenorhabditis elegans* results in a completely penetrant egg-laying defect. In screens for extragenic suppressors of the *sel-12* egg-laying defect, we have isolated mutations in at least five genes. We report here the cloning and characterization of *spr-3* and *spr-4* that encode large basic C₂H₂ zinc finger proteins. Suppression of *sel-12* by *spr-3* and *spr-4* requires the activity of the second presenilin gene, *hop-1*. Mutations in both *spr-3* and *spr-4* de-repress *hop-1* transcription in the early larval stages when *hop-1* expression is normally nearly undetectable. Since *sel-12* and *hop-1* are functionally redundant, this suggests that mutations in *spr-3* and *spr-4* bypass the need for one presenilin by stage-specifically de-repressing the transcription of the other. Both *spr-3* and *spr-4* code for proteins similar to the human REST/NRSF (Re1 silencing transcription factor/neural-restrictive silencing factor) transcriptional repressors. As other *spr* genes encode proteins homologous to components of the CoREST co-repressor complex that interacts with REST, and the INHAT (*inhibitor of acetyltransferase*) co-repressor complex, our data suggest that all *spr* genes may function through the same mechanism that involves transcriptional repression of the *hop-1* locus.

Introduction

Presenilins are a class of polytopic proteins found throughout the plant and animal kingdoms. They are part of high molecular weight complexes containing additional components, including APH-2/Nicastrin, APH-1 and PEN-2 (Capell et al., 1998; Francis et al., 2002; Li et al., 2000; Thinakaran et al., 1998; Yu et al., 1998). This complex assembles and matures in the ER and Golgi and is subsequently transported to the cell membrane where it is required for the intra-membranous proteolytic cleavage of certain type I transmembrane proteins. These include the amyloid precursor protein APP and Notch-type receptors (De Strooper et al., 1999; De Strooper et al., 1998; Fortini, 2001). It has been proposed that presenilins themselves provide aspartyl protease activity and are responsible for the γ -secretase cleavage involved in generating β -amyloid fragments from the amyloid precursor protein (APP) (Steiner et al., 2000; Wolfe et al., 1999).

Mutations in either of the human presenilin genes, PS1 and PS2, are dominant and cause early onset Alzheimer's disease. They result in an increase in the ratio of the 42 amino acid variant to the 40 amino acid variant of β -amyloid, but do not alter the total amount of presenilin-dependent γ -secretase cleavage (reviewed in (Selkoe, 2001)). The 42 amino acid variant of β -amyloid is highly insoluble and tends to aggregate, nucleating the senile plaques found in brains of Alzheimer's disease patients (reviewed in (Sisodia and St George-Hyslop, 2002)).

Presenilin activity is also required for the S3 cleavage of Notch receptors after ligand binding (Struhl and Adachi, 1998). Like the γ -secretase cleavage of APP, this cleavage occurs within the transmembrane domain and releases the Notch intracellular domain (NICD). The release of the NICD is essential for Notch signaling, because the liberated NICD fragment enters the nucleus where it interacts with the transcription factor CSL [CBP, suppressor of hairless, lag-1] (De Strooper et al., 1999; Song et al., 1999) and additional co-activators such as *sel-8/lag-3* or mastermind (Doyle et al., 2000; Freyer et al., 2002; Petcherski and Kimble, 2000).

The *C. elegans* genome encodes three presenilin genes, *sel-12*, *hop-1*, and *spe-4* that are homologous to human PS1 and PS2. *spe-4* is the most divergent member of the presenilin family and appears to have a specific role in spermatogenesis (Arduengo et al., 1998; L'Hernault and Arduengo, 1992). The two other presenilins are much more similar to the human homologues and are absolutely essential for signaling through the two *C. elegans*

Notch-type receptors, LIN-12 and GLP-1 (Levitan and Greenwald, 1995; Li and Greenwald, 1997; Westlund et al., 1999). The absence of both *sel-12* and *hop-1* genes leads to a completely penetrant lethal phenotype that resembles either a complete loss of GLP-1 or a complete loss of LIN-12 signaling [the exact phenotype depends on how the double mutants are constructed as both *sel-12* and *hop-1* have partial maternal effects, (Westlund et al., 1999)]. On their own, mutations in *hop-1* have no obvious phenotype, while mutations in *sel-12* lead to an egg-laying defect (Egl) (Levitan and Greenwald, 1995; Westlund et al., 1999). *sel-12* and *hop-1* seem to have largely overlapping roles, since *hop-1* can rescue the *sel-12* Egl defect when expressed from a *sel-12* promoter (Li and Greenwald, 1997; Westlund et al., 1999). Not only the sequence, but also the function of presenilins is evolutionarily conserved, as both human presenilins PS1 and PS2 can also rescue the *sel-12* Egl defect when expressed under the control of appropriate promoters (Baumeister et al., 1997; Levitan et al., 1996).

In order to understand more about the biological role of presenilins, we have been studying the *sel-12* gene in *C. elegans*. Mutations in *sel-12* were first identified for their ability to suppress a *lin-12* gain-of-function mutation (Levitan and Greenwald, 1995). This suggests that *sel-12* mutations reduce *lin-12* signaling and that the SEL-12 protein normally facilitates *lin-12* signaling (Levitan and Greenwald, 1995). However, mutations in *sel-12* do not completely eliminate *lin-12* signaling, presumably due to residual presenilin activity supplied by *hop-1* (Li and Greenwald, 1997; Westlund et al., 1999). Different levels of LIN-12 activity are required to control at least five post-embryonic signaling events (Eimer et al., 2002a). In *sel-12* null mutants only two of these are affected to a varying degree (Eimer et al., 2002a)(Cinar et al., 2001). This indicates that the presenilin activity supplied by *hop-1* is sufficient for most *lin-12* signaling events and that some *lin-12* signaling events appear to be more sensitive to presenilin dosage than others (Eimer et al., 2002a).

To further elucidate the function of the *sel-12* gene, one can study mutations that bypass the need for *sel-12*. Mutations in four genes, *sel-10*, *spr-1*, *spr-2*, and *spr-5*, have already been shown to suppress the *sel-12* egg-laying defect. Mutations in *sel-10* were first found in a screen for genes that suppresses a weak *lin-12* loss of function mutant (Hubbard et al., 1997). *sel-10* is similar to the yeast gene CDC4, and acts as an E3 ubiquitin ligase that targets the intra-cellular domains of LIN-12 and GLP-1 proteins for degradation (Gupta-Rossi et al., 2001; Hubbard et al., 1997). *sel-10* mutations also weakly suppress mutations in *sel-12*, but do completely bypass the need for *sel-12*. In a screen similar to the one reported here, Wen *et al.* have identified four genes that strongly suppress the Egl defect of *sel-12* (suppressors of presenilin) and have described the cloning and characterization of one of

them, *spr-2* (Wen et al., 2000). Mutations in *spr-2* almost completely bypass the need for *sel-12*. The biochemical role of SPR-2 is presently unclear, but it may affect chromatin structure and/or transcription (Wen et al., 2000).

In this paper, we report the results of several screens for strong suppressors of *sel-12* and the isolation of 25 independent mutations. These mutations lie in several of the same complementation groups identified by Wen *et al.* as well as in some additional genes, indicating that neither screen has reached saturation. We also report the cloning and characterization of two suppressor genes, *spr-3* and *spr-4*, that code for C₂H₂ zinc finger proteins similar to the transcriptional repressors REST/NRSF. *spr-3* and *spr-4* mutants bypass the need for *sel-12* by up-regulating the transcription of the other presenilin, *hop-1*. Since two other presenilin suppressors that were also identified in this screen, *spr-1* and *spr-5*, encode proteins of the CoREST/HDAC complex (Eimer et al., 2002b; Jarriault and Greenwald, 2002) that interacts with REST, we propose that the *spr* proteins assemble into one or more repressor complexes that normally repress the *hop-1* locus in the early larval stages. Mutations in components of these complexes remove a repressor activity leading to a higher basal level of *hop-1* presenilin activity.

Materials and Methods

General handling and mutations used. Worms were handled according to standard procedures (Sulston and Hodgkin, 1988) and grown at 20°C unless otherwise stated. The following mutations were used:

LG I: *hop-1(lg1501)*, *dpy-5(e61)*, *ego-1(om71)*, *unc-55(e1170)*, *spr-4(ar208)*, *daf-8(e1393)*, *unc-75(e950)*, *unc-101(m1)*, *unc-59(e261)*

LG V: *dpy-11(e224)*, *unc-76(e911)*

LG X: *sel-12(ar171)*, *ar131*, *by125*, *lg1401*, *dpy-23(e830)*, *spr-3(ar209)*, *lon-2(e678)*, *mnDp31*, *mnDp32*.

All mutations were obtained from the Caenorhabditis Genetics Center except *sel-12(ar131)*, *sel-12(ar171)*, *spr-3(ar209)* and *spr-4(ar208)* (kindly provided by Iva Greenwald), *hop-1(lg1501)* [described in Wittenburg et al., 2000], *sel-12(by125)* and *sel-12(lg1401)* [described in Eimer et al., 2002b].

Isolation of mutants. Ethylmethanesulfonate (EMS) and Ultra Violet light/tetramethylpsoralen (UV/TMP) mutagenesis were done according to published procedures (Anderson, 1995; Sulston and Hodgkin, 1988). The mutator screen is presented in another paper (Eimer et al., 2002b). We looked in one EMS (16 000 haploid genomes) and one UV/TMP screen (8 000 haploid genomes) for dominant suppressor mutations but did not identify any. We screened for recessive suppressor mutations in a similar manner to (Wen et al., 2000). Mutants were retained when the *spr; sel-12(ar171)* double mutants displayed essentially wild-type egg-laying behavior and the vast majority of their progeny (>90%) did not become Egl. All mutations were out-crossed five times before further phenotypic analysis. For each type of screen, below are listed the mutagens used, the number of haploid genomes screened and the mutations identified:

EMS: 24 300; *by105, by107, by108, by109, by112, by113, by114, by116, by117, by119.*

UV/TMP: 41 600; *by118, by128, by129, by130, by131, by132, by133, by134, by135, by136, by137, by139, by140.*

Mutator generated mutations: 9 600; *by101, by110.*

Complementation tests. Complementation tests were done according to standard procedures (Sulston and Hodgkin, 1988). Assignment of complementation groups:

spr-1: by133.

spr-3: ar209, by108, by109, by110, by131(byDf1), by135, by136, by137.

spr-4: ar208, by105, by107, by112, by114, by129, by130, by132.

spr-5: by101, by113, by119, by128, by134, by139.

Uncharacterized: *by116, by117, by118, by140.*

Genetic mapping. Suppressor mutations were genetically mapped using standard techniques (Sulston and Hodgkin, 1988) maintaining, where possible, the *spr* mutation in a homozygous *sel-12(ar171)* background. The position of *spr-4* was refined further by single nucleotide polymorphism (SNP) mapping done essentially as described (Jakubowski and Kornfeld, 1999).

Transgenic rescue of *spr-3* and *spr-4*. We injected into the strain *sel-12(ar171) spr-3(by108)* to rescue *spr-3* and into the strain *spr-4(by105); sel-12(ar171)* to rescue *spr-4* and then looked for anti-suppressor activity of injection mixes (i.e. restoration of a *sel-12* phenotype). All test clones and PCR products were injected at 20 ng/μl with 100ng/μl pRF4 (*rol-6*) and 20ng/μl pBY218 (*ttx-3::GFP*, (Hobert et al., 1997)) as co-injection markers.

Gene structure of *spr-3* and *spr-4*. We sequenced two *spr-3* cDNAs, yk64e9 and yk247c5, kindly provided by Yuji Kohara. We found that the two cDNAs have a very similar structure, yet yk247c5 has an additional intron in the largest exon of the gene. However, on staged Northern blots (see Figures 2, 4A) and by RT-PCR on each developmental stage, only a single transcript, similar in length to yk64e9, could be detected (data not shown). In the process of sequencing the cDNAs we also discovered a sequencing error in the genomic sequence from the cosmids F46H6 and C07A12 near the 5' end of *spr-3*, which put the first ATG out of frame (data not shown). This error was communicated to the *C. elegans* sequencing consortium and the genomic sequence has been updated. To determine the 5' end of the *spr-3* transcript we performed PCR on a random primed cDNA library, kindly provided by Bob Barstead, using SL1 and SL2 forward primers (Spieth et al., 1993) and gene specific reverse primers (RB1080 CATACTTGACGGCATCATCGG; RB1079 CATCTGCTTCTCGCTCGAGAATCG). We found that *spr-3* is trans-spliced to SL1 but not to SL2. The SL1 specific product was sequenced and was found to start just 5' to the 5' ends of the two sequenced cDNAs at a predicted splice acceptor site.

To determine the structure of *spr-4* we sequenced the nearly-full length cDNA, yk646c12, in its entirety and found that it matched the predicted gene C09H6.1 (Z81466) except that yk646c12 lacks the first five nucleotides of the ORF and the last exon starts six nucleotides more 3' than in the annotated C09H6.1. As the cDNA, yk1178d11, uses a weak acceptor for this last exon, as annotated in Wormbase [<http://www.wormbase.org/>], *spr-4* appears to be alternatively spliced. The two transcripts encode identical proteins except for a difference of two amino acids in the region between the 17th and 18th zinc fingers (Figure 5C).

Comparisons with predicted *Caenorhabditis briggsae* genes. Access to the unpublished draft genomic sequence of *Caenorhabditis briggsae* is available from the Wellcome Trust Sanger Institute (http://www.sanger.ac.uk/Projects/C_briggsae/) or from the Genome Sequencing Center at Washington University, St. Louis

(<http://genome.wustl.edu/projects/cbriggsae/>). The local synteny between *C. elegans* and *C. briggsae* and a preliminary prediction for *C. briggsae* spr genes can be checked there.

The *C. briggsae spr-3* gene. We identified a possible *spr-3* homologue in *C. briggsae* on the contig c010301474. We purified total *C. briggsae* mixed stage RNA with a Qiagen RNAeasy kit according to the manufacturer's instructions (Qiagen, Hilden). To determine its gene structure, we performed RT-PCR with various combinations of primers. We amplified a PCR product using the primers RB1627 TACTTGCCACTTGTGTCCAAG and RB1629 TGGTGAACTTTTACCCAGCG from reverse transcribed first strand cDNAs generated with the primer RB1629. This PCR product was sequenced and found to contain the central and 3' portions of the *C. briggsae spr-3* gene.

Expression constructs: An *spr-3::EGFP promoter* fusion was made by cloning EGFP at the *spr-3* ATG behind 4kb of *spr-3* promoter sequence. This construct also contained the *spr-3* 3'UTR. Translational fusion constructs were made by inserting EGFP into a rescuing genomic construct either at the ATG (N-terminal fusion) or before the TAA stop codon (C-terminal fusion), but transgenic lines generated with these constructs did not rescue *spr-3* and did not have detectable GFP fluorescence. The Baculovirus expression construct was made by inserting the *spr-3* cDNA into the transfer vector pBY1296 (Eimer et al., 2002b) fusing a GST-myc-tag N-terminally to *spr-3*. The resulting construct was co-transformed along with linearized BaculoGold DNA (Becton-Dickinson/Pharming) into Sf9 cells to generate recombinant viruses.

RNAi by feeding. We subcloned a 2.7kb *HindIII/XhoI* fragment from the cDNA yk356a2 [kindly provided by Y. Kohara] into L4440 [pPD129.36, kindly provided by A. Fire] cut *HindIII/XhoI* to generate a C28G1.4 RNAi feeding vector. A full-length *hop-1* cDNA was amplified by PCR and cloned as a *SmaI/NotI* fragment into L4440 creating pBY1575. Genes were transiently inactivated by RNAi through feeding of the *E. coli* strain HT115(DE3) expressing double stranded RNA of the gene of interest (Timmons et al., 2001; Timmons and Fire, 1998). The dsRNA expression was induced as described (Kamath et al., 2001) and the worms were transferred as L4 larvae onto seeded plates containing 50µg/ml ampicillin and 1mM IPTG. After 24h the parental worm was transferred to a new plate also containing ampicillin and IPTG. The progeny on the second RNAi plate were then scored for the relevant phenotypes. In the case of *sel-12(ar171)* animals, the parental worms were kept on the first

RNAi plate until they died with a bag of worm phenotype and only the last progeny were scored for the RNAi phenotype.

Northern blots. RNA was isolated from mixed stage plates or staged plates and prepared with an RNAsasy kit according to the manufacturer's instructions (Qiagen, Hilden). For most Northern blots, 5µg of total RNA per lane was denatured at 65 °C for 5min and then loaded onto a 0.8% agarose RNA gel. The gel was run overnight to separate fragments and blotted onto Hybond N+ membranes according to (Sambrook, 1989). For the L1 Northern blots, 20µg of total RNA was used per lane. Probes were labeled with $\alpha^{32}\text{P}$ dCTP using a Megaprime labeling kit according to the manufacturer's instructions (Amersham, Freiburg, Germany). Blots were hybridized and washed according to the procedure of (Church and Gilbert, 1984) at 65 °C. All Northern blots were probed with an *ama-1* specific probe (Johnstone and Barry, 1996) as a loading control. For each blot we first made a blot with 5µg per lane of total RNA and probed it with *ama-1*. We then used the results of this probing to adjust the amount of RNA loaded to get equal amounts of mRNA per blot. For the quantification of relative transcript levels, blots were placed on a storage phosphor screen (Molecular Dynamics) for several days and were read with a Storm 860 scanner (Molecular Dynamics). The intensity of bands was determined using ImageQuant version 4.2 (Molecular Dynamics) using the User Method of Volume Quantitation. Volumes were adjusted for background intensity.

For staged Northern blots, worms were synchronized at the L1 stage by alkaline hypochlorite treatment (Sulston and Hodgkin, 1988). Then synchronized L1 larvae were spotted onto 9cm plates seeded with OP50 and allowed to grow for six hours, 18 hours, 30 hours, 42 hours and 54 hours for L1, L2, L3, L4, and young adult stages, respectively. Worms were inspected visually before harvesting to confirm that the worms were at the correct stage.

Results

The *sel-12* suppressor screen. To isolate mutations that bypass the need for *sel-12*, we performed several screens for suppressors of the egg-laying defect of *sel-12(ar171)* mutants, using chemical (EMS, UV/TMP) and genetic (Eimer et al., 2002b) mutagenesis protocols. The different screens were chosen to induce a range of types of mutations and to get some alleles with Restriction Fragment Length Polymorphisms (RFLPs). We recovered no dominant suppressor but did isolate 25 strong recessive suppressor mutations. Twenty of the 25 mutations fall into only three complementation groups, defined by the alleles *by108*, *by105* and *by101*. *by101* was mapped to the right arm of chromosome I between *unc-101* and *unc-59* very near to *unc-59*, *by105* was mapped genetically to the cluster on LGI between *daf-8* and *unc-55*, while *by108* was mapped to LGX between *dpy-23* and *lon-2* (see supplemental data).

Subsequently, Wen *et al.* identified four suppressors of presenilin (*spr* genes) in a similar screen and described the cloning and characterization of one of them, *spr-2* (Wen et al., 2000). Wen *et al.* mapped *spr-1*, *spr-2*, *spr-3* and *spr-4* to chromosomes V, IV, X and I, respectively. By complementation analysis with *spr-3(ar209)* and *spr-4(ar208)* (kindly provided by I. Greenwald, New York), we determined that *by108* and *by105* are alleles of *spr-3* and *spr-4* (Eimer et al., 2002b), respectively. Consequently, we defined a new gene, *spr-5*, with the reference allele *by101* (Eimer et al., 2002b). We examined the remaining five suppressor mutations found in our screens to see if they could be *spr-1* or *spr-2* alleles. None of the remaining five alleles have a mutation in the coding region of *spr-2*. However, *by133* shows close linkage to *dpy-11* on chromosome V and maps to a similar region as *spr-1* (see supplemental data). *spr-1* has recently been cloned (Jarriault and Greenwald, 2002) and we have found that *by133* contains a mutation in this gene (Eimer et al., 2002b). The remaining four suppressor mutations have not been pursued in detail, but by complementation tests define three additional genes (data not shown). The fact that we found no *spr-2* alleles and that we have found mutations in genes not identified by (Wen et al., 2000) indicates that saturation was not reached in either screen. The rest of this paper will report the cloning and characterization of two of the major complementation groups, *spr-3* and *spr-4*.

***spr-3* and *spr-4* potently and specifically suppress *sel-12*.** Roughly $\frac{3}{4}$ of all *sel-12(ar171)* adult animals display a protruding vulva (Pvl, Figure 1), a defect that is strongly correlated with, and presumably caused by, the misspecification of the π lineage (Eimer et al., 2002a). Almost all *sel-12* animals retain too many eggs in the uterus (an egg-laying defective or Egl

phenotype) and these eggs hatch and develop within the mother, leading to a terminal ‘bag of worms’ (Bag) phenotype (Table 1).

The Egl defect severely limits the number of progeny generated (Table 1). Mutations in *spr-3* completely suppress all aspects of the *sel-12* egg-laying defect (Figure 1). *sel-12(ar171) spr-3* double mutants also display a nearly wild type brood size (Table 1) indicating that *spr-3* mutations restore normal egg-laying behavior and normal fertility.

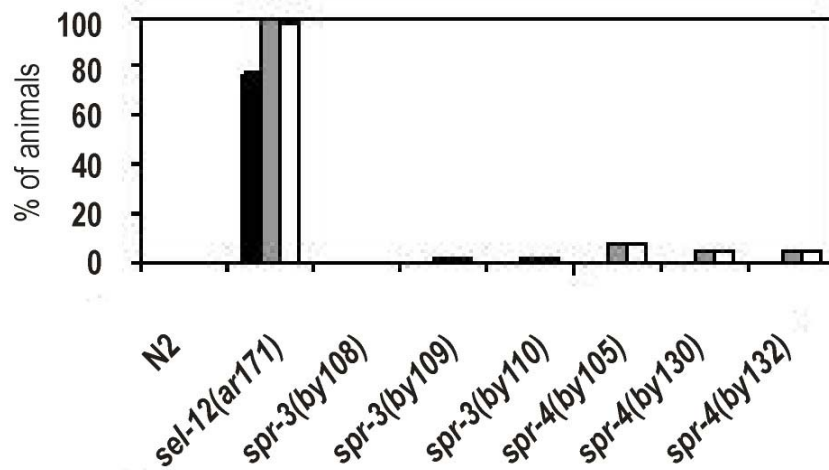


Figure 1: Mutations in *spr-3* and *spr-4* potentially suppress the egg-laying defect of *sel-12* mutants. The percentage of animals that exhibit a protruding vulva (Pvl=black), an egg-laying defect (Egl=grey) and that die of internal hatching (Bag=white) are shown for the wild type (N2), *sel-12*, and three separate alleles each of *spr-3* and *spr-4* in a *sel-12(ar171)* background. The number of animals examined were: N2, 100; *ar171*, 95; *by108*, 97; *by109*, 99; *by110*, 99; *by105*, 92; *by130*, 95; *by132*, 87.

They also respond to neurotransmitters that stimulate egg-laying (data not shown). *spr-4* mutations, on the other hand, lead to a less completely penetrant suppression of the *sel-12* phenotype and in all alleles, roughly 5% of *spr-4; sel-12(ar171)* animals still become Egl (Figure 1). This Egl phenotype is similar to *sel-12(ar171)* except that no Pvl animals are seen. This suggests that in these remaining Egl animals at least part of the *sel-12* phenotype was rescued. However, those *spr-4; sel-12(ar171)* double mutant animals that do lay eggs display a nearly wild type brood size (Table 1). Mutations in *spr-3* and *spr-4* also suppress all other *sel-12* alleles tested (*ar131*, *by125*, *lg1401* for *spr-3*, and *ar131* for *spr-4*; Table 1 and data not shown). On their own, mutations in *spr-3* and *spr-4* have no obvious phenotype, except perhaps a slightly reduced brood size (Table 1 and data not shown).

For *spr-3* we examined a clear null mutation (*by131* aka *byDfl*) in more detail. Surprisingly even this mutation, a 31kb deletion that deletes five genes including *spr-3* and both its upstream and downstream neighbor (Figure 2b), has no obvious phenotype (Table 1 and data not shown) indicating that none of the deleted genes is essential. Taken together these results

show that *spr-3* and *spr-4* are potent and specific suppressors of *sel-12* that are able to suppress all aspects of the *sel-12* phenotype.

Table 1: The brood size of *spr-3* and *spr-4* mutants

Genotype	Broods	Progeny
N2	20	314 ± 26
<i>sel-12(ar131)</i>	20	126 ± 61
<i>sel-12(ar171)</i>	20	61 ± 16
<i>sel-12(ar131) spr-3(by108)*</i>	20	226 ± 33
<i>sel-12(ar171) spr-3(by108)*</i>	20	283 ± 27
<i>sel-12(ar171) spr-3(by108); byEx134[†]</i>	20	53 ± 26
<i>byDf1[‡]</i>	20	230 ± 25
<i>sel-12(ar171) byDf1[‡]</i>	19	205 ± 63
<i>spr-4(by130); sel-12(ar171)[§]</i>	20	239 ± 33

* Similar results were obtained with the alleles *by109* and *by110* (data not shown)

[†]*byEx134* is an extra-chromosomal array containing a 9.3 kb *Bam*HI fragment from F46H6 (see Figure 2B), pBY218 and pRF4. Twenty rollers were picked as L4s and their brood size was determined.

[‡]Similar results were obtained with the *spr-3* allele *by135* (data not shown).

[§]Similar results were obtained with the *spr-4* alleles *by105* and *by132* (data not shown).

SPR-3 is a C2H2 zinc finger protein. Genetic mapping placed *spr-3* on chromosome X between *dpy-23(e840)* and *lon-2(e678)*, very close to *dpy-23* (Figure 2A). *dpy-23(e840)* is a roughly 100kb deletion with left and right breakpoints in the cosmids C15H3 and F02E8, respectively (Gian Garriga, personal communication). We started sequentially injecting the sequenced cosmids from F02E8 to the right. *spr-3* was completely rescued by the cosmid F46H6 but not by the partially overlapping cosmid C07A12 (Figure 2B). We then injected a series of purified restriction fragments, sub-clones and PCR products from F46H6 (Figure 2B). All injected products containing the entirety of the predicted gene C07A12.5 gave complete rescue of *spr-3* (Figure 2B, Table 1 and data not shown). The minimal rescuing fragment was narrowed down to 4.1kb containing C07A12.5 as the only predicted open reading frame.

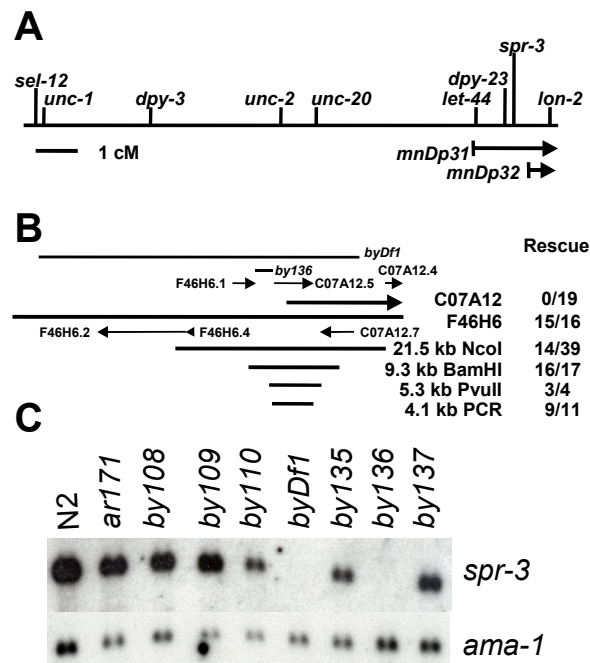


Figure 2: The positional cloning of *spr-3*. **A)** By three factor mapping *spr-3* was mapped to the interval between *dpy-23*(*e840*) and *lon-2*, outside of the duplication *mnDp32* (see supplemental data) Note that *spr-3* was previously mapped between *dpy-3* and *unc-2*, close to *unc-2* (Wen et al., 2000). **B)** Rescue of *spr-3*. *spr-3* was rescued by the cosmid F46H6 but not the partially overlapping cosmid C07A12, both shown in thick bars. The cosmid C07A12 extends further to the right. ORFs on F46H6 are named and indicated by lines with arrows. Two *spr-3* alleles generated by UV/TMP mutagenesis are large rearrangements. *byDf1* deletes 31kb of the cosmid F46H6, while *by136* is a complex rearrangement that affects the promoter of C07A12.5. By injecting a series of restriction fragments, subclones and PCR products (see thick bars below F46H6) the minimal rescuing region was narrowed down to a 4.1 kb fragment (using RB950 CAGTATACAACACTACGCTCTCC and RB951 ATCCAACACTCCTAAGTCCG), which only contains the C07A12.5 open reading frame. The number of lines that rescued is indicated on the right for each construct. **C)** Northern blot with RNA from N2, *sel-12*(*ar171*) and 7 *spr-3* alleles in a *sel-12*(*ar171*) background probed with a *spr-3* cDNA. No message is detectable in strains harboring either of the two large rearrangements, *byDf1* and *spr-3*(*by136*).

spr-3 encodes a novel, basic protein (predicted pI=9.1) of 684 amino acids. The only recognizable domains in SPR-3 are seven putative C₂H₂ zinc finger and several regions that may act as nuclear localization signals (Figure 3A, B). The *spr-3* alleles *ar209*, *by108*, *by110*, and *by137* mutations are all amino acid to stop codon mutations at various positions in the protein (Figure 3B). The *by135* mutation is a single base pair deletion, which shifts frame after amino acid 183 and truncates the protein at 210 amino acids. The *by109* mutation is a C596Y transition in the second cysteine of the sixth zinc finger, indicating that this finger is essential for SPR-3 function. *by131* is a deletion of 31 069 bases from position 3052 of F46H6 to position 6698 of C07A12 with a single A base pair insertion. This mutation deletes F46H6.2/*dgk-2*, F46H6.4, F46H6.1/*rhi-1*, C07A12.5/*spr-3*, and part of C07A12.7 and is clearly null for *spr-3* function (Figure 2B). Since *by131* deletes several genes we have renamed it *byDfl*. By a combination of PCR, Southern blotting and sequencing, we determined that there are no alterations in the coding sequence of *by136*. However, *by136* has a complex promoter rearrangement in C07A12.5 (data not shown). By Northern analysis a single transcript is detectable in *by108*, *by109*, *by110*, *by135* and *by137* lanes at nearly wild type levels while no transcript is detectable for *byDfl* and *by136* (Figure 2C) indicating that *by136* is also null for *spr-3* function.

SPR-3 is broadly expressed and nucleary localized. The *spr-3* transcript is expressed in all stages but at different levels. The message is present in high amounts in eggs, L2, and adult stages, but more weakly expressed in the L1, L3 and L4 stages (Figure 4A). To determine the expression pattern of *spr-3*, we made a promoter fusion to EGFP. This construct is very broadly expressed in the embryo, larval stages and in the adult (Figure 4B, C). When expressed in Sf9 insect cells using a Baculovirus expression system, SPR-3 is localized in the nucleus (Figure 4D, E). Attempts to purify SPR-3 from insect cells failed. SPR-3 remained in the nuclear fraction even after DNase treatment and high salt extraction (data not shown). It is therefore likely that SPR-3 is present in a nuclear sub-compartment or attached to the nuclear periphery.

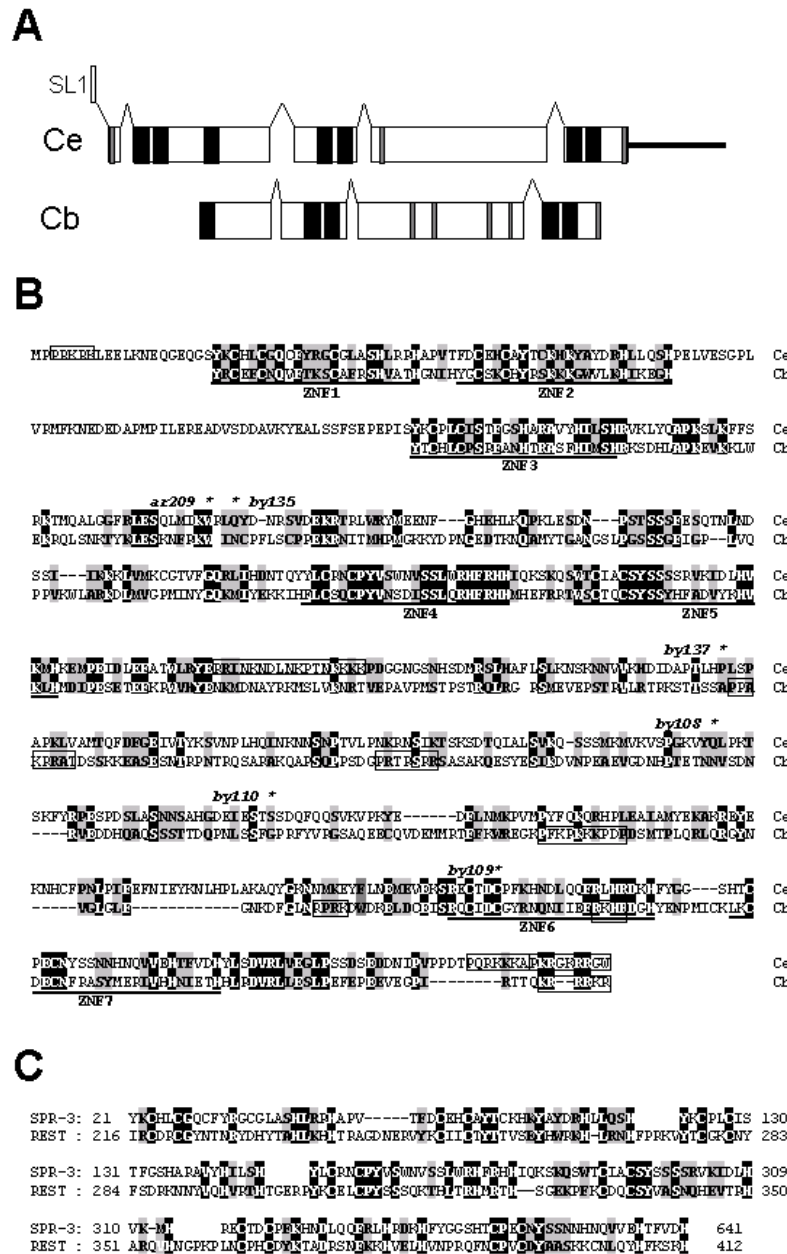


Figure 3: The structure of SPR-3 from *C. elegans* and *C. briggsae*. **A)** The determined structure of *C. elegans* SPR-3 and the 3' end of the *C. briggsae* homologue. In black boxes are indicated the location of the predicted C₂H₂ zinc fingers and in grey are the locations of sequences that might act as nuclear localization signals. In the region confirmed, the structure of the *C. elegans* and *C. briggsae* transcripts are very similar. **B)** An alignment of the *C. elegans* and partial *C. briggsae* sequences of SPR-3. Also shown is a region 5' of the determined sequence of the *C. briggsae* SPR-3 that is similar to the zinc fingers 1 and 2 of the *C. elegans spr-3* gene and is predicted to be part of the *C. briggsae spr-3* gene. Identical amino acids are highlighted in black and similar amino acids are indicated in grey. Predicted zinc fingers are underlined and regions containing sequences that could act as nuclear localization signals are boxed. The positions of point mutations are shown with an asterisk. **C)** Alignment of the zinc fingers regions of SPR-3 with REST (*Homo sapiens*). Identical amino acids are highlighted in black and similar in grey. Gaps in the alignment are indicated by hyphens and gaps between segments of SPR-3 are indicated by blank spaces.

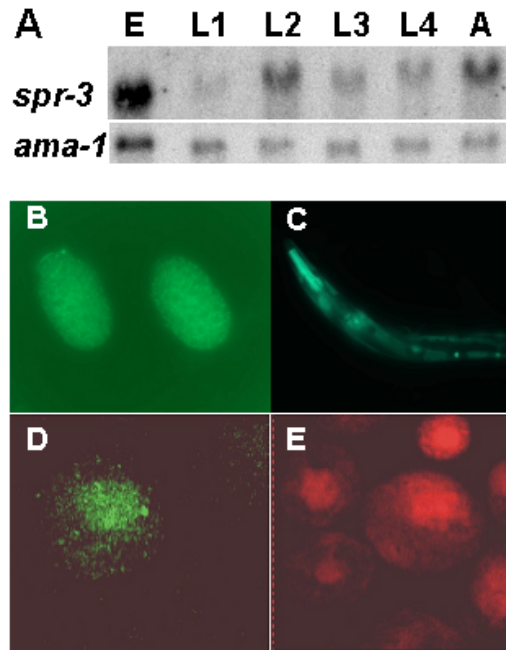


Figure 4: The expression pattern of *spr-3*. **A)** The stage specific expression of the *spr-3* transcript with *ama-1* shown as a control; E=eggs, L1-L4= first –fourth larval stages, A=adult. **B,C)** An *spr-3*::EGFP promoter fusion is expressed broadly throughout the animal. *spr-3* is expressed uniformly in eggs (B) and very broadly in the adult (C) with strong expression in the pharynx. **D, E)** Expression of a GST-myc tagged *spr-3* Baculovirus construct expressed in insect Sf9 cells and detected with a fluoresceine-isothiocyanate coupled goat-anti-mouse secondary antibody. **D)** Fluorescence and **E)** propidium iodide staining of the same cells.

The *spr-3* gene has evolved rapidly. We were unable to identify any clear homologues of SPR-3 in the sequence databases. To understand better what regions of the protein could be important for its function, we tried to identify homologues in *Caenorhabditis briggsae*, *C. elegans*' closest known relative (Blaxter et al., 1998). By RT-PCR, we have isolated a large fragment of this transcript and determined that it has a similar exon/intron structure to *spr-3* in *C. elegans* (see Figure 3 A,B). However, the *C. briggsae* gene is only 22% identical and 45% similar to *C. elegans spr-3* (see Figure 3B), with most of the similarity confined to the zinc finger regions. The predicted 5' end of the *C. briggsae spr-3* gene is significantly diverged from the *C. elegans spr-3*. However, in the predicted 5' region of *C. briggsae* SPR-3, there is a region similar to zinc fingers 1 and 2 of *C. elegans* SPR-3 (Figure 3B).

SPR-3 is similar to transcriptional repressors. The fact that SPR-3 is only weakly conserved in *C. briggsae*, with similarity largely confined to the zinc finger domains, suggests that the regions between the zinc fingers are under little selective pressure and that the zinc fingers and nuclear localization signals may be the only functional domains of the protein. If this were the case, then we would expect that most mutations that result in amino acid substitutions would have no phenotypic consequences. Consistent with this, only one of eight

spr-3 alleles is a missense mutation, and this mutation affects a conserved cysteine of one of the zinc fingers. SPR-3 contains three pairs of adjacent zinc fingers and one lone zinc finger separated by non-conserved linkers. Therefore, to analyze the zinc finger regions of the protein, we concatenated the sequences of just the zinc fingers, along with the short linkers between tandem fingers, and searched the databases for similarity. This sequence is similar to many C₂H₂ zinc finger proteins and is most similar to members of the REST family of transcriptional repressors (Figure 3C). This suggests that SPR-3 may also function as a transcriptional repressor.

SPR-4 belongs to a family of C₂H₂ proteins related to transcriptional repressors. *spr-4* was mapped between *unc-55* and *daf-8* on LGI; close to, but to the right of, the single nucleotide polymorphism (SNP) v120a11.s1@186 on cosmid F18C12 (Figure 5A, B). Near this point is the gene C09H6.1, the gene with the greatest similarity in *C. elegans* to C07A12.5 (Figure 5B). By probing *spr-4* alleles on a Southern blot with yk18b7, a C09H6.1 cDNA, we could identify clear polymorphisms in two UV/TMP generated *spr-4* alleles, *by130* and *by132* (data not shown). Injection of either of two cosmids that overlap C09H6, F34G10 and C48B11, gave partial rescue of *spr-4* (data not shown). Both of these cosmids contain a 12kb *PvuII* fragment which contains the entire coding region of C09H6.1, 2 kb of 3' sequence as well as 4.5 kb of 5' sequence extending almost to the next gene upstream (Figure 5B). We subcloned the *PvuII* fragment from F34G10 into pBSIISK- cut with *PvuII* and found that this rescues *spr-4* as well as the original cosmids (data not shown).

spr-4 codes for a large protein with 1309 amino acids (Figure 5C) containing 18 C₂H₂ zinc finger domains. One of the zinc fingers, labeled ZNF7, is below threshold by Pfam (<http://www.cgr.ki.se/Pfam/>) but this region is highly conserved in *C. briggsae* (data not shown) indicating that it may represent a functional domain. A possible splice variant has also been suggested based on the sequence of the yk1178d11 cDNA (see Materials and Methods). SPR-4 is also predicted to be nuclearly localized and contains several nuclear localization signals (NLS), including a bipartite NLS. We have identified the mutations in three *spr-4* alleles (Figure 5C). *by130* contains a 64bp deletion and 8bp insertion at position 1165 of the message. This deletion shifts frame at amino acid 389 and truncates the predicted protein at position 404 (Figure 5C). The *by112* allele is a Q97stop mutation (Figure 5C). By Southern analysis, *by132* contains a ~500 bp deletion near the 3' end of the gene (data not shown).

SPR-4 has clear homologues in *C. briggsae* (data not shown), and in the more distantly related nematodes *Pristionchus pacificus* (AI989188) and *Parastrongyloides tricosuri*

(BM513702) (Jim McCarter, personal communication). SPR-4 also has strong similarity ($e=3 \times 10^{-43}$) to C28G1.4 in *C. elegans* (NM 077098.1). Twenty-one of the first 34 amino acids are identical between SPR-4 and C28G1.4. This region is followed in both proteins by a highly acidic stretch suggesting that this region forms a functional domain (Figure 5C). The central portion of C28G1.4 does not resemble any other protein but C28G1.4 is 34% identical to SPR-4 in the N-terminal section from ZNF13 to the end of the protein and contains all zinc fingers in this region except ZNF15, suggesting that SPR-4 and C28G1.4 may have a related function (Figure 5C). However, RNA interference by feeding (Kamath et al., 2001) of C28G1.4 has no obvious effects on the wild type strain N2 nor does it influence the Egl defect of *sel-12(ar171)* and *sel-12(ar131)* (data not shown). dsRNAi against C28G1.4 also does not produce any synthetic effect in either a *spr-4(by105); sel-12(ar171)* or a *spr-4(by105)* background (data not shown). These results may suggest that an RNAi effect was not induced by the bacterial feeding approach, however, RNAi by injection of purified double stranded RNA from yk356a2, a C28G1.4 cDNA, also induced no phenotype (Maeda et al., 2001). Interestingly, there is no C28G1.4 homologue present in the draft *C. briggsae* assembly, suggesting that C28G1.4 may have recently diverged from an ancestral *spr-4* like gene or that this gene is under very low selective pressure or can be lost without phenotypic effects.

SPR-4 also has similarity to a large number of zinc finger proteins from other metazoans. SPR-4 is most similar to members of the REST family of transcriptional repressors (Figure 5D) but it also has weaker similarity to other known transcriptional repressors, such as members of the CTCF/CCCTC binding factor, suggesting that SPR-4, like SPR-3, may also function as a transcriptional repressor.

***hop-1* transcription is regulated by *spr-3* and *spr-4*.** Since both SPR-3 and SPR-4 encode C₂H₂ zinc finger proteins that are probably nuclearly localized and might act as transcription factors, we looked for possible targets regulated by *spr-3* and *spr-4*. Therefore, we probed Northern blots prepared with mixed stage, or staged RNA, from *spr-3* and *spr-4* mutants with several genes involved in *lin-12* or *glp-1* signaling. No significant differences in transcript levels were seen between any of the strains when we probed with *lin-12*, *glp-1*, *lag-1*, *apx-1* or *sup-17* (data not shown). Although we did not probe exhaustively, this suggested that *spr-3* and *spr-4* might not have obvious effects on the transcription of genes involved in the *lin-12* and *glp-1* pathways.

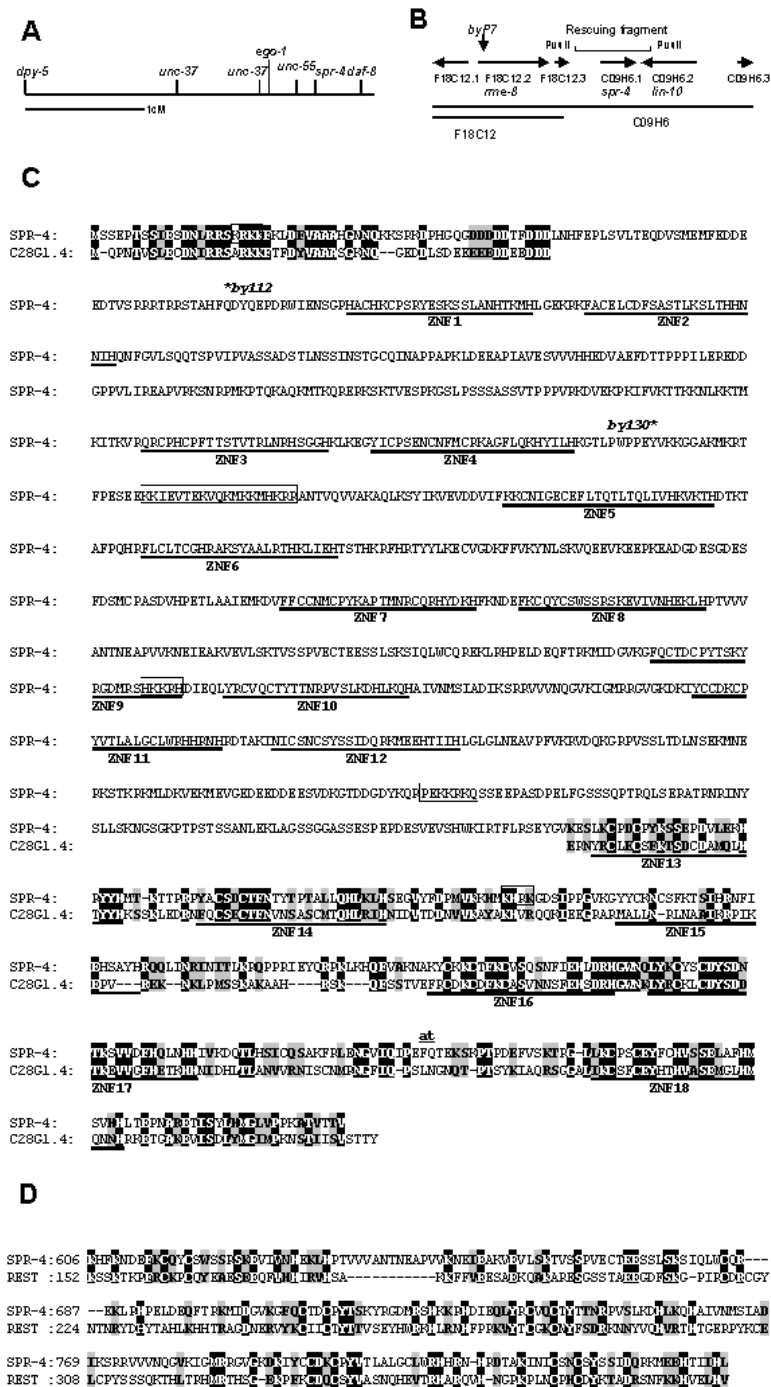


Figure 5: The cloning of *spr-4*. **A)** The genetic position of *spr-4* (also see supplemental data). **B)** Physical map near C09H6.1. *spr-4* was mapped close to but to the right of byP7 (SNP v120a11.s1@186). The extent of the 12kb *PvuII* rescuing fragment is shown. **C)** The predicted SPR-4 protein aligned with the 5' end of C28G1.4 and the 3' end of G28G4.4. Identical amino acids are highlighted in black while similar amino acids are highlighted in grey. The 18 putative C2H2 zinc fingers of SPR-4 are underlined and regions that could act as nuclear localization signals are boxed. The two amino acids present only in the alternatively spliced form of SPR-4 are overlined and labeled AT. Mutations are indicated with an asterisk. **D)** Alignment of SPR-4 with REST (*Homo sapiens*). Highlighting is as for part C.

We then investigated whether *spr-3* and *spr-4* might bypass the need for *sel-12* by up-regulating one of the other presenilin genes, *spe-4* or *hop-1*. Results from mixed stage blots suggested that *hop-1* and *spe-4* may be differentially expressed (data not shown). Therefore, we then probed staged Northern blots. Transcript levels of the three *C. elegans* presenilin genes in the various developmental stages have not been reported previously. We find, consistent with its only known role in spermatogenesis, that *spe-4* is only expressed in the L4 larval stage when hermaphrodites produce sperm (Figure 6 A,C).

sel-12 is expressed strongly and uniformly throughout development (Figure 6B and 6C), consistent with the strong and ubiquitous expression of a *sel-12::EGFP* promoter fusion (Baumeister et al., 1997). Surprisingly, *hop-1* has a very dynamic expression. It is most strongly expressed in the adult stage, more weakly in the embryo and is almost undetectable in the L1 stage (Figure 6A,C). *hop-1* expression slowly increases through the remaining larval stages.

In *spr-3* and *spr-4* mutants, we found no differences in the temporal pattern of expression of *sel-12* or *spe-4*, but we did see an increase in *hop-1* expression in the L1, L2 and L3 larval stages, those stages, in which *hop-1* expression is lowest (data not shown). Since the egg-laying defect in *sel-12* animals is due to developmental defects occurring in the mid-larval stages, the suppression of *sel-12* by *spr* genes could be explained by stage specific alterations in gene expression. To confirm this result, and to directly compare different strains, we prepared a Northern blot with L1 RNA from N2, *sel-12(ar171)* and several *spr* strains and probed it with *hop-1*.

Since the expression of *hop-1* is lowest in the L1 stage, we reasoned that increased expression in this stage might be easiest to detect. We increased the amount of total RNA used from 5µg/lane to 20µg/lane because the expression of *hop-1* in wild type worms is near the detection level. We tested L1 RNA prepared from N2, *sel-12(ar171)*, four *spr-5* alleles, one *spr-4* allele and three *spr-3* alleles (Figure 7). In all *spr* strains tested, *hop-1* is upregulated. This suggests that all *spr* genes may use the same mechanism to bypass the requirement for *sel-12*. *spr-4* up-regulates *hop-1* expression 11 fold while *spr-3* alleles upregulate *hop-1* between four and 12 fold (Figure 7). These data were confirmed by a separate experiment, for which we looked at *hop-1* expression in the L1 stage in all seven *spr-3* alleles isolated in our screens. In all *spr-3* alleles *hop-1* was more strongly expressed than the controls (see supplemental information).

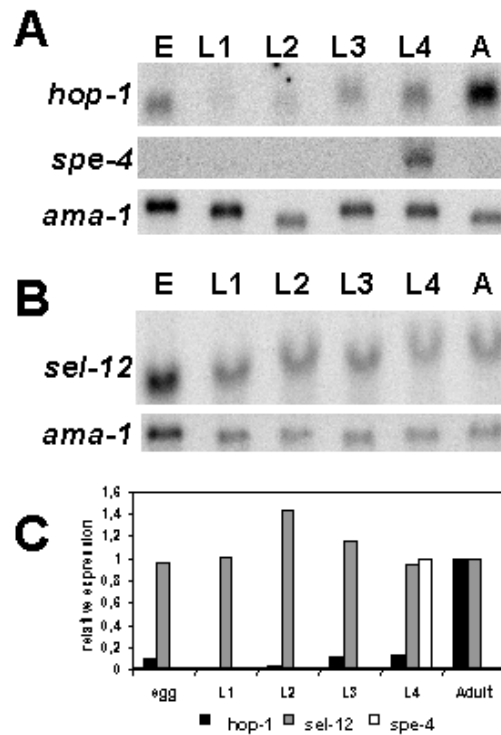


Figure 6: The stage specific expression of *sel-12*, *spe-4* and *hop-1* transcripts. Stages are as for Figure 4A. **A)** The stage specific expression of *hop-1* and *spe-4* from the same blot, with *ama-1* as an equal loading control. **B)** The stage specific expression of *spr-3* and *sel-12* from probing the same blot with *ama-1* expression as a loading control. **C)** The relative expression of the various presenilin genes from parts A and B above, after correction for equal loading.

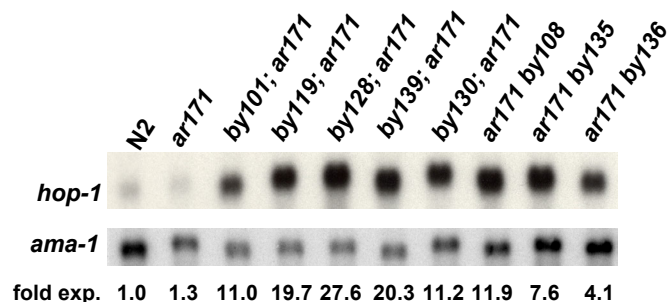


Figure 7: Mutations in *spr-3* and *spr-4* de-repress the expression of the *hop-1* message in the L1 stage. Expression of the *hop-1* message with *ama-1* loading control in the L1 stage for N2 (wild type), *sel-12(ar171)*, four *spr-5* alleles (*by101*, *by119*, *by128*, *by139*), one *spr-4* allele (*by130*) and three *spr-3* alleles (*by108*, *by135*, *by136*). All *spr* mutants are in a *sel-12(ar171)* background. Below the bands are listed the fold expression of *hop-1* compared to N2, after correction for equal loading. The first six lanes have also been published as Figure 6 in (Eimer et al., 2002b). Preliminary experiments with 5µg/lane RNA gave qualitatively similar results. Also see a supplemental figure for additional *spr-3* alleles (see supplemental information).

***spr-3* and *spr-4* do not suppress the synthetic lethality of *hop-1*; *sel-12* double mutants.** If the *spr* genes bypass the need for *sel-12* by upregulating the expression of *hop-1*, then *spr-3* and *spr-4* mutations should not suppress the synthetic lethal phenotype induced by reducing both *hop-1* and *sel-12* activity. This is exactly what we find. RNAi by feeding of the *hop-1* gene in a *sel-12(ar171) spr-3(by108)* strain or a *spr-4(by105); sel-12(ar171)* strain induces the same range of phenotypes as seen when one induces RNAi of *hop-1* in *sel-12(ar171)* [Table 2, (Li and Greenwald, 1997)]. Most animals display a lethal phenotype (Emb, Lag, Ste) consistent with a strong reduction of *lin-12* and/or *glp-1* signaling, but those few animals that do produce progeny are Egl. This indicates that *spr-3* and *spr-4* mutations do not bypass the need for presenilins *per se*, but only for *sel-12* and that this effect is dependent on the activity of *hop-1*. We confirmed this result by constructing *hop-1; sel-12 spr-3* triple mutant strains (Table 3). Similar experiments with *spr-4* have not been done due to the genetic proximity of *spr-4* and *hop-1*.

We find that *spr-3* does not affect the phenotype of *hop-1; sel-12* double mutants as has also been shown for *spr-1*, *spr-2* and *spr-5* (Eimer et al., 2002b; Jarriault and Greenwald, 2002; Wen et al., 2000). Furthermore, 43% of all *hop-1(lg1501)/dpy-5(e61) I; sel-12(ar171) spr-3(by108)* animals with only one remaining copy of *hop-1* and no functional *sel-12* gene display an Egl phenotype (Table 3). As *sel-12(ar171) spr-3(by108)* animals are never Egl (see Figure 1) this indicates that in a *sel-12 spr-3* background *hop-1* is haploinsufficient. In *sel-12 spr-3* mutants, presenilin activity is very near the threshold necessary for correct egg-laying and reducing *hop-1* activity by half brings the worms below this threshold. Taken together, all of these results are consistent with *spr-3* and *spr-4* suppressing *sel-12* by up-regulating *hop-1*.

Table 2: *hop-1* activity is required for *spr-3* and *spr-4* mediated suppression of the *sel-12* egg-laying defect.

Genotype	Phenotype	<i>hop-1</i> RNAi	n [‡]
	without RNAi*	phenotypes [†]	
N2	WT	WT	(30/30)
<i>sel-12(ar171)</i>	Egl	Egl; Ste; Emb; Lag	(30/30)
<i>sel-12(ar171) spr-3(by108)</i>	WT	Egl; Ste; Emb; Lag	(48/50) [§]
<i>sel-12(ar171); spr-4(by105)</i>	WT [¶]	Egl; Ste; Emb; Lag	(50/50)

* RNAi with the empty vector resulted in the same phenotypes as seen without RNAi.

[†] Phenotypes obtained by RNA interference against *hop-1* through bacterial feeding of dsRNA of *hop-1*. Phenotypes as described in Li and Greenwald (1997): Egl egg-laying defective; Ste sterile; Emb embryonic lethal; Lag *lin-12* and *glp-1*.

[‡] The number in brackets corresponds to the number of parental L4 worms who's progeny show the annotated phenotypes.

[§] Two lines showed a Gro phenotype and did not develop.

[¶] Approximately 5% of the animals showed an Egl phenotype (see Figure 1).

Table 3: *hop-1* is haploinsufficient in a *sel-12 spr-3* background.

Progeny of <i>hop-1(lg1501)/dpy-5(e61) I; sel-12(ar171) spr-3(by108)</i> hermaphrodites			
Phenotype*	Genotype [†]	Number ^{‡‡}	Percent
Dpy	<i>dpy-5; sel-12 spr-3</i>	50/197	25.4
Pvl Ste	<i>hop-1; sel-12 spr-3</i>	56/197	28.4
WT	<i>dpy-5/hop-1; sel-12 spr-3</i>	51/197	25.9
Egl [§]	<i>dpy-5/hop-1; sel-12 spr-3</i>	38/197	19.3

* Phenotypes are: Dpy=Dumpy, Pvl= protruding vulva, Ste= sterile; WT= wild type, and Egl= egg-laying defective. The Pvl Ste animals had a phenotype very similar to *hop-1; sel-12* double mutants and strong *lin-12* loss-of-function mutants.

[†] All worms are the progeny of *hop-1(lg1501)/dpy-5(e61) I; sel-12(ar171) spr-3(by108)* hermaphrodites. The genotypes were inferred from the phenotypes. We verified for several animals that the Egl animals had the genotype noted. In a separate cross, 20/20 Egl progeny of a *+/hop-1(lg1501); sel-12(ar171) spr-3(by108)* strain were heterozygous for *hop-1*.

[‡] The broods of three Egl animals were scored.

[§] Forty three percent of all animals heterozygous for *hop-1* displayed an Egl phenotype.

Discussion

The difference in expression patterns may explain the phenotypes of *sel-12* and *hop-1*.

Although *sel-12* and *hop-1* have very similar biochemical functions and are interchangeable in transgenic experiments, mutations in *sel-12* and *hop-1* result in different phenotypes. This suggests that although these genes may encode functionally equivalent proteins, the genes are not redundant. The different phenotypes may be explained by their different expression patterns. *sel-12* is strongly and uniformly expressed while *hop-1* expression is dynamic and very low throughout most of the larval stages. Thus, in the absence of *hop-1* expression, there is still enough of (*sel-12*) presenilin activity at all times of development and consequently, *hop-1* mutants have only a very mild phenotype. However, in the absence of *sel-12* expression, there are probably insufficient copies of the *hop-1* transcript in the early larval stages to completely compensate for the loss of *sel-12* expression. Therefore, *sel-12* mutants only display post-embryonic defects.

All *spr* genes may function through the same mechanism. Here we provide evidence that the mechanism by which mutants of *spr-3* and *spr-4* suppress *sel-12* loss-of-function alleles involves de-repression of *hop-1* transcription in those stages in which *hop-1* expression alone does not suffice. Similarly, we have shown recently that SPR-1 and SPR-5 proteins interact, and that *spr-5* up-regulates *hop-1* expression at the same developmental stages as mutations in *spr-3* and *spr-4* (Eimer et al., 2002b). This suggests that *spr-1*, *spr-3*, *spr-4* and *spr-5* all suppress *sel-12* by up-regulating *hop-1*, replacing one presenilin by another. Similarly, mutations in *spr-2* genetically bypass the need for *sel-12*, but do not bypass the need for both *sel-12* and *hop-1* (Wen et al., 2000). Although *hop-1* activity is required for the suppression mechanism, Wen *et al.* did not find evidence for *hop-1* transcriptional de-repression (Wen et al., 2000). However, the stage specific de-repression of *hop-1* transcription we have seen would not be detectable on a mixed stage Northern blot. Thus, we propose that *spr-2* may also bypass the need for *sel-12* by the same mechanism as *spr-3*, *spr-4* and *spr-5*.

Up-regulation of *hop-1* transcription in the early larval stages can explain the suppression of *sel-12* by *spr-3* and *spr-4*. Mutations in *spr-3* and *spr-4* clearly de-repress the transcription of *hop-1* in the early larval stages. However, even in the suppressor strains, the

absolute *hop-1* transcript levels in the early larval stages are still much lower than in the adult stage. We believe that the stage-specific increase in *hop-1* expression is sufficient to explain why *spr-3* and *spr-4* suppress *sel-12*. Even in a strong, putative null *sel-12* mutant, there is sufficient *hop-1* protein in the larval stages to enable most *lin-12*-dependent developmental decisions to occur correctly. In *sel-12* mutants the ventral uterine /anchor cell decision, lateral inhibition in the vulval precursors and the sex myoblast/coelomocyte decision are not affected (Levitan and Greenwald, 1995), indicating that there is sufficient presenilin activity, provided by HOP-1, present in many cell types. In *sel-12(ar131)* even the π cell fate is executed correctly in the vast majority of animals and in *sel-12(ar171)* it is executed correctly in some animals, while in a *sel-12 hop-1* double mutants 100% of animals have a defective vulval uterine connection (Cinar et al., 2001; Eimer et al., 2002a). This indicates that in *sel-12* mutants the expression of *hop-1* is almost sufficient for wild-type π cell induction. Therefore, it is likely that small increases in *hop-1* expression could be sufficient to completely compensate for the loss of *sel-12* in all developmental decisions.

There are also reasons to believe that small amounts of presenilin message may be sufficient to provide adequate levels of presenilin activity. Presenilins are normally found as part of a high molecular weight complex (Capell et al., 1998; Li et al., 2000; Thinakaran et al., 1998; Yu et al., 1998). This complex is assembled in the ER and Golgi, and proteins that are not incorporated into this complex are not targeted to the cell membrane and are rapidly degraded (Ratovitski et al., 1997). Presenilins may be required in small amounts because the amount of other components of the complex are limiting for assembly (Edbauer et al., 2002). Consequently, it has been found that, in cell culture, presenilins cannot be over-produced (Thinakaran et al., 1996). Furthermore, as the presenilin complex is thought to have enzymatic activity, the levels of the complex necessary for its biochemical function may normally be in vast excess of what is required. Thus, even if the amount of the complex present at the cell membrane in *spr; sel-12* double mutants should be slightly lower than the wild type levels, the wild type phenotype of the double mutants indicates that it suffices to ensure sufficient levels of *lin-12* signaling.

Is the increased expression of *hop-1* in the early larval stages seen in *spr-3* and *spr-4* mutants sufficient to rescue the later larval defects seen in *sel-12* mutants? We have several reasons to believe this is the case. Firstly, the cell signaling events that lead to the π cell induction and the correct alignment of the sex muscles, occur prior to the developmental changes (Cinar et al., 2001; Eimer et al., 2002a) and presenilin activity is presumably required at the time of signaling. Secondly, our initial experiments suggested that the relative

expression of *hop-1* is increased in the L1, L2 and L3 stages in both *spr-3* and *spr-4* mutants. We chose to pursue this further in the L1 stage because we thought the up-regulation of *hop-1* expression might be most obvious at this stage. Furthermore, it has been demonstrated in cell culture that, once assembled, the high molecular weight presenilin complex is very stable over a long time period (Edbauer et al., 2002; Ratovitski et al., 1997). Finally, we have indications that the presenilin complex is necessary in small amounts and can persist for up to 24 hours in *C. elegans* because we see rescue of sex myoblast/coelomocyte cell fate decision in *hop-1;sel-12* double mutants with maternally provided *hop-1* (Eimer et al., 2002a). Thus, presenilin protein produced in the embryo is sufficiently stable and produced in sufficient amounts for a cell fate decision occurring in the L2 stage.

Do *spr-3* and *spr-4* perform a conserved function? Although SPR-3 and SPR-4 do not have clear mammalian homologues, they may be performing a similar function to known transcriptional repressors. Both SPR-3 and SPR-4 resemble known transcriptional repressors, especially REST/NRSF (Re1 silencing transcription factor/neural–restrictive silencing factor) in different vertebrates. The C₂H₂ zinc finger factor REST mediates repression of neuronal genes in non-neuronal cells, by recruiting the co-repressor complexes Sin3 and CoREST (Humphrey et al., 2001). Both of these co-repressor complexes contain multiple proteins including histone deacetylases, and presumably repress transcription in part by removing activating acetyl groups from histones H3 and H4 at the target locus. It is possible that SPR-3 and SPR-4 may also function by recruiting conserved co-repressor complexes to the *hop-1* locus. Three other *spr* genes, *spr-1*, *spr-2* and *spr-5*, encode proteins similar to components of known co-repressor *sel-12* (Eimer et al., 2002b; Jarriault and Greenwald, 2002; Wen et al., 2000). SPR-2 is a member of the Nucleosome Assembly Protein (NAP) family and is most similar to the human oncogene SET (Wen et al., 2000). Human SET was purified as part of the INHAT (*inhibitor of acetyltransferases*) co-repressor complex, which helps to repress transcription by binding to histones and masking them from being acetyltransferase substrates for p300/CBP and PCAF (Seo et al., 2001). Recently it has been shown that up-regulation of SET also inhibits demethylation of methylated DNA and may integrate the epigenetic states of DNA and associated histones (Cervoni et al., 2002). In another paper, we have reported the identification and characterization of SPR-5 that encodes a polyamine oxidase-like protein most similar to a known component of the CoREST co-repressor complex (Eimer et al., 2002b). The core CoREST complex contains only six proteins (Hakimi et al., 2002). *spr-1* encodes a homologue of the MYB domain containing protein CoREST (Eimer et al., 2002b;

Jarriault and Greenwald, 2002), an additional component of the CoREST co-repressor complex. We have shown that SPR-1 and SPR-5 interact biochemically *in vitro* and *in vivo* (Eimer et al., 2002b). This suggests that a similar complex is present in *C. elegans* and functions to repress *hop-1* transcription. Interestingly, CoREST has been found to associate with at least two large, basic C₂H₂ zinc finger protein, ZNF217 and REST (You et al., 2001) and may be a general co-repressor complex that is recruited to different loci in different cell types by binding to a different C₂H₂ zinc finger proteins. Recent work also suggests that CoREST may interact with components of the SWI-SNF complex (Battaglioli et al., 2002) and may be involved in silencing of chromosomal regions (Lunyak et al., 2002).

The proteins encoded by the *spr* genes may form one or more transcriptional repressor complexes. Thus, SPR-3 and SPR-4 may recruit one or more conserved co-repressor complexes, including one similar to the CoREST co-repressor complex, to target loci. We propose the following model for how the *spr* genes are functioning. The fact that loss of function mutations in either *spr-3* or *spr-4* suppress *sel-12* and de-repress *hop-1* transcription, suggest that both SPR-3 and SPR-4 are normally recruited to the *hop-1* locus. There they associate with co-repressor proteins similar to members of the INHAT and CoREST corepressor complexes. It is unclear if the two zinc finger proteins co-operatively bind the co-repressor proteins, or if each zinc finger protein associates with a different complex. The assembled complex (or complexes), probably acts as a basal repressor of *hop-1* transcription that is overridden in later developmental stages.

The mammalian INHAT and CoREST complexes were purified and studied by biochemical approaches. However, as yet little is known about their biological function. The data now available on *spr* gene function suggest that INHAT and CoREST complexes can be studied both genetically and biochemically in *C. elegans*. We suggest that through *C. elegans* genetics we may identify additional genes that interact with these complexes and we may help to elucidate their biological function.

Acknowledgements

We thank Gian Garriga, Sophie Jarriault, Iva Greenwald, Jim McCarter, the Sanger Institute and the Genome Sequencing Center, Washington University, St Louis, for communicating unpublished information, Jean-Claude Labbé for advice on RNA isolation and Northern analysis, Jonathan Hodgkin and Iva Greenwald for strains, Yuji Kohara for cDNA clones, Bob Barstead for a cDNA library, and Alan Coulson for cosmid clones. Some strains used in this work were provided by the *Caenorhabditis* Genetics Center.

References

- Anderson, P.** (1995). Mutagenesis. In *Methods in Cell Biology. Caenorhabditis elegans: Modern Biological Analysis of an Organism.*, vol. 48 (ed. H. F. E. a. D. C. Shakes), pp. 31-58. San Diego: Academic Press, Inc.
- Arduengo, P. M., Appleberry, O. K., Chuang, P. and L'Hernault, S. W.** (1998). The presenilin protein family member SPE-4 localizes to an ER/Golgi derived organelle and is required for proper cytoplasmic partitioning during *Caenorhabditis elegans* spermatogenesis. *J Cell Sci* **111**, 3645-54.
- Battaglioli, E., Andres, M. E., Rose, D. W., Chenoweth, J. G., Rosenfeld, M. G., Anderson, M. E. and Mandel, G.** (2002). REST repression of neuronal genes requires components of the hSWI.SNF complex. *J Biol Chem* **277**, 41038-45.
- Baumeister, R., Leimer, U., Zweckbronner, I., Jakubek, C., Grunberg, J. and Haass, C.** (1997). Human presenilin-1, but not familial Alzheimer's disease (FAD) mutants, facilitate *Caenorhabditis elegans* Notch signalling independently of proteolytic processing. *Genes Funct* **1**, 149-59.
- Blaxter, M. L., De Ley, P., Garey, J. R., Liu, L. X., Scheldeman, P., Vierstraete, A., Vanfleteren, J. R., Mackey, L. Y., Dorris, M., Frisse, L. M. et al.** (1998). A molecular evolutionary framework for the phylum Nematoda. *Nature* **392**, 71-5.
- Capell, A., Grunberg, J., Pesold, B., Diehlmann, A., Citron, M., Nixon, R., Beyreuther, K., Selkoe, D. J. and Haass, C.** (1998). The Proteolytic Fragments of the Alzheimer's Disease-associated Presenilin-1 Form Heterodimers and Occur as a 100-150-kDa Molecular Mass Complex. *J. Biol. Chem.* **273**, 3205-3211.
- Cervoni, N., Detich, N., Seo, S.-b., Chakravarti, D. and Szyf, M.** (2002). The oncoprotein Set/TAF-1 {beta}, an inhibitor of histone acetyltransferase, inhibits active demethylation of DNA, integrating DNA methylation and transcriptional silencing. *J. Biol. Chem.*, M202256200.
- Church, G. M. and Gilbert, W.** (1984). Genomic sequencing. *Proc Natl Acad Sci U S A* **81**, 1991-5.
- Cinar, H. N., Sweet, K. L., Hosemann, K. E., Earley, K. and Newman, A. P.** (2001). The SEL-12 Presenilin Mediates Induction of the *Caenorhabditis elegans* Uterine pi Cell Fate. *Dev Biol* **237**, 173-82.
- De Strooper, B., Annaert, W., Cupers, P., Saftig, P., Craessaerts, K., Mumm, J. S., Schroeter, E. H., Schrijvers, V., Wolfe, M. S., Ray, W. J. et al.** (1999). A presenilin-1-dependent gamma-secretase-like protease mediates release of Notch intracellular domain. *Nature* **398**, 518-22.
- De Strooper, B., Saftig, P., Craessaerts, K., Vanderstichele, H., Guhde, G., Annaert, W., Von Figura, K. and Van Leuven, F.** (1998). Deficiency of presenilin-1 inhibits the normal cleavage of amyloid precursor protein. *Nature* **391**, 387-90.
- Doyle, T. G., Wen, C. and Greenwald, I.** (2000). SEL-8, a nuclear protein required for LIN-12 and GLP-1 signaling in *Caenorhabditis elegans*. *Proc Natl Acad Sci U S A* **97**, 7877-81.
- Edbauer, D., Winkler, E., Haass, C. and Steiner, H.** (2002). Presenilin and nicastrin regulate each other and determine amyloid beta -peptide production via complex formation. *PNAS* **99**, 8666-8671.
- Eimer, S., Donhauser, R. and Baumeister, R.** (2002a). The *Caenorhabditis elegans* presenilin *sel-12* is required for mesodermal patterning and muscle function. *Dev Biol* **251**, 178-92.
- Eimer, S., Lakowski, B., Donhauser, R. and Baumeister, R.** (2002b). Loss of *spr-5* bypasses the requirement for the *C. elegans* presenilin *sel-12* by derepressing *hop-1*. *EMBO J.* **21**, 5787-5796.

- Fortini, M. E.** (2001). Notch and presenilin: a proteolytic mechanism emerges. *Curr Opin Cell Biol* **13**, 627-34.
- Francis, R., McGrath, G., Zhang, J., Ruddy, D. A., Sym, M., Apfeld, J., Nicoll, M., Maxwell, M., Hai, B., Ellis, M. C. et al.** (2002). *aph-1* and *pen-2* Are Required for Notch Pathway Signaling, gamma-Secretase Cleavage of betaAPP, and Presenilin Protein Accumulation. *Dev Cell* **3**, 85-97.
- Freyer, C., Lamar, E., Turbachova, I., Kintner, C. and Jones, K.** (2002). Mastermind mediates chromatin-specific transcription and turnover of the Notch enhancer complex. *Genes & Development* **16**, 1397-1411.
- Gupta-Rossi, N., Le Bail, O., Gonen, H., Brou, C., Logeat, F., Six, E., Ciechanover, A. and Israel, A.** (2001). Functional interaction between SEL-10, an F-box protein, and the nuclear form of activated Notch1 receptor. *J Biol Chem* **276**, 34371-8.
- Hakimi, M.-A., Bochar, D. A., Chenoweth, J., Lane, W. S., Mandel, G. and Shiekhattar, R.** (2002). A core-BRAF35 complex containing histone deacetylase mediates repression of neuronal-specific genes. *PNAS* **99**, 7420-7425.
- Hobert, O., Mori, I., Yamashita, Y., Honda, H., Ohshima, Y., Liu, Y. and Ruvkun, G.** (1997). Regulation of interneuron function in the *C. elegans* thermoregulatory pathway by the *ttx-3* LIM homeobox gene. *Neuron* **19**, 345-57.
- Hubbard, E. J., Wu, G., Kitajewski, J. and Greenwald, I.** (1997). *sel-10*, a negative regulator of *lin-12* activity in *Caenorhabditis elegans*, encodes a member of the CDC4 family of proteins. *Genes Dev* **11**, 3182-93.
- Humphrey, G. W., Wang, Y., Russanova, V. R., Hirai, T., Qin, J., Nakatani, Y. and Howard, B. H.** (2001). Stable histone deacetylase complexes distinguished by the presence of SANT domain proteins CoREST/kiaa0071 and Mta-L1. *J Biol Chem* **276**, 6817-24.
- Jakubowski, J. and Kornfeld, K.** (1999). A local, high-density, single-nucleotide polymorphism map used to clone *Caenorhabditis elegans cdf-1*. *Genetics* **153**, 743-52.
- Jarriault, S. and Greenwald, I.** (2002). Suppressors of the egg-laying defective phenotype of *sel-12* presenilin mutants implicate the CoREST corepressor complex in LIN-12/Notch signaling in *C. elegans*. *Genes Dev.* **16**, 2713-2728.
- Johnstone, I. L. and Barry, J. D.** (1996). Temporal reiteration of a precise gene expression pattern during nematode development. *Embo J* **15**, 3633-9.
- Kamath, R. S., Martinez-Campos, M., Zipperlen, P., Fraser, A. G. and Ahringer, J.** (2001). Effectiveness of specific RNA-mediated interference through ingested double-stranded RNA in *Caenorhabditis elegans*. *Genome Biol* **2**, RESEARCH0002.
- Levitani, D., Doyle, T. G., Brousseau, D., Lee, M. K., Thinakaran, G., Slunt, H. H., Sisodia, S. S. and Greenwald, I.** (1996). Assessment of normal and mutant human presenilin function in *Caenorhabditis elegans*. *Proc Natl Acad Sci U S A* **93**, 14940-4.
- Levitani, D. and Greenwald, I.** (1995). Facilitation of *lin-12*-mediated signalling by *sel-12*, a *Caenorhabditis elegans* S182 Alzheimer's disease gene. *Nature* **377**, 351-4.
- L'Hernault, S. W. and Arduengo, P. M.** (1992). Mutation of a putative sperm membrane protein in *Caenorhabditis elegans* prevents sperm differentiation but not its associated meiotic divisions. *J Cell Biol* **119**, 55-68.
- Li, X. and Greenwald, I.** (1997). HOP-1, a *Caenorhabditis elegans* presenilin, appears to be functionally redundant with SEL-12 presenilin and to facilitate LIN-12 and GLP-1 signaling. *Proc Natl Acad Sci U S A* **94**, 12204-9.
- Li, Y.-M., Lai, M.-T., Xu, M., Huang, Q., DiMuzio-Mower, J., Sardana, M. K., Shi, X.-P., Yin, K.-C., Shafer, J. A. and Gardell, S. J.** (2000). Presenilin 1 is linked with gamma-secretase activity in the detergent solubilized state. *PNAS* **97**, 6138-6143.
- Lunyak, V. V., Burgess, R., Prefontaine, G. G., Nelson, C., Sze, S. H., Chenoweth, J., Schwartz, P., Pevzner, P. A., Glass, C., Mandel, G. et al.** (2002). Corepressor-

- dependent silencing of chromosomal regions encoding neuronal genes. *Science* **298**, 1747-52.
- Maeda, I., Kohara, Y., Yamamoto, M. and Sugimoto, A.** (2001). Large-scale analysis of gene function in *Caenorhabditis elegans* by high-throughput RNAi. *Curr Biol* **11**, 171-6.
- Petcherski, A. G. and Kimble, J.** (2000). LAG-3 is a putative transcriptional activator in the *C. elegans* Notch pathway. *Nature* **405**, 364-8.
- Ratovitski, T., Slunt, H. H., Thinakaran, G., Price, D. L., Sisodia, S. S. and Borchelt, D. R.** (1997). Endoproteolytic Processing and Stabilization of Wild-type and Mutant Presenilin. *J. Biol. Chem.* **272**, 24536-24541.
- Sambrook, J., Fritsch, E.F., T. Maniatis.** (1989). Molecular cloning: a laboratory manual, (ed.: Cold Spring Harbor Laboratory Press, Cold Spring Harbor, N. Y.
- Selkoe, D. J.** (2001). Alzheimer's disease: genes, proteins, and therapy. *Physiol Rev* **81**, 741-66.
- Seo, S. B., McNamara, P., Heo, S., Turner, A., Lane, W. S. and Chakravarti, D.** (2001). Regulation of histone acetylation and transcription by INHAT, a human cellular complex containing the set oncoprotein. *Cell* **104**, 119-30.
- Sisodia, S. and St George-Hyslop, P.** (2002). Gamma-secretase, Notch, Abeta and Alzheimer's disease: where do the presenilins fit in? *Nature Reviews Neuroscience* **3**, 281-290.
- Song, W., Nadeau, P., Yuan, M., Yang, X., Shen, J. and Yankner, B. A.** (1999). Proteolytic release and nuclear translocation of Notch-1 are induced by presenilin-1 and impaired by pathogenic presenilin-1 mutations. *Proc Natl Acad Sci U S A* **96**, 6959-63.
- Spieth, J., Brooke, G., Kuersten, S., Lea, K. and Blumenthal, T.** (1993). Operons in *C. elegans*: polycistronic mRNA precursors are processed by trans-splicing of SL2 to downstream coding regions. *Cell* **73**, 521-32.
- Steiner, H., Kostka, M., Romig, H., Basset, G., Pesold, B., Hardy, J., Capell, A., Meyn, L., Grim, M. L., Baumeister, R. et al.** (2000). Glycine 384 is required for presenilin-1 function and is conserved in bacterial polytopic aspartyl proteases. *Nat Cell Biol* **2**, 848-51.
- Struhl, G. and Adachi, A.** (1998). Nuclear access and action of notch in vivo. *Cell* **93**, 649-60.
- Sulston, J. and Hodgkin, J.** (1988). Methods. In *The Nematode Caenorhabditis elegans.*, (ed. W. Wood), pp. 587-606. Cold Spring Harbor: Cold Spring Harbor Laboratory Press.
- Thinakaran, G., Borchelt, D. R., Lee, M. K., Slunt, H. H., Spitzer, L., Kim, G., Ratovitsky, T., Davenport, F., Nordstedt, C., Seeger, M. et al.** (1996). Endoproteolysis of presenilin 1 and accumulation of processed derivatives in vivo. *Neuron* **17**, 181-90.
- Thinakaran, G., Regard, J., Bouton, C., Harris, C., Price, D., Borchelt, D. and Sisodia, S.** (1998). Stable association of presenilin derivatives and absence of presenilin interactions with APP. *Neurobiol Dis* **4**, 438-453.
- Timmons, L., Court, D. L. and Fire, A.** (2001). Ingestion of bacterially expressed dsRNAs can produce specific and potent genetic interference in *Caenorhabditis elegans*. *Gene* **263**, 103-12.
- Timmons, L. and Fire, A.** (1998). Specific interference by ingested dsRNA. *Nature* **395**, 854.
- Wen, C., Levitan, D., Li, X. and Greenwald, I.** (2000). *spr-2*, a suppressor of the egg-laying defect caused by loss of *sel-12* presenilin in *Caenorhabditis elegans*, is a member of the SET protein subfamily. *Proc Natl Acad Sci U S A* **97**, 14524-9.
- Westlund, B., Parry, D., Clover, R., Basson, M. and Johnson, C. D.** (1999). Reverse genetic analysis of *Caenorhabditis elegans* presenilins reveals redundant but unequal roles for *sel-12* and *hop-1* in Notch-pathway signaling. *Proc Natl Acad Sci U S A* **96**, 2497-502.
- Wittenburg, N., Eimer, S., Lakowski, B., Rohrig, S., Rudolph, C. and Baumeister, R.** (2000). Presenilin is required for proper morphology and function of neurons in *C. elegans*. *Nature* **406**, 306-9.

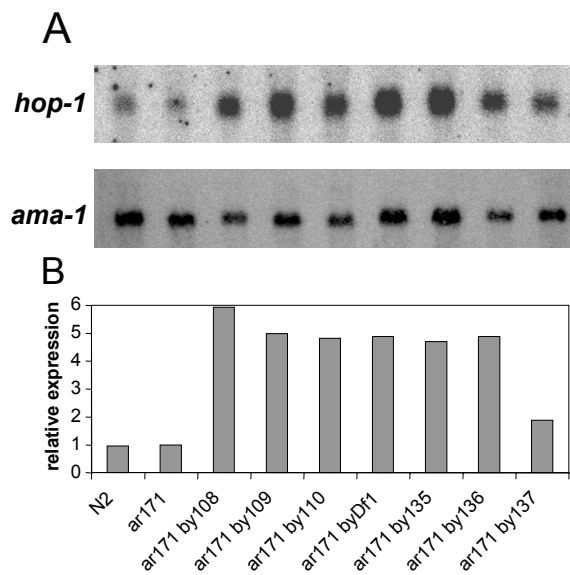
- Wolfe, M. S., Xia, W., Ostaszewski, B. L., Diehl, T. S., Kimberly, W. T. and Selkoe, D. J.** (1999). Two transmembrane aspartates in presenilin-1 required for presenilin endoproteolysis and gamma-secretase activity. *Nature* **398**, 513 - 517.
- You, A., Tong, J. K., Grozinger, C. M. and Schreiber, S. L.** (2001). CoREST is an integral component of the CoREST- human histone deacetylase complex. *Proc Natl Acad Sci U S A* **98**, 1454-8.
- Yu, G., Chen, F., Levesque, G., Nishimura, M., Zhang, D.-M., Levesque, L., Rogaeva, E., Xu, D., Liang, Y., Duthie, M. et al.** (1998). The Presenilin 1 Protein Is a Component of a High Molecular Weight Intracellular Complex That Contains beta -Catenin. *J. Biol. Chem.* **273**, 16470-16475.

Lakowski et al., supplemental data

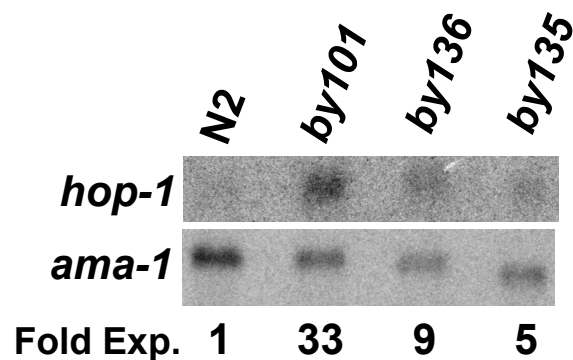
Table 1. The fine¹ genetic mapping of *spr-1*, *spr-3*, *spr-4* and *spr-5*.

Cross	picked	result
<i>spr-1</i>(by133)		
<i>dpy-11 unc-76/spr-1, sel-12</i>	Dpy non Unc and Unc non Dpy	<i>dpy-11</i> 9 <i>spr-1</i> 36 <i>unc-76</i>
<i>spr-3</i>(by108)		
<i>dpy-23 lon-2/spr-3</i>	Lon non Dpy	<i>dpy-23</i> 8 <i>spr-3</i> 41 <i>lon-2</i>
<i>sel-12 spr-3 lon-1; mnDp32</i>		<i>mnDp32</i> does not contain <i>spr-3</i>
<i>spr-4</i>(by105)		
<i>unc-13 spr-4 daf-8 unc-29/ego-1 unc-29; sel-12</i>	Unc-13 non Daf	<i>unc-13</i> 4 <i>ego-1</i> 1 <i>spr-4</i> 6 <i>daf-8</i>
<i>dpy-5 spr-4/unc-55; sel-12</i>	Spr non Dpy	<i>dpy-5</i> 52 <i>unc-55</i> 4 <i>spr-4</i>
<i>dpy-5unc-55 spr-4/+²; sel-12</i>	Spr non Dpy	<i>dpy-5</i> 60 <i>unc-55</i> 0 <i>byP4</i> 3 <i>byP5</i> 0 <i>byP7</i> 1 <i>byP8</i> 0 <i>spr-4</i>
<i>spr-5</i>(by101)		
<i>unc-75 spr-5 /; sel-12</i>	all	Egl 153, Unc 81, WT 7
<i>unc101 unc-59/ spr-5; sel-12</i>	Spr-5 ³	<i>unc-101</i> 17 <i>spr-5</i> 1 <i>unc-59</i>

1) Additional mapping data will be submitted to Wormbase. 2) SNP mapping done with the Hawaiian strain outcrossed twice with *unc-13 lin-11* to remove many unlinked polymorphisms. *byP4* = [vr77h09.s1@284](#) (position 7673 on *Cosmid F55D12*), *byP5* = [yw19d07.s1@263](#) (6926 on *H05L14*), *byP7* = [v120a11.s1@186](#) (23323 on *F18C12*) and *byP8* = [yy40e07.s1@715](#) (18265 on *T02E1*). The presence of *byP4* was determined by *KpnI* restriction digest and all other polymorphisms were detected by sequencing. 3) Of approximately 200 *spr* worms, 17 were heterozygous for *unc-101* and 1 was heterozygous for *unc-59*.



Supplemental figure 1: Mutations in the *spr-3* gene de-repress the expression of the *hop-1* gene in the L1 stage. A) *hop-1* mRNA concentration, with *ama-1* control, in the L1 stage from N2, *sel-12(ar171)* and most *sel-12(ar171) spr-3* strains. B) The relative expression of *hop-1* for the bands shown in A, after adjusting for equal loading.



Supplemental figure 2: Mutations in *spr-3* and *spr-5* de-repress the expression of the *hop-1* gene in the L1 stage in a *sel-12(+)* background. *hop-1* mRNA with *ama-1* loading control in the L1 stage for N2 (wild type), *spr-5(by101)*, *spr-3(by136)* and *spr-5(by135)*. All *spr* strains are in a *sel-12(+)* background. Below the bands are listed the fold expression of *hop-1* compared to N2, after correction for equal loading. Experimental methods are the same as for the Figure 7 in the paper.

CHAPTER VIII

**SPE-4, the third presenilin homolog in *C. elegans*, is a
non functional presenilin**

prepared for publication as:

Yamasaki A., **Eimer S.**, Baumeister R., Haass C. and Steiner H.

Expression of the *C. elegans* presenilin *spe-4* in human cells: functional implications for γ -secretase assembly and activity.

Introduction

Mutations in the human genes that code for the presenilins PS1 and PS2 lead to an autosomal dominant form of early onset Alzheimer's disease (Selkoe, 2001).

Presenilins have also been shown to be required for proteolysis and subsequent signaling of several type I transmembrane receptors like the amyloid precursor protein (APP) and the Notch receptors (De Strooper et al., 1999; De Strooper et al., 1998; Steiner and Haass, 2001). Although presenilins are widely distributed in nature, they seem to be restricted to multicellular organisms, since no presenilins have been identified in yeast or bacteria (Czech et al., 2000). However, presenilins share regions of similarity with a novel type of bacterial aspartyl proteases that are polytopic transmembrane proteins. Furthermore, these conserved motifs have been shown to be required for presenilin activity in *C. elegans* (Steiner et al., 2000). It is likely that presenilins exhibit proteolytic activity and are the long elusive γ -secretase. Furthermore, the notion that presenilins might belong to novel family of intramembraneous proteases is supported by the recent finding that the signal peptide protease (SPP) family of transmembrane proteases contain the same signature motif, which is required for SPP activity (Weihofen et al., 2002). SPPs catalyze the intramembrane proteolysis of some signal peptides after they have been cleaved off from the preprotein (Lemberg and Martoglio, 2002).

Phylogenetic analysis of the presenilin family suggests that presenilins have emanated from a common ancestor and that a duplication took place in those organisms that have two presenilin paralogs (Martinez-Mir et al., 2001).

In contrast to all organisms tested so far, the *C. elegans* genome codes for three presenilin genes *sel-12*, *hop-1*, and *spe-4*. The somatically expressed *sel-12* and *hop-1* have been shown to be required for signaling through the *C. elegans* Notch type receptors *lin-12* and *glp-1* (Levitan and Greenwald, 1995; Westlund et al., 1999). In *C. elegans*, *sel-12* is expressed during all developmental stages in probably all tissues (Baumeister et al., 1997). In contrast, *spe-4* is expressed only during spermatogenesis in the larval stage L4 (B. Lakowski, S. Eimer and R. Baumeister, submitted) (L'Hernault and Arduengo, 1992). *spe-4* expression is thereby restricted to the spermatheca (Arduengo et al., 1998). Therefore, it seems that *spe-4* has acquired a specialized role restricted to sperm development in *C. elegans*. SPE-4 is also more divergent in its degree of sequence conservation compared to the other *C. elegans* presenilins and to human PS1 (Table 1).

Nevertheless, SPE-4 contains several of the determinants that are considered to be required for presenilin function (Figure 1):

- (i) SPE-4 has been predicted to adopt the same transmembrane topology as has been shown for the other presenilins (Li and Greenwald, 1996; Li and Greenwald, 1998).
- (ii) SPE-4 contains the two aspartate residues in the transmembrane regions 6 and 7 which are critical for presenilin activity (Steiner et al., 2000).
- (iii) The PALP motif that is present in all presenilin family members is also conserved in SPE-4 (Tomita et al., 2001).

Therefore, SPE-4 contains all the residues and the topology that has been shown to be crucial for presenilin function although its sequence identity with the other presenilins is low (Table 1). However, there are still some differences. Compared to SEL-12 and the human presenilins, SPE-4, like HOP-1, contains only a short N-terminus. However, HOP-1 has been shown to be fully capable of replacing SEL-12 function in *C. elegans* (Li and Greenwald, 1997). Furthermore, the cytoplasmic loop between the transmembrane regions 6 and 7 is much larger than that of the other presenilins (Figure 1). However, this loop is largely variable among the presenilin family members and has been shown to be dispensable for presenilin function in human cells (Saura et al., 2000). Furthermore, even endoproteolysis of the presenilins seems not to be always required for function since the FAD variant PS1delta exon9, lacking the conserved cleavage site, is able to facilitate LIN-12/Notch-signaling in *C. elegans* (Baumeister et al., 1997). However, one region where SPE-4 is clearly different from any other presenilin cloned so far is its shorter C-terminus. All other presenilins have the same length of the C-terminus (Figure 1) (Czech et al., 2000).

It has been shown for *hop-1* and the human presenilins PS1 and PS2 that they are able to replace *sel-12* in *C. elegans* when expressed under the control of the *sel-12* promoter. (Baumeister et al., 1997; Levitan et al., 1996; Li and Greenwald, 1997). Hence, proteins that provide presenilin activity able to rescue the egg-laying defect (Egl) caused by loss of function mutations in *sel-12* (Levitan and Greenwald, 1995). We therefore wondered whether *spe-4* might also be able to replace *sel-12* when expressed under the control of the *sel-12* promoter. On the other hand, if *spe-4* is not able to rescue the *sel-12* Egl defect than one can consider SPE-4 as a non functional presenilin. In this respect it might be possible to substitute parts of SPE-4 with corresponding parts of the human presenilins or *sel-12* in order to re-gain rescuing activity. By this it should be possible to find new determinants of the presenilin function through defined local replacements.

Analysis of SPE-4 function

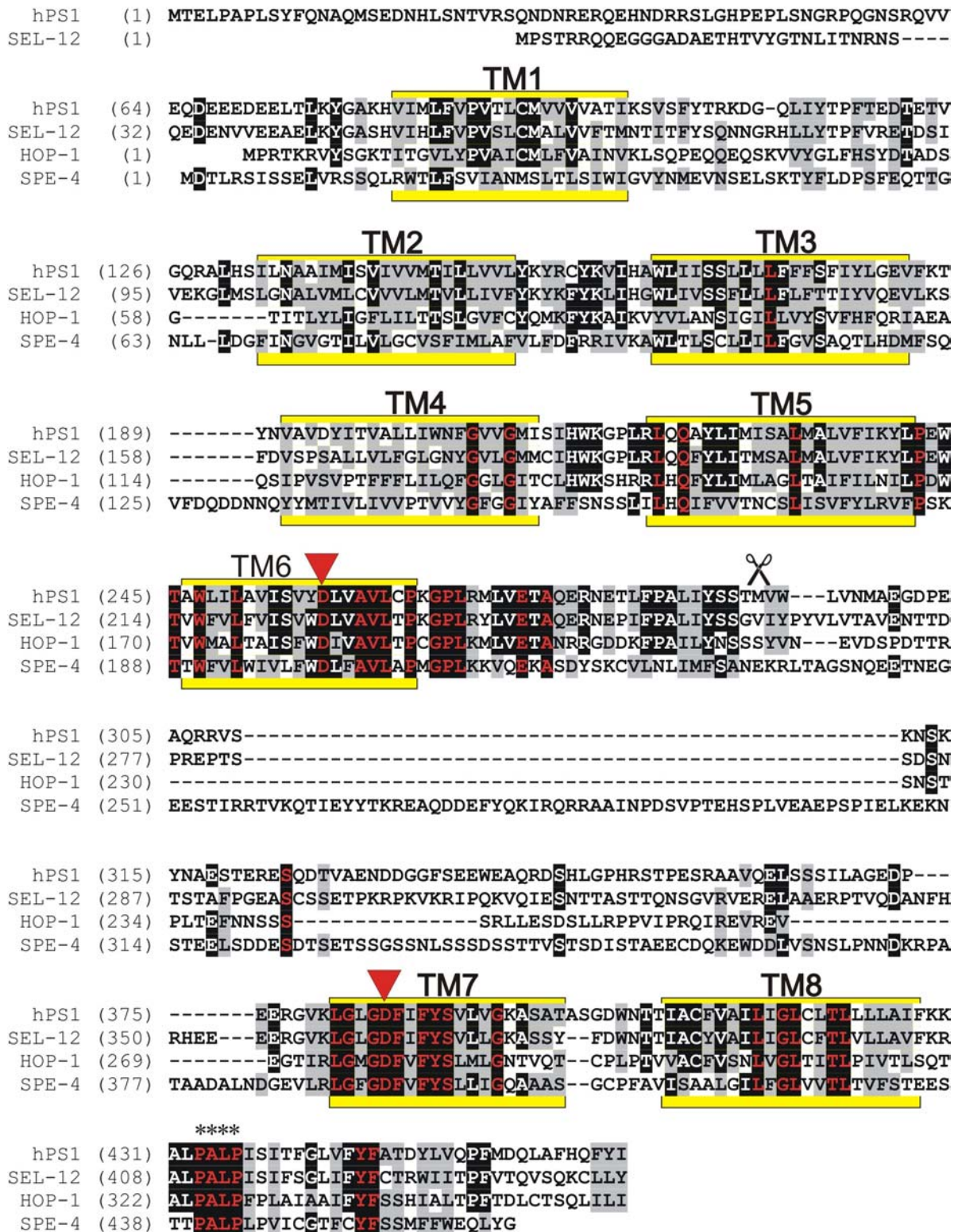


Figure 1: Sequence alignments of the *C. elegans* presenilin homologs SEL-12 (accession number AF171064), HOP-1 (AF021905) and SPE-4 (NM059694) with the human PS1 (AH004968). Similar residues are highlighted in grey, conserved residues that are identical in 75% of the aligned sequences are highlighted in black boxes with white letters. Positions that are invariant in all aligned sequences are represented by black boxes with red letters. The predicted transmembrane spanning segments (TM) are surrounded by yellow boxes. The position of the presumptive active site aspartate residues in TM6 and TM7 are indicated by red triangles (▼). The location of the presenilin cleavage site in human PS1 is marked by scissors and the location of the conserved PALP motive by asterisks (*).

Table 1: Sequence conservation of the *C. elegans* presenilins.

	<i>identity/similarity [%]*</i>			
	human PS1	SEL-12	HOP-1	SPE-4
human PS1	100	51/69	30/50	23/42
Ce SEL-12		100	30/49	22/42
Ce HOP-1			100	23/42
Ce SPE-4				100

* The Blast2 program available at the NCBI site was used to calculate the percentage of amino acid identity and similarity.

Results

Phylogenetic analysis of the presenilins in *C. elegans*

The whole genomes of the closely related nematodes *Caenorhabditis elegans* and *Caenorhabditis briggsae* have been sequenced (Guiliano et al., 2002; Kent and Zahler, 2000; The *C. elegans* Sequencing Consortium, 1998). Both species are estimated to have separated approximately 100 million years ago (Coghlan and Wolfe, 2002). Sequences that are not subjected to selective pressure should have diverged between *C. elegans* and *C. briggsae*, since nematodes evolve faster than other organisms (Coghlan and Wolfe, 2002). Therefore, if the similarities between SPE-4 and the somatic presenilins SEL-12 and HOP-1 are just accidental, they should have further diverged when compared to *C. briggsae*. Blast searches using the *C. briggsae* Blast server revealed that *C. briggsae*, like *C. elegans*, contains three presenilins, Cb SEL-12, Cb HOP-1, and Cb SPE-4, which correspond to *C. elegans* Ce SEL-12, Ce HOP-1, and Ce SPE-4, respectively (Figure 2). Cb SEL-12, Cb HOP-1, and Cb SPE-4 exhibit the same degree of homology to the human PS1 as their *C. elegans* counterparts (Figure 2).

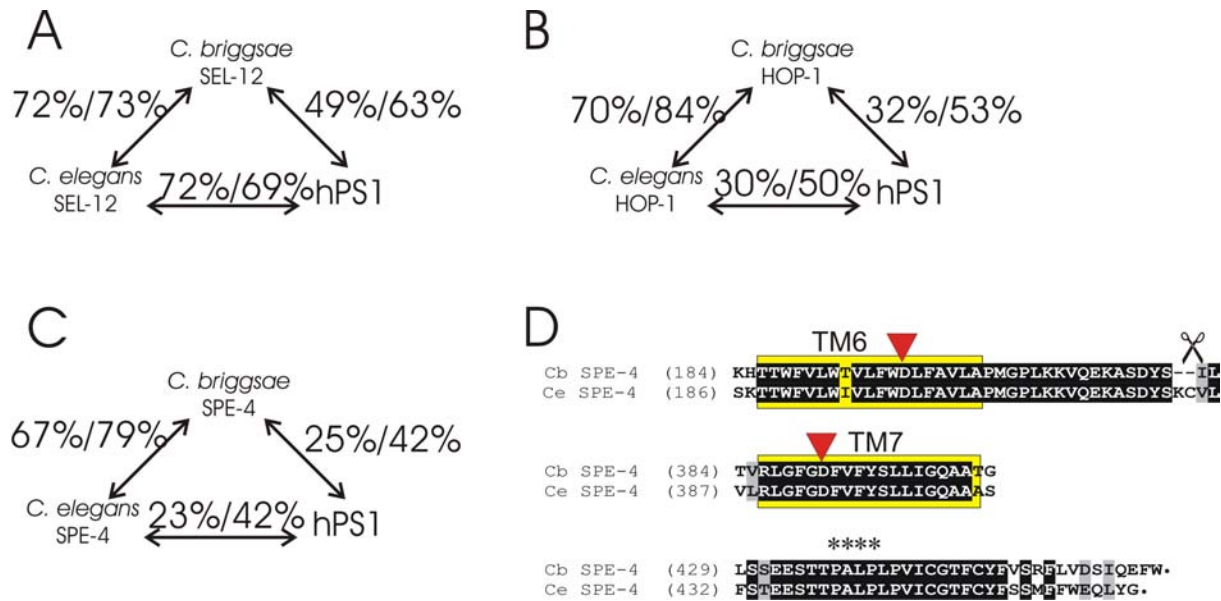


Figure 2: Comparison of the sequence conservation between the *C. elegans* and *C. briggsae* presentin homologs for (A) SEL-12, (B) HOP-1 and (C) SPE-4 relative to human presentin PS1. The *C. briggsae* presentin homologs were assembled by Blast search using the *C. briggsae* whole genome shot gun assembly as described in Material and Methods. The numbers above the arrows correspond to first the percentage of sequence identity and second the similarity between two sequences aligned. (D) Partial alignments between the *C. elegans* and *C. briggsae* SPE-4 proteins are shown comprising the conserved regions in TM6 and TM7 and the PALP motive. The site that corresponds to the autocatalytic cleavage site in the human presentilins is marked by scissors, although no processing for SPE-4 has been demonstrated, yet. Note the differences in the C-terminal extensions between *C. elegans* and *C. briggsae* SPE-4 (last two rows).

Although there is no complete sequence of Cb SEL-12 available in the database, the portion available reveals the highest similarity to the human PS1 (Figure 2A). As in the case of *C. elegans*, the Cb HOP-1 is more divergent than the SEL-12 presentilins, but still shows 32% sequence identity and 53% similarity to human PS1 (Figure 2B). Surprisingly, the Cb SPE-4 homolog shows the same degree of sequence conservation on the protein level than the other presentilins between *C. elegans* and *C. briggsae*, suggesting that there is a selective pressure to conserve the protein sequence of all the presentin homologs (Figure 2). A comparison of the protein sequences of Cb and Ce SPE-4 revealed that all of the known regions necessary for presentin function are also conserved (Figure 2D). *C. briggsae* SPE-4 also contains both presumptive active site aspartates located in the transmembrane domains TM6 and TM7 (Figure 2D).

Furthermore, the GXGD motive surrounding the aspartate in TM7 which has also been shown to be present in the bacterial (Steiner et al., 2000) and the SPP proteases (Weihofer et al., 2002) is conserved in *C. briggsae* (Figure 2D). In addition, the PALP motive following TM8 which is present in all presentin family members is also conserved between Ce and Cb SPE-4 (Figure 2D). A strong indication that this motif is also critical for SPE-4 function during spermatogenesis in the *C. elegans* are animals that carry a mutation in the first proline

of the PALP motif in SPE-4, which display the same sterility like complete loss-of-function mutants (Arduengo et al., 1998). This suggests that there is a selective pressure to conserve those sequences known to be required for presenilin function also within the SPE-4 protein.

However, in contrast to SEL-12 and HOP-1, the length of the C-terminus in SPE-4 is not conserved (Figure 2). Both the Ce and Cb SPE-4 molecules have shorter C-termini compared to the other presenilins (Czech et al., 2000) and, moreover, the length of the C-terminus is also divergent between *C. elegans* and *C. briggsae* SPE-4 (Figure 2D). The conservation of the known presenilin determinants between the *C. elegans* and *C. briggsae* SPE-4 makes it likely that it may also function as a presenilin. Furthermore, the data suggest that, so far, nematodes are the only organism to have three presenilin orthologs encoded in their genome.

Is SPE-4, a functional presenilin?

The second somatic presenilin in *C. elegans* HOP-1 is already very divergent from SEL-12 (Figure 1). However, *hop-1* is able to fully rescue the egg laying (Egl) defect caused by mutations in *sel-12* when expressed under the control of the *sel-12* promoter (Table 2) (Li and Greenwald, 1997). Since the similarities between HOP-1 and SEL-12 are in the same range as those of SPE-4 and SEL-12 (Table 1), it might be possible that SPE-4 provides some presenilin function. In this case it should be able to replace *sel-12* like *hop-1* or the human PS1 when expressed in *sel-12* mutant animals (Baumeister et al., 1997; Levitan et al., 1996; Li and Greenwald, 1997).

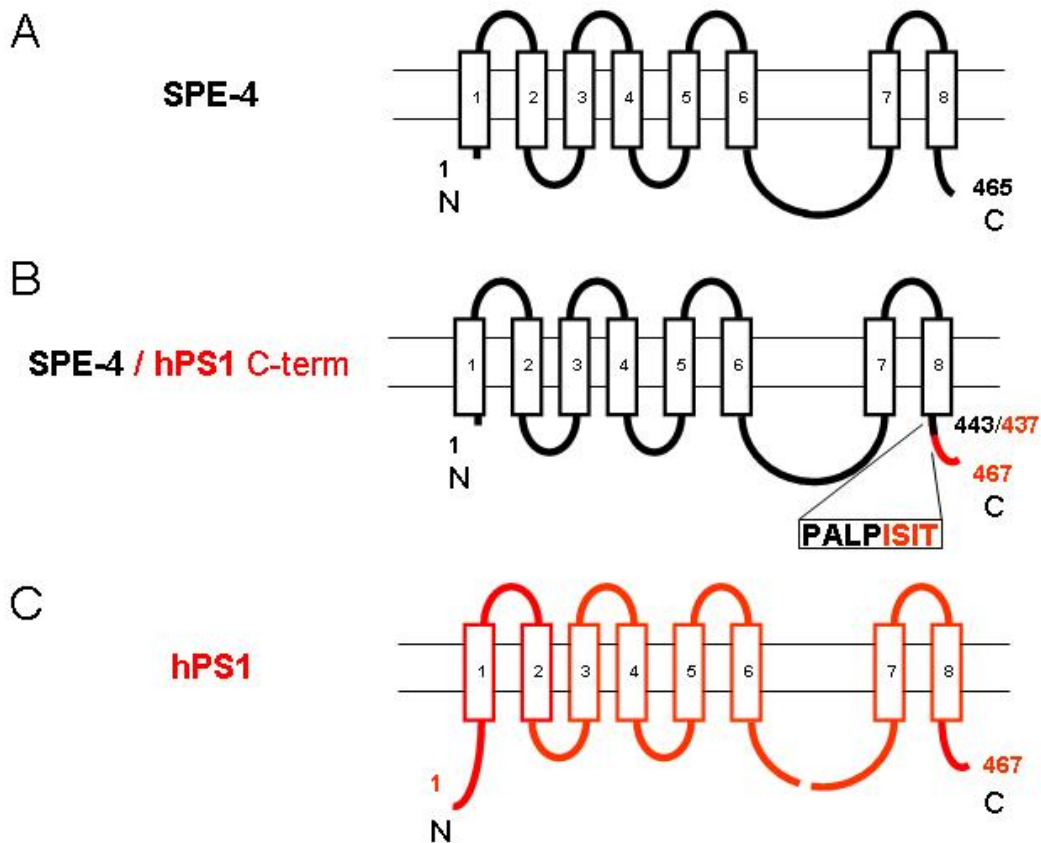


Figure 3: Graphical representation of the different SPE-4 molecules used to rescue experiments the *sel-12* Egl defect. **(A)** SPE-4 wild type sequence, **(B)** SPE-4/hPS1 C-terminus fusion protein (with the fusion site after the conserved PALP motif) contains the C-terminus from the human PS1. **(C)** Wild type human PS1 sequence. All constructs were expressed in *C. elegans sel-12* mutant animals under the control of the *sel-12* promoter.

Table 2: Rescuing activity of the *sel-12* Egl defect for the different presenilins expressed in *C. elegans*.

Strain	Transgene	Genotype	egg-laying behaviour ^s			
			+++	++	+	-
N2	-	wild type	50	0	0	0
BR1129	-	<i>sel-12(ar171)</i>	0	0	0	50
BR1964	PS1 wt	<i>sel-12(ar171)</i>	45	3	1	0
BR2002	<i>sel-12</i>	<i>sel-12(ar171)</i>	48	2	0	0
BR2993	<i>hop-1</i>	<i>sel-12(ar171)</i>	50	0	0	1
Line1	<i>spe-4</i>	<i>sel-12(ar171)</i>	0	0	0	34
Line2	<i>spe-4</i>	<i>sel-12(ar171)</i>	0	0	0	27
Line3	<i>spe-4</i>	<i>sel-12(ar171)</i>	0	0	0	16
Line4	<i>spe-4/PS1</i> C-term	<i>sel-12(ar171)</i>	0	0	0	42
Line5	<i>spe-4/PS1</i> C-term	<i>sel-12(ar171)</i>	0	0	0	38

^s For each transgenic animal the number of eggs laid were counted and were grouped into the following categories: +++, over 50 eggs progeny laid by an individual animal; ++, 15-50 eggs laid; +, 5-15 eggs laid; -, 0-5 eggs laid.

In order to test the ability of SPE-4 to act as a presenilin, we expressed *spe-4* under the control of the *sel-12* promoter in *sel-12(ar171)* mutant hermaphrodites and scored the Egl defect in the transgenic animals. The *sel-12(ar171)* mutation leads to a completely penetrant Egl defect and animals carrying this mutation never lay eggs (Baumeister et al., 1997; Eimer et al., 2002a; Levitan and Greenwald, 1995). Instead, *sel-12* mutants accumulate the fertilized eggs in the uterus and die consequently with a "bag of worms" phenotype (Levitan and Greenwald, 1995) as the progeny hatches inside the mother. Unlike *hop-1* and human PS1, *spe-4* is not able to rescue the *sel-12* Egl defect when expressed under the *sel-12* promoter (Table 2). *sel-12* mutant hermaphrodites carrying a *sel-12::spe-4* array never lay any eggs like the *sel-12* mutants alone (Figure 2), suggesting that *C. elegans* SPE-4 is unable to replace SEL-12 function.

However, as reported before, one of the differences between SPE-4 and the other presenilins is its shorter C-terminus. Therefore, it is likely that presenilins require a unique C-terminal elongation. In order to test this hypothesis, the *C. elegans spe-4* cDNA was fused to the human PS1 3' end after the conserved PALP motive as shown in Figure 3. This engineered *spe-4/hPS1* C-term cDNA is able to replace the endogenous PS1 and PS2 when overexpressed in human cells (Aya Yamasaki and Harald Steiner, personal communication). Unlike the wild type *C. elegans* SPE-4, it is now able to enter the presenilin complex and replaces the endogenous presenilins. However, SPE-4/hPS1 C-term act as dominant negative presenilin, blocking beta amyloid peptide production and Notch signaling (Aya Yamasaki and Harald Steiner, personal communication). In this respect SPE-4/hPS1 C-term acts like a PS1 or PS2 protein carrying a mutation in one of the aspartates required for function.

In order to test whether SPE-4/hPS1 C-term would be functional as a presenilin in *C. elegans*, we expressed *spe-4/hPS1* C-term under the control of the *sel-12* promoter and scored the rescue of *sel-12* Egl defect. Like wild type SPE-4, SPE-4/hPS1 C-term is not able to replace *sel-12* in *C. elegans* and transgenic *sel-12::spe-4/hPS1* C-term *sel-12(ar171)* hermaphrodites remain Egl (Table 2). However, the majority of the transgenic *sel-12(ar171)* animals expressing either *spe-4* wild type or *spe-4/hPS1* C-term are sterile, (65/77) and (67/80) respectively, and produce only unfertilized oocytes (Figure 4). The oocytes that left the gonad often develop into giant oocytes that contain large vacuoles (Figure 4). Furthermore, the sterile animals show a stacked oocytes (Sto) phenotype that is indicative of defective sperm, fewer sperm than normal, or no sperm (Eckmann et al., 2002). In some animals the gonad is even torn apart from the uterus at the position of the spermatheca and the

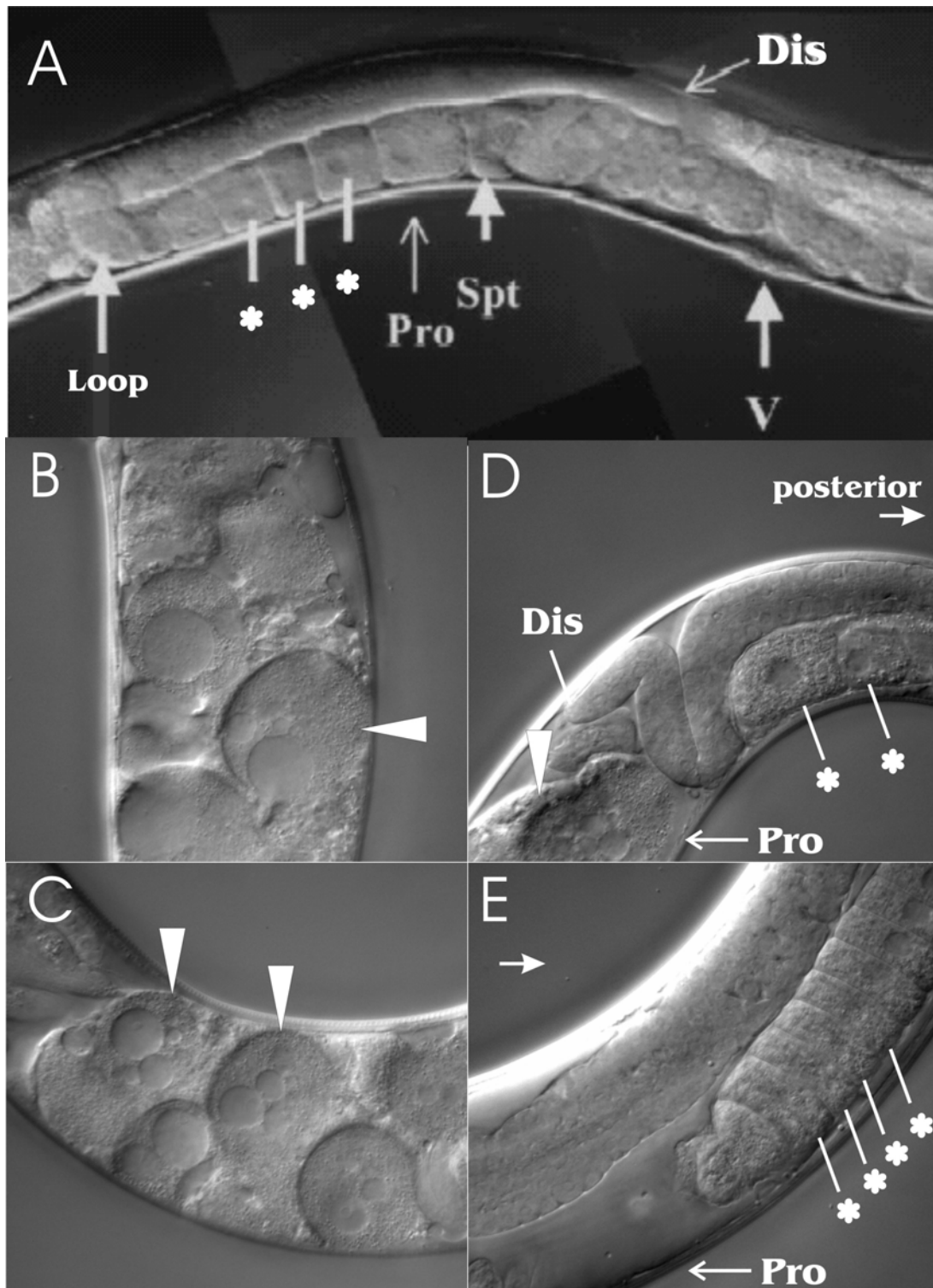


Figure 4: Midbody region of (A) a wild type hermaphrodite and (B-E) *sel-12(ar171)* animals carrying extrachromosomal arrays expressing the *spe-4* wild type cDNA under the control of the *sel-12* promoter. The distal (Dis) and proximal (Pro) parts of the gonad, oocytes in the proximal half of the gonad (asterisks), spermatheca (Spt), and vulva (V) are indicated. White triangles mark the giant oocytes in animals expressing *sel-12::spe-4*. (D-E) the proximal part of the gonad is torn apart from the uterus at the position of the spermatheca. Note that in (D) the gonad is pushed into the posterior of the body cavity. [Picture (A) was taken from Dufourcq et al, 2002.]

disconnected gonad arm is pushed into the posterior of the animal (Figure 4). This neomorphic phenotypes have not been observed with any of the other presenilins or mutants thereof, when being expressed in *C. elegans*. Therefore, we conclude that SPE-4 is not able to function as a presenilin in *C. elegans* although it contains some of the motives present in presenilins.

Discussion

Genetic and biochemical studies have shown that presenilins are not only able to lead to familial forms of Alzheimer's disease by aberrantly processing the amyloid beta peptid when mutated, but are also essential for Notch signaling (Kopan and Goate, 2000; Levitan and Greenwald, 1995; Sastre et al., 2001; Selkoe, 2001). Presenilins have been shown to be an integral component of high molecular weight complexes (Capell et al., 1998; Edbauer et al., 2002; Li et al., 2000; Seeger et al., 1997; Yu et al., 1998). The other complex components known so far are conserved throughout evolution (Francis et al., 2002; Goutte et al., 2002; Kopan and Goate, 2002; Lai, 2002; Steiner et al., 2002). It has been demonstrated that the cell surface display of this proteolytically active complex is tightly regulated and it needs all components for assembly and trafficking (Chung and Struhl, 2001; Edbauer et al., 2002; Goutte et al., 2002; Steiner et al., 2002). However, the precise role of presenilins in the process of complex formation and the interactions required for complex assembly are not well understood. In order to shed light on the hierarchical processes that govern complex assembly and maturation, it is important to know the contributions of each component in this process, especially since in the case of the presenilins the molecules are only stabilized when incorporated into the complexes (Tomita et al., 2001). The presence of three presenilin homologs in *C. elegans*, which are highly divergent in their protein sequence (Table 1), offers a unique possibility to detect the structural components and motives that are indispensable for presenilin function. Therefore, it might be possible to dissect the interactions required for complex assembly.

Although the sequence identity between the *C. elegans* presenilin SEL-12 and HOP-1 is only 30%, they have been shown to be functionally interchangeable (Eimer et al., 2002b; Li and Greenwald, 1997). Since most of the motives that are conserved between SEL-12 and HOP-1 are also found in SPE-4, it was likely that SPE-4 might also be able to function as a presenilin in *C. elegans*. However, SPE-4 has no detectable presenilin activity when expressed in *sel-12* mutant animals. This is still true even when the shorter C-terminus is exchanged with the corresponding part of the human PS1 (Figure 3). This draws the attention

to the motives that are missing in SPE-4 relative to the other presenilins (Figure 1). The biggest differences can be found in the loop region which is almost twice the size in SPE-4 as compared to the other presenilins. However, the entire large cytoplasmic loop has been shown to be dispensable for function of the human PS1 (Saura et al., 2000). Another major difference is found in the N-terminal sequences between the transmembrane segments TM1 and TM5. It will be very interesting to see whether introduction of N-terminal sequences from PS1 into SPE-4 will be able to render SPE-4 active as presenilin. However, in mammalian cell culture the exchange of the C-terminus in SPE-4 already leads to its association with nicastrin and its incorporation into the presenilin complex, since it is able to replace the endogenous PS1 and PS2 (Aya Yamasaki and Harald Steiner, personal communication). This suggests that part of the interaction domain with nicastrin/APH-2 might be located at the C-terminus. However, there are still additional components missing since the incorporated SPE-4/hPS1 C-term behaves as a dominant negative presenilin in cell culture (Aya Yamasaki and Harald Steiner, personal communication). In this respect it acts like a presenilin in which the active site aspartates have been mutated (Yu et al., 2000).

In *C. elegans* however, expression of either of the forms of SPE-4 also leads to the appearance of a novel phenotype (Figure 4). The degree of gonad destruction is reminiscent of that seen in the *C. elegans gon-10*, a mutant defective in the histone deacetylase HDA-1, which also affects gonad morphogenesis (Dufourcq et al., 2002). This phenotype was not detected during expression of any other presenilin in *C. elegans* nor during expression of mutant forms thereof (Baumeister et al., 1997; Levitan et al., 1996). Therefore, this might reflect a novel property of the SPE-4 protein. The expression of *spe-4* is normally restricted to the spermatheca and is required for sperm maturation (Arduengo et al., 1998; L'Hernault and Arduengo, 1992). But the exact role of SPE-4 during spermatogenesis is still unclear. Furthermore, it is also unclear whether SPE-4 is involved in proteolytic signaling and what the possible substrates might be. Maybe the ectopic expression of *spe-4* offers a way to deduce the processes it is involved in.

Material and Methods

Plasmid constructions and injections

All standard molecular methods were done according to Current Protocols. The *sel-12* cDNA was obtained by PCR from a *C. elegans* mixed stage cDNA library (kindly provided by Bob Barstead, Oklahoma) using the primers RB541/ RB542 and confirmed by sequencing. This *sel-12* cDNA (Genbank accession number AF171064) differs at its 3' end from the previously published sequence (Levitan and Greenwald, 1995). This *sel-12* cDNA was cloned as a *Sma*I/*Not*I fragment under the control of a 2.8-kilobase (kb) *sel-12* promoter fragment starting at the translational start ATG of *sel-12* to generate pBY895 (Wittenburg et al., 2000). The cDNAs of *spe-4* wt and *spe-4*/hPS1 C-terminus and human PS1 were PCR amplified (Aya Yamasaki and Harald Steiner unpublished) using *pfu* DNA polymerase (Stratagene) according to the manufacturers protocol. For the amplification of *spe-4* wt, *spe-4*/PS1 C-terminus and hPS1 the primers RB1370 / RB1372, RB1370 / RB1371 and RB968 / RB1371 were used, respectively. The PCR products were each subcloned into pBY895 as a *Sma*I/*Not*I fragment replacing the *sel-12* cDNA. Therefore the *spe-4* wt cDNA, *spe-4*/hPS1 C-term, and hPS1 were placed under the control of the *sel-12* promoter yielding the *C. elegans* expression vectors pBY1587, pBY1588, and pBY1100, respectively. The *sel-12::hop-1* rescue construct was created by amplification of the *hop-1* cDNA from a *C. elegans* cDNA library (kindly provided by Bob Barstead, Oklahoma) using the primers RB925 / RB926 and subcloning the PCR product into pBY895 as a *Sma*I/*Not*I fragment resulting in pBY1218. All constructs were confirmed by sequencing. To determine if the presenilin constructs are able to rescue *sel-12* mutant hermaphrodites, all constructs were each injected into *sel-12(ar171)* mutant hermaphrodites at a concentration of 20ng/μl together with pBY1153 (*sel-12::gfp*) at 20ng/μl as a coinjection marker.

Scoring of the *sel-12* Egl rescue

After germline injection, GFP positive animals were isolated that stable inherit the array to their progeny thereby creating an independent line. To score the ability of the arrays to rescue the Egl defect of *sel-12(ar171)* animals, GFP positive worms that showed a broad and

uniform gfp expression were singled as L4 to new plates and their egg-laying behaviour was scored at 20°C .

Comparison of *C. elegans* and *C. briggsae* presenilins

The *C. elegans* presenilin protein sequences were compared with the *C. briggsae* whole genome shot gun sequences using the TBlastN search algorithm. The preliminary *C. briggsae* genome sequence is accessible via the *C. briggsae* Blast server at:

http://www.sanger.ac.uk/Projects/C_briggsae/blast_server.shtml.

Acknowledgement

I would especially like to thank Roland Donhauser for his excellent technical help with the injections. Additionally, I would like to thank Christine Baumeister for providing the strain carrying the hop-1 array. Furthermore, I would like to thank Bob Barsted for providing the *C. elegans* mixed stage cDNA library and all members of the Baumeister lab for their help and discussions.

Supplementary information

Oligo table:

Primer	Target	Sequence 5' - 3'
RB541	<i>sel-12</i>	GAG GTA CCC GGG CAA AAA ATG CCT TCC ACA AGG AGA CAA CAG G
RB542	<i>sel-12</i>	GTG AAT TCG CGG CCG CTT AAT ATA ATA AAC ACT TTT GAG AGA CTT GTG
RB968	hPS1	ATT CGG ATC CCC GGG CAA AAA ATG ACA GAG TTA CCT GCA CCG
RB925	<i>hop-1</i>	GAC CAT GGT ACC CGG GCA AAA AAT GCC AAG AAC AAA AAG AGT GTA C
RB926	<i>hop-1</i>	CGA GAG CTC GCG GCC GCA TCT TTA GAA CAA CCC GGT CAC
RB1370	<i>spe-4</i>	GGG CAA AAA ATG GAC ACC CTT CGA TCG ATT
RB1371	hPS1	CAC CTC GAG CGG CCG CTA GAT ATA AAA TTG ATG GAA TGC
RB1372	<i>spe-4</i>	CAC CTC GAG CGG CCG CTC ATC CGT AAA GTT GCT CCC A

References

- Arduengo, P. M., Appleberry, O. K., Chuang, P., and L'Hernault, S. W. (1998). The presenilin protein family member SPE-4 localizes to an ER/Golgi derived organelle and is required for proper cytoplasmic partitioning during *Caenorhabditis elegans* spermatogenesis. *J Cell Sci* **111**, 3645-54.
- Baumeister, R., Leimer, U., Zweckbronner, I., Jakubek, C., Grunberg, J., and Haass, C. (1997). Human presenilin-1, but not familial Alzheimer's disease (FAD) mutants, facilitate *Caenorhabditis elegans* Notch signalling independently of proteolytic processing. *Genes Funct* **1**, 149-59.
- Capell, A., Grunberg, J., Pesold, B., Diehlmann, A., Citron, M., Nixon, R., Beyreuther, K., Selkoe, D. J., and Haass, C. (1998). The proteolytic fragments of the Alzheimer's disease-associated presenilin-1 form heterodimers and occur as a 100-150-kDa molecular mass complex. *J Biol Chem* **273**, 3205-11.
- Chung, H. M., and Struhl, G. (2001). Nicastrin is required for Presenilin-mediated transmembrane cleavage in *Drosophila*. *Nat Cell Biol* **3**, 1129-32.

- Coghlan, A., and Wolfe, K. H. (2002). Fourfold faster rate of genome rearrangement in nematodes than in *Drosophila*. *Genome Res* **12**, 857-67.
- Czech, C., Tremp, G., and Pradier, L. (2000). Presenilins and Alzheimer's disease: biological functions and pathogenic mechanisms. *Prog Neurobiol* **60**, 363-84.
- De Strooper, B., Annaert, W., Cupers, P., Saftig, P., Craessaerts, K., Mumm, J. S., Schroeter, E. H., Schrijvers, V., Wolfe, M. S., Ray, W. J., Goate, A., and Kopan, R. (1999). A presenilin-1-dependent gamma-secretase-like protease mediates release of Notch intracellular domain. *Nature* **398**, 518-22.
- De Strooper, B., Saftig, P., Craessaerts, K., Vanderstichele, H., Guhde, G., Annaert, W., Von Figura, K., and Van Leuven, F. (1998). Deficiency of presenilin-1 inhibits the normal cleavage of amyloid precursor protein. *Nature* **391**, 387-90.
- Dufourcq, P., Victor, M., Gay, F., Calvo, D., Hodgkin, J., and Shi, Y. (2002). Functional Requirement for Histone Deacetylase 1 in *Caenorhabditis elegans* Gonadogenesis. *Mol Cell Biol* **22**, 3024-34.
- Eckmann, C. R., Kraemer, B., Wickens, M., and Kimble, J. (2002). GLD-3, a bicaudal-C homolog that inhibits FBF to control germline sex determination in *C. elegans*. *Dev Cell* **3**, 697-710.
- Edbauer, D., Winkler, E., Haass, C., and Steiner, H. (2002). Presenilin and nicastrin regulate each other and determine amyloid beta -peptide production via complex formation. *Proc Natl Acad Sci U S A*.
- Eimer, S., Donhauser, R., and Baumeister, R. (2002a). The *Caenorhabditis elegans* Presenilin *sel-12* Is Required for Mesodermal Patterning and Muscle Function. *Dev Biol* **251**, 178-92.
- Eimer, S., Lakowski, B., Donhauser, R., and Baumeister, R. (2002b). Loss of *spr-5* bypasses the requirement for the *C.elegans* presenilin *sel-12* by derepressing *hop-1*. *Embo J* **21**, 5787-5796.
- Francis, R., McGrath, G., Zhang, J., Ruddy, D. A., Sym, M., Apfeld, J., Nicoll, M., Maxwell, M., Hai, B., Ellis, M. C., Parks, A. L., Xu, W., Li, J., Gurney, M., Myers, R. L., Himes, C. S., Hiesch, R., Ruble, C., Nye, J. S., and Curtis, D. (2002). *aph-1* and *pen-2* are required for Notch pathway signaling, gamma-secretase cleavage of betaAPP, and presenilin protein accumulation. *Dev Cell* **3**, 85-97.
- Goutte, C., Tsunozaki, M., Hale, V. A., and Priess, J. R. (2002). APH-1 is a multipass membrane protein essential for the Notch signaling pathway in *Caenorhabditis elegans* embryos. *Proc Natl Acad Sci U S A* **99**, 775-779.
- Guiliano, D. B., Hall, N., Jones, S. J., Clark, L. N., Corton, C. H., Barrell, B. G., and Blaxter, M. L. (2002). Conservation of long-range synteny and microsynteny between the genomes of two distantly related nematodes. *Genome Biol* **3**, RESEARCH0057.
- Kent, W. J., and Zahler, A. M. (2000). Conservation, regulation, synteny, and introns in a large-scale *C. briggsae*-*C. elegans* genomic alignment. *Genome Res* **10**, 1115-25.
- Kopan, R., and Goate, A. (2000). A common enzyme connects notch signaling and Alzheimer's disease. *Genes Dev* **14**, 2799-806.
- Kopan, R., and Goate, A. (2002). Aph-2/Nicastrin: an essential component of gamma-secretase and regulator of Notch signaling and Presenilin localization. *Neuron* **33**, 321-4.
- Lai, E. C. (2002). Notch cleavage: Nicastrin helps Presenilin make the final cut. *Curr Biol* **12**, R200-2.
- Lemberg, M. K., and Martoglio, B. (2002). Requirements for signal Peptide peptidase-catalyzed intramembrane proteolysis. *Mol Cell* **10**, 735-44.
- Levitan, D., Doyle, T. G., Brousseau, D., Lee, M. K., Thinakaran, G., Slunt, H. H., Sisodia, S. S., and Greenwald, I. (1996). Assessment of normal and mutant human presenilin function in *Caenorhabditis elegans*. *Proc Natl Acad Sci U S A* **93**, 14940-4.

- Levitan, D., and Greenwald, I. (1995). Facilitation of *lin-12*-mediated signalling by *sel-12*, a *Caenorhabditis elegans* S182 Alzheimer's disease gene. *Nature* **377**, 351-4.
- L'Hernault, S. W., and Arduengo, P. M. (1992). Mutation of a putative sperm membrane protein in *Caenorhabditis elegans* prevents sperm differentiation but not its associated meiotic divisions. *J Cell Biol* **119**, 55-68.
- Li, X., and Greenwald, I. (1996). Membrane topology of the *C. elegans* SEL-12 presenilin. *Neuron* **17**, 1015-21.
- Li, X., and Greenwald, I. (1997). HOP-1, a *Caenorhabditis elegans* presenilin, appears to be functionally redundant with SEL-12 presenilin and to facilitate LIN-12 and GLP-1 signaling. *Proc Natl Acad Sci U S A* **94**, 12204-9.
- Li, X., and Greenwald, I. (1998). Additional evidence for an eight-transmembrane-domain topology for *Caenorhabditis elegans* and human presenilins. *Proc Natl Acad Sci U S A* **95**, 7109-14.
- Li, Y. M., Lai, M. T., Xu, M., Huang, Q., DiMuzio-Mower, J., Sardana, M. K., Shi, X. P., Yin, K. C., Shafer, J. A., and Gardell, S. J. (2000). Presenilin 1 is linked with gamma-secretase activity in the detergent solubilized state. *Proc Natl Acad Sci U S A* **97**, 6138-43.
- Martinez-Mir, A., Canestro, C., Gonzalez-Duarte, R., and Albalat, R. (2001). Characterization of the amphioxus presenilin gene in a high gene-density genomic region illustrates duplication during the vertebrate lineage. *Gene* **279**, 157-64.
- Sastre, M., Steiner, H., Fuchs, K., Capell, A., Multhaup, G., Condron, M. M., Teplow, D. B., and Haass, C. (2001). Presenilin-dependent gamma-secretase processing of beta-amyloid precursor protein at a site corresponding to the S3 cleavage of Notch. *EMBO Rep* **2**, 835-41.
- Saura, C. A., Tomita, T., Soriano, S., Takahashi, M., Leem, J. Y., Honda, T., Koo, E. H., Iwatsubo, T., and Thinakaran, G. (2000). The nonconserved hydrophilic loop domain of presenilin (PS) is not required for PS endoproteolysis or enhanced abeta 42 production mediated by familial early onset Alzheimer's disease-linked PS variants. *J Biol Chem* **275**, 17136-42.
- Seeger, M., Nordstedt, C., Petanceska, S., Kovacs, D. M., Gouras, G. K., Hahne, S., Fraser, P., Levesque, L., Czernik, A. J., George-Hyslop, P. S., Sisodia, S. S., Thinakaran, G., Tanzi, R. E., Greengard, P., and Gandy, S. (1997). Evidence for phosphorylation and oligomeric assembly of presenilin 1. *Proc Natl Acad Sci U S A* **94**, 5090-4.
- Selkoe, D. J. (2001). Alzheimer's disease: genes, proteins, and therapy. *Physiol Rev* **81**, 741-66.
- Steiner, H., and Haass, C. (2001). Nuclear signaling: a common function of presenilin substrates? *J Mol Neurosci* **17**, 193-8.
- Steiner, H., Kostka, M., Romig, H., Basset, G., Pesold, B., Hardy, J., Capell, A., Meyn, L., Grim, M. L., Baumeister, R., Fichteler, K., and Haass, C. (2000). Glycine 384 is required for presenilin-1 function and is conserved in bacterial polytopic aspartyl proteases. *Nat Cell Biol* **2**, 848-51.
- Steiner, H., Winkler, E., Edbauer, D., Prokop, S., Basset, G., Yamasaki, A., Kostka, M., and Haass, C. (2002). PEN-2 is an integral component of the gamma-secretase complex required for coordinated expression of presenilin and nicastrin. *J Biol Chem* **277**, 39062-5.
- The *C. elegans* Sequencing Consortium. (1998). Genome sequence of the nematode *C. elegans*: a platform for investigating biology. The *C. elegans* Sequencing Consortium. *Science* **282**, 2012-8.
- Tomita, T., Watabiki, T., Takikawa, R., Morohashi, Y., Takasugi, N., Kopan, R., De Strooper, B., and Iwatsubo, T. (2001). The first proline of PALP motif at the C terminus of

- presenilins is obligatory for stabilization, complex formation, and gamma-secretase activities of presenilins. *J Biol Chem* **276**, 33273-81.
- Weihofen, A., Binns, K., Lemberg, M. K., Ashman, K., and Martoglio, B. (2002). Identification of signal peptide peptidase, a presenilin-type aspartic protease. *Science* **296**, 2215-8.
- Westlund, B., Parry, D., Clover, R., Basson, M., and Johnson, C. D. (1999). Reverse genetic analysis of *Caenorhabditis elegans* presenilins reveals redundant but unequal roles for *sel-12* and *hop-1* in Notch-pathway signaling. *Proc Natl Acad Sci U S A* **96**, 2497-502.
- Wittenburg, N., Eimer, S., Lakowski, B., Rohrig, S., Rudolph, C., and Baumeister, R. (2000). Presenilin is required for proper morphology and function of neurons in *C. elegans*. *Nature* **406**, 306-9.
- Yu, G., Chen, F., Levesque, G., Nishimura, M., Zhang, D. M., Levesque, L., Rogaeva, E., Xu, D., Liang, Y., Duthie, M., St George-Hyslop, P. H., and Fraser, P. E. (1998). The presenilin 1 protein is a component of a high molecular weight intracellular complex that contains beta-catenin. *J Biol Chem* **273**, 16470-5.
- Yu, G., Chen, F., Nishimura, M., Steiner, H., Tandon, A., Kawarai, T., Arawaka, S., Supala, A., Song, Y. Q., Rogaeva, E., Holmes, E., Zhang, D. M., Milman, P., Fraser, P. E., Haass, C., and George-Hyslop, P. S. (2000). Mutation of conserved aspartates affects maturation of both aspartate mutant and endogenous presenilin 1 and presenilin 2 complexes. *J Biol Chem* **275**, 27348-53.

Curriculum vitae

Name Stefan Eimer
Geburtsdatum 07.03.71
Geburtsort Kronach
Familienstand unverheiratet

Schulbildung:

1977 - 1981 Grundschule, Leck/Nordfriesland
1981 Grundschule, Troisdorf-Spich
1981 - 1984 Stadt-Gymnasium Altenforst, Troisdorf
1984 - 1992 Gymnasium Bad Aibling, Bad Aibling
Erlangung der Allgemeinen Hochschulreife

Hochschulstudium:

1992 Chemie- und Biochemie- Studium an der Universität Bayreuth
1997 Diplomhauptprüfung Biochemie an der Universität Bayreuth
1997 Diplomarbeit unter Anleitung von Prof. Dr. Christian Lehner an der Universität Bayreuth
Thema: Untersuchungen zur Funktion und Wechselwirkung des *Drosophila melanogaster* Proteins Pimples bei der Schwesterchromatidentrennung
1998 - 2002 Anfertigung der Dissertation unter der Anleitung von Prof. Dr. Ralf Baumeister am Genzentrum der Ludwig-Maximilians Universität München
Thema: Analysis and suppression of mutant presenilin *sel-12* in *Caenorhabditis elegans*

Abbreviations

aa	amino acid
A β	beta amyloid peptide
AC	anchor cell
AD	Alzheimer's Disease
<i>aph</i>	anterior pharynx missing
APP	amyloid precursor protein
BLAST	basic local alignment search tool
bp	base pair
<i>C. briggsae</i>	<i>Caenorhabditis briggsae</i>
<i>C. elegans</i>	<i>Caenorhabditis elegans</i>
CC	coelomocyte
cDNA	complementary DNA
cM	centi Morgan
DNA	deoxyribonucleic acid
dsRNA	double stranded RNA
DTC	distal tip cell
<i>E. coli</i>	<i>Escherichia coli</i>
Egl	egg-laying defective
FAD	familial Alzheimer's disease
FAD	flavin adenine dinucleotide cofactor
GFP	green fluorescent protein
Glp	germline proliferation
HDAC	histone deacetylase
GST	glutathione S-transferase
IPTG	isopropyl-thio-galactoside
<i>lin</i>	lineage defective
mRNA	messenger RNA
Muv	multi vulva phenotype
NLS	nuclear localisation signal
nt	nucleotide
ORF	open reading frame
PAGE	polyacrylamide gel electrophoresis
PAO	polyamine oxidase

PCR	polymerase chain reaction
<i>pen</i>	presenilin enhancer
PS	presenilin
Pvl	protruding vulva
RNA	ribonucleic acid
RNAi	double stranded RNA mediated interference
RT	reverse transcriptase
<i>S. cerev.</i>	<i>Saccharomyces cerevisiae</i>
SDS	sodium dodecyl sulfate
<i>sel</i>	suppressor enhancer of <i>lin-12</i>
SL	splice leader
SM	sex myoblast
<i>spr</i>	suppressor of presenilin
Sto	stacked oocytes
Unc	uncoordinated
utse	uterine seam cell
VPC	vulva precursor cell
VU	ventral uterine cell